UNIVERSITY OF KWAZULU-NATAL

SYNTHESIS, CHARACTERISATION AND ANTIBACTERIAL ACTIVITY OF QUINOLINE CHALCONE HYBRIDS

2019

GILLEAN PAMELA FRASER

SUPPLEMENTARY MATERIAL
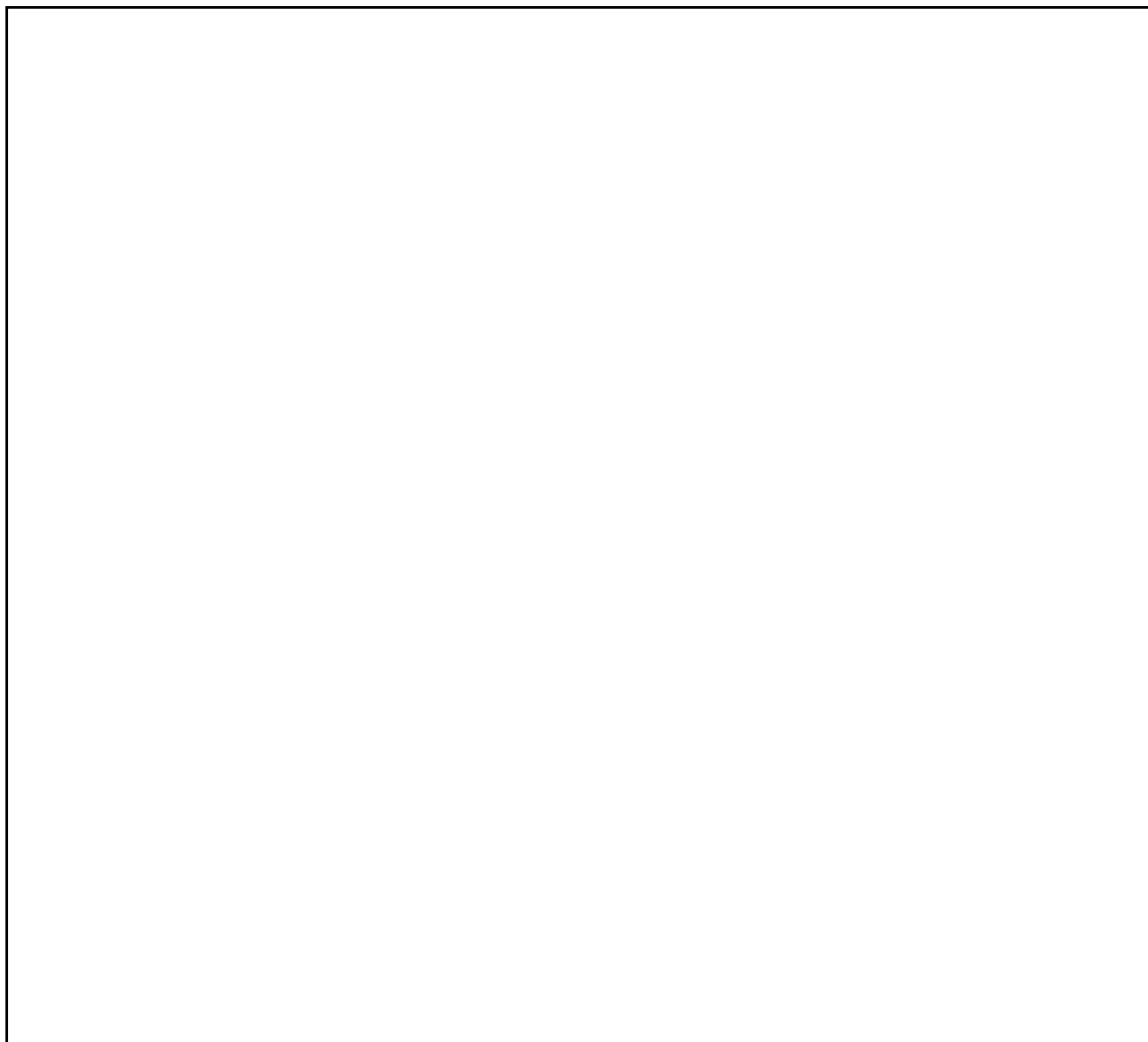
SYNTHESIS, CHARACTERISATION AND ANTIBACTERIAL ACTIVITY OF QUINOLINE CHALCONE HYBRIDS

GILLEAN FRASER

2019

A thesis submitted to the School of Chemistry and Physics in the College of Agriculture, Engineering and Science for the fulfilment of the degree of Master of Science.

Preface

I hereby declare that the thesis entitled "**Synthesis, characterisation and antibacterial activity of quinoline chalcone hybrids**" submitted to the University of KwaZulu-Natal for the award of the degree of Master of Science in Chemistry under the supervision of Professor Neil A. Koorbanally represents original work by the author and has not been submitted in full or part for any degree or diploma at this or any other University.

Where use was made of the work of others it has been duly acknowledged in the text. This work was carried out in the School of Chemistry and Physics, University of KwaZulu-Natal, Westville campus, Durban, South Africa.

Signed: _____   Date: _____

Gillean Pamela Fraser, BSc (HONS)

As the candidate's supervisor, I have approved this dissertation for submission

Signed: _____   Date: _____

Professor Neil A. Koorbanally, PhD (Natal)

DECLARATIONS

DECLARATION 1 – PLAGIARISM

I, **Gillean Pamela Fraser**, declare that

1. The research reported in this thesis is my original research, except where otherwise indicated.

2. This thesis has not been submitted for any degree or examination at any other university.

3. This thesis does not contain other persons' data, pictures, graphs or other information, unless specifically acknowledged as being sourced from other persons.

4. This thesis does not contain other persons' writing, unless specifically acknowledged as being sourced from other researchers. Where other written sources have been quoted, then:

   a. Their words have been rewritten but the general information attributed to them have been referenced.

   b. Where their exact words have been used, then their writing has been placed in italics and inside quotation marks and referenced.

5. This thesis does not contain text, graphics or tables copied and pasted from the Internet, unless specifically acknowledged, and the source being detailed in the thesis and in the References sections.

Signed ……………………………………………………………

Sam's Speech (taken from the Lord of the Rings: Two Towers)

Frodo: I can't do this, Sam.

Sam: I know, it's all wrong. By rights we shouldn't even be here.

But we are.

It's like in the great stories Mr. Frodo.

The ones that really mattered.

Full of darkness and danger they were,

and sometimes you didn't want to know the end, because how could the end be happy?

How could the world go back to the way it was when so much bad happened?

But in the end, it's only a passing thing, this shadow.

Even darkness must pass.

A new day will come.

And when the sun shines it will shine out the clearer.

Those were the stories that stayed with you, that meant something.

Even if you were too small to understand why.

But I think, Mr. Frodo, I do understand. I know now.

Folk in those stories had lots of chances of turning back only they didn't.

Because they were holding on to something.

Frodo: What are we holding on to, Sam?

***Sam*: That there's some good in this world, Mr. Frodo. And it's worth fighting for.**

ACKNOWLEDGEMENTS

List of Abbreviations

APT	attached proton test
bd	broad doublet
bs	broad singlet
°C	degrees Celsius
^{1}H NMR	proton nuclear magnetic resonance spectroscopy
^{13}C NMR	carbon-13 nuclear magnetic resonance spectroscopy
COSY	correlation spectroscopy
d	doublet
dd	doublet of doublets
ddd	doublet of doublet of doublets
DMF	dimethylformamide
DMSO	dimethyl sulfoxide
DMSO-d_6	deuterated dimethyl sulfoxide
FTIR	Fourier transform infrared
HMBC	heteronuclear multiple bond correlation
HRMS	high resolution mass spectrometry
HSQC	heteronuclear single quantum coherence
Hz	hertz
IR	infrared
LC-MS	liquid chromatography–mass spectrometry
MBC	minimum bactericidal concentration
mp	melting point
MHA	Mueller-Hinton agar
MHz	megahertz
NHP	*N*-hydroxyphthalimide
NOESY	nuclear Overhauser effect spectroscopy
PIDA	phenyliodine(III) diacetate
rt	room temperature
s	singlet
t	triplet
TFA	trifluoroacetic acid
TLC	thin layer chromatography
TMS	tetramethylsilane
UV	ultraviolet

Abstract

Nine novel quinoline-chalcone hybrids were synthesized via a base-catalysed Claisen-Schmidt condensation of 6-fluoroquinoline-2-carbaldehyde, 8-fluoroquinoline-2-carbaldehyde or 6,8-difluoroquinoline-2-carbaldehyde with 4'-Br, 4'-Cl and 4'-F substituted acetophenones. The 2-methylquinoline intermediates were prepared by the Doebner-Miller reaction and oxidized to their corresponding quinoline-2-carbaldehydes before being condensed with the acetophenones. The structures of the quinoline chalcones were characterized by 1D and 2D NMR spectroscopy and confirmed by HRMS. The synthesised hybrid molecules were evaluated for their antibacterial activity against six standard bacterial strains, namely the Gram-positive *Staphylococcus aureus* and methicillin-resistant *Staphylococcus aureus* (MRSA), and the Gram-negative *Escherichia coli*, *Klebsiella pneumoniae*, *Pseudomonas aeruginosa* and *Salmonella typhimurium*. The synthesized compounds showed better or comparable antibacterial activity to known drugs (ciprofloxacin and levofloxacin) in the same assay, the most active being the 6,8-difluoroquinoline derivative with a *para* bromo moiety on the acetophenone derived portion of the molecule, showing MBC values of 5.2 and 20.9 μM against *S. aureus* and MRSA respectively.

Keywords: quinoline, chalcone, hybrid molecules, antibacterial activity

STRUCTURES OF THE SYNTHESISED COMPOUNDS REPORTED IN THIS

THESIS
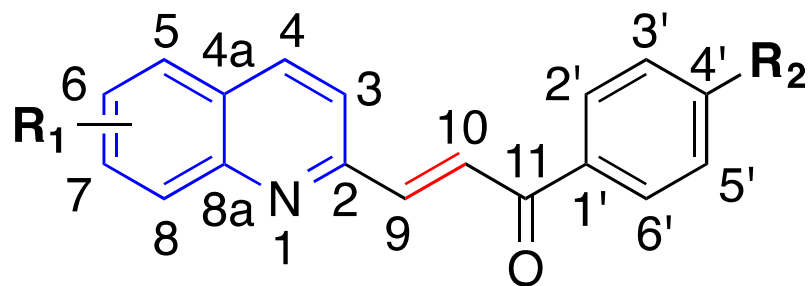
8a-i

	R₁	R₂		R₁	R₂		R₁	R₂
8a	6-F	Br	**8d**	6,8-diF	Br	**8g**	8-F	Br
8b	6-F	Cl	**8e**	6,8-diF	Cl	**8h**	8-F	Cl
8c	6-F	F	**8f**	6,8-diF	F	**8i**	8-F	F

Contents

List of Figures

List of Schemes

List of Tables

Chapter 1. Introduction

The startling rise of antibiotic-resistance is a major worldwide concern and as such, the search for new and alternative drugs is an important pursuit for modern chemists. The synthesis of antibiotics in large quantities and their extensive use in hospitals have made this worse (Neu, 1992). Between 1940 and 1980, the development and introduction of new antibiotics peaked, which may have contributed to the antibiotic resistance crisis (Martens and Demain, 2017). A decline in Natural Products research and merging of pharmaceutical companies (resultant companies were less productive) may have also contributed to this epidemic (Martens and Demain, 2017).

Bacterial resistance occurs when bacteria change their structure or form, such that it reduces or eliminates antibiotic binding, thereby reducing or eliminating their efficacy. Bacteria are able to develop resistance as a result of chromosomal changes, exchange of genetic material or by concealing their cell walls. Beside these known resistant pathogens, other opportunistic organisms have emerged, which are resistant to many drugs.

Methicillin-resistant *S. aureus* (MRSA) is a prime example of a bacterial species resistant to many drugs. This is a strain of *S. aureus*, resistant to penicillin-derived antibiotics such as methicillin, as the name suggests. In the mid-1980s, fluoroquinolone antimicrobial agents such as ciprofloxacin inhibited MRSA at < 2 μg/mL, and the threat of MRSA appeared as though it was being eradicated. However, this was not the case. It was later shown that less than 20% of MRSA was inhibited by any of the commercially available fluoroquinolone antibiotics (Neu, 1992). This example highlights the need for the discovery of newer hit and lead compounds for the development of antibiotics to fight the problem of antibiotic resistance.

1.1. Quinolines

The quinoline skeleton (**Figure 1.1**) has attracted attention due to it being present in a variety of bioactive synthetic and natural products. Quinolines consist of a benzene ring fused to a pyridine ring and are particularly attractive for use in drug discovery due to their relatively high chemical stability, low toxicity and aromaticity (Bindu et al., 2014).
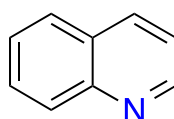
Figure 1.1 The quinoline skeleton

There are many naturally occurring compounds containing the quinoline moiety that are either used as lead compounds for the development of new more potent drugs or are already on the market as pharmaceutical drugs (Kumar et al., 2009). An example of this is quinine (**1.1**), isolated from the bark of the cinchona tree, and used in the treatment of malaria (Kumar et al., 2009). This discovery prompted the development of more potent drugs such as chloroquine, primaquine and mefloquine (**1.2–1.4**) (**Figure 1.2**) (Kumar et al., 2009).

| Quinine | Chloroquine | Primaquine | Mefloquine |
| **1.1** | **1.2** | **1.3** | **1.4** |
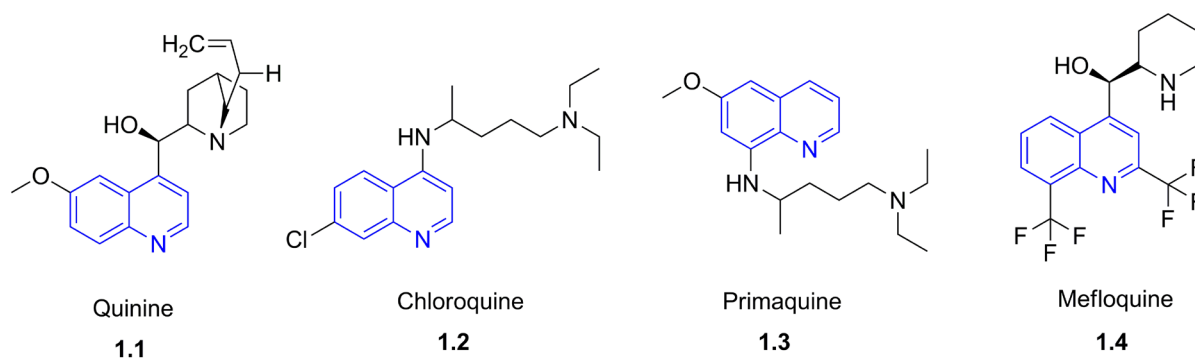
Figure 1.2 Various biologically active compounds that contain a quinoline moiety

1.1.1. Bioactivity

The quinoline core has many biological applications, amongst which is antimalarial (Kaur et al., 2010), antidepressant (Kumar et al., 2011) and antibacterial (Manjunatha et al., 2012) activity. Quinolines and their oxo-derivatives, specifically 3-substituted quinoline-2-ones (**1.5**) (**Figure 1.3**) (Sahu et al., 2002; Egan, 2006), have been of particular interest in cancer research, as they are good lead molecules for KDR kinase inhibition (Fraley et al., 2002).
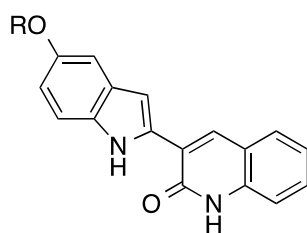
1.5

Figure 1.3 Quinoline-2-one based compound with antitumour properties

A volatile alkaloid quinoline-4-carbonitrile (**1.6**) (**Figure 1.4**) was isolated from a floral extract of *Quisqalis indica*. A catalytic reduction converted it to quinoline-4-methylamine, which has subsequently shown enhanced bioactivities. Both the isolated compound, quinoline-4-carbonitrile, and floral extract have shown potential antioxidant and anti-inflammatory properties (Rout et al., 2019). This enhanced antioxidant activity was thought to be due to synergistic interactions amongst phenolics (10.1%) and quinoline-4-carbonitrile (19.7%) in the essential oil (Rout et al., 2019).
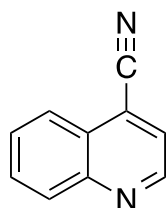
1.6

Figure 1.4 The chemical structure of quinoline-4-carbonitrile

Nine previously undescribed carbazole and quinoline alkaloids, and 14 known derivatives, were isolated from the leaves and stems of *Clausena dunniana*. One of the compounds, 4-methoxyfuro[2,3-b]quinoline (**1.7**) (**Figure 1.5**) was shown to have good anti-inflammatory activity when evaluated in nitric oxide inhibitory assays, with an IC_{50} value of 60.4 μM. This activity was just six-fold lower than dexamethasone, the standard, which had an IC_{50} value of 10.7 μM (Cao et al., 2018). This work provided a scientific basis for the plant's reported use in traditional medicine as an anti-inflammatory agent.
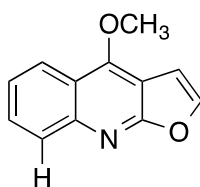
1.7

Figure 1.5 The chemical structure of 4-methoxyfuro[2,3-*b*]quinoline

A series of quinoline hybrids bearing bioactive pharmacophores were synthesised to identify possible hits for antibiotics. While most quinoline hybrids showed a narrow spectrum of activity in inhibiting only Gram-negative bacteria, compounds **1.8** and **1.12** (**Figure 1.6**) showed approximately 25% of the activity of the standard levofloxacin against *E. coli*, with MIC values of 25 μg/mL each. Additionally, **1.9** and **1.11** demonstrated broad-spectrum activity. Structure-activity relationship studies showed that methyl and ethyl groups substituted on the thidiazole moiety showed enhanced activity against both Gram-negative and Gram-positive bacteria in comparison to their non-methylated analogues, and the other quinoline hybrids synthesised (Rizk et al., 2019).

1.8: R = H
1.9: R = CH₃
1.10: R = Br

1.11: R₁ = CH₃
1.12: R₁ = C₂H₅
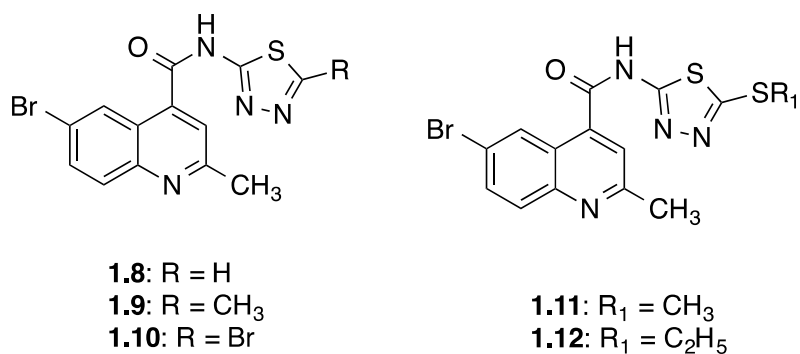
Figure 1.6 Quinoline-carboxamide-thidiazole conjugate molecules with antibacterial activity

Malaria is also treated using a variety of quinoline based compounds, the most well-known of which being chloroquine, although there are many other quinoline based compounds in use or under development (**Figure 1.2** and **Figure 1.7**). These compounds are particularly successful as they act during the blood stages of the parasite's life cycle, although some act during the hepatic stages as well (Baird and Reickmann, 2003).

1.13 Hydroxychloroquine

1.14 Tafenoquine
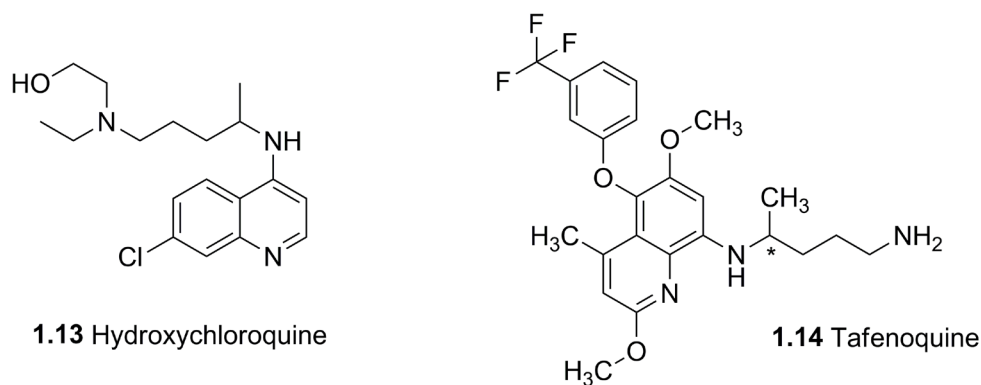
Figure 1.7 Promising antimalarial quinolines currently in use

Fluoroquinolones are the largest class of quinolone antibiotics, and are generally broad-spectrum drugs (effective against Gram-negative and Gram-positive bacteria). One of the most widely used antibiotics worldwide is ciprofloxacin (**Figure 1.8**), patented in 1980 and introduced in 1987 (Alapi and Fischer, 2006). It has an MIC₉₀ of ≤1 µg/L against all species of *Enterobacteriaceae* and most *Haemophilus* species, including *β*-lactamase negative and

positive strains (Campoli-Richards et al., 1988). Other examples of fluoroquinolones include levofloxacin, a broad-spectrum antibiotic usually prescribed with antipyretics (Shinozaki et al., 2019) and also used with rifampin to treat joint infections (Meléndez-Carmona et al., 2019), and ofloxacin, a broad-spectrum antibiotic, used primarily to treat urinary tract infections (Onyango et al., 2018) and simple skin and soft tissue infections (Pavithra et al., 2018).

Figure 1.8 Structures of popular fluorinated quinolones: ofloxacin (**1.15**) and ciprofloxacin (**1.16**)

1.1.2. Synthesis

A variety of traditional methods are used to synthesise quinolines. Among them are the Skraup, Doebner−von Miller, Friedländer, Pfitzinger, Conrad−Limpach, Combes and Vilsmeier-Haack syntheses (Sriramurthy and Kwon, 2010). Most of these make use of anilines or acetanilides and carbonyl compounds and can be synthesised in a single step. Variety is introduced by using different anilines, acetanilides or carbonyl compounds in the synthesis.

The Skraup reaction is well-established and involves the dehydrogenation of glycerol to form the highly reactive acrolein, which further condenses with aniline to form the quinoline (**Scheme 1.1**). In general, a variety of quinolines may be synthesised using the Skraup reaction depending on the substituents on the aniline. Jin et al. (2017) synthesised quinolines by a continuous flow Skraup reaction with quinoline selectivity of between 41–57%. (Jin et al., 2017).

Scheme 1.1 Skraup reaction for the synthesis of quinoline

Closely related to the Skraup synthesis is the Doebner-Miller reaction, which also uses an aromatic amine and proceeds through the formation of dihydroquinoline. In this synthesis, aniline and two molecules of aldehyde are heated in the presence of hydrochloric acid to form a Schiff base. Thereafter, two molecules of this Schiff base self-condense and form the quinoline nucleus (Cheeseman, 1960) (**Scheme 1.2**). The mechanism for the Doebner-Miller reaction is under debate, although the most commonly accepted mechanism is shown in **Scheme 1.3** (Li, 2014). This is a popular synthetic method used to synthesise quinolines, however low yields are sometimes reported due to by-products forming. Nevertheless, this method is popularly used since it results in a 2-methyl group being placed on the quinoline framework. This methyl group can be oxidised to the aldhehyde, creating a site where conjugation can take place on the quinoline scaffold. Leir (1977) found that by adding an equimolar amount of zinc chloride to the reaction mixture, all of the basic products precipitated out as a brown, curdy solid.
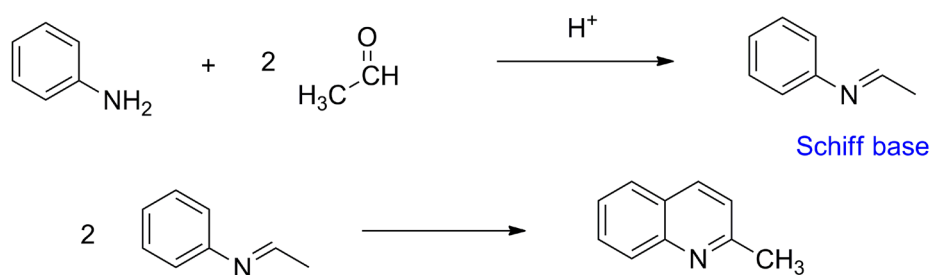
Scheme 1.2 Doebner-Miller synthesis of quinaldine

7
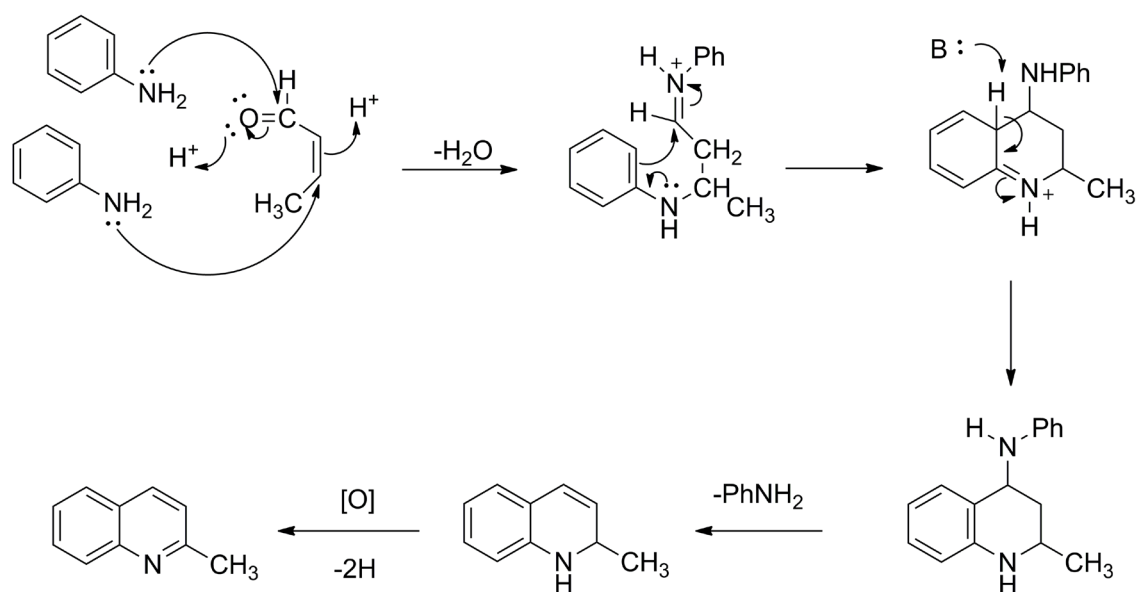
Scheme 1.3 The accepted Doebner-Miller mechanism

The Friedlander synthesis occurs between an *ortho* aminobenzaldehyde or *ortho* amino phenylketone and carbonyl compound with a reactive methylene group (**Scheme 1.4**). The reaction can either be acid or base catalysed and involves a condensation reaction, followed by cyclodehydration (Li, 2014).
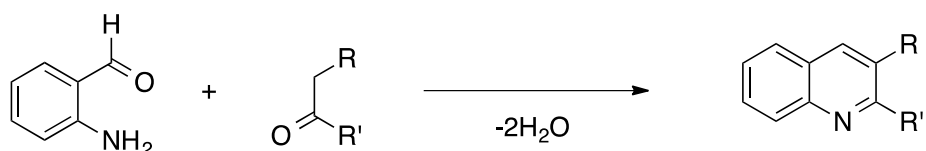
Scheme 1.4 The Friedlander synthesis of quinolines

The Combes synthesis forms 2,4-substituted quinolines and occurs by the condensation of aniline with β-diketones in the presence of an acid catalyst (**Scheme 1.5**) (Aribi et al., 2016).
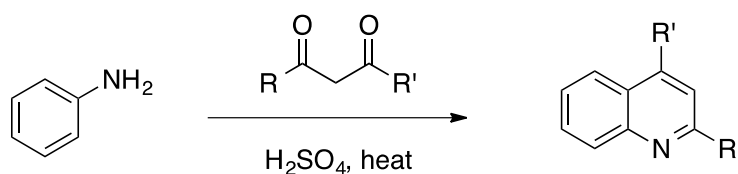
Scheme 1.5 Combes quinoline synthesis

The Vilsmeier-Haack reaction (**Scheme 1.6**) makes use of DMF, in aqueous solution, with an acid chloride to synthesise an aryl aldehyde from an electron rich aromatic ring. First, an iminium salt, fittingly named the "Vilsmeier reagent", is formed by the reaction of DMF with the acid chloride, which reacts with the electron rich aromatic ring thereby losing aromaticity. Aromaticity is restored during a deprotonation step, followed by the formation of another iminium intermediate by the loss of a chloride ion. The iminium intermediate then hydrolyses to form the final products during aqueous work-up (Vilsmeier et al., 1927). Ali et al. (2001) used the Vilsmeier-Haack reaction to successfully cyclise acetanilides in micellar media (**Scheme 1.7**). The mechanism of the Vilsmeier-Haack reaction to synthesise quinolines is shown in Govender (2018).
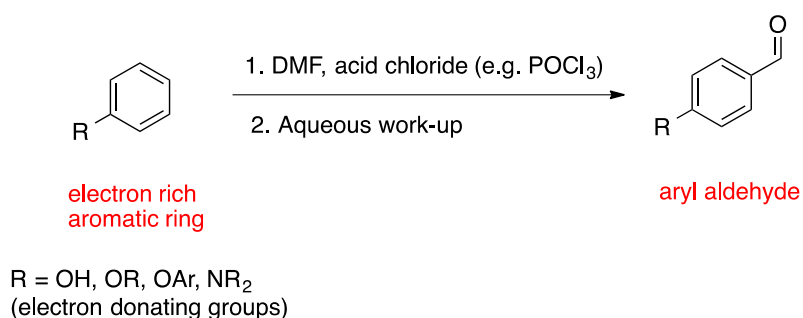
Scheme 1.6 General Vilsmeier-Haack reaction
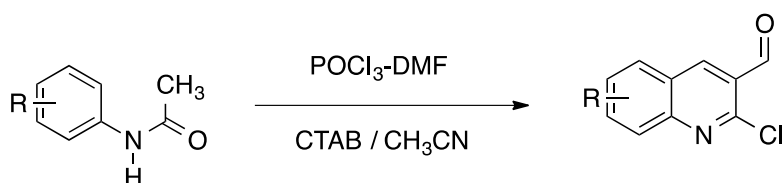
Scheme 1.7 Formation of quinolines by the Vilsmeier-Haack reaction in micellar media

Although commonly used, the reactions described previously in this chapter often take place in harsh conditions, either using a strong acid or base, or at high temperatures (Kouznetsov et al., 2005; Madapa et al., 2008). In addition, the Friedlander synthesis in particular is limited due to the instability of coupling partners (Kouznetsov et al., 2005; Madapa et al., 2008; Marco-Contelles et al., 2009), since the self-condensation of both coupling partners can lead to side-products and lower the reaction efficiency (Vander Mierde et al., 2008).

The Skraup reaction, although well-established, is relatively under-exploited and usually makes use of harsh or toxic reagents, for example concentrated sulfuric acid, nitrobenzene and a variety of metal salts and strong antioxidants (Wang et al., 2010). Jin et al. (2017) described an improved Skraup synthesis of both mono- and bis-quinolines, from commercially available solketal (a protected form of glycerol), using niobium phosphate (NbP) as a catalyst, which plays three important roles in the synthesis, namely deprotection, dehydration and annulation (**Scheme 1.8**) (Jin et al., 2017).
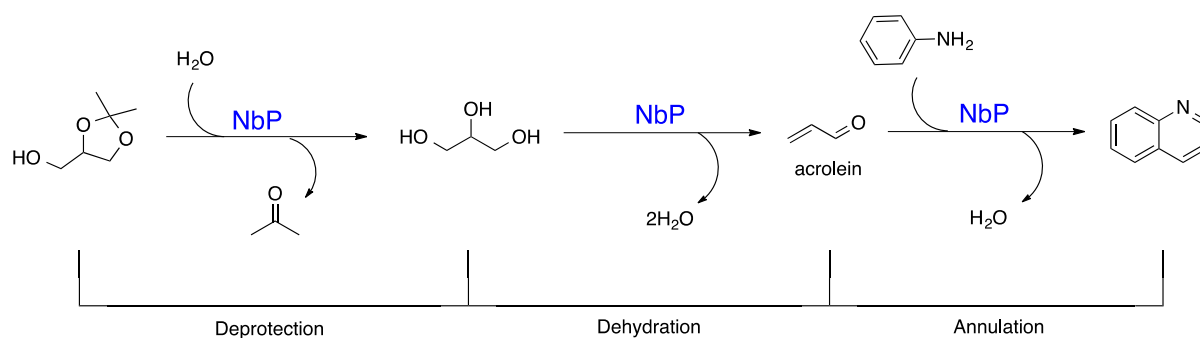
Scheme 1.8 Improved Skraup synthesis of quinolines using a niobium phosphate catalyst

Among other methods, a one-pot double-Michael reaction has been developed as an improved method for the synthesis of 3-substituted quinolines. By replacing one pro-nucleophilic group with an electrophilic group, and by the presence of an *N*-tosyl group in the substrate, the pro-

nucelophilic group was activated and self-condensation was completely inhibited (**Scheme 1.9**) (Khong and Kwon, 2012).
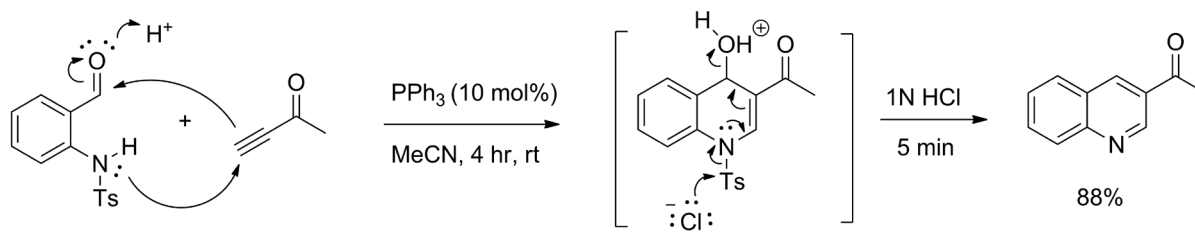
Scheme 1.9 One-pot phosphine-catalyzed synthesis of quinoline

In the last few years, 1,3-disubstituted imidazo [1,5-a]-quinolines have received increasing attention for their strong fluorescence, as they can be used as fluorescence probes (Shen et al., 2018, Song et al., 2018) or as cell imaging reagents (Volpi et al., 2018). As such, many new methods to synthesise these quinolines have been developed. One such synthetic method involves a solvent-free microwave-assisted synthesis, where activated MnO_2 is used as an oxidant, starting from the relevant ketones and amines (**Scheme 1.10**) (Herr et al., 2019).
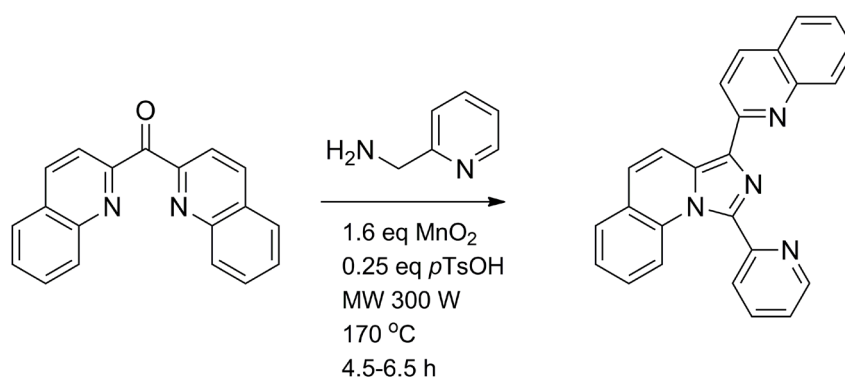
Scheme 1.10 Synthetic scheme showing the formation of 1,3-disubstituted imidazo [1,5-a]-quinoline

In the search for more efficient solvent-free synthetic methods, the last few years have seen a huge interest in catalytic synthetic methods. Zeolites have also been reportedly used for their

synthesis (Brosius et al., 2006; López-Sanz et al.,2010). Guo et al. (2016) developed a method using arylamines and aldehydes over a mesoporous MCM-41/Cp$_2$ZrCl$_2$ material to synthesise substituted alkylquinolines in yields of 29–81%. Grigor'eva et al. (2019) investigated the activity and selectivity of various crystalline and amorphous aluminosilicates, as well as an ASM mesoporous aluminosilicate, in the synthesis of 2-ethyl-3-methylquinoline, via the reaction of aniline with propionic aldehyde (**Scheme 1.11**).

This reaction produced two main products namely 2-ethyl-3-methylquinoline and 2-ethyl-3-methyl-*N*-phenyl-1,2,3,4-tetrahydroquinoline-4-amine, as well as minor products *N*-propylaniline, condensation products of propionic aldehyde and 2,3-dialkyldihydroquinoline. They found that the catalysts H-Beta and H-MOR, with a crystallinity of close to 100% and specific surface area of 625 and 393 m^2/g respectively, produced the best results with 99% conversion of aniline each (Grigor'eva et al., 2019).
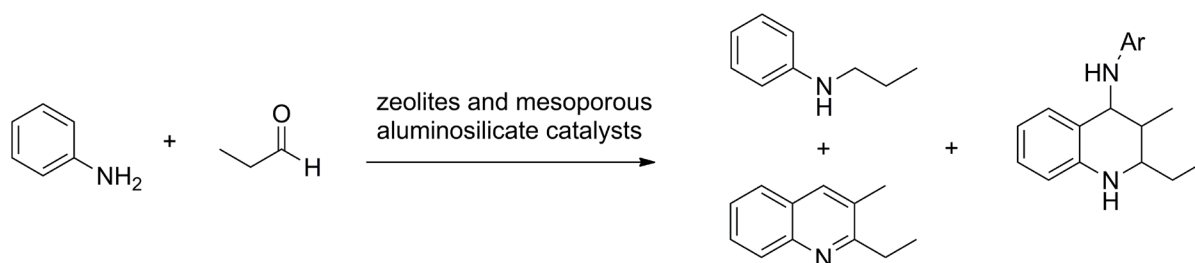
Scheme 1.11 Synthetic route to 2-ethyl-3-methylquinoline with zeolites and mesoporous aluminosilicate catalysts

To introduce aryl groups onto quinolines, (benzo[h]quinoline-10-yl)methanol was reacted with various arylboronic acids, in the presence of 7 mol% (PPh$_3$)$_3$RhCl catalyst and 1 equivalent of CuCl in xylene (**Scheme 1.12**). The advantage to this method is that the reaction is environmentally friendly, since it reduces waste associated with separation and purification (Yu et al., 2016).
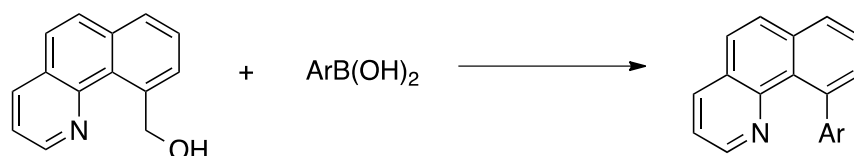
Scheme 1.12 Synthetic scheme to aryl quinolines

In an effort to develop a series of quinoline-benzothiazole conjugate molecules as potential anticancer compounds, Bindu et al. (2019) developed a four-stage synthetic route using a range of substituted acetoacetanilides with eco-friendly *p*-TSA as a catalyst (**Scheme 1.13**). The final products, *N*-(benzo[d]thiazol-2-yl)-2-hydroxyquinoline-4-carboxamides were produced in good yields of up to 96%.
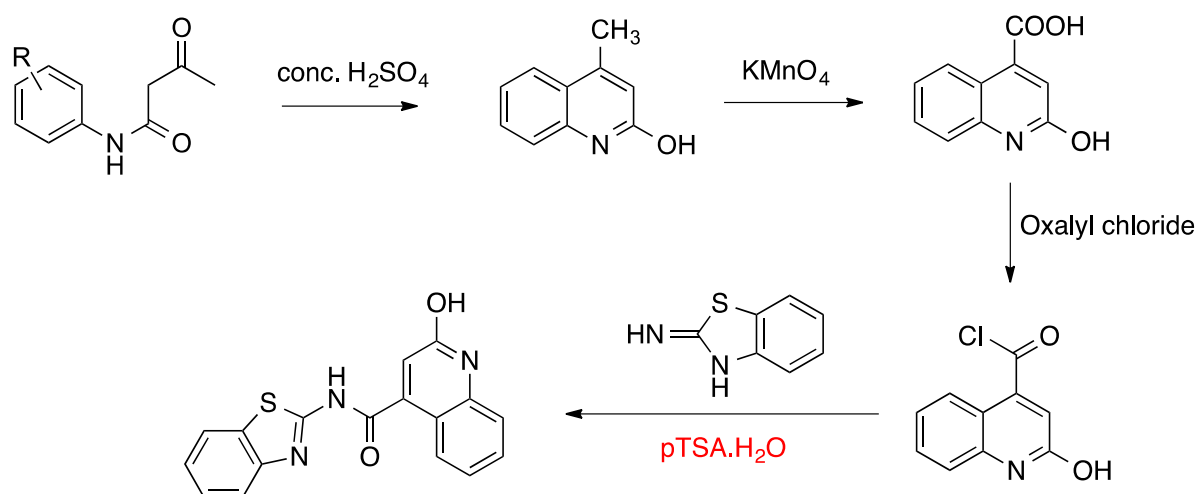
Scheme 1.13 Synthesis of *N*-(benzo[d]thiazol-2-yl)-2-hydroxyquinoline-4-carboxamides

A heterogeneous ionic organic solid catalyst (IOS), 1,3-bis(carboxymethyl)-imidazolium chloride (bcmim-Cl), was used in the coupling of 2-aminophenyl carbonyl compounds with ketones for the synthesis of quinolines (**Scheme 1.14**). It was hypothesised that the functionalised salt, bcmim-Cl, can favour the reaction in the absence of a solvent. Catalysed reactions produced yields of 72% as opposed to 10% for the uncatalysed reactions. This

reaction occurs at temperatures of 100 °C and fivefold the amount of ketone (Gisbert et al., 2019).

Scheme 1.14 Quinolines synthesised by an ionic organic catalyst (bcmim-Cl)

In addition to the large number of by-products formed using traditional methods for some of the quinaldine syntheses, they are generally not environmentally friendly. Safari et al. (2009) developed a greener method for the synthesis of quinaldine derivatives under microwave irradiation using no solvent, and hydrochloric acid as a catalyst (**Scheme 1.15**). This increased yields, shortened reaction times and provided a green alternative method.
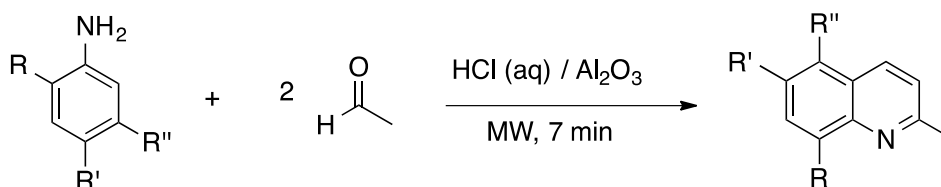
Scheme 1.15 Green, microwave-assisted substituted-quinaldine synthesis

Tetrahydrocurcumin and zingerone are biologically active molecules that originate from turmeric and ginger respectively. Manjunatha et al. (2012) proposed a method of synthesising quinoline derivatives from these two naturally occurring molecules. The reaction proceeded by adding either 2-aminoacetophenone, 2-aminobenzophenone or a substituted 2-aminobenzophenone to tetrahydrocurcumin or zingerone (**Scheme 1.16**). The reaction occurred with a TFA catalyst at 100°C and formed between 30 and 120 minutes in good yields of between 56–90% (Manjunatha et al., 2012).

14
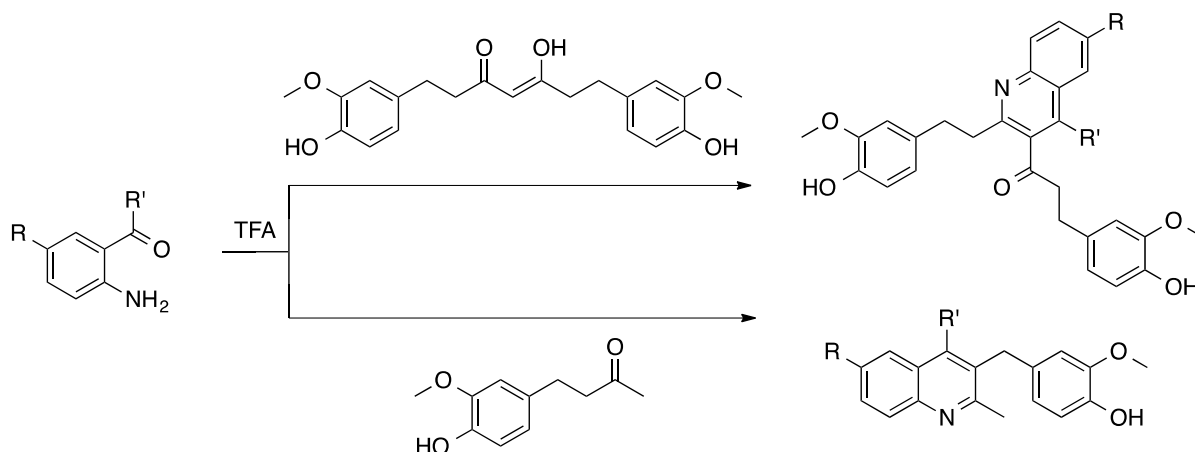
Scheme 1.16 Quinoline synthesis from tetrahydrocurcumin and zingerone

1.2. Chalcones

Chalcones are α,β-unsaturated ketones with two aromatic benzene rings (**Figure 1.9**). Their ketovinyl moiety is very reactive and contributes significantly to its pharmacological activity. A prominent class of secondary metabolites, chalcones are also precursors of flavonoids, and exhibit a wide range of biological activity including anticancer (Rao et al., 2004), anti-inflammatory (Ko et al., 2003) and anti-invasive (Parmar et al., 2003).

Trans (E)   *Cis (Z)*
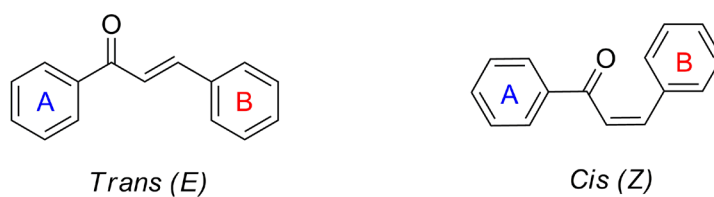
Figure 1.9 The two configurations of chalcone

1.2.1. Bioactivity

The substitution patterns on the two aromatic rings of chalcones was shown to influence its bioactivity. For example, by introducing 2,5-dichlorothiophene to the basic skeleton of chalcones (**1.17** in **Figure 1.10**), broad-spectrum antibacterials were synthesised (Tomar et al., 2007). On the other hand, chalcones that contain heterocyclic alkyl *para* substituents such as

1.18 (**Figure 1.10**), exhibit a narrow spectrum of antibacterial activity, being only effective against Gram-positive bacteria (Nowakowska et al., 2008).
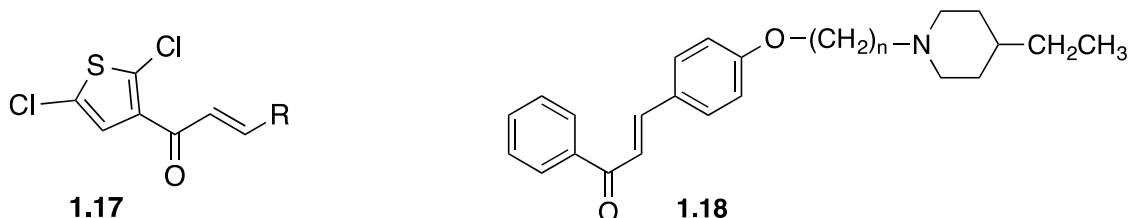
Figure 1.10 Antibacterial chalcones with dichlorothiophene and heterocyclic alkyl side chains

To investigate the structure-activity relationship of chalcones, Ávila et al. (2008) synthesised a library of oxygenated and prenylated chalcones (**Figure 1.11**) and tested them against standard antibacterial strains. It was found that a 2'-hydroxyl group, a highly common feature of naturally occurring chalcones, was present in every active compound, and most likely stabilizes the molecule through hydrogen bonding. They also found that an isoprenyl group on ring B does not lead to increased activity. Overall, it was concluded that a certain level of lipophilicity was required for activity (Ávila et al., 2008).

The chalcone with a 2-hydroxy-5-halo substitution pattern on the A ring (**1.22**) (**Figure 1.12**) was found to have the best antifungal activity against *C. albicans*, and chalcone **1.23** with a *para* fluorinated aromatic group (**Figure 1.12**) was shown to be the best hit compound, with broad-spectrum activity against *C. parapsilosis*, *C. krusei*, *C. glabrata*, *C. tropicalis*, *C. neoformans* and *Rhodotorula mucilaginosa*. This was a significant finding, since some of the strains have increased resistance to azole drugs. In addition, the most active compounds were found to be non-toxic (Bonvicini et al., 2019).
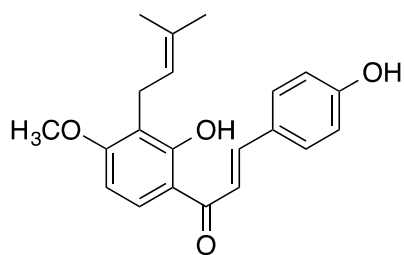
1.19: 4-hydroxyderricin

B. cereus: MIC = 3.9 μg/mL
S. aureus: MIC = 7.8 μg/mL
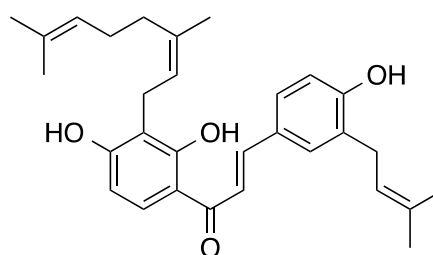
1.20: 2',4,4'-trihydroxy-3-prenyl-3'-geranylchalcone

B. cereus: MIC = 15.6 μg/mL
S. aureus: MIC = 31.2 μg/mL
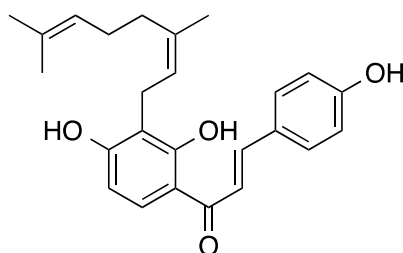
1.21: 2',4,4'-trihydroxy-3'-geranylchalcone

B. cereus: MIC = 15.6 μg/mL
S. aureus: MIC = 31.2 μg/mL

Figure 1.11 The three most active compounds used in antibacterial structure-activity relationship study
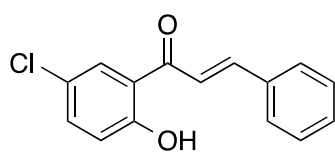
1.22
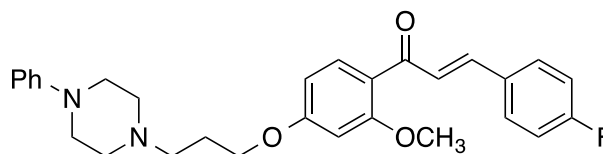
1.23

Figure 1.12 Halogen substituted antifungal chalcones, including those with *O*-alkylpiperizinyl side chains

17

According to a review by Sulzipio et al. (2018), some of the most biologically successful metal chalcone complexes contain either manganese, ruthenium (high antifungal affinity), cobalt, nickel, copper (although many are cytotoxic), zinc, gallium or tellurium (high antibacterial affinity) (Sulzipio et al., 2018). For example, thiosemicarbazone ligands (**1.24**, **Figure 1.13**) possessing chalcone moieties showed better antibacterial activity, typically by about 50%, upon zinc (II) complexation. Their antifungal properties were, however, strongly compromised (Da Silva et al., 2013).
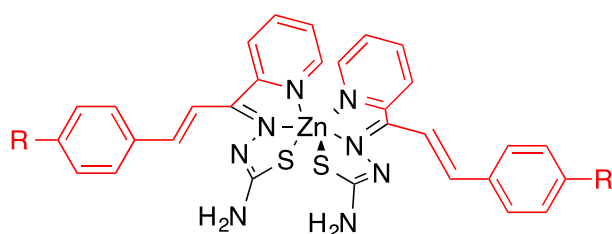
1.24

Figure 1.13 Chalcone-zinc complex

Chalcones with a 2,4,6-trihydroxy substitution pattern were found to be non-toxic, whereas a 2-hydroxy-4,6-dimethoxy substitution pattern was found to be toxic and to suppress cell proliferation (Choi et al., 2018). Zenger et al. (2015) also showed that hydroxyl groups on the A ring reduce toxicity, and that methoxy groups increase antiproliferative activity. Choi also found that the substituents on the B ring did not affect activity (Choi et al., 2018). Furthermore, they found that only high concentrations of chalcones in the presence of Bone Morphogenetic Protein 2 (BMP-2), a type of protein involved in inducing osteogenesis of stem cells, brought about significant osteogenesis of C2C12 cells. Interestingly, 2,4,6,4'-tetrahydroxychalcone **(1.25)** (**Figure 1.14**) inhibited the growth of S*treptococcus mutans*, a major causative agent of dental caries (Choi et al., 2018).

1.25
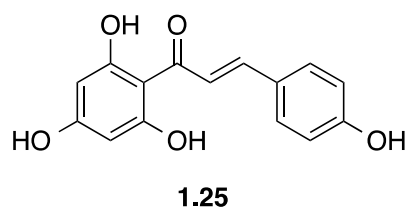
Figure 1.14 The structure of 2,4,6,4'-tetrahydroxychalcone

Dihydrotriazine groups joined to chalcones by an *O*-alkylated linker (**1.26–1.27**) (**Figure 1.15**) were found to down-regulate expression of iNOS (nitric oxide synthase, an enzyme that catalyses NO production) and COX-2 (an enzyme inhibitor) in LPS-stimulated RAW 264.7 cells, and to inhibit nitric oxide secretion, dependent on the dosage (Gan et al., 2018). Additionally, concentrations between 5–20 µM of the two compounds were non-toxic. The triazine alone demonstrated negligible anti-inflammatory effects on RAW 264.7 cells and human monocytes, suggesting that the chalcone pharmacophore in the molecule is responsible for their anti-invasive and anti-inflammatory activities (Gan et al., 2018).

Triazine pharmacophore

1.26

1.27
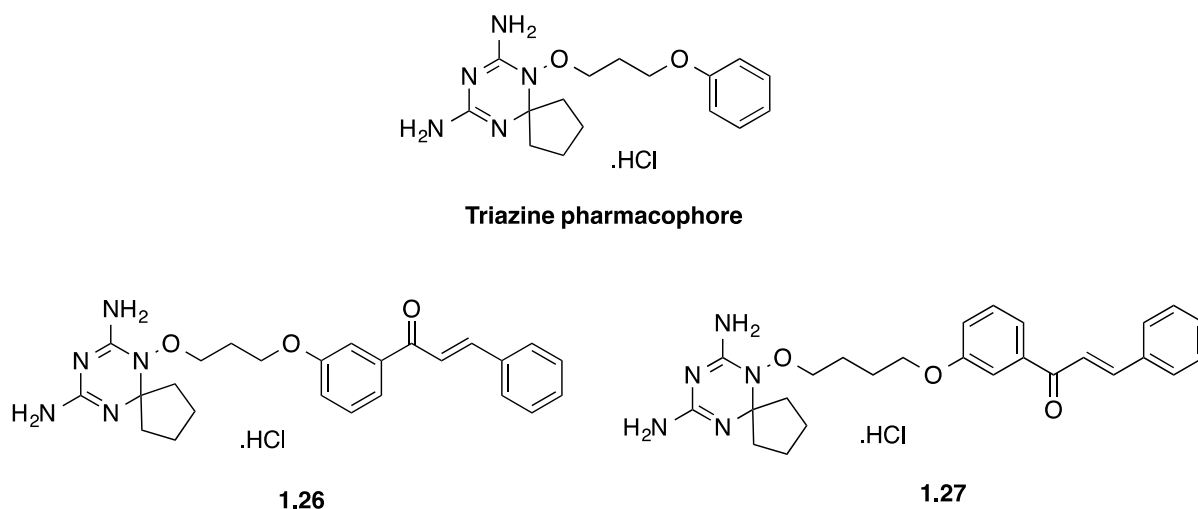
Figure 1.15 Chalcones linked to triazines via an *O*-alkylated linker

Millepachine (MIL) (**1.28**) (**Figure 1.16**) is a natural chalcone found in the Chinese herbal medicine, *Millettia pachycarpa* Benth. It was found to have a strong antitumor effect against

numerous human cancer cells, both *in vitro* and *in vivo* (Wu et al., 2013). MIL was found to inhibit the proliferation of cisplatin-sensitive and cisplatin-resistant ovarian cancer cells, whereas the classic chemotherapeutic agent cisplatin (**1.29**) (**Figure 1.16**) inhibited the proliferation of cisplatin-sensitive cells, and only exhibited 30% inhibition of cisplatin-resistant cells, at a concentration of 20 μM (Wu et al., 2018).
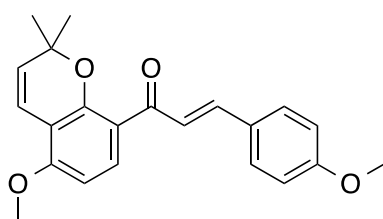
Millepachine (MIL)
1.28

Cisplatin-sensitive cells: IC$_{50}$ = 4 μM

Cisplatin-resistant cells: IC$_{50}$ = 4 μM
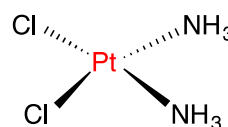
cis-diamminedichloridoplatinum(II) (CDDP)
1.29

Cisplatin-sensitive cells: IC$_{50}$ = 2.5 μM

Cisplatin-resistant cells: 30% inhibition (concentration = 20 μM)

Figure 1.16 Millepachine, a natural chalcone (**1.28**) and CDDP, a commonly used chemotherapeutic agent (**1.29**)

1.2.2. Synthesis

The Claisen-Schmidt condensation is a useful reaction in the formation of chalcones, and usually occurs between an aldehyde or ketone possessing an α-hydrogen, with an aromatic carbonyl compound lacking an α-hydrogen. This reaction is successful due to the formation of the very reactive enolate anion, which attacks an activated carbonyl group, forming the aldol intermediate (**Scheme 1.17**). This hydroxy group is eliminated after enolization, via an E1cB mechanism. Hydroxy groups are normally not good leaving groups; however, they are on this occasion, due to the highly conjugated nature of the chalcone. Since the hydroxyl group is eliminated from the final intermediate in a unimolecular reaction, and since the final

intermediate is a conjugate base of the aldol, the reaction is referred to as an E1cB reaction (cB = conjugate base).
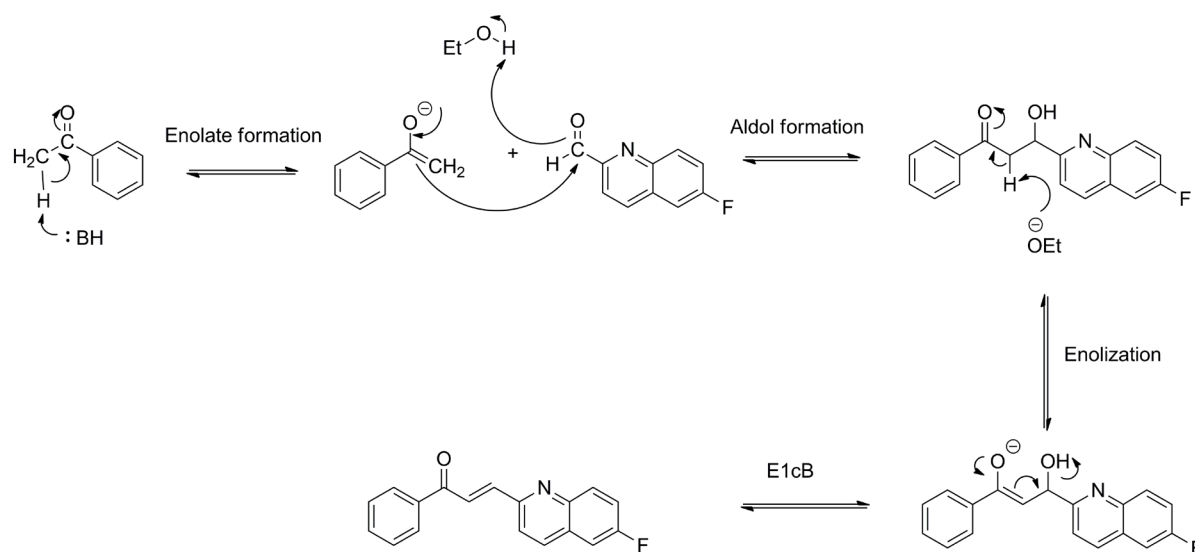
Scheme 1.17 Mechanism of chalcone formation with quinoline-2-carbaldehydes and acetophenones

More recently, furanochalcones were reported to be synthesised from their 1-[6-(trifluoromethyl)benzofuran-2-yl]ethanone and benzaldehyde precursors in basic media with high yields being reported (**Scheme 1.18**) (El Shehry et al., 2019).
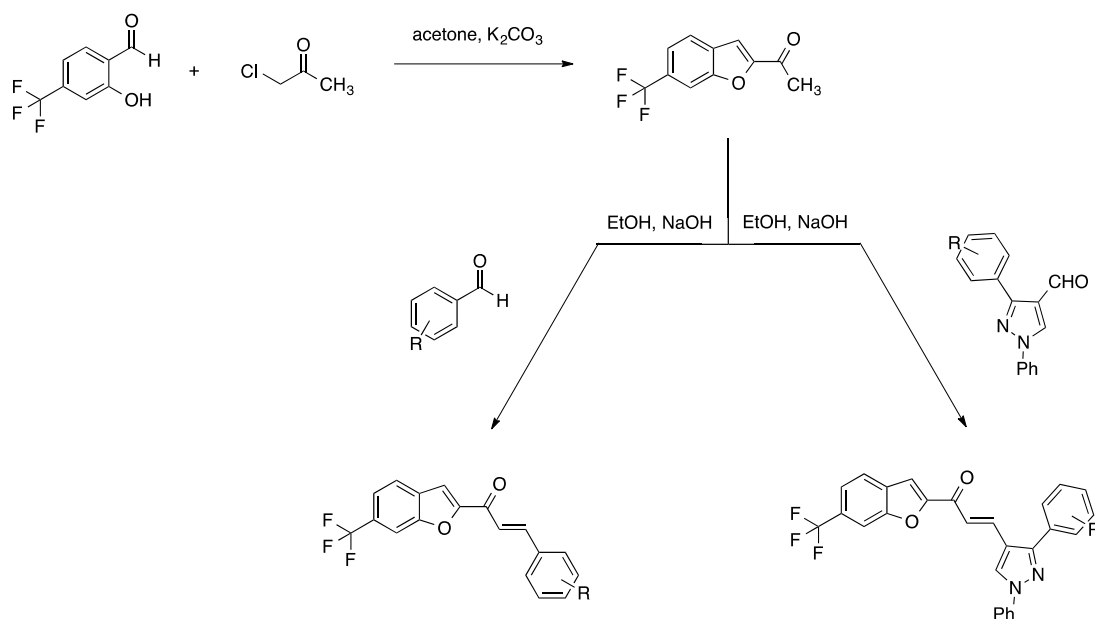
Scheme 1.18 Synthetic scheme producing furanochalcones

21

Although the Claisen-Schmidt condensation is the most common and widely used method for the synthesis of chalcones, some alternative synthetic methods have appeared in recent years (Wu et al., 2019; Tang et al., 2019). Most recent work focused on synthesising chalcones, and then hybridising and derivatising them to develop bioactive leads (Ahmad et al., 2017; Dave and Rahatgaonkar, 2011). There is also a growing effort to make synthetic procedures greener by using heterogeneous catalysts to replace traditional strong acid/alkali homogeneous catalysts (Tang et al., 2019).

Tang et al. (2019) developed a green method for the preparation of chalcones, using a fluorinated 4-dimethylaminopyridine (DMAP) catalyst. Thereafter, the benzaldehyde and acetophenone precursors are added and heated. Although this reaction is greener, the catalyst is quite expensive. They also used a hydrotalcite catalyst in an ionic liquid, consisting of an imidazolium salt of 1,3-dibutyl-2-methyltetrafluoroborate. This allowed the reaction to be carried out at a high temperature before adding the benzaldehyde and acetophenone precursors. The reactions reached completion within 2-4 hours. Although this method is highly efficient, the ionic liquid is very expensive.

In addition, Tang et al. (2019) have also used metal oxides such as MgO, MnO_2 and Y_2O_3 to prepare chalcones by an oxidative condensation. The metal oxide catalyses the reaction between an acetophenone and benzaldehyde in a pressure bottle, producing the chalcone. The disadvantage of this method is that the reaction time is long, and the conversion rate of ketone low. They also used a hydroxyapatite-loaded potassium fluoride catalyst with the respective acetophenones and benzaldehydes in ethanol or water. The reaction is carried out in a reactor. A major problem with this reaction is that the catalyst flows too easily. Yields greater than 85%

are achieved, presenting promising alternatives to the traditional Claisen-Schmidt condensation.

Although heterogeneous catalysis in the formation of chalcones is largely accepted as an improved, greener method, there are still drawbacks. For example, in strong basic conditions, there is poor selectivity to chalcones due to the heterogeneous nature of the catalyst. As such, there have been few efforts to improve the selectivity of chalcones using acid catalysts, however they remain largely under-reported (Shylesh et al., 2007).

One such method is described by Xu et al. (2008), who reported a synthesis of chalcones using a novel catalyst – solid sulfonic acid from bamboo. In their work-up, they tested various catalysts for their efficacy in the Claisen-Schmidt reaction, among which were Amberlyst-15, sulfuric acid, boric acid, sodium bicarbonate and citric acid, which produced chalcones in yields of between 18–82%. Bamboo char sulfonic acid, however, afforded a 94% yield, with no side products detected by GC analysis. The selectivity of the reaction avoided the need for separation and purification, making it a greener method. Interestingly, they found that electron donor groups in the benzaldehyde precursor decreased the yields of **1.30** and **1.31** (**Figure 1.17**). In contrast, electron donor groups in the acetophenone precursor increased yields. Impressively, their catalyst was re-used three times, with no decrease in the selectivity of the chalcone (Xu et al., 2008).
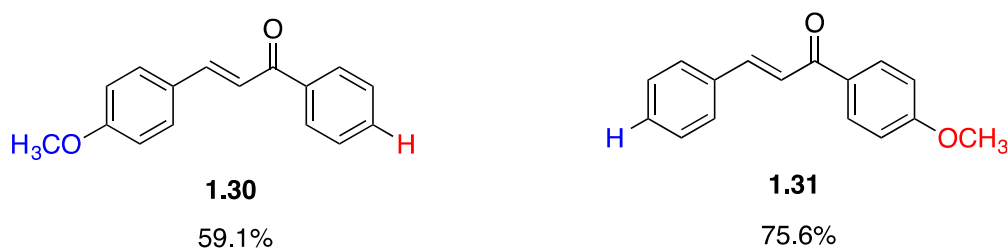
Figure 1.17 Chemical structures of methoxy chalcones **1.30** and **1.31**

Although the Claisen-Schmidt condensation is by far the most common method for the synthesis of chalcones, coupling reactions such as carbonylative Heck coupling (Wu et al., 2004), Sonogashira isomerization coupling (Takahashi et al., 1980) and Suzuki-Miyaura coupling (Selepe and Van Heerden, 2013) are also prominent. Other methods of synthesising chalcones include the continuous-flow deuteration reaction (Hsieh et al., 2015) and using phenylmethanol with acetophenones (Mahapatra et al., 2015).

In the Heck coupling reaction (**Scheme 1.19**), the phenyl halide undergoes carbonylative vinylation with styrene, using palladium as the catalyst and in the presence of carbon monoxide (Wu et al., 2010).
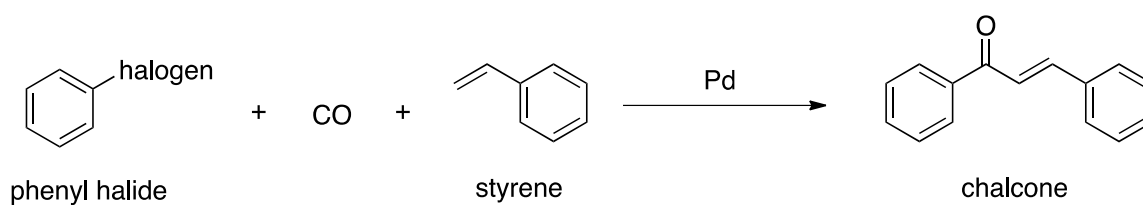
Scheme 1.19 Heck coupling reaction to form chalcones over Pd catalyst

In the Sonogashira coupling reaction, catalysed by $PdCl_2(PPh_3)_2$, equimolecular concentrations of propargyl alcohol and electron-deficient phenyl-halide are used (**Scheme 1.20**) (Takahashi et al., 1980).
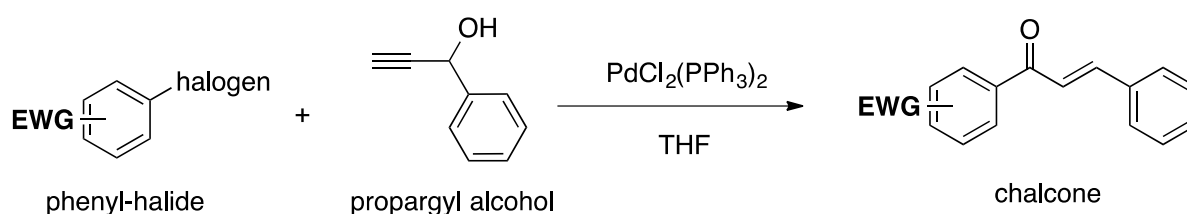
Scheme 1.20 Synthesis of chalcones by the Sonogashira coupling reaction

The Suzuki-Miyaura coupling reaction can take place via two different routes, either coupling styrylboronic acid and benzoyl chloride in the presence of anhydrous toluene, or by coupling cinnamoyl chloride and phenylboronic acid. Both make use of $CsCO_3$ and a $Pd(PPh_3)_4$ catalyst (**Scheme 1.21** and **Scheme 1.22**) (Selepe and Van Heerden, 2013).

benzoyl chloride   styrylboronic acid   chalcone
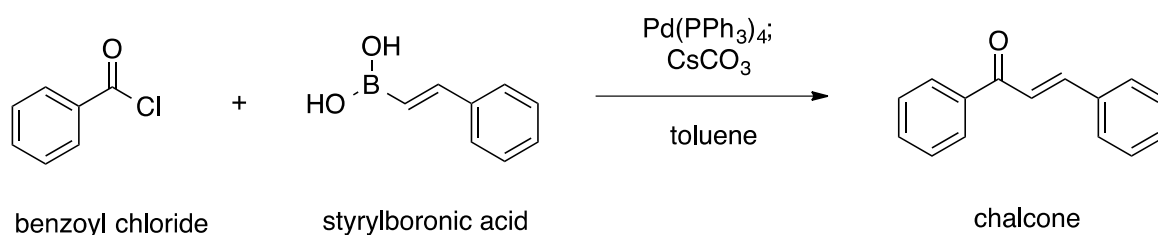
Scheme 1.21 Chalcone formation by coupling styrylboronic acid and benzoyl chloride

phenylboronic acid   cinnamoyl chloride   chalcone
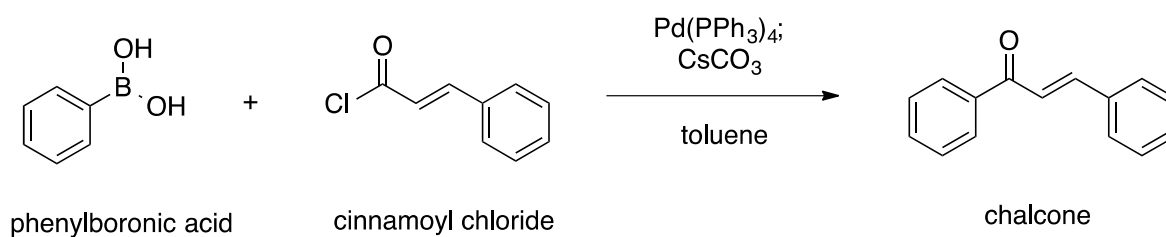
Scheme 1.22 Chalcone formation from phenylboronic acid and cinnamoyl chloride

The continuous-flow deuteration reaction starts using the same conditions as the Sonogashira reaction, with the coupling of phenylacetylenes and benzoyl chlorides to form ynones. Thereafter, deuteration is carried out with an H-Cube® system where a D_2O deuterium source replaces the H_2O hydrogen source (**Scheme 1.23**) (Hsieh et al., 2015).

benzoyl chloride   phenylacetylene   ynone   deuterium-containing chalcone
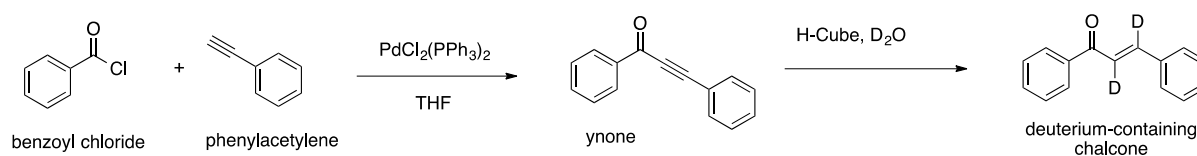
Scheme 1.23 Continuous-flow synthesis of deuterated chalcones

In an alternate synthesis acetophenones are reacted with phenylmethanol with an oxidising agent, CrO$_3$. This forms benzaldehyde in situ and proceeds via a Claisen-Schmidt condensation thereafter (**Scheme 1.24**) (Mahapatra et al., 2015).

| acetophenone | phenylmethanol | | chalcone |
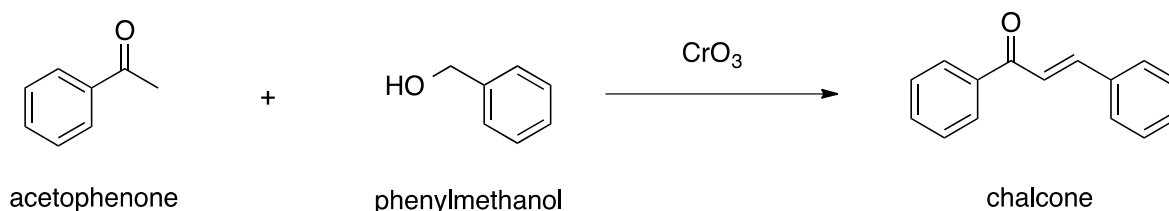
Scheme 1.24 One-pot, efficient and green synthesis of chalcones

1.3. Quinoline chalcone hybrids

The molecular hybridisation approach to forming bioactive molecules has received interest in recent years. It is hypothesised that hybrid molecules containing the structures of both the quinoline and chalcone framework will lead to enhanced bioactivity or activity in more than one bioassay. Both pharmacophores either work alone or in conjunction to augment each other's effects. This is best demonstrated in anti-ulcer studies of quinoline-chalcone hybrids against cold restraint induced gastric ulcer (CRU) models in rats, where the individual quinolines and chalcones did not show significant activity, but the hybrids did, demonstrating the synergy between both core structures (Sashidhara et al., 2015).

1.3.1. Synthesis and bioactivity

Although the synthesis of quinoline-2-chalcones is very uncommon, some novel quinoline-2-one based chalcones have been synthesized and tested for their potential antitumour activity (Abonia et al., 2012). Their synthesis involved a Claisen-Schmidt condensation between the acetophenone and carbaldehyde (**Scheme 1.25**). This method was used to synthesise four

quinoline-chalcone hybrids, where compound **1.32** (**Figure 1.18**), a symmetrical compound,

displayed GI$_{50}$ values ≤1.0 μM for 13 of the 50 cell lines tested (Abonia et al., 2012).
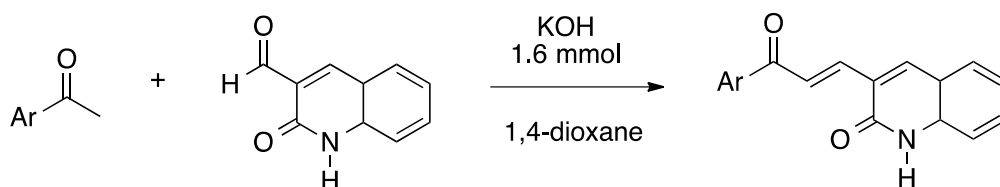
Scheme 1.25 Formation of quinoline chalcones with antitumour activity
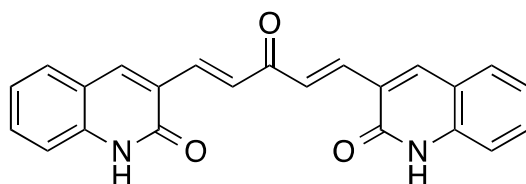
Figure 1.18 Compound **1.32**: 3,3'-((1*E*,4*E*)-3-oxopenta-1,4-diene-1,5-diyl)*bis*(quinolin-2(1*H*)-one) with antitumour activity

A series of quinoline-2-yl chalcone hybrids were also synthesised by the Claisen-Schmidt

condensation between quinoline-2-carbaldehydes and acetophenones (Gopaul and

Koorbanally, 2016) (**Scheme 1.26**). In this synthetic design, the methylquinolines were first

synthesised, oxidised to the aldehyde, and then condensed with various acetophenones. The

quinoline moiety contained a chloro group at C-6 and the acetophenone portion had a variety

of substituents, both electron donating and withdrawing. For the hydroxy quinoline chalcones,

they had proceeded via the *O*-prenylated chalcones and then hydrolysed the *O*-prenyl group to

the hydroxy group using a mixture of BF$_3$Et$_2$O and 1,4-dioxane.
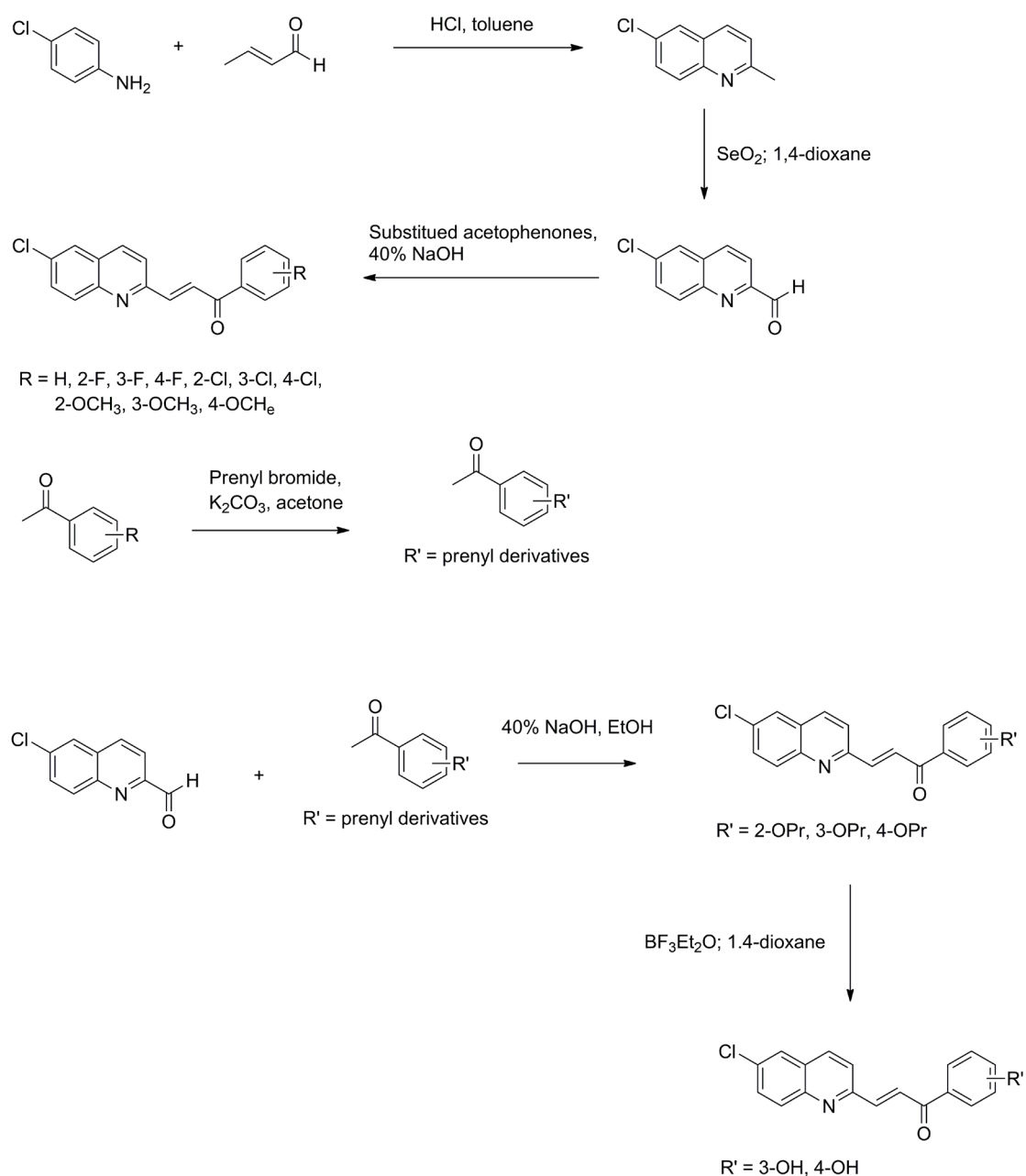
Scheme 1.26 Synthetic scheme to 6-chloroquinoline-chalcone hybrids

Chalcones were also synthesised by tagging on other molecules to it via linkers. A microwave assisted nucleophilic substitution reaction and Williamson etherification were used to join a quinoline to a chalcone at C-8 via an oxygen (**Scheme 1.27**) (Coa et al., 2017). A propyl linker was first linked to the quinoline, which was subsequently linked to the chalcone on the carbonyl side. The Williamson etherification reaction is subject to many side reactions, such as that catalysed by the highly reactive alkoxide ions generated in the reaction. In addition, there is

often competition with the base-catalysed elimination of the alkylating agent (Morrison and Boyd, 1992).
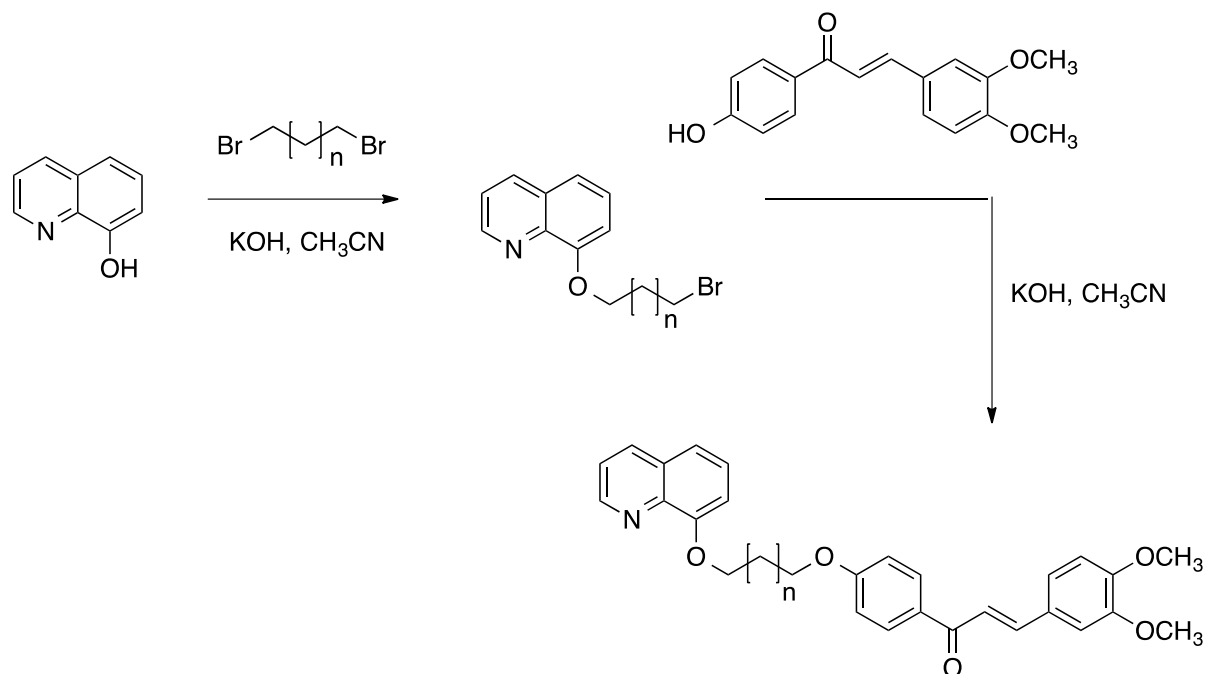
Scheme 1.27 Synthetic pathway to quinoline-chalcone hybrids

Tseng et al. synthesised quinoline-chalcone hybrid molecules in a three step reaction (**Scheme 1.28**), consisting of a thermal decarboxylation of 3-(4-methoxyphenyl)-2-methylquinoline, which was then oxidised to 3-(4-methoxyphenyl)quinoline-2-carbaldehyde using SeO_2, and finally the 2-phenylquinolinylchalcones (**1.33**–**1.42**) were synthesised by a Claisen-Schmidt condensation reaction of the appropriate acetophenone and quinoline-2-carbaldehyde. A basic catalyst was used for all condensation reactions except compound **1.42**, which could only be synthesised using an acid catalyst due to the strong electron-withdrawing effect of the NO_2 group (**Scheme 1.28**) (Tseng et al., 2013).

The chalcone derivative **1.33** (R = 4-H) was very active against both lung and cancer cell lines with IC_{50} values of 1.41 and 0.86 μM respectively. This antiproliferative activity against lung

cancer cell lines was increased by introducing an electron-withdrawing group such as a nitro or fluorine group on the A ring, as compounds **1.34** (R = 4-F) and **1.44** had IC$_{50}$ values of 0.82 and 0.77 μM respectively, compared to the standard topotecan, which had an IC$_{50}$ value of 6.02 μM. On the other hand, electron-donating groups on the A ring were shown to inhibit activity altogether, as compounds **1.35** (R = 4-OH), **1.36** (R = 4-OCH$_3$) and **1.41** (R = 4-NH$_2$) were inactive against all cell lines tested.

1.33: R = 4-H
1.34: R = 4-F
1.35: R = 4-OH
1.36: R = 4-OCH$_3$
1.37: R = 2,4-OCH$_3$
1.38: R = 2,6-OCH$_3$
1.39: R = 3,4-OCH$_3$
1.40: R = 3,5-OCH$_3$
1.41: R = 4-NH$_2$

1.42
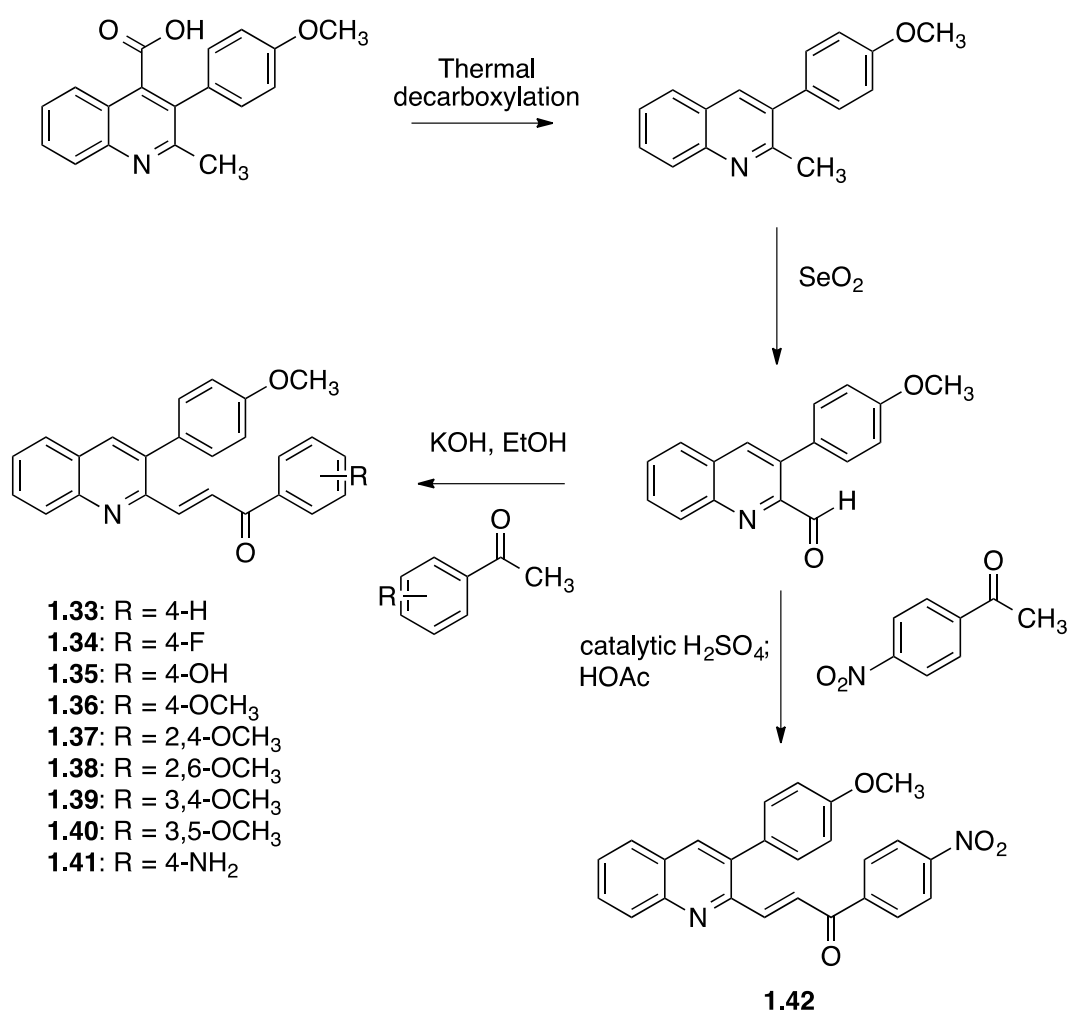
Scheme 1.28 Synthesis of anticancer quinoline chalcone hybrids **1.33–1.42**

Xu et al. (2019) synthesised a library of 30 quinoline chalcone hybrids (**Scheme 1.29**) by first preparing the quinoline intermediates, and then reacting them with MEM

(methoxyethoxymethyl ether)-protected isovanillin derivatives for 2 hours at room temperature in ethanol, with NaOH as the basic catalyst.
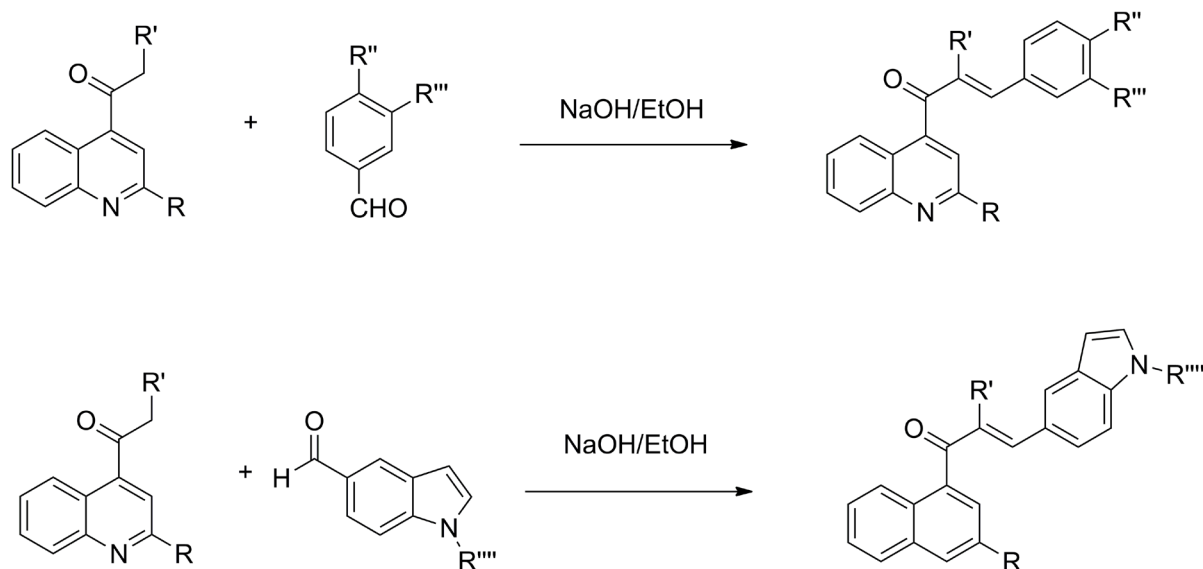
Scheme 1.29 Synthesis of target antiproliferative quinoline chalcones

Among the compounds synthesised, compound **1.43** (**Figure 1.19**) showed the best antiproliferative activity against five human cell cancer lines, with IC_{50} values as low as 15 nM against several cell lines. In addition, all the synthesised compounds showed better tubulin aggregation activity (IC_{50} between 1.78–2.58 μM) than the standard, CA-4 (a microtubule destabilising agent, combretastatin-A4) with an IC_{50} of 2.88 μM (Xu et al., 2019).
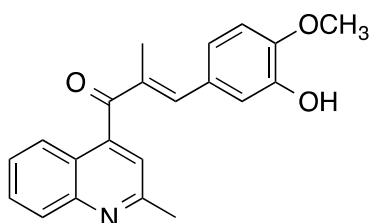
Figure 1.19 The chemical structure of chalcone **1.43**

In similar work, Li et al. (2019) synthesised a range of quinoline-4-chalcones from quinoline-4-ketones and MEM-protected benzaldehydes (**Scheme 1.30**). Compounds **1.44** and **1.45** (**Figure 1.20**) exhibited anticancer activity against four cancer cell lines and produced excellent anticancer activity against human chronic myelogenous leukaemia cell K562 with IC_{50} values of 11 and 9 nM respectively, comparable to that of CA-4 with an IC_{50} value of 11 nM. The activity of these two compounds improved due to the methyl substituent at the α-position of the unsaturated carbonyl group, which agrees with previous reports (Ducki et al., 1998; Yan et al., 2016).
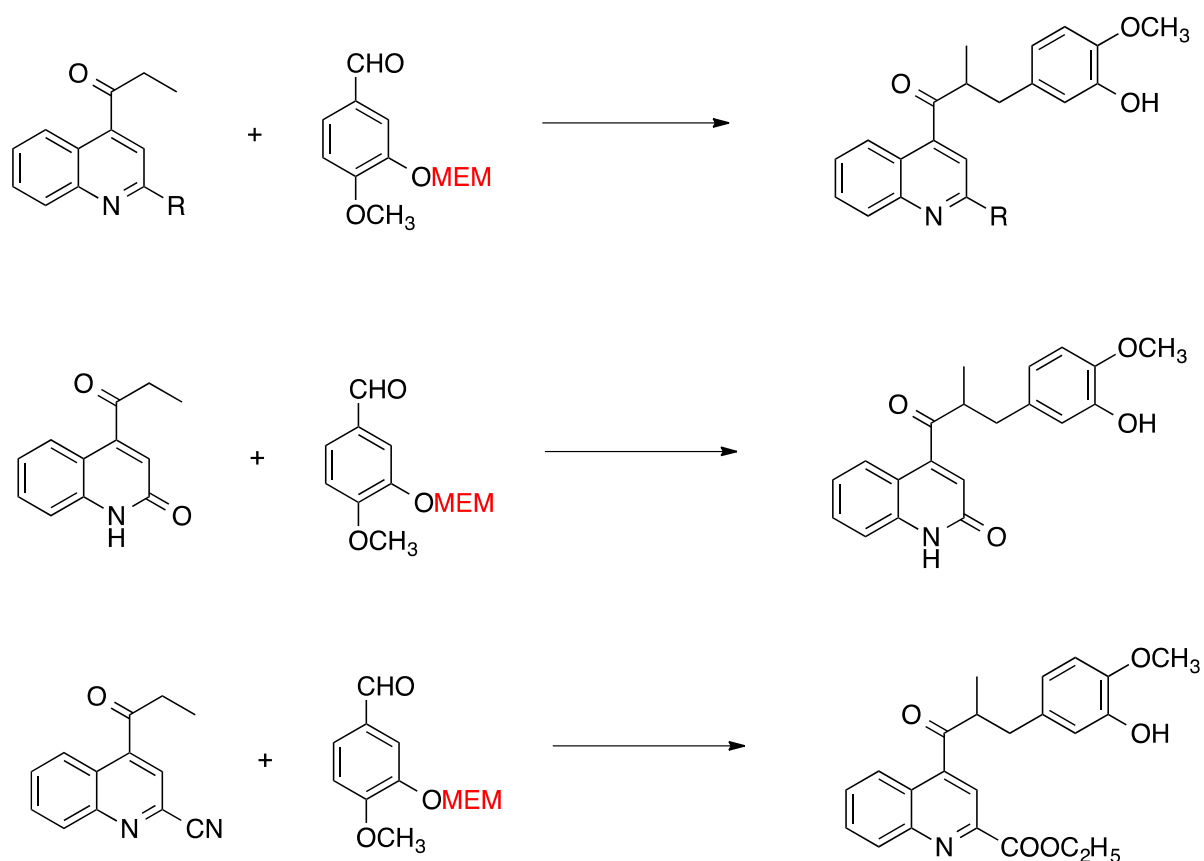
Scheme 1.30 Synthetic pathway to anticancer lead compounds with MEM protection
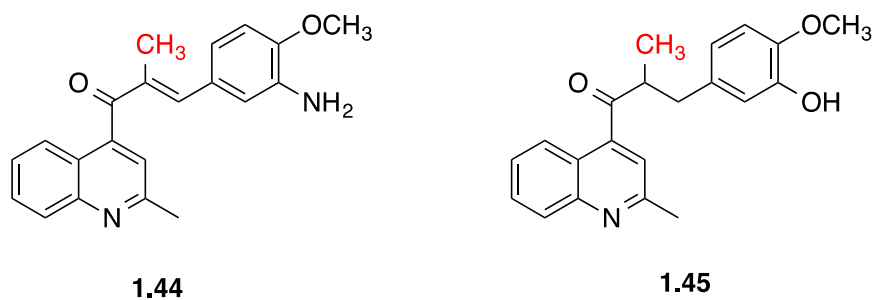
Figure 1.20 Anticancer quinoline-4-chalcones

Sashidhara et al. (2015) synthesised a library of quinoline chalcone hybrids by first attaching a diamine linker to the 4-position, and by subsequently putting a benzaldeyde at the other end of the linker through an imidazole intermediate, before condensing it with various acetophenones (**Scheme 1.31**). The *para* methoxy derivative **1.46** (**Figure 1.21**) of the series was shown to have the best anti-ulcer activity, with 85% protection compared to the control, Sucralfate, which had 65% protection. Interestingly, neither of the individual scaffolds were active as anti-ulcer compounds, but their conjugate molecule was (Sashidhara et al., 2015).
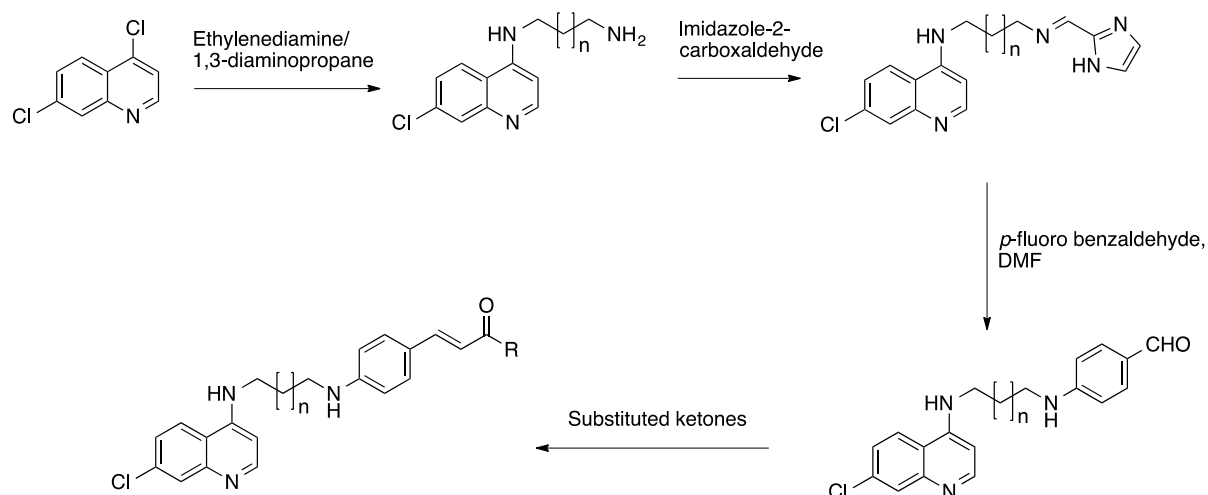
Scheme 1.31 Synthesis of anti-ulcer quinoline chalcones through a diamine linker

33
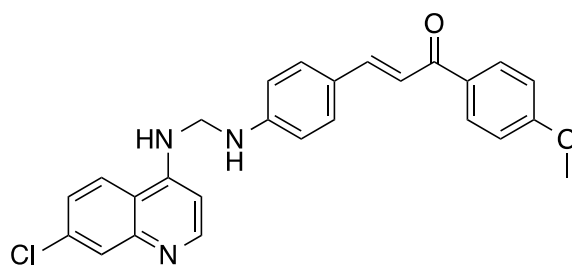
Figure 1.21 The chemical structure of the quinoline hybrid **1.46** with anti-ulcer activity

Ultrasound irradiation is known to produce better yields, shorten reaction times and is a clean process (Cella and Stefani, 2008). Polo et al. (2019) synthesised quinoline-chalcone hybrids (**Scheme 1.32**) by an ultrasound-assisted synthesis of quinoline acetophenone precursors (linked by an amide bond) with various benzaldehydes. The carboxamide intermediate was synthesised from commercially available quinoline-3-carboxylic acid, which was activated by thionyl chloride, forming the acyl chlorides, and condensed with *para*-aminoacetophenone. This ultrasound step produced the conjugate molecules in yields of 53–92% in reaction times as short as 20 minutes. Thionyl chloride was used as a chlorinating agent to convert the acid to the acyl chloride and the sulphur ends up in the by-products, HCl and SO_2. The purpose of the sodium hydrogen carbonate was to remove the acidic hydrogen from the aniline.
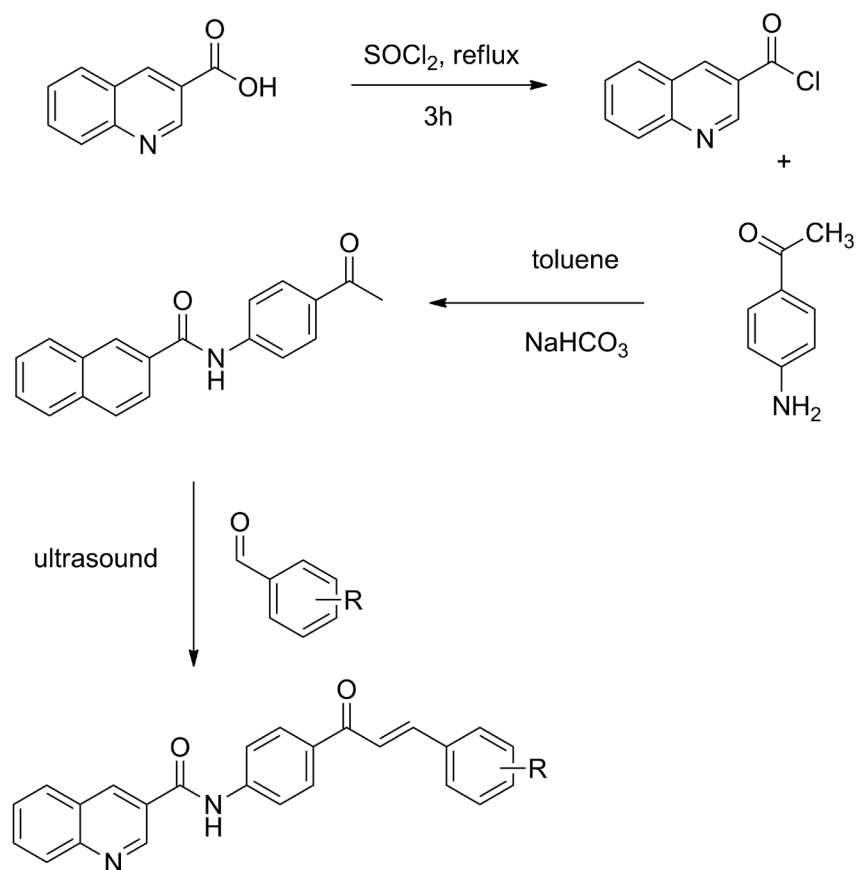
Scheme 1.32 Ultrasound-assisted synthesis of quinoline chalcone hybrids

The synthesised compounds were tested *in vitro* as dual acetylcholinesterase (AChE)-butyrylcholinesterase (BuChE) inhibitors, enzymes responsible for the onset of Alzheimer's disease. Compounds **1.47**–**1.49** (**Figure 1.22**) showed moderate to good activity in inhibiting AChE, with IC_{50} values of 45.3, 7.5 and 12.6 μM respectively. Although galanthamine, a well-known AChE inhibitor was active in the same assay with an IC_{50} of 0.57 μM, these compounds could be considered hits (Polo et al., 2019).
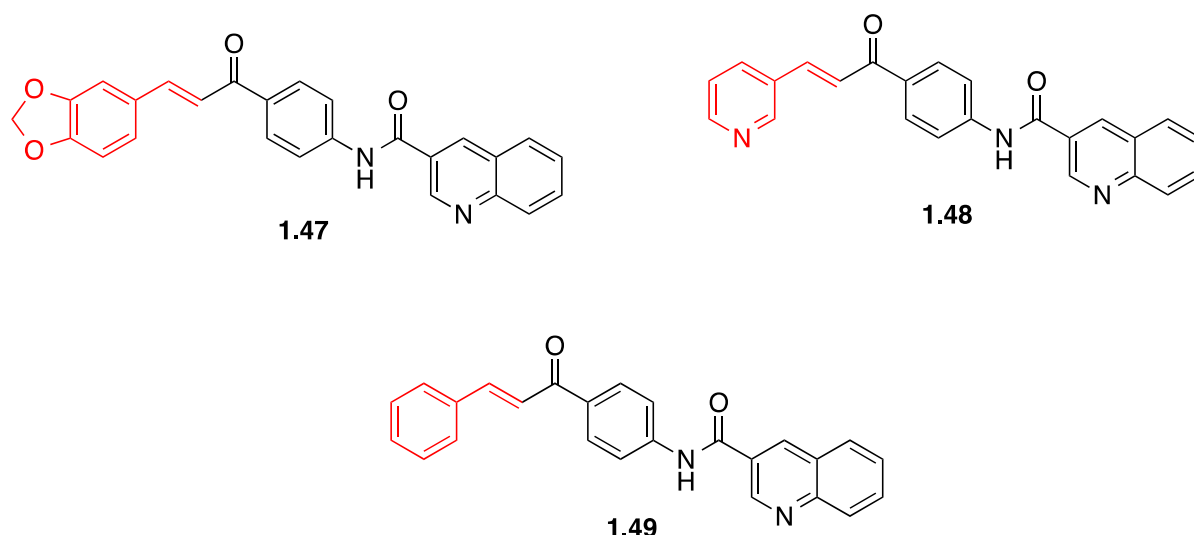
Figure 1.22 Quinoline carboxamide chalcone inhibitors of acetylcholinesterase-butyrylcholinesterase

Another set of quinoline-3-chalcone hybrids were synthesised from quinoline-3-carbaldehydes and commercially available acetyl thiophenes and acetophenones and tested for their dual inhibition of AChE and BuChE (Rizvi et al., 2012; Shah et al., 2018). They were synthesised from aniline precursors, which were acetylated and cyclised in the presence of phosphoryl chloride via the Vilsmeier-Haack reaction to form formyl quinolines that undergo a Claisen-Schmidt condensation, forming quinoline chalcone hybrids (**Scheme 1.33**) (Meth-Cohn et al., 1981).

Most of the compounds were shown to inhibit BChE only and not AChE, thought to be because BChE has a larger active site than AChE, and therefore can accommodate bulky groups attached to both sides of the chalcone (Shah et al., 2018). The most potent compound of the series was **1.50** (**Scheme 1.33**) with an IC_{50} value of 0.56 μM.
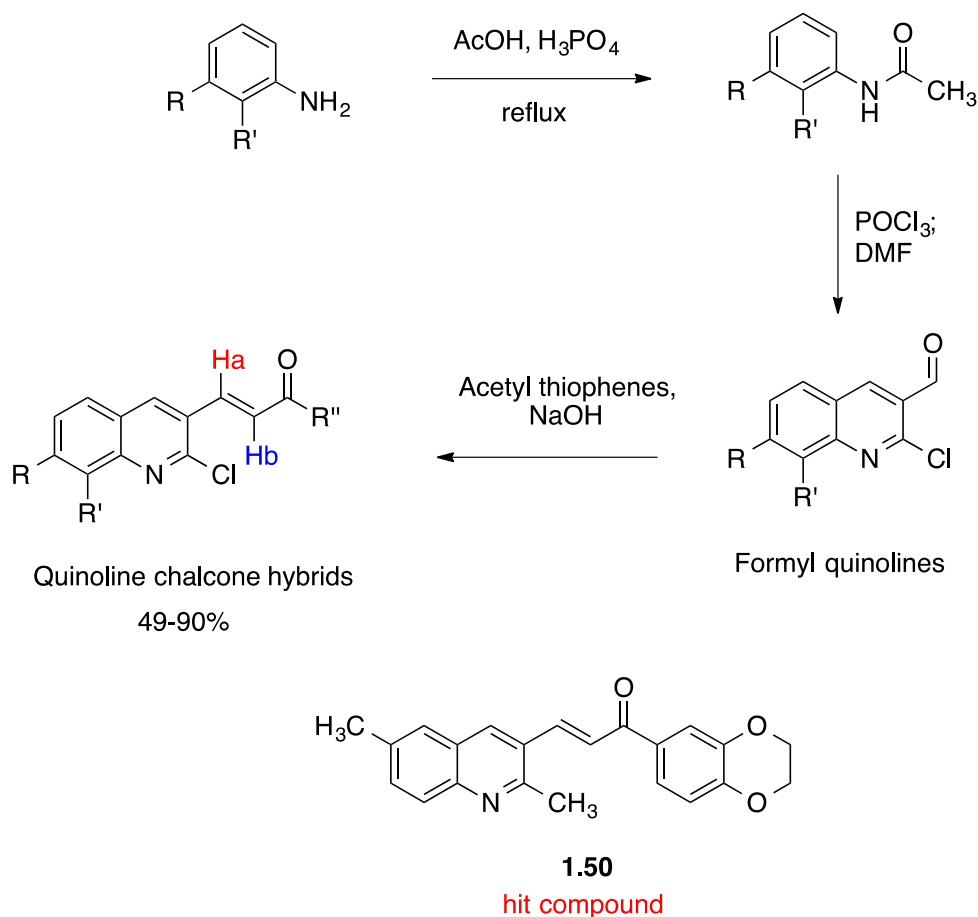
Scheme 1.33 Formation of quinoline chalcone hybrid molecules for AChE and BChE inhibition and hit compound **1.50**

Abbas et al. (2018) synthesised four quinoline chalcones (**Scheme 1.34**) by first forming the chalcones and quinoline-4-carbohydrazides separately and then reacting these two moieties. The chalcones were formed by the normal Claisen-Schmidt condensation, and the quinoline-4-carboxamides from isatin and acetophenones, forming 2-aryl-quinoline-4-carboxylic acids, which then underwent a Fischer esterification to form ethyl esters and then carbohydrazides with hydrazine hydrate.
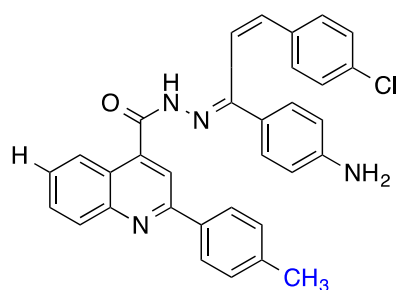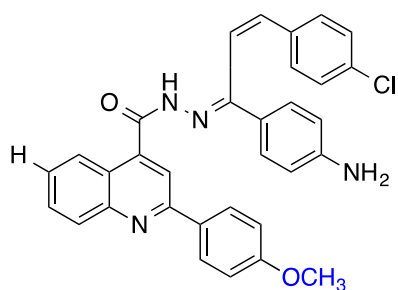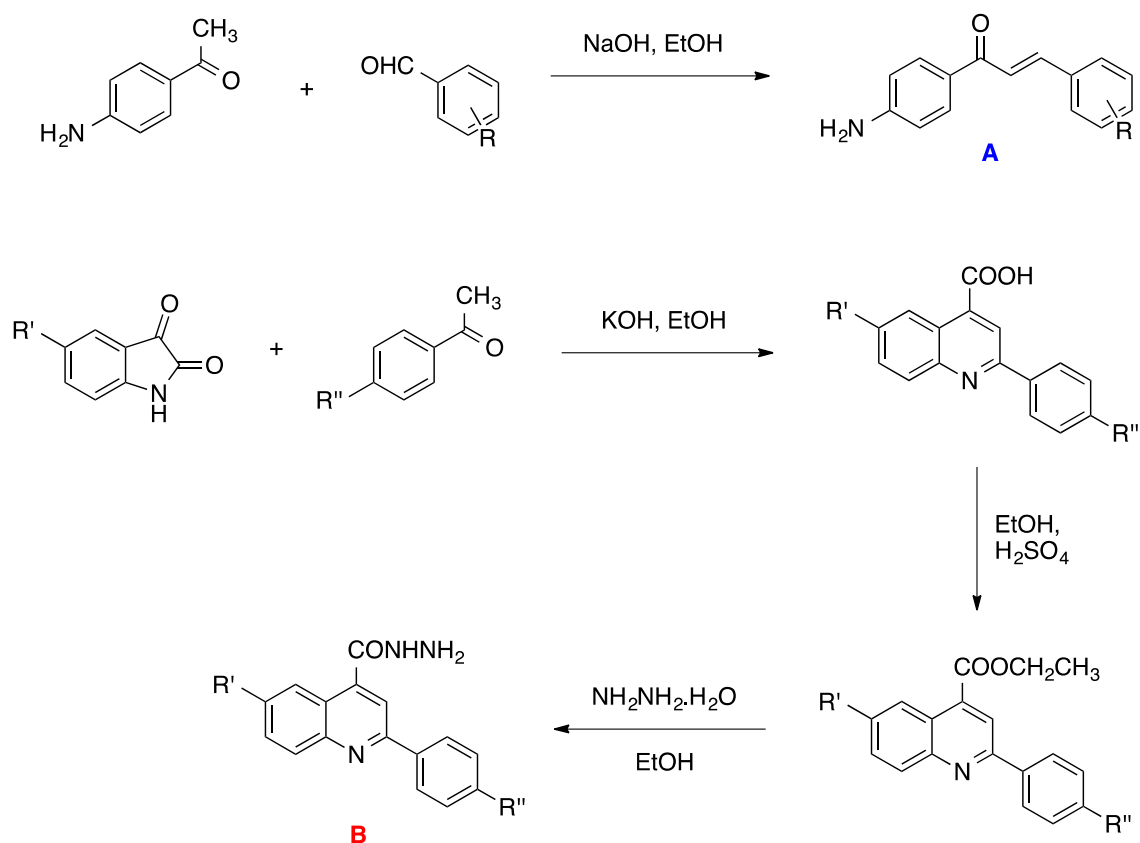
Scheme 1.34 Formation of quinoline chalcone hybrids by Claisen-Schmidt condensation, preparation of intermediates and hit compounds **1.51** and **1.52**

Compounds **1.51** and **1.52** (**Scheme 1.34**) showed good anticancer activity against various human cancer cells with GI$_{50}$ values of 0.3–52 μM. In addition, small cell lung cancer and chronic myeloid leukaemia were both very sensitive to compounds **1.51** and **1.52**, with GI$_{50}$ values of 0.3–6 μM (Abbas et al., 2018).

The Claisen-Schmidt reaction is still the most common and reliable method for the synthesis of chalcones in hybrids, although the use of a basic or acidic catalyst varies dependent on the substituents of the reactants. As such, this methodology was used in the current work.

1.4. Derivatisation of chalcones

As previously mentioned, the ketovinyl moiety of the chalcone is highly reactive and as such, there are many reports in the literature on its derivatization. Chalcone derivatives have shown impressive pharmacological activity, possessing antibacterial, antifungal, antiviral, antiparasitic, anticancer, antileishmanial and antitubercular activity (Crombie and Mistry, 1990).

Chalcones were converted to pyrimidine derivatives using guanidine carbonate in a basic medium (**Scheme 1.35**) (Dave and Rahatgaonkar, 2011). However, none of the compounds showed appreciable activity in antibacterial studies.
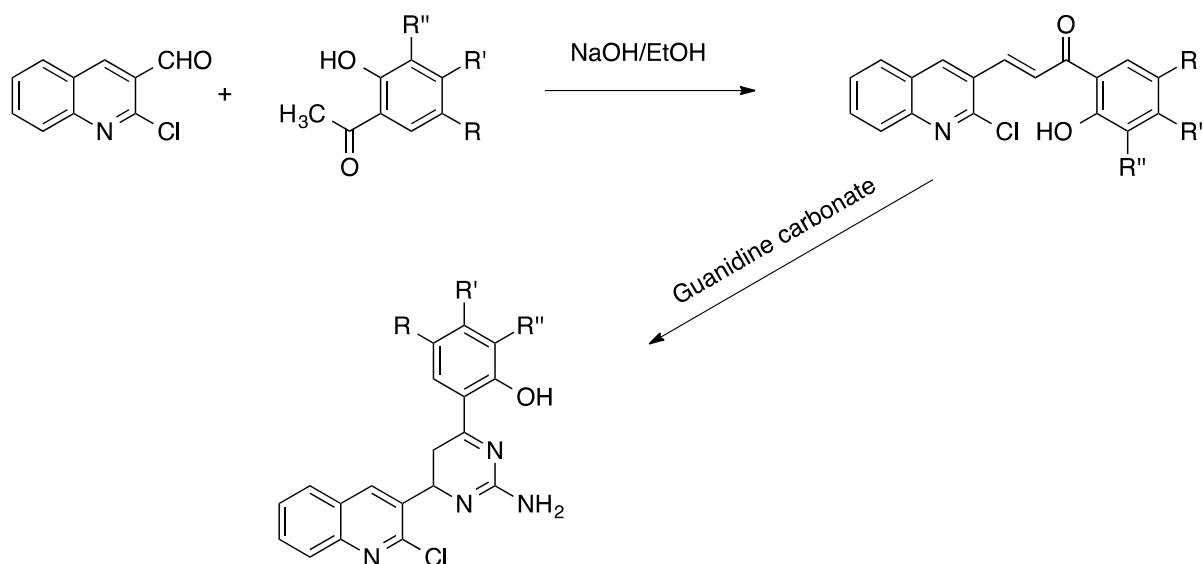
Scheme 1.35 Synthetic route to pyrimidine derivatives via chalcones

Ahmad et al. (2017) performed a number of reactions with the chalcone moiety (**Scheme 1.36**) to form various derivatives to treat *Candida albicans*, a yeast strain. The derivatives showed moderate to good antifungal activity, with the two most active derivatives being **1.56** and **1.57**, with MIC values of 2 μg/mL each for fluconazole susceptible strains, and 8 μg/mL each for fluconazole resistant strains.
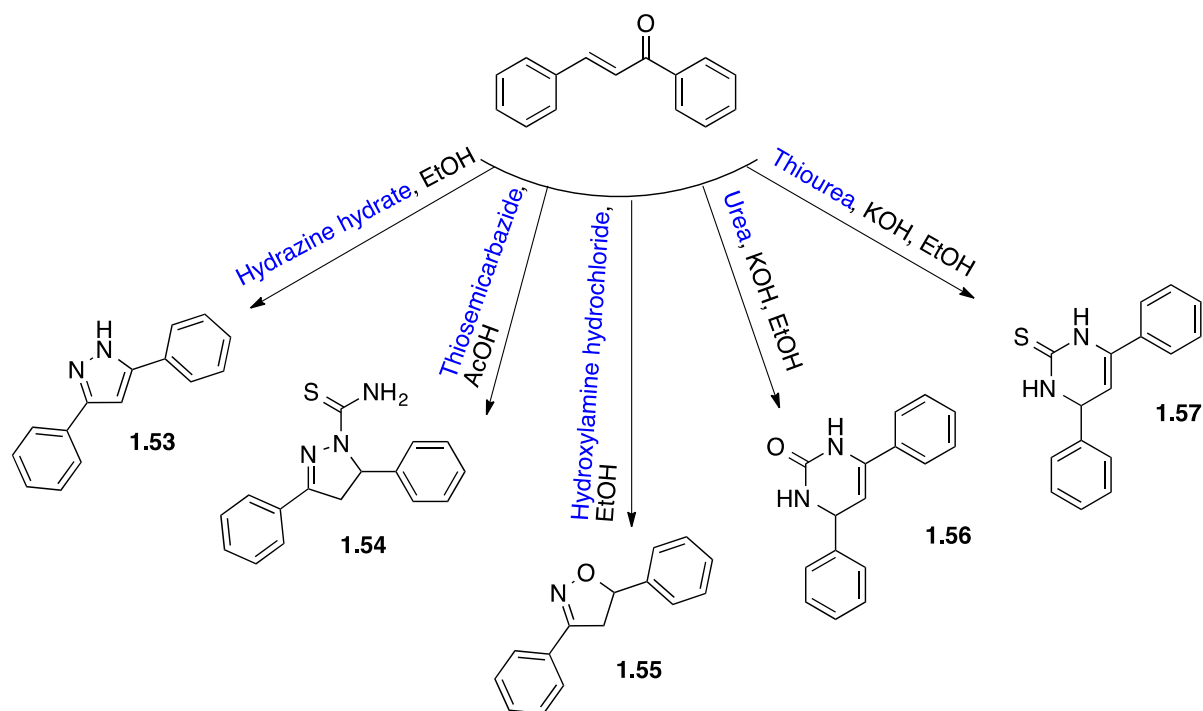
Scheme 1.36 Various reactions used to derivatise the *α,β*-unsaturated moiety

In an effort to produce greener synthetic methods, with no solvents, microwave reactions with chalcones and thiosemicarbazide, phenyl-hydrazine, guanidine hydrochloride and thiourea were carried out to form pyrazoline (**1.58**), pyrazole thioamide (**1.59**), amino pyrimidine (**1.60**) and thiopyrimidine (**1.61**) derivatives respectively (**Scheme 1.37**) (Khan et al., 2019). They showed better antibacterial activity than the parent chalcone, with MICs of between 16–128 µg/mL against *S. aureus* and *S. pyogenes*.
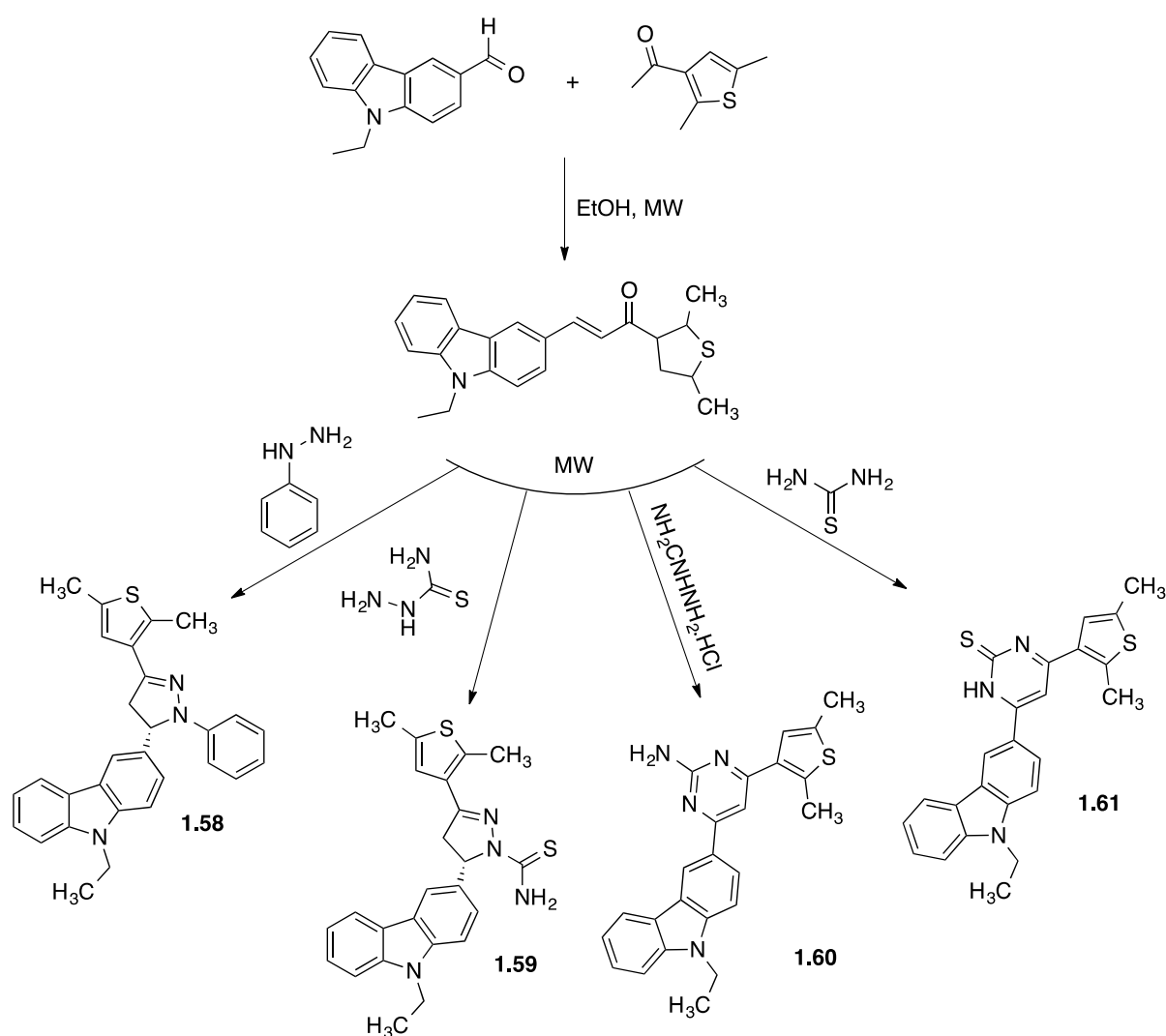
Scheme 1.37 Microwave-assisted synthesis of chalcones and cyclized derivatives

1.5. Fluorinated molecules

Fluorine atoms are known to influence the lipophilicity, electronegativity, basicity and bioavailability of compounds that are of medicinal importance (Harsanyi and Sandford, 2015; Filler and Saha, 2009). Interestingly, introducing a fluorine atom next to a basic group can reduce its basicity. This is important in medicinal compounds where basic groups typically decrease the bioavailability of a drug. The introduction of a fluorine atom does not have significant steric effects on a molecule, since the size of fluorine is very similar to the size of hydrogen, but fluorine can induce significant changes in the conformation of a molecule through electrostatic interactions with other groups (Purser et al., 2008; Dawadi et al., 2015). It is now a well-established strategy to fluorinate bioactive molecules to improve their pharmaceutical effectiveness, biological half-life and bioabsorption (Böhm et al, 2004; Kirk, 2006; Purser et al., 2008).

As such, it is no surprise that some of the most popular and top-performing drugs are fluorinated, including fluoroquinolones such as ofloxacin (**1.15**) and ciprofloxacin (**1.16**), commonly used antibiotics (**Figure 1.8**). Beside the fluoroquinolones, there are many other fluorinated pharmaceuticals on the market today. For example, statins are used in the treatment of hypercholesterolemia. This is a group of 3-hydroxy-3-methylglutaryl CoA (HMG-CoA) reductase inhibitors that are highly effective. In particular rosuvastatin (marketed as Crestor, **1.62**) containing a *para* fluorinated phenyl moiety, was the fourth best-selling drug in 2013 (Ridker et al., 2008; Zhou et al., 2016). Another highly successful drug on the market is fluticasone propionate (**1.63**) (**Figure 1.23**), an oral inhaler, used to treat asthma (Calverley et al., 2007; Zhou et al., 2016). This molecule contains two fluorine atoms on the main scaffold of the drug and another in the thioester side chain.
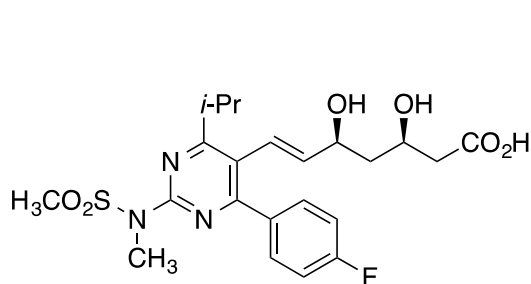
Rosuvastatin (**1.62**)

Treats hypercholesterolemia
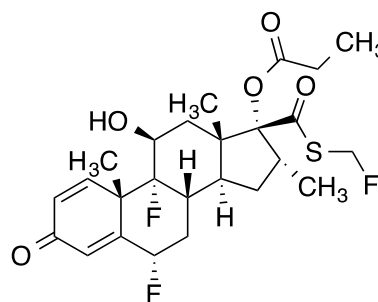
Fluticasone propionate (**1.63**)

Treats asthma

Figure 1.23 Fluorinated molecules for treatment of hypercholesterolemia and asthma

Triple combination therapy is now the standard treatment for HIV, with the most successful combination being that of two fluorinated drugs, emtricitabine (**1.64**) and efavirenz (**1.65**) (**Figure 1.24**), together with tenofovir (marketed as Atripla) (Zhou et al., 2016). These drugs work by inhibiting HIV 1 reverse transcriptase, an enzyme responsible for virus replication (Gallant et al., 2006).
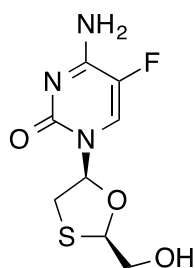
Emtricitabine (**1.64**)
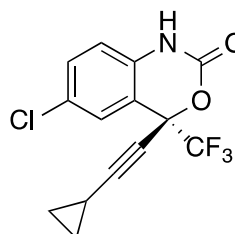
Efavirenz (**1.65**)

Treats HIV infection

Figure 1.24 Fluorinated drugs for the treatment of HIV

1.6. Hypothesis, aims and objectives

Hypothesis

Since both the quinoline and chalcone moieties each have significant biological activity on their own, it is hypothesised that a hybrid molecule containing both these pharmacophores may exhibit enhanced activity, as the two moieties either work alone or in conjunction to augment each other's effects. Furthermore, introducing a fluorine atom at the same position on the quinoline backbone as that of popular fluoroquinolones, such as ciprofloxacin and levofloxacin, may also lead to enhanced antibacterial activity.

Aim: To identify hit fluoroquinoline-chalcone derivatives that could be developed further into antibiotics.

Objectives

1. To synthesise a small library of quinoline-chalcone derivatives, fluorinated on the quinoline ring and with varying substituents on the chalcone moiety.

2. To characterise the synthesised compounds using NMR spectroscopy and mass spectrometry.

3. To determine the antibacterial activity of the synthesised compounds.

4. To investigate the best substitution pattern on the quinoline core structure for antibacterial activity and the effect that different halogens have when substituted at the *para* position of the chalcone moiety.

Chapter 2.   Results and Discussion

2.1. Chemistry

Nine novel quinoline-chalcone hybrids (**8a**–**i**) were synthesized from substituted fluoroanilines in three steps. This involved addition of the fluoroanilines to crotonaldehyde under acidic conditions producing 6- and 8-monofluorinated, and 6,8-difluorinated 2-methylquinoline intermediates (**1**–**3**), which were further oxidized by selenium dioxide to the 2-carbaldehydes (**4**–**6**) in yields of 65, 62 and 55% respectively. This reaction was carefully monitored by TLC to ensure that oxidation to the carboxylic acid did not occur. The quinoline-2-carbaldehydes **4**–**6** were isolated and purified after the reaction and condensed with *para* halogenated acetophenones (**7a**–**c**) by a Claisen-Schmidt condensation to produce the quinoline-chalcone hybrids **8a**–**i** in yields of 46–77% after isolation and purification (**Scheme 2.1**).
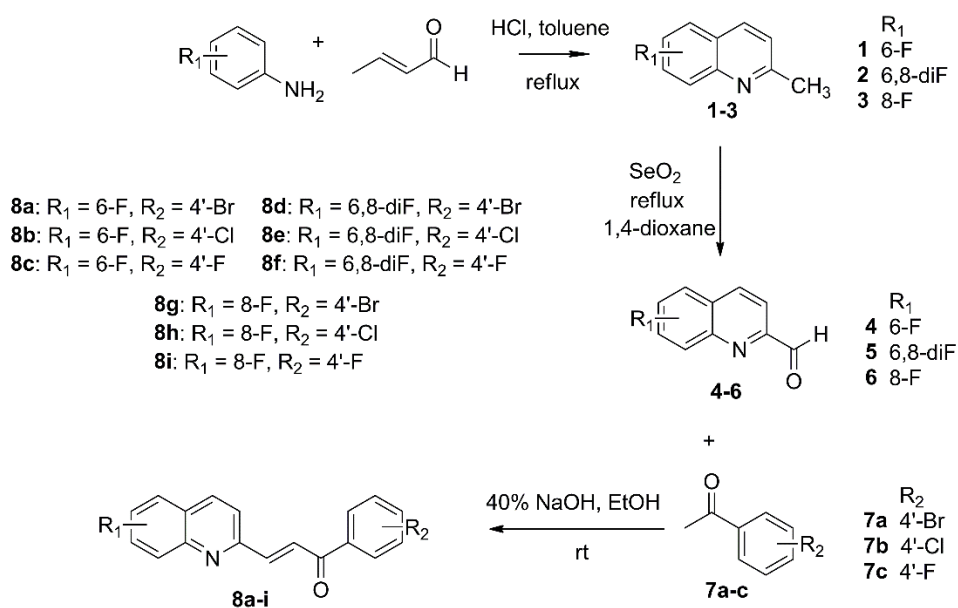
Scheme 2.1 Reaction scheme for quinoline-chalcone hybrids (**8a**–**i**)

In general, compounds difluorinated on the quinoline ring resulted in lower yields than those monofluorinated on the quinoline scaffold (**Table 2.1**). Although the fluorine atom withdraws

electrons more by induction than donation, this effect could possibly be due to its electron donating effect, deactivating the aldehyde carbon to nucleophilic addition in the Claisen Schmidt reaction (**Table 2.1**). In both the 6,8-difluoro and 8-fluoro scaffolds, the compounds with fluorine at the 4'-position exhibited higher melting points than compounds with bromine or chlorine at the same position. This was possibly due to a greater degree of intermolecular forces (intermolecular H-bonding) than the bromo or chloro-substituted compounds on the same scaffold. The 4',6-difluoro derivative (**8c**) is an exception and it is hypothesised that the 8-fluoro substituent has a role to play in hydrogen bonding, increasing the melting point.

Table 2.1   Yields of the final step of the Claisen-Schmidt condensation of quinoline-2-carbaldehydes and acetophenones

No.	R₁	R₂	Melting point °C	Yield %
8a	6-F	Br	188–190	62
8b	6-F	Cl	187–189	72
8c	6-F	F	170–172 (dec.)	66
8d	6,8-diF	Br	185–187 (dec.)	46
8e	6,8-diF	Cl	185–187 (dec.)	48
8f	6,8-diF	F	202–204	69
8g	8-F	Br	178–180	77
8h	8-F	Cl	188–190	72
8i	8-F	F	200–202	64

*dec = decomposed

The reaction of substituted fluoroanilines and crotonaldehyde required a biphasic solvent system consisting of aqueous HCl and toluene, since crotonaldehyde polymerises in an acidic environment. Crotonaldehyde was therefore used in excess during the reaction. By taking this approach, the aldehyde is contained in the organic solvent while the aniline and acid are contained in the aqueous medium. This allows the reaction to occur at the phase boundary of

the two immiscible solvents (Matsugi et al., 2000). Oxidation of the fluoro-2-methylquinolines (**1**–**3**) to the fluoro-2-carbaldehydes (**4**–**6**) was achieved using selenium dioxide, a good oxidizing agent for methyl groups in particular. The reduction of Se (from +4 to 0) was observed as a black deposit that appeared towards the end of the oxidation step due to an accumulation of elemental selenium. The solvent, 1,4-dioxane, was chosen due to its high boiling point and poor ability to be oxidized. In the base-catalysed Claisen-Schmidt condensation, conjugate elimination of a poor leaving group (OH⁻) was favoured rather than water elimination due to the extended conjugated system of the chalcone.

Various derivative reactions were attempted with the chalcone moiety. For this purpose, the 6-fluoroquinoline-4'-chlorochalcone **8b** was used. Attempts were made to synthesise pyrimidine derivatives with urea in the presence of potassium hydroxide, a strong Lewis base, pyrimidine thiones with thiourea, pyrazole carbothioic acid amides with thiosemicarbazides, isoxazoles with hydroxylamine hydrochloride, and pyrazolines with hydrazine hydrate (**Scheme 2.2**). Disappointingly, none of the reactions worked, despite several attempts. The reason for this is unknown, however the presence of deactivating halogens on the molecule may contribute to these reactions not occurring.

2.2. Structural elucidation

Formation of the quinoline carbaldehyde intermediates was confirmed using ^{1}H NMR spectroscopy (**Figure 2.1**). For example, in the quinoline-6-carbaldehyde intermediate **4**, the aldehyde proton could be seen at δ 10.18. The H-3 and H-4 resonances were identified as a pair of doublets at δ 8.02 and 8.24 with a J value of 8.6 Hz. H-8 overlapped with the H-4 resonance. This resonance was coupled to H-7, which was also coupled to the 6-F group and H-5, resulting in a doublet of doublet of doublets (ddd) at δ 7.57 with $J_{H7,H8}$ = 8.9 Hz, $J_{H7,F}$ =

8.9 Hz, and $J_{H7,5}$ = 2.8 Hz. Both $J_{H7,H8}$ and $J_{H7,F}$ had equal coupling constants and hence the ddd appeared as a triplet of doublets (td). H-5, being coupled to the fluorine and H-7, appeared as a dd at δ 7.49 with J values of 8.6 and 2.8 Hz.

R$_1$ = 6-F; 6,8-diF; 8-F
R$_2$ = 4'-Br, 4'-Cl, 4'-F
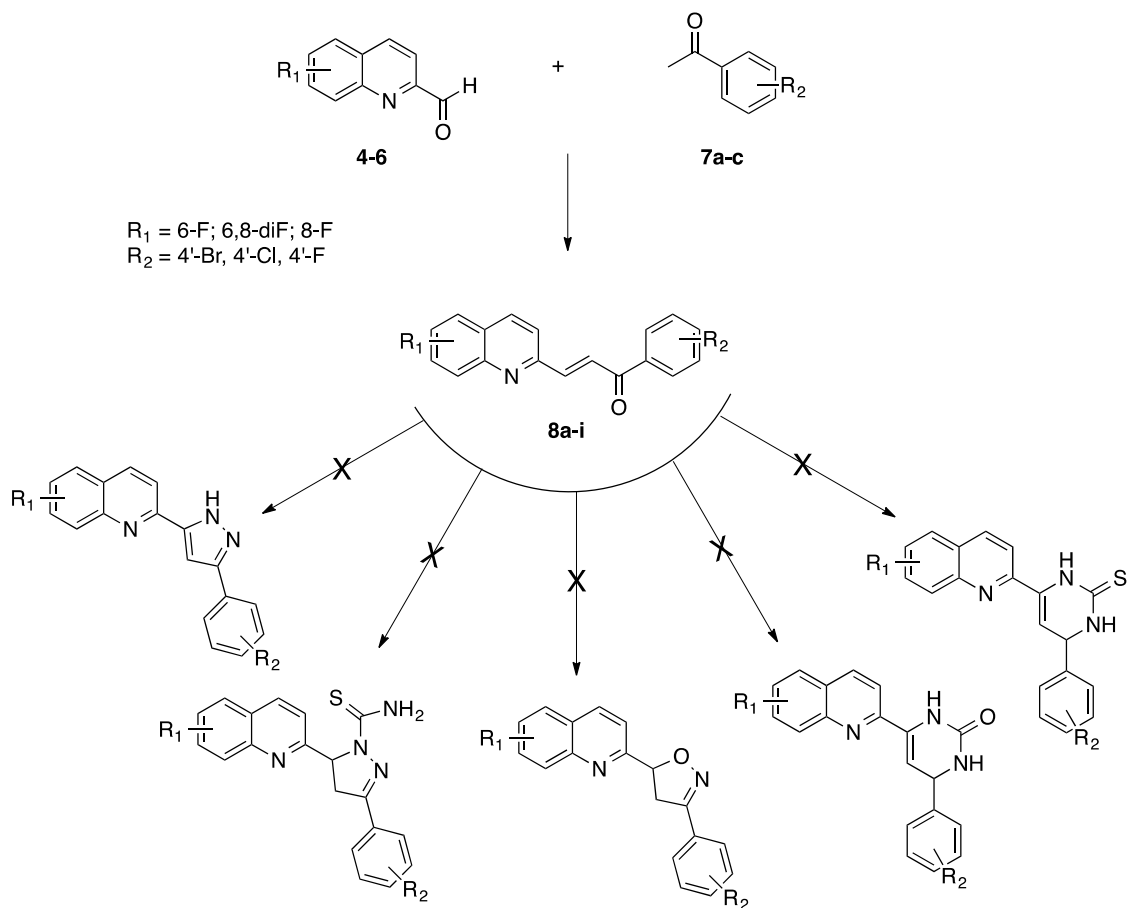
Scheme 2.2 Attempted derivatisation reactions on the quinoline-chalcone hybrids
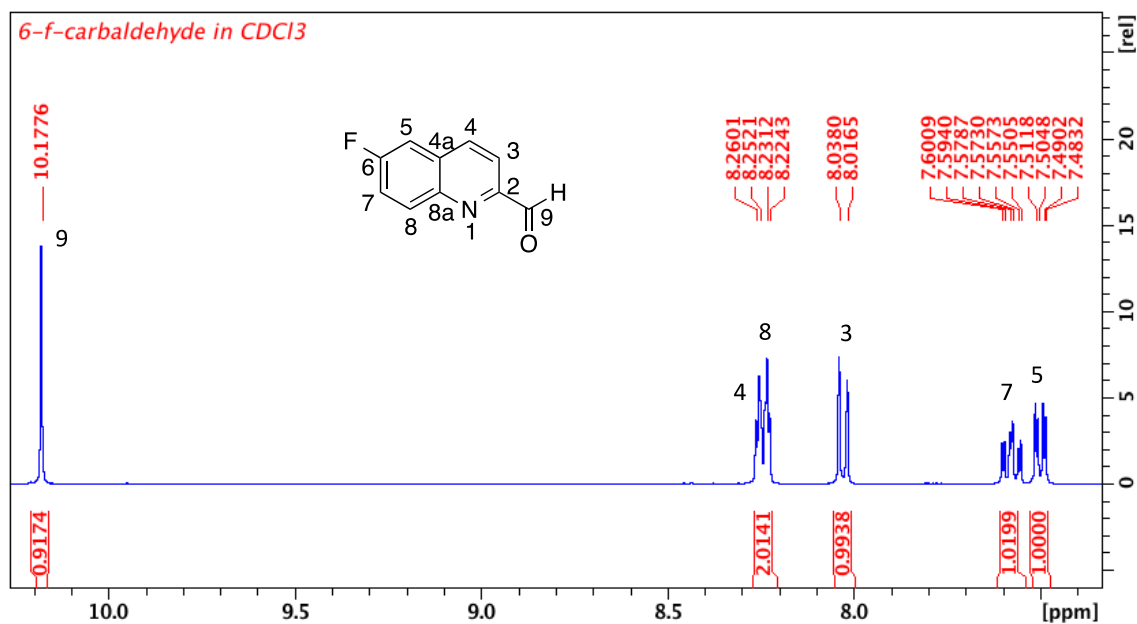
Figure 2.1 ^{1}H NMR spectrum of quinoline-6-carbaldehyde (**4**)

Conversion to the quinoline-chalcone hybrids **8a**–**i** was confirmed by the disappearance of the aldehyde proton singlet, which in **8a** occurred at δ 10.18 (**Figure 2.1**) and by the appearance of two characteristic pairs of doublets, one pair with large coupling constants of 15.4 Hz at δ 8.11 and 7.93, typical of *trans* coupled protons across a double bond (H-10 and H-9 respectively), and the other with smaller coupling constants of J = 8.5 Hz, typical of *ortho* coupling (**Figure 2.2**). The resonances at δ 7.98 and 7.68 were attributed to H-2'/6' and H-3'/5' respectively. The quinoline proton resonances were very similar to the quinoline carbaldehyde intermediate **4**, with the exception of H-3, which was significantly more shielded, now at δ 7.66, than it was in the quinoline intermediate at δ 8.02. This is probably due to the added electron donation by the newly bonded pi system of the chalcone.
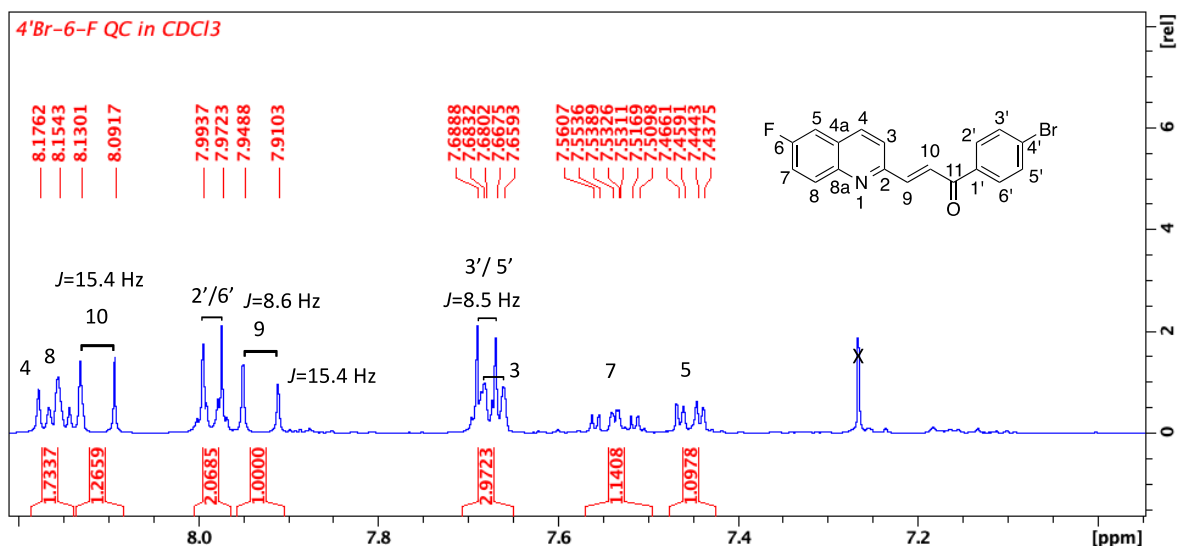
Figure 2.2 ^{1}H NMR spectrum of *(E)-3-(6-fluoroquinolin-2-yl)-1-(4-bromophenyl)prop-2-en-1-one* (**8a**)

The ^{13}C NMR was useful in confirming the fluorine at position-6 as this fluorine splits the *ipso* C-6 resonance into a doublet with a large, characteristic coupling constant of 250.6 Hz (**Figure 2.3**). In general, the further away the carbon is from the fluorine, the smaller the coupling constant. As such, *ipso* carbons directly attached to a fluorine typically exhibit coupling constants between 240–260 Hz, whereas *ortho* carbon resonances have coupling constants between 20–25 Hz, and *meta* carbon resonances between 8–12 Hz. In this way, C-4 and C-8 were identified. They were initially identified from the HSQC spectrum, since H-8 and H-4 could be characteristically identified. C-4 appeared as a doublet with $J = 5.8$ Hz and C-8 a doublet with $J = 9.3$ Hz (**Figure 2.4**). C-5 and C-7 were both doublets with similar coupling constants of $J = 21.9$ and 26.1 Hz respectively (**Figure 2.5**). These carbon resonances were also differentiated using the HSQC spectrum, since H-5 and H-7 could be identified by their splitting pattern.
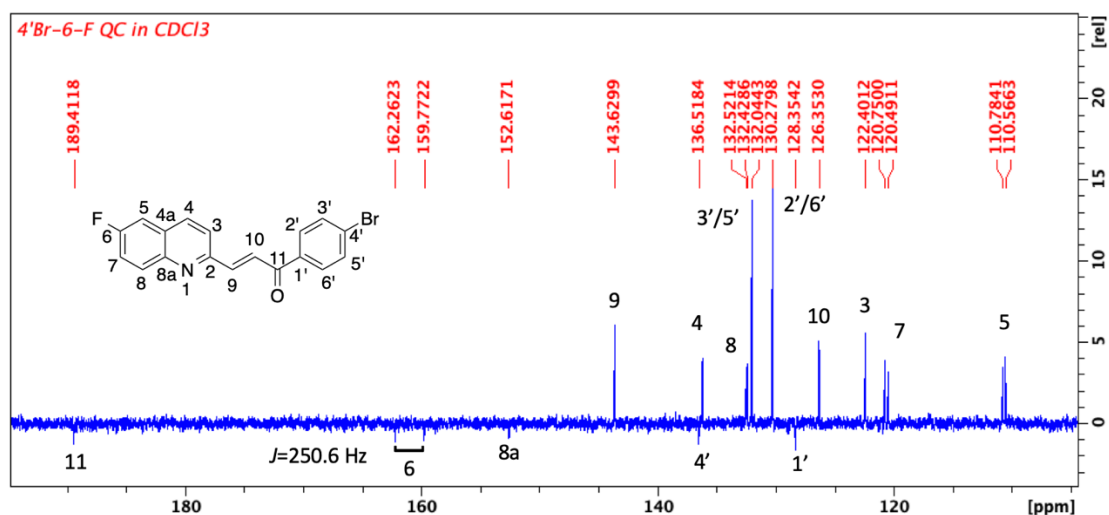
Figure 2.3 APT NMR spectrum of *(E)-3-(6-fluoroquinolin-2-yl)-1-(4-bromophenyl)prop-2-en-1-one* (**8a**)

The intensity of the signals of C-3'/5' and C-2'/6' suggested that these signals were those of two equivalent carbon resonances. They were differentiated by an HMBC correlation of H-2'/6' to C-11, the carbonyl peak at δ 189.4. The quaternary carbons C-1' and C-4' were assigned due to HMBC correlations with H-3'/5' and H-2'/6' respectively, the more deshielded resonance at δ 136.5 being assigned to C-4'. C-8a was assigned due to its HMBC correlation to H-9 (**Figure 2.6**). C-2 and C-4a could not be detected on the ^{13}C NMR spectrum.
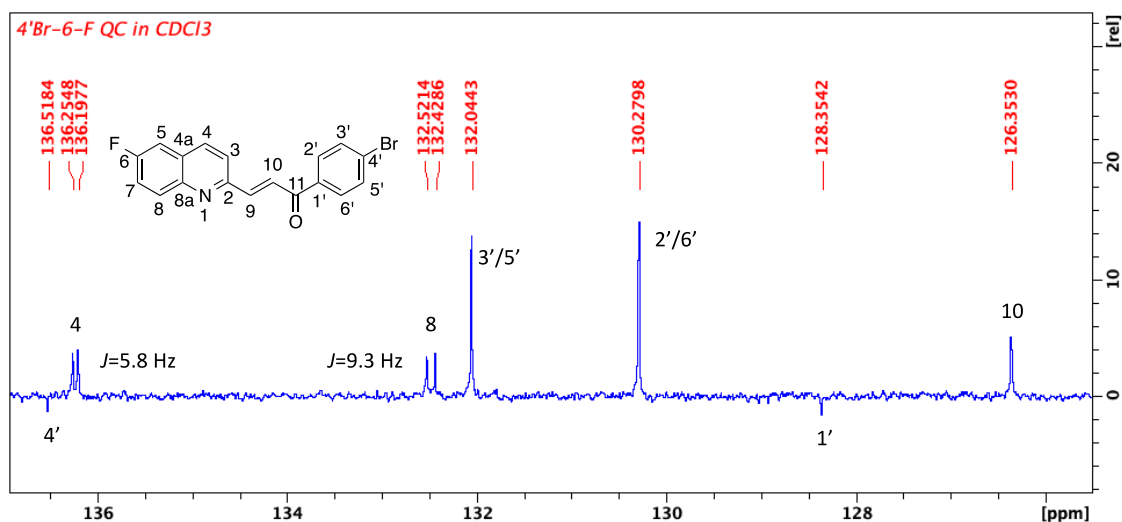
Figure 2.4 Expanded APT NMR spectrum of *(E)-3-(6-fluoroquinolin-2-yl)-1-(4-bromophenyl)prop-2-en-1-one* (**8a**) showing the coupling constants of C-4 and C-8
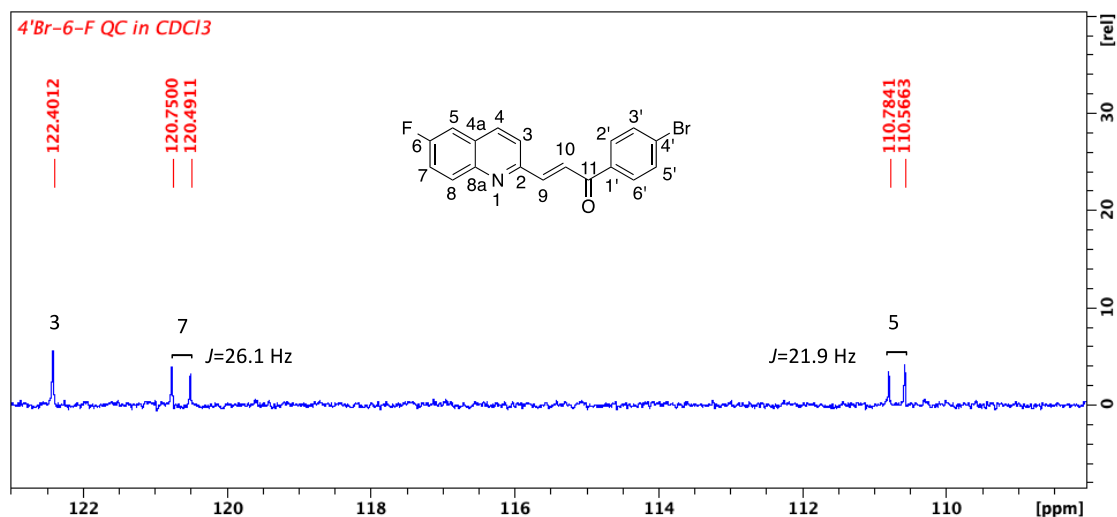
Figure 2.5 Expanded APT NMR spectrum of *(E)-3-(6-fluoroquinolin-2-yl)-1-(4-bromophenyl)prop-2-en-1-one* (**8a**) showing the coupling constants of C-5 and C-7
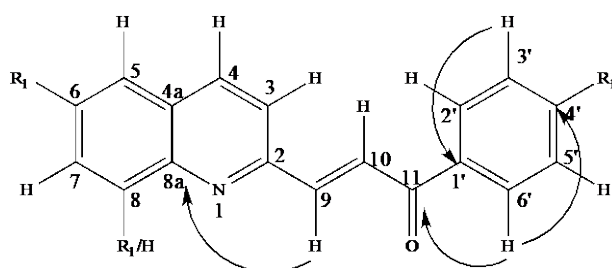
Figure 2.6 Selected HMBC correlations used in the elucidation of compound **8a**

For the difluorinated compounds, three pairs of doublets, typical of the quinoline chalcones with a *para* substituted aromatic ring were present. These were the two *trans* coupled olefinic proton doublets at δ 7.93 and 8.12, H-9 and H-10 with J = 15.2 Hz, two *ortho* coupled aromatic doublet resonances, H-2'/6' and H-3'/5' at δ 7.97 and 7.67 (J = 8.6 Hz), and the two doublets of H-3 and H-4 at δ 7.73 and 8.18 (J = 8.6 Hz). The resonances of H-5 and H-7 overlapped as a two-proton multiplet at δ 7.28–7.30 (**Figure 2.7**).

The *ipso* carbon resonances of C-6 and C-8 could not be clearly differentiated from the noise but were in the region of δ 160 and δ 170 respectively (**Figure 2.8**). This could be inferred

from correlations on the HMBC spectrum. Interestingly, as illustrated in **Figure 2.9,** the eight

peaks between δ 105.8 and 106.8 were the two double doublets of C-5 and C-7. For C-5, this

resonance couples with F-6 first (J = 21.6 Hz) and then F-8 (J = 5.1 Hz), resulting in the first

dd. C-7 is *ortho* coupled to both F-6 and F-8 with coupling constants of 29.4 Hz and 22.4 Hz,

resulting in the second double doublet. A closer look at C-4 (**Figure 2.10**) reveals that this

resonance is also J^4 coupled to the two fluorine atoms and appears as a double doublet with J

values of 5.6 and 5.3 Hz.
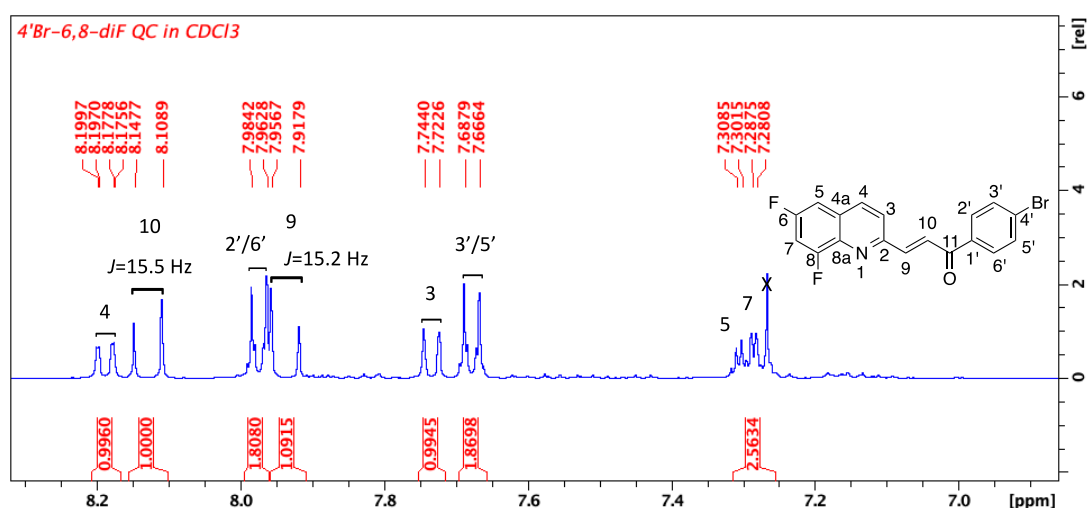
Figure 2.7 ^{1}H NMR spectrum of *(E)-3-(6,8-difluoroquinolin-2-yl)-1-(4-bromophenyl)prop-2-en-1-one* (**8d**)
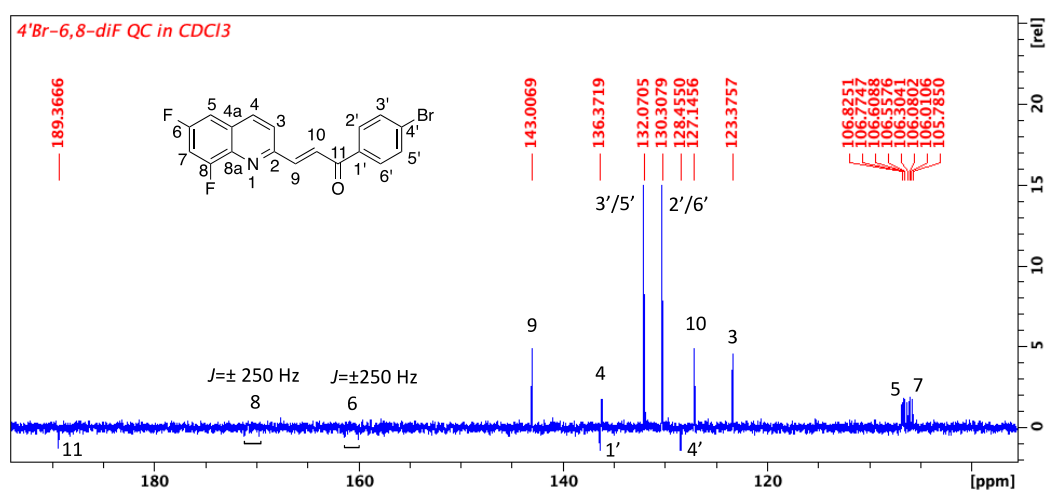
Figure 2.8 APT NMR spectrum of *(E)-3-(6,8-difluoroquinolin-2-yl)-1-(4-bromophenyl)prop-2-en-1-one* (**8d**)
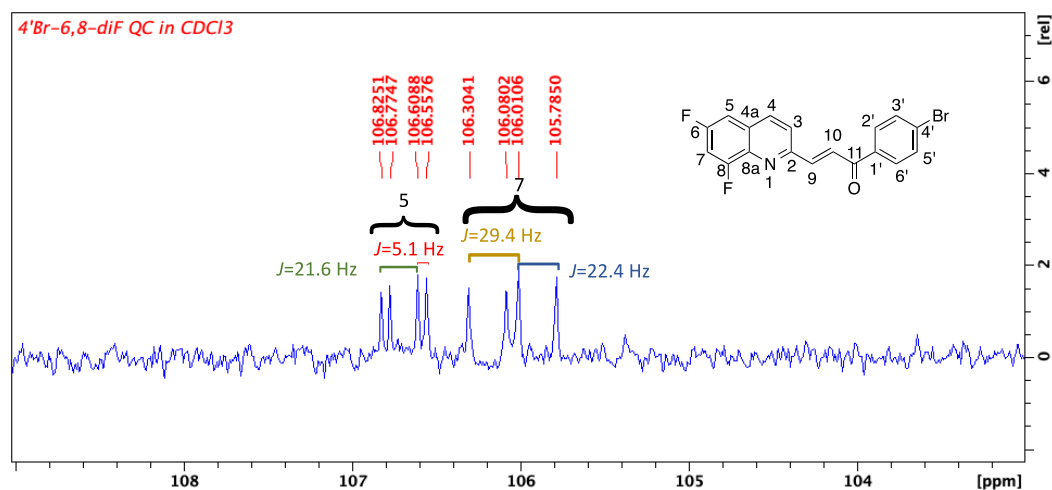
Figure 2.9 Expanded APT NMR spectrum of *(E)-3-(6,8-difluoroquinolin-2-yl)-1-(4-bromophenyl)prop-2-en-1-one* (**8d**) δ 104–108
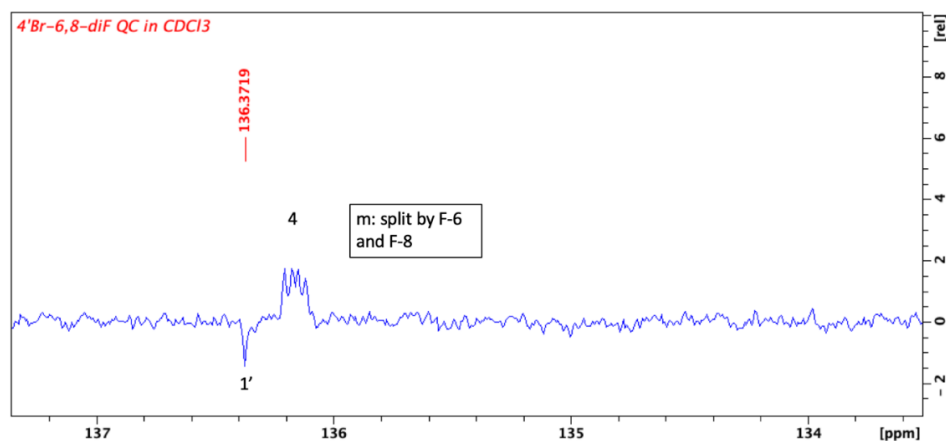
Figure 2.10 Expanded APT NMR spectrum of *(E)-3-(6,8-difluoroquinolin-2-yl)-1-(4-bromophenyl)prop-2-en-1-one* (**8d**) δ 134–137

The ^{13}C NMR spectra of those compounds with a *para* fluorinated aromatic ring (**8c, f** and **i**) was particularly useful in assigning the C-2'/6' and C-3'/5' aromatic carbon resonances (**Figure 2.11**). C-2'/6', *meta* to F-4' is split with a smaller coupling constant of 9.3 Hz, while H-3'/5', being *ortho* to F-4', is split with a larger *J* value of 22.0 Hz (**Figure 2.11**). This also aided in distinguishing between H-2'/6' and H-3'/5' in the HSQC spectrum. In the same way, the carbon resonances of C-5, C-6 and C-7 were determined in 6- or 8- monofluorinated quinolines. For example, in **8h**, the 8-fluorinated quinoline, C-5 had the smallest *J* value (4.6 Hz), followed by C-6 (6.9 Hz) and then C-7 with the largest *J* value (19.1 Hz) (**Figure 2.12**). Once the carbon

54

resonances were assigned, the HSQC was used to identify the proton resonances, H-5, H-6 and

H-7.
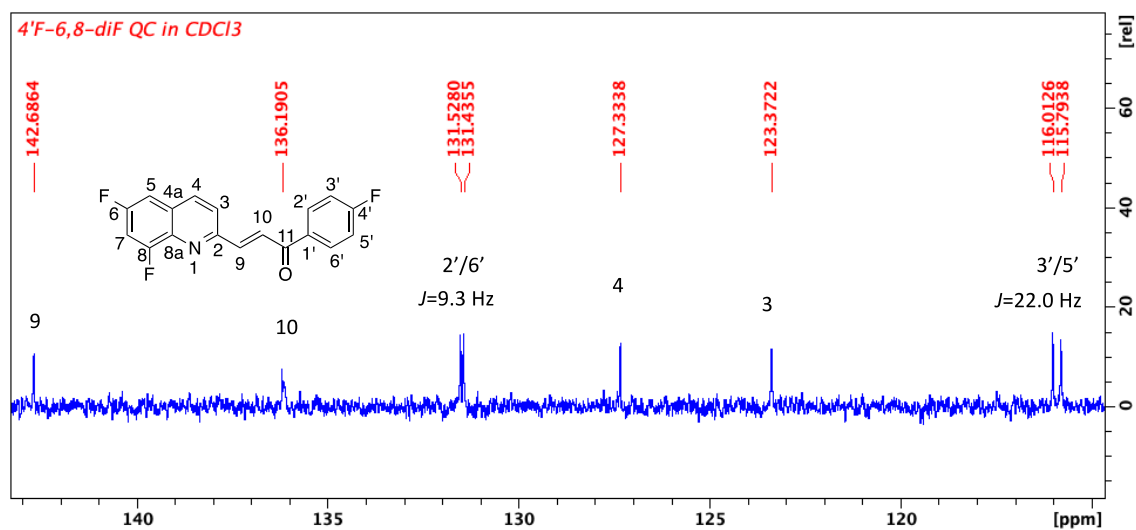
Figure 2.11 Expanded ^{13}C NMR spectrum of *(E)-3-(6,8-difluoroquinolin-2-yl)-1-(4-fluorophenyl)prop-2-en-1-one* (**8f**)
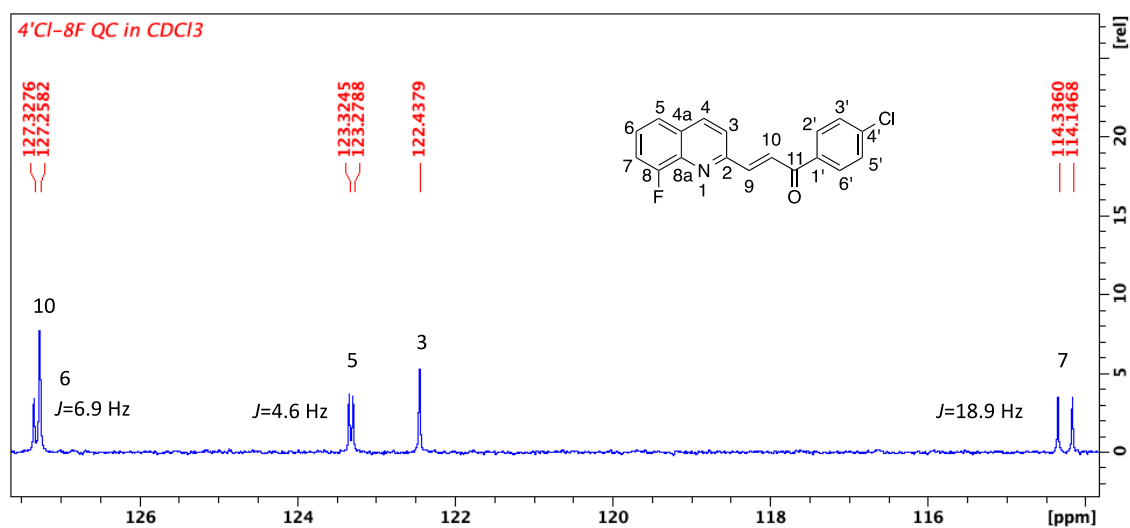
Figure 2.12 Expanded ^{13}C NMR spectrum of *(E)-3-(8-fluoroquinolin-2-yl)-1-(4-chlorophenyl)prop-2-en-1-one* (**8h**)

Thus, using a range of 1D and 2D NMR spectra, most ^{1}H and ^{13}C resonances could be unequivocally assigned and the structures of the compounds verified. The presence of fluorine in the molecule was used to our advantage in the assignments, as fluorine coupling to carbon was used for easy identification of the carbon resonances. Further confirmation was obtained by High Resolution Mass Spectrometry (HRMS), where the exact mass of the compounds was observed.

2.3. Bioactivity

The quinoline-chalcone hybrids (**8a**–**i**) were tested for their antibacterial activity against two Gram +ve and four Gram -ve strains, being initially screened by the disk diffusion method and the active compounds being tested by the broth microdilution method to determine the MBC values of the active compounds. Standard antibiotics, ciprofloxacin and levofloxacin, were used in the same assay for comparison. Compounds **8a**–**i** were not active against the four Gram -ve strains, but were very active against the two Gram +ve strains, *Staphylococcus aureus* (SA) and Methicillin resistant *Staphylococcus aureus* (MRSA) (**Table 2.2**).

Table 2.2 Minimum bactericidal concentration of compounds **8a**–**i** (MBC in μM)

	R$_1$	R$_2$	*S. aureus*	MRSA
8a	6-F	Br	21.9	174.5
8b	6-F	Cl	**6.3**	200.5
8c	6-F	F	**3.3**	-
8d	6,8-diF	Br	**5.2**	**20.9**
8e	6,8-diF	Cl	23.7	189.6
8f	6,8-diF	F	24.9	-
8g	8-F	Br	-	-
8h	8-F	Cl	**7.8**	-
8i	8-F	F	**7.8**	-
Cipro			94.3	188.6
Levo			21.6	86.5

Cipro = ciprofloxacin; Levo = Levofloxacin; MRSA = methicillin resistant *S. aureus*
- indicates activity >500 μM

All synthesized compounds, with the exception of **8g**, showed excellent activity against *S. aureus*, at < 30 μM, better than the standards, ciprofloxacin and levofloxacin, which had MBCs of 94.3 and 21.6 μM respectively. Five compounds were active at <10 μM against *S. aureus*, the 6-fluoroquinoline derivative with *para* chloro and fluorophenyl chalcone moieties (**8b** and **8c**), the 6,8-difluoroquinoline-4-bromo chalcone derivative (**8d**) and the 8-fluoroquinoline derivatives with *para* chloro and fluoro chalcone moieties (**8h** and **8i**). Although the 6,8-difluoroquinoline derivative with a *para* bromo substituted chalcone moeity (**8d**) was very active against *S. aureus*, removing the 6-fluoro group from this molecule, leaving only the 8-F group (**8g**), resulted in no activity. Removing the 8-fluoro (**8a**) group, leaving only the 6-fluoro substituent resulted in good activity, but was still four-fold lower than **8d**. This indicates that when a *para* bromo group is present on the phenyl portion of the quinoline chalcone, the 6,8-difluoro substitution pattern on the quinoline moiety is best for activity against *S. aureus*.

With the exception of **8g** (*para* bromo derivative of the 8-fluorinated quinoline), all compounds were active against *S. aureus*, regardless of whether the quinoline ring was 6-fluorinated, 8-fluorinated, or 6,8-difluorinated. The most active of all compounds against *S. aureus* was the 6-fluoroquinoline-4'-fluorochalcone (**8c**). This indicates that the smaller halogens, fluorine and chlorine, are better substituted on the phenyl ring than the larger and more polarisable bromo substituent. Incidentally, this is not the case for the 6,8-difluoroquinolines, where the bromo substituent on the phenyl ring showed the best antibacterial activity.

Interestingly, only when bromo and chloro substituents were present on the phenyl ring of the fluoroquinoline-chalcone hybrids, were they active against MRSA and this too, only occurred with the 6-fluoro and 6,8-difluoroquinoline derivatives. Compounds with a *para* fluorophenyl derivative (**8c**, **8f** and **8i**) and with an 8-fluoroquinoline moiety (**8g**–**i**) showed no activity

against MRSA. Compounds **8a**, **8b** and **8e** had activity comparable to ciprofloxacin against MRSA, at approximately 200 μM. Compound **8d**, however had excellent activity against MRSA at 20.9 μM, four-fold better than levofloxacin. Thus, although the 6,8-difluorinated quinoline chalcones with *para* chloro and fluorophenyl moieties were not as active as the other compounds, the 6,8-difluoroquinoline with a *para* bromophenyl substituent was the best of the series, being active at 5.2 μM against *S. aureus* and 20.9 μM against MRSA. This compound can be considered a hit compound against *S. aureus* and MRSA and is worth developing and investigating further, perhaps with other Gram +ve strains.

Chapter 3.   Experimental

3.1. General experimental procedures

All chemicals and reagents were supplied by Sigma-Aldrich *via* Capital Lab, South Africa and were reagent grade. Column chromatography was used to purify samples using silica gel 60 (0.063–0.200 mm) as the stationary phase and varying ratios of hexane:ethyl acetate as the mobile phase. Reactions were monitored on TLC (thin-layer chromatography) using Merck Kieselgel 60 F_{254} fluorescent plates and visualised under UV light at 254 nm. Melting points were measured using a capillary tube in a SMP11 Stuart melting point apparatus. IR spectra were recorded on a Perkin Elmer Spectrum 100 FT-IR spectrometer with a universal attenuated total reflectance sampling accessory. ^{1}H and ^{13}C NMR spectra were recorded at 298K with 10 mg samples dissolved in 0.5 mL of $CDCl_3$ in 5-mm NMR tubes using a 400-MHz Bruker Avance NMR spectrometer (9.4T; Bruker, Germany) (400.22 MHz for ^{1}H and 100.63 MHz for ^{13}C). Coupling constants (J) are reported in Hertz (Hz) and chemical shifts (δ) are reported in parts per million (ppm). With reference to the internal standard, TMS, the ^{1}H and ^{13}C chemical shifts of the deuterated solvent, $CDCl_3$ were δ 7.24 and 77.0 respectively. NMR data was processed using Bruker TopSpin 3.5 software.

3.2. Synthesis

General procedure for the synthesis of the 2-methylquinoline derivatives (**1**–**3**)

Crotonaldehyde (67.5 mmol, 4.73 g) in toluene was added dropwise to a warm (~40 °C) solution of 2-, 2-/4- or 4-fluoroaniline (45.0, 38.7, 45.0 mmol respectively; 5.00 g) in aqueous HCl and refluxed for 14 h at 100 °C. Upon completion, the reaction mixture was cooled, and the toluene layer discarded. The aqueous layer was basified using $NaHCO_3$ and extracted with ethyl acetate, dried over anhydrous $MgSO_4$ and concentrated using a rotary evaporator. Purification of the crude product was carried out using column chromatography on silica gel

using hexane:ethyl acetate (95:5). Of the three compounds, only compound **1** was isolated in 71% yield, purified and characterised. This was to ensure that a reaction occurred. Compounds **2**–**3** were not purified and used straight after the extraction for the next step.

General procedure for the synthesis of quinoline-2-carbaldehydes (**4**–**6**)

Selenium dioxide (45.1 mmol, 5.00 g) was added to a cool solution of **1, 2** or **3** (45.1 mmol) in 1,4-dioxane (30 mL) and refluxed at 100 °C for 20 min. The reaction was monitored by TLC as described above, until completion. Thereafter, the mixture was cooled and filtered through celite. The reaction mixture was then extracted with ethyl acetate, dried over anhydrous $MgSO_4$ and concentrated using a rotary evaporator. Purification of the crude product by column chromatography on silica gel using a hexane:ethyl acetate (95:5) mobile phase yielded **4, 5** and **6** in yields of 65, 62 and 55% respectively.

General procedure for the synthesis of quinoline chalcones (**8a**–**i**)

Substituted acetophenones (**7a**–**c;** 2.5, 3.2 and 3.6 mmol respectively; 0.50 g) were dissolved in absolute ethanol (20 mL). Thereafter, 4–6 drops of 40% NaOH (aq) were added whilst stirring at room temperature. Compounds **4, 5** or **6** (0.9, 1.0, 1.1 mmol respectively; 0.20 g), was then added to the solution and allowed to stir for 15 min, after which the reaction mixture was cooled in an ice bath, where it precipitated out of solution. When precipitation did not occur spontaneously, 2–4 drops ice water were added to the solution to encourage precipitation. The products were then filtered, washed with hexane and dried under vacuum to produce the quinoline chalcones in yields of between 46–77%.

3.3. *In vitro* antimicrobial studies

Compounds **8a**–**i** were preliminarily screened against two Gram +ve strains (*Staphylococcus aureus* ATCC 25923 and Methicillin resistant *Staphylococcus aureus* ATCC BAA-1683) and four Gram –ve strains (*Escherichia coli* ATCC 25922, *Pseudomonas aeruginosa* ATCC 27853, *Salmonella typhimurium* ATCC 14026 and *Klebsiella pneumonia* ATCC 314588) by the disc diffusion method. Briefly, bacterial micro-organisms were grown overnight at 37 °C in nutrient broth (Biolab, South Africa) and adjusted to a 0.5 McFarland standard using distilled water. Mueller-Hinton agar (MHA) (Biolab, South Africa) plates were prepared by dissolving 38 g of agar in 1 L of water and pouring these into sterile petri dishes, which were then allowed to set and dry at room temperature. They were then inoculated with the respective strains of bacteria by streaking a swab (dipped into the micro-organism solution) evenly over the entire sterile agar surface. A solution of a 1.0 mg/mL was prepared for each compound **8a**–**i**, from which 5 μL was impregnated directly onto Mueller-Hinton plates. They were then left to incubate for 24 h at 37 °C. The compounds that showed a zone of inhibition for respective strains were considered active. Those active in four or more strains were chosen to determine their MBC (minimum bactericidal concentration).

MBC assay

A swab of the microbial cultures (adjusted to a 0.5 McFarland standard) were prepared and evenly streaked over the sterile agar plates. The selected compounds were serially diluted with DMSO to obtain concentrations of 0.24 to 500 μg/mL. A volume of 5 μL of the prepared concentrations were directly spotted onto the MHA plates containing the respective bacterial strains and incubated at 37 °C for 20 h. The lowest concentration showing a zone of inhibition was recorded as the minimum bactericidal concentration (MBC). DMSO was used as a control

and levofloxacin and ciprofloxacin were used as standards. All experiments were conducted in triplicate and were reproducible.

3.4. Chemical data

Some quaternary resonances in the ^{13}C NMR spectra could not be detected, possibly due to the NMR parameters used when acquiring the spectra. These are indicated in each case below.

(E)-3-(6-fluoroquinolin-2-yl)-1-(4-bromophenyl)prop-2-en-1-one (**8a**), pale yellow crystalline

solid; 62% yield, mp 188–190 ºC, IR (neat) υ_{max}: 1682 cm^{-1} (C=O stretch); ^{1}H NMR (CDCl$_3$, 400 MHz) δ 8.18 (1H, d, J = 8.4 Hz, H-4), 8.15 (1H, d, J = 8.7 Hz, H-8), 8.11 (1H, d, J = 15.4 Hz, H-10), 7.98 (2H, d, J = 8.6 Hz, H-2'/6'), 7.93 (1H, d, J = 15.4 Hz, H-9), 7.68 (2H, d, J = 8.6 Hz, H-3'/5'), 7.67 (1H, d, J = 8.4 Hz, H-3), 7.54 (1H, ddd, J = 8.7, 8.7, 2.8 Hz, H-7), 7.45 (1H, dd, J = 8.7, 2.8 Hz, H-5); ^{13}C NMR (CDCl$_3$, 100MHz) δ 189.4 (C-11), 161.0 (d, J = 250.6 Hz, C-6), 152.6 (d, J = 2.9 Hz, C-8a), 143.6 (C-9), 136.5 (C-4'), 136.2 (d, J = 5.8 Hz, C-4), 132.5 (d, J = 9.3 Hz, C-8), 132.0 (C-3'/5'), 130.3 (C-2'/6'), 128.4 (C-1'), 126.4 (C-10), 122.4 (C-3), 120.6 (d, J = 26.1 Hz, C-7), 110.7 (d, J = 21.9 Hz, C-5); HRMS: 356.0098 [M+H]$^{+}$ (calcd. for C$_{18}$H$_{12}$BrFNO, 356.0086). *C-2 and C-4a could not be detected.

(E)-3-(6-fluoroquinolin-2-yl)-1-(4-chlorophenyl)prop-2-en-1-one (**8b**) white crystalline solid;

72% yield, mp 187–189 ºC, IR (neat) υ_{max}: 1660 cm^{-1} (C=O stretch); ^{1}H NMR (CDCl$_3$, 400 MHz) δ 8.09 (1H, d, J = 8.4 Hz, H-4), 8.16 (1H, d, J = 7.3 Hz, H-8), 8.12 (1H, d, J = 15.5 Hz, H-10), 8.05 (2H, d, J = 8.6 Hz, H-2'/6'), 7.93 (1H, d, J = 15.4 Hz, H-9), 7.67 (1H, d, J = 8.4 Hz, H-3), 7.53 (1H, m, H-7), 7.51 (2H, d, J = 8.6 Hz, H-3'/5'), 7.45 (1H, dd, J = 8.7, 2.8 Hz, H-5); ^{13}C NMR
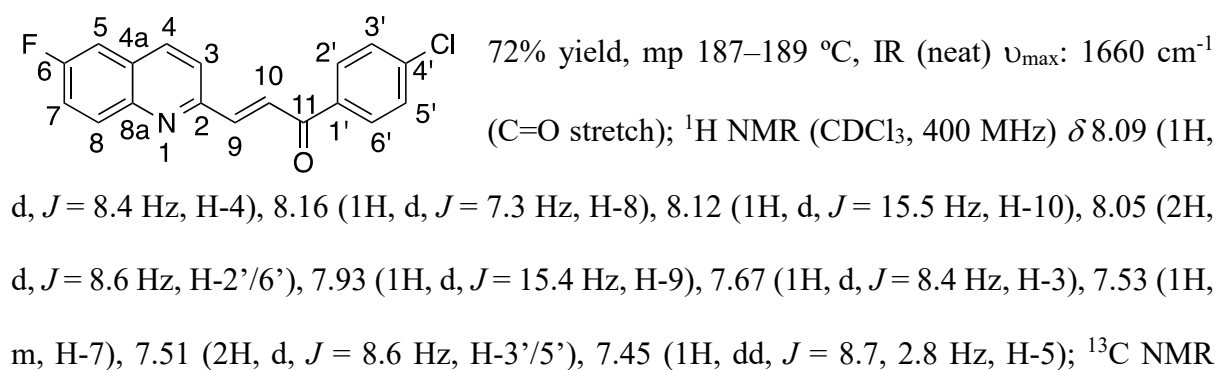
(CDCl$_3$, 100 MHz) δ 189.2 (C-11), 161.0 (d, J = 250.6 Hz, C-6), 152.6 (d, J = 3.0 Hz, C-8a), 145.5 (C-2), 143.6 (C-9), 139.6 Hz (C-4'), 136.2 (d, J = 5.5 Hz, C-4), 136.1 (C-1'), 132.5 (d, J = 9.1 Hz, C-8), 130.2 (C-2'/6'), 129.1 (C-3'/5'), 126.4 (C-10), 122.4 (C-3), 120.6 (d, J = 26.0 Hz, C-7), 110.7 (d, J = 21.8 Hz, C-5); HRMS: 312.0595 [M+H]$^+$ (calcd. for C$_{18}$H$_{11}$ClFNO, 312.0591). *C-4a could not be detected

(E)-3-(6-fluoroquinolin-2-yl)-1-(4-fluorophenyl)prop-2-en-1-one (**8c**) white crystalline solid; 66% yield, decomposed 170–172 ºC, IR (neat) υ_{max}: 1663 cm^{-1} (C=O stretch); **^{1}H NMR** (CDCl$_3$, 400 MHz) δ 8.12–8.18 (5H, m, H-4, H-8, H-10, H-2'/6'), 7.93 (1H, d, J = 15.5 Hz, H-9), 7.67 (1H, d, J = 8.5 Hz, H-3), 7.53 (1H, ddd, J = 8.4, 8.4, 2.8 Hz, H-7), 7.45 (1H, dd, J = 8.7, 2.8 Hz, H-5), 7.21 (2H, t, J = 8.6 Hz, H-3'/5'); **^{13}C NMR** (CDCl$_3$, 100 MHz) δ 188.9 (C-11), 165.9 (d, J = 255.3 Hz , C-4'), 160.9 (d, J = 250.4 Hz, C-6), 152.7 (d, J = 2.9 Hz, C-8a), 145.5 (C-2), 143.3 (C-9), 136.2 (d, J = 5.6 Hz, C-4), 139.7 (C-1'), 132.4 (d, J = 9.4 Hz, C-8), 131.4 (d, J = 9.4 Hz, C-2'/6'), 128.9 (d, J = 10.2 Hz, C-4a), 126.5 (C-10), 122.4 (C-3), 120.6 (d, J = 26.0 Hz, C-7), 115.9 (d, J = 21.9 Hz, C-3'/5'), 110.7 (d, J = 21.9 Hz, C-5); HRMS: 296.0885 [M+H]$^+$ (calcd. for C$_{18}$H$_{11}$F$_2$NO, 296.0887).
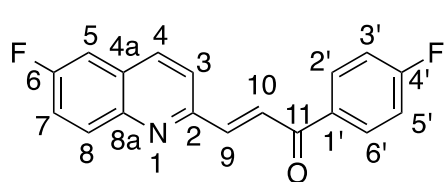
(E)-3-(6,8-difluoroquinolin-2-yl)-1-(4-bromophenyl)prop-2-en-1-one (**8d**) white crystalline solid; 46% yield, decomposed 185–187 ºC, IR (neat) υ_{max}: 1662 cm^{-1} (C=O stretch); **^{1}H NMR** (CDCl$_3$, 400 MHz) δ 8.19 (1H, d, J = 8.8 Hz, H-4), 8.12 (1H, d, J = 15.2 Hz, H-10), 7.97 (2H, d, J = 8.6 Hz, H-2'/6'), 7.94 (1H, d, J = 15.2 Hz, H-9), 7.73 (1H, d, J = 8.8 Hz, H-3), 7.68 (2H, d, J = 8.6 Hz, H-3'/5'), 7.28-7.30 (2H, m, H-5, H-7); **^{13}C NMR** (CDCl$_3$, 100 MHz) δ 189.4 (C-11), 170.5 (d, J = 250.0 Hz, C-8), 160.9 (d, J = 250.0 Hz, C-6),
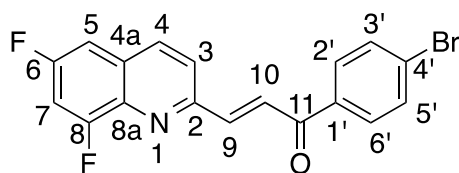
143.0 (C-9), 136.4 (C-1'), 136.2 (d, J = 3.2 Hz, C-4), 132.1 (C-3'/5'), 130.3 (C-2'/6'), 128.5 (C-4'), 127.2 (C-10), 123.4 (C-3), 106.6 (1H, dd, J = 21.6, 5.1 Hz, C-5), 106.1 (1H, dd, J = 29.4, 22.4 Hz, C-7); HRMS: 374.0004 [M+H]$^+$ (calcd. for $C_{18}H_{11}BrF_2NO$, 373.9992). *C-2, C-4a and C-8a could not be detected.

(E)-3-(6,8-difluoroquinolin-2-yl)-1-(4-chlorophenyl)prop-2-en-1-one (**8e**) white crystalline solid, 48% yield), mp 185–187 ºC, IR (neat) υ_{max}: 1661 cm^{-1} (C=O stretch); **^{1}H NMR** (CDCl$_3$, 400 MHz) δ 8.19 (1H, d, J = 8.6 Hz, H-4), 8.14 (1H, d, J = 15.5 Hz, H-10), 8.05 (2H, d, J = 8.5 Hz, H-2'/6'), 7.94 (1H, d, J = 15.5 Hz, H-9), 7.73 (1H, d, J = 8.6 Hz, H-3), 7.51 (2H, d, J = 8.5 Hz, H-3'/5'), 7.27-7.31 (2H, m, H-5, H-7); **^{13}C NMR** (CDCl$_3$, 100 MHz) δ 189.2 (C-11), 161.0 (d, J = 247.1 Hz, C-6), 142.9 (C-9), 139.7 (C-4'), 136.2 (m, C-4), 136.1 (C-1'), 130.2 (C-2'/6'), 129.1 (C-3'/5'), 127.2 (C-10), 123.4 (C-3), 106.7 (1H, dd, J = 21.4, 5.1 Hz, C-5), 106.1 (1H, dd, J = 29.5, 22.6 Hz, C-7); HRMS: 330.0502 [M+H]$^+$ (calcd. for $C_{18}H_{11}ClF_2NO$, 330.0497). *C-2, C-8, C-4a and C-8a could not be detected.
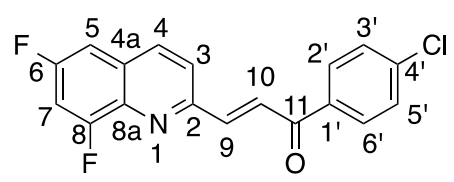
(E)-3-(6,8-difluoroquinolin-2-yl)-1-(4-fluorophenyl)prop-2-en-1-one (**8f**) white crystalline solid; 69% yield, mp 202–204 ºC, IR (neat) υ_{max}: 1658 cm^{-1} (C=O stretch); **^{1}H NMR** (CDCl$_3$, 400 MHz) δ 8.13–8.20 (4H, H-2'/6', H-4, H-10), 7.93 (1H, d, J = 15.5 Hz, H-9), 7.73 (1H, d, J = 8.5 Hz, H-3), 7.28-7.31 (2H, m, H-5, H-7), 7.21 (2H, t, J = 8.6 Hz, H-3'/5'); **^{13}C NMR** (CDCl$_3$, 100MHz) δ 191.2 (C-11), 142.7 (C-9), 136.2 (C-10), 131.5 (d, J = 9.3 Hz, C-2'/6'), 127.3 (C-4), 123.4 (C-3), 115.9 (d, J = 22.0 Hz, C-3'/5'), 106.5 (2C, m, C-5, C-7); HRMS: 314.0795 [M+H]$^+$ (calcd. for $C_{18}H_{11}F_3NO$, 314.0793). *The singlet resonances of C-2, C-4a, C-8a, C-6, C-8, C-4' and C-1' could not be detected.
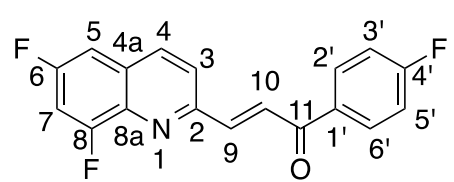
(E)-3-(8-fluoroquinolin-2-yl)-1-(4-bromophenyl)prop-2-en-1-one (**8g**) white crystalline solid;

77% yield, mp 178–180 ºC, IR (neat) υ_{max}: 1679 cm^{-1} (C=O stretch); **^{1}H NMR** (CDCl$_3$, 400 MHz) δ 8.24 (1H, d, J = 8.5 Hz, H-4), 8.14 (1H, d, J = 15.5 Hz, H-10), 7.97 (2H, d, J = 8.6 Hz, H-2'/6'), 7.96 (1H, d, J = 15.5 Hz, H-9), 7.82 (1H, d, J = 8.6 Hz, H-5), 7.72 (1H, d, J = 8.5 Hz, H-3), 7.67 (2H, d, J = 8.6 Hz, H-3'/5'), 7.49-7.56 (1H, m, H-6), 7.42-7.48 (1H, m, H-7); **^{13}C NMR** (CDCl$_3$, 100 MHz) δ 189.5 (C-11), 157.5 (d, J = 258.4 Hz, C-8), 153.5 (C-2), 143.4 (C-9), 136.8 (d, J = 3.1 Hz, C-4), 136.7 (C-1'), 132.1 (C-3'/5'), 130.3 (C-2'/6'), 129.7 (C-10), 128.4 (d, J = 10.2 Hz, C-8a), 127.3 (d, J = 8.0 Hz, C-6), 123.3 (d, J = 4.7 Hz, C-5), 122.4 (C-3), 114.2 (d, J = 19.1 Hz, C-7); HRMS: 356.0098 [M+H]$^+$ (calcd. for C$_{18}$H$_{11}$BrFNO, 356.0086). *C-4a and C-4' could not be detected.

(E)-3-(8-fluoroquinolin-2-yl)-1-(4-chlorophenyl)prop-2-en-1-one (**8h**) white crystalline solid;

72% yield, mp 188–190 ºC, IR (neat) υ_{max}: 1635 cm^{-1} (C=O stretch); **^{1}H NMR** (CDCl$_3$, 400 MHz) δ 8.23 (1H, d, J = 8.5 Hz, H-4), 8.14 (1H, d, J = 15.5 Hz, H-10), 8.05 (2H, d, J = 8.6 Hz, H-2'/6'), 7.96 (1H, d, J = 15.5 Hz, H-9), 7.71 (1H, d, J = 8.5 Hz, H-3), 7.62 (1H, d, J = 8.1 Hz, H-5), 7.49-7.53 (3H, m, H-6, H-3'/5'), 7.44 (1H, ddd, J = 10.6, 8.0, 1.2 Hz, H-7); **^{13}C NMR** (CDCl$_3$, 100 MHz) δ 189.3 (C-11), 159.6 (d, J = 258.5 Hz, C-8), 153.5 (C-2), 143.4 (C-9), 139.7 (C-4a), 136.7 (d, J = 3.0 Hz, C-4), 136.0 (C-1'), 130.3 (C-2'/6'), 129.8 (d, J = 2.2 Hz, C-8a), 129.1 (C-3'/5'), 127.3 (C-10), 127.3 (d, J = 6.9 Hz, C-6), 123.3 (d, J = 4.6 Hz, C-5), 122.4 (C-3), 114.3 (d, J = 18.9 Hz, C-7); HRMS: 312.0597 [M+H]$^+$ (calcd. for C$_{18}$H$_{11}$ClFNO, 312.0591). *C-4' could not be detected.

(E)-3-(8-fluoroquinolin-2-yl)-1-(4-fluorophenyl)prop-2-en-1-one (**8i**) white crystalline solid;
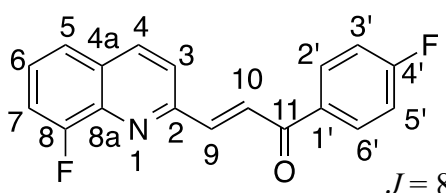
64% yield), mp 200–202 ºC, IR (neat) υ_{max}: 1658 cm^{-1} (C=O stretch); **^{1}H NMR** (CDCl$_3$, 400 MHz) δ 8.24 (1H, d, J = 8.6 Hz, H-4), 8.14–8.19 (3H, m, H-10, H-2'/6'), 7.96 (1H, d, J = 15.5 Hz, H-9), 7.72 (1H, d, J = 8.5 Hz, H-3), 7.63 (1H, d, J = 8.1 Hz, H-5), 7.52 (1H, ddd, J = 7.9, 7.9, 5.3 Hz, H-6), 7.44 (1H, ddd, J = 10.2, 7.9, 1.4 Hz, H-7); **^{13}C NMR** (CDCl$_3$, 100 MHz) δ 189.9 (C-11), 165.5 (d, J = 255.2 Hz, C-4'), 157.5 (d, J = 258.3 Hz, C-8), 153.6 (C-2), 143.1 (C-9), 138.5 (C-1'), 136.7 (d, J = 2.9 Hz, C-4), 131.5 (d, J = 9.3 Hz, C-2'/6'), 129.7 (d, J = 2.8 Hz, C-4a), 127.4 (C-10), 127.2 (d, J = 8.0 Hz, C-6), 123.3 (d, J = 4.8 Hz, C-5), 122.4 (C-3), 115.8 (d, J = 21.8 Hz, C-3'/5'), 114.2 (d, J = 18.9 Hz, C-7); HRMS: 296.0892 [M+H]$^+$ (calcd. for C$_{18}$H$_{11}$F$_3$NO, 296.0887). *C-8a could not be detected.

Chapter 4.   Conclusion

Nine fluorinated quinoline chalcone hybrids were synthesised in good yields from a Doebner-Miller reaction between fluorinated anilines and crotonaldehyde to form quinoline intermediates. The quinoline-2-carbaldehydes were oxidized successfully with SeO_2 to functionalise the 2-position for further reactions and to hybridise the quinoline framework. Formation of quinoline chalcone hybrids took place via an easy Claisen-Schmidt condensation between the oxidized quinolines and *para*-substituted acetophenones. Thus, the reaction series carried out was efficient in forming quinoline chalcone hybrids, which have the attributes of both quinolines and chalcones. Beside forming chalcones from the aldehydes, a number of other reactions can be carried out with this functional group, for example, forming imines with various amines, and therefore the quinoline-2-carbaldehyde intermediate is an important intermediate in quinoline hybrid synthesis.

A full structural elucidation of all the compounds synthesised was carried out and will provide a basis for the identification of similar molecules in future research. It was shown that although the ^{13}C NMR of fluorinated quinoline chalcones looked complex, since doublets and double doublets now appeared in the spectrum, this was actually quite useful in assigning the carbon resonances and, indirectly, the proton resonances of the respective compounds. Typical coupling constants allowed these resonances to be positioned either *ortho*, *meta* or *para* to the fluorine substituent.

All compounds were inactive against the Gram-negative strains, however, most compounds were active against the Gram-positive *S. aureus* in the range of 3.3 to 24.9 μM, comparable to levofloxacin and approximately 4-fold better than ciprofloxacin. An exception is the 8-fluoro-4'-bromo derivative **8g**, which was inactive against all strains. Compound **8d**, containing 6,8-

difluoro substituents on the quinoline moiety and a bromine group at the *para* position on the acetophenone moiety, showed the best antibacterial activity at 5.2 μM against *S. aureus* and 20.9 μM against MRSA. This activity was approximately 4-fold better than levofloxacin, the better of the two standard antibiotics used for comparison. This was therefore identified as a hit compound amongst this series. Gopaul and Koorbanally synthesised similar quinoline chalcone hybrids, however, they were chlorinated on the quinoline ring, rather than fluorinated. The chlorinated quinoline hybrids they synthesised were all inactive in preliminary antimicrobial assays, whereas the fluorinated quinoline chalcone hybrids in this work were active in antibacterial assays. This highlights the necessity of a fluorine substituent on the quinoline moiety for antibacterial activity.

Unfortunately, attempts to derivatise this series of quinoline chalcone hybrids using known reactions were unsuccessful. This may be due to the presence of deactivating halogens on both the A and B rings.

Future work will involve the modification of compound **8d** (6,8-diF, 4'-Br) to improve its activity, as this compound was identified as a hit compound against Gram-positive bacterial strains. It is hoped that through further testing and analysis, a substantial structure-activity relationship will be established, in particular how the presence of the halogens affects the activity of the molecule as a whole. Cytotoxicity studies must also be carried out on the active compounds to ascertain whether the strong antibacterial activity is not due to the compound itself being cytotoxic.

Chapter 5. References

Abbas, S.H., El-Hafeez, A.A.A., Shoman, M.E., Montano, M.M., Hassan, H.A. New quinoline/chalcone hybrids as anti-cancer agents: design, synthesis and evaluations of cytotoxicity and PI3K inhibitory activity. *Bioorg. Chem.* **2019**, 82, 360−377.

Abonia, R., Insuasty, D., Castillo, J., Insuasty, B., Quiroga, J., Nogueras, M., Cobo, J. Synthesis of novel quinoline-2-one based chalcones of potential anti-tumour activity. *Eur. J. Med. Chem.* **2012**, 57, 29−40.

Ahmad, A., Wani, M.Y., Patel, M., Sobral, A.J.F., Duse, A.G., Aqlan, F.M., Al-Bogami, A.S. Synergistic and antifungal effect of cyclized chalcone derivatives and fluconazole against *Candida albicans. Med. Chem. Commun.* **2017**, 8, 2195−2207.

Alapi, E.M., Fischer, J. Table of selected analogue classes, In: *Analogue-based Drug Discovery*, Fischer, J., Ganellin, C.R. (Eds), John Wiley and Sons, New Jersey, **2006**, 441−552.

Ali, M.M., Tasneem, K.C., Rajanna, K., Sai Prakash, P.K. An efficient and facile synthesis of 2-chloro-3-formyl quinolines from acetanilides in micellar media by Vilsmeier-Haack cyclisation. *Syn. Lett.* **2001**, 2, 251−253.

Aribi, F., Schmitt, E., Panossian, A., Vors, J.P., Pazenok, S., Leroux, F. A new approach toward the synthesis of 2,4-bis(fluoroalkyl)-substituted quinoline derivatives using fluoroalkyl amino reagent chemistry. *Org. Chem. Front.* **2016**, 3, 1392−1415.

Ávila, H.P., Smânia, E.F.A., Monache, F.D., Smânia Júnior, A. Structure-activity relationship of antibacterial chalcones. *Bioorg. Med. Chem.* **2008**, 16, 9790−9794.

Baird, J., Rieckmann, K. Can primaquine therapy for vivax malaria be improved? *Trends Parasitol.* **2003**, 19, 115−120.

Bindu, B., Vijayalakshmi, S., Manikandan, A. Discovery, synthesis and molecular substantiation of *N*-(benzo[d]thiazol-2-yl)-2-hydroxyquinoline-4-carboxamides as anticancer agents. *Bioorg. Chem.* **2019**, 91, Article ID: 103171, https://doi.org/10.1016/j.bioorg.2019.103171.

Bindu, P.J., Mahadevan, K.M., Ravikumar Naik, T.R., Harish, B.G. Synthesis, DNA binding, docking and photocleavage studies of quinolinyl chalcones. *Med. Chem. Commun.* **2014**, 5, 1708−1717.

Böhm, H.J., Banner, D., Bendels, S., Kansy, M., Kuhn, B., Müller, K., Obst-Sander, U., Stahle, M. Fluorine in medicinal chemistry. *ChemBioChem.* **2004**, 5, 637−643.

Bonvicini, F., Gentilomi, G.A., Bressan, F., Gobbi, S., Rampa, A., Bisi, A., Belluti, F. Functionalisation of the chalcone scaffold for the discovery of novel lead compounds targeting fungal infections. *Molecules* **2019**, 24, 1−26.

Brinkman, M., Bogdan, B., Carriere, D., Velki, M., Smith, K., Meyer-Alert, H., Müller, Y., Thalmann, B., Bluhm, K., Schiwy, S., Hotz, S., Salowsky, H., Tiehm, A., Hecker, M., Hollert, H. Bioactivation of quinolines

in a recombinant estrogen receptor transactivation assay is catalysed by *N*-methyltransferases. *Chem. Res. Toxicol.* **2019**, 32, 698−707.

Brosius, R., Gammon, D., Van Laar, F., Van Steen, E., Bert, S., Jacobs, P. Vapour-phase synthesis of 2-methyl- and 4-methylquinoline over BEA* zeolites. *J. Catal.* **2006**, 239, 362−368.

Calverley, P.M.A., Anderson, J.A., Celli, B., Ferguson, G.T., Jenkins, C., Jones, P.W., Yates, J.C., Vestbo, J. Salmeterol and fluticasone propionate and survival in chronic obstructive pulmonary disease. *N. Engl. J. Med.* **2007**, 356, 775−789.

Campoli-Richards, D., Monk, J.P., Price, A., Benfield, P., Todd, P.A., Ward, A. Ciprofloxacin: A review of its antibacterial activity, pharmacokinetic properties and therapeutic use. *Drugs* **1988**, 35, 373−447.

Cao, N., Chen, Y., Ma, X., Zeng, K., Zhao, M., Tu, P., Li, J., Jiang, Y. Bioactive carbazole and quinoline alkaloids from *Clausena dunniana*. *Phytochemistry* **2018**, 151, 1−8.

Cella, R. and Stefani, H.A. Ultrasound in heterocycles chemistry. *Tetrahedron* **2009**, 65, 2619−2641.

Cheeseman, G.W.H. The synthesis and tautomerism of some 2-substituted pyrazines. *J. Chem. Soc.* **1960**, 47, 242.

Choi, D., Park, J.C., Lee, H.N., Moon, J.H., Ahn, H., Park, K., Hong, J. *In vitro* osteogenic differentiation and antibacterial potential of chalcone derivatives. *Mol. Pharmaceutics* **2018**, 15, 3197−3204.

Coa, J.C., Gárcia, E., Carda, M., Agut, R., Vélez, I.D., Muñoz, J.A., Yepes, L.M., Robledo, S.M., Cardona, W.I. Synthesis, leishmanicidal, trypanocidal and cytotoxic activites of quinoline-chalcone and quinoline-chromone hybrids. *Med. Chem. Res.* **2017**, 26, 1405−1414.

Crombie, M., Mistry, J. The phytoalexins of oat leaves: 4*H*-3,1-benzoxazin-4-ones or amides? *Tetrahedron Lett.* **1990**, 31, 2647−2648.

Da Silva, J.G., Despaigne, A.A.R., Louro, S.R.W., Bandeira, C.C., Souza-Fagundes, E.M., Beraldo, H. Cytotoxic activity, albumin and DNA binding of new copper(II) complexes with chalcone-derived thiosemicarbazones. *Eur. J. Med. Chem.* **2013**, 65, 415−426.

Dave, S.S., Rahatgaonkar, A.M. Synthesis and anti-microbial evaluation of new quinoline scaffold derived pyrimidine derivatives. *Arab. J. Chem.* **2011**, 9, S451−S456.

Dawadi, S., Viswanathan, K., Boshoff, H.I., Barry, III, C.E., Aldrich, C.C. Investigation and conformational analysis of fluorinated nucleoside antibiotics targeting siderophore biosynthesis. *J. Org. Chem.* **2015**, 80, 4835−4850.

Ducki, S., Forrest, R., Hadfield, J.A., Kendall, A., Lawrence, N.J., McGown, A.T., Rennison, D. Potent antimitotic and cell growth inhibitory properties of substituted chalcones. *Bioorg. Med. Chem. Lett.* **1998**, 8, 1051−1056.

Egan, T.J. Interactions of quinoline antimalarials with hematin in solution. *J. Inorg. Biochem.* **2006**, 100, 916–926.

El Shehry, M.F., Ewies, E.F., Zayed, E.M. Synthesis of new pyrazole derivatives, their anti-inflammatory and analgesic activities and molecular docking studies. *Russ. J. Gen. Chem.* **2019**, 89, 492–498.

Filler, R., Saha, R. Fluorine in medicinal chemistry: a century of progress and a 60-year retrospective of selective highlights. *Future Med. Chem.* **2009**, 1, 777–791.

Fraley, M.E., Rubino, R.S., Hoffman, W.F., Hambaugh, S.R., Arrington, K.L., Hungate, R.W., Bilodeau, M.T., Tebben, A.J., Rutledge, R.Z., Kendall, R.L., McFall, R.C., Huckle, W.R., Coll, K.E., Thomas, K.A. Optimisation of a pyrazolo[1,5-a]pyrimidine class of KDR kinase inhibitors: improvements in physical properties enhance cellular activity and pharmokinetics. *Bioorg. Med. Chem. Lett.* **2002**, 12, 3537–3541.

Gallant, J.E., DeJesus, E., Arribas, J.R., Pozniak, A.L., Gazzard, B., Campo, R.E., Lu, B., McColl, D., Chuck, S., Enejosa, J., Toole, J.J., Cheng, A.K. Tenofovir EF, emtricitabine, and efavirenz vs. zidovudine, lamivudine, and efavirenz for HIV. *N. Eng. J. Med.* **2006**, 354, 251–260.

Gan, F., Zhang, R., Ng, H., Karuppasamy, M., Seah, W., Hseun Yeap, W., Ong, S., Hadadi, E., Wong, S., Chui, W., Chew, E. Novel dual-targeting anti-proliferative dihydrotriazine-chalcone derivatives display suppression of cancer cell invasion and inflammation by inhibiting the NF-κB signalling pathway. *Food Chem. Toxicol.* **2018**, 116, 238–248.

Gisbert, P., Albert-Soriano, M., Manuel Pastor, I. Metal-free robust catalyst mediated C-C and C-N bond formation: an effective and sustainable access to quinoline and acridine derivatives. *Eur. J. Org. Chem.* **2019**, 30, 4928–4940.

Gopaul, K., Koorbanally, N.A. Synthesis and structure elucidation of a series of chloroquinoline-2-chalcones by the Doebner-Miller reaction. *Magn. Reson. Chem.* **2016**, 54, 677–683.

Govender, H. Synthesis and biological activity of quinoline derivatives. PhD Thesis. University of KwaZulu-Natal, **2018**, p.10.

Grigor'eva, N.G., Kostyleva, S.A., Gataulin, A.R., Khazipova, A.N., Narender, N., Kutepov, B.I. Aluminosilicates with different porous structures in the synthesis of 2-ethyl-3-methylquinoline. *Petrol Chem.* **2019**, 59, 719–725.

Guo, Q., Liao, L., Teng, W., Ren, S., Wang, X., Lin, Y., Meng, F. Synthesis of quinoline derivatives from anilines and aldehydes catalysed by Cp_2ZrCl_2 and recyclable Cp_2ZrCl_2/MCM-41 system. *Catal. Today* **2015**, 263, 117–122.

Harsanyi, A., Sandford, G. Organofluorine chemistry: applications, sources and sustainability. *Green Chem.* **2015**, 17, 2081–2086.

Herr, J.M., Rössiger, C., Albrecht, G., Yanagi, H., Göttlich, R. Solvent-free microwave-assisted synthesis of imidazo[1,5-a]pyridine and -quinoline derivatives. *Synth. Commun.* **2019**, 49, 2931–2940.

Hsieh, C. -T., Ötvös, S.B., Wu, Y. -C., Mándity, I.M., Chang, F.-R., Fülöp, F. Highly selective continuous-flow synthesis of potentially bioactive deuterated chalcone derivatives. *ChemPlusChem* **2015**, 80, 859−864.

Jin, J., Guidi, S., Abada, Z., Amara, Z., Selva, M., George, M.W., Poliakoff, M. Continuous niobium phosphate catalysed Skraup reaction for quinoline synthesis from solketal. *Green Chem.* **2017**, 19, 2439−2447.

Kaur, K., Jain, M., Reddy, R.P., Jain, R. Quinolines and structurally related heterocycles as antimalarials. *Eur. J. Med.* **2010**, 45, 3245−3264.

Khan, S.S., Asiri, A.M., Al-Ghamdi, N.S.M., Asad, M., Zayed, M.E.M, Elroby, S.A.K., Aqlan, F.M., Wani, M.Y., Sharma, K. Microwave assisted synthesis of chalcone and its polycyclic heterocyclic analogues as promising antibacterial agents: *in vitro, in silico* and DFT studies. *J. Mol. Struct.* **2019**, 1190, 77−85.

Khong, S., Kwon, O. One-pot phosphine-catalyzed syntheses of quinolines. *J. Org. Chem.* **2012**, 77, 8257−8267.

Kirk, K.L. Fluorine in medicinal chemistry: recent therapeutic applications of fluorinated small molecules. *J. Fluor. Chem.* **2006**, 127, 1013−1029.

Ko, H., Tsao, L., Yu, K., Liu, C., Wang, J., Lin, C. Structure-activity relationship studies on chalcone derivatives: the potent inhibition of chemical mediators release. *Bioorg. Med. Chem.* **2003**, 11, 105−111.

Kouznetsov, V.V., Vargas Mendéz, L.Y., Meléndez Gómez, C.M. Recent progress in the synthesis of quinolines. *Curr. Org. Chem.* **2005**, 9, 141−161.

Kumar, S., Bawa, S., Drabu, S., Gupta, H., Machwal, L., Kumar, R. Synthesis, antidepressant and antifungal evaluation of novel 2-chloro-8-methylquinoline amine derivatives. *Eur. J. Med. Chem.* **2011**, 46, 670−675.

Kumar, S., Bawa, S., Gupta, H. Biological activities of quinoline derivatives. *Mini-Rev. Org. Chem.* **2009**, 9, 1648−1654.

Leir, C.M. An improvement in the Doebner-Miller synthesis of quinolines. *J. Org. Chem.* **1977**, 42, 911−913.

Li, J. J. Name reactions: A collection of detailed reaction mechanisms, 5th Edition, Springer, Berlin. **2014**

Li, B., Yuan, Y., Hu, J., Zhao, Q., Zhang, D., Chen, N. Protective effect of Bu-7, a flavonoid extracted from *Clausena lansium*, against rotenone injury in PC12 cells. *Acta Pharm. Sin.* **2011**, 32, 1321−1326.

Li, W., Xu, F., Shuai, W., Sun, H., Yao, H., Ma, C., Xu, S., Yao, H., Zhu, Z., Yang, D.H., Chen, Z.S., Xu, J. Discovery of novel quinoline-chalcone derivatives as potent antitumor agents with microtubule polymerisation inhibitory activity. *J. Med. Chem.* **2019**, 62, 993−1013.

López-Sanz, J., Pérez-Mayoral, E., Procházková, D., Martín-Aranda, R.M., López-Peinado, A.J. Zeolites promoting quinoline synthesis via Friedländer reaction. *Top. Catal.* **2010**, 53, 1430−1437.

Madapa, S., Tusi, Z., Batra, S. Advances in the syntheses of quinoline and quinoline-annulated ring systems. *Curr. Org. Chem.* **2008**, 12, 1116−1183.

Mahapatra, D.K., Bharti, S.K., Asati, V. Chalcone scaffolds as anti-infective agents: Structural and molecular target perspectives. *Eur. J. Med. Chem.* **2015**, 101, 496−524.

Manjunatha, J.R., Bettadaiah, B.K., Negi, P.S., Srinivas, P. Synthesis of quinoline derivatives of tetrahydrocurcumin and zingerone and evaluation of their antioxidant and antibacterial attributes. *Food Chem.* **2013**, 136, 650−658.

Marco-Contelles, J., Pérez-Mayoral, E., Samadi, A., Carmo Carreiras, M., Soriano, E. Recent advances in the Friedländer reaction. *Chem. Rev.* **2009**, 109, 2652−2671.

Martens, E. and Demain, A.L. The antibiotic resistance crisis, with a focus on the United States. *J. Antibiot.* **2017**, 70, 520−526.

Matsugi, M., Tabusa, F. and Minamikawa, J.-i. Doebner-Miller synthesis in a two-phase system: Practical preparation of quinolines. *Tetrahedron Lett.*, **2000**, 41, 8523-8525.

Meléndez-Carmona, M.A., Muñoz-Gallego, I., Viedma, E., Lora-Tamayo, J., Chaves, F. Intraosteoblastic activity of levofloxacin and rifampin alone and in combination against clinical isolates of methicillin-susceptible *Staphylococcus aureus* causing prosthetic joint infection. *Int. J. Antimicrob.* **2019**, 54, 356−360.

Meth-Cohn, O., Narine, B., Tarnowski, B. A versatile new synthesis of quinoline and related fused pyridines, Part 5. The synthesis of 2-chloroquinoline-3-carbaldehydes. *J. Chem. Soc., Perkin Trans. 1* **1981**, 1520−1530.

Morrison, R.N., Boyd, R.T. Functional derivatives of carboxylic acids. *In*: Organic Chemistry. 2nd Ed, Allyn & Bacon, Boston, 1992, p. 659−700.

Neu, H.C. The Crisis in Antibiotic Resistance. *Science* **1992**, 257, 1064−1073.

Nowakowska, Z., Kędzia, B., Schroeder, G. Synthesis, physicochemical properties and antimicrobial evaluation of new (*E*)-chalcones. *Eur. J. Med. Chem.* **2008**, 43, 707−713.

Onyango, H.A., Ngugi, C., Maina, J., Kiiru, J. Antimicrobial susceptibility profiles and associated risk factors. *Adv. Microbiol.* **2018**, 8, 175−187.

Parmar, V.S., Sharma, N.K., Husain, M., Watterson, A.C., Kumar, J., Samuelson, L.A., Cholli, A.L., Prasad, A.K., Kumar, A., Malhotra, S., Kumar, N., Jha, A., Singh, A., Singh, I., Himanshu, Vats, A., Shakil, N.A., Trikha, S., Mukherjee, S., Sharma, S.K., Singh, S.K., Kumar, A., Jha, H.N., Olsen, C.E., Stove, C.P., Bracke, M.E., Mareel, M.M. Synthesis, characterisation and *in vitro* anti-invasive activity screening of polyphenolic and heterocyclic compounds. *Bioorg. Med. Chem.* **2003**, 913−929.

Pavithra, P.S., Mehta, A., Verma, R.S. Aromadendrene oxide 2, induces apoptosis in skin epidermoid cancer cells through ROS mediated mitochondrial pathway. *Life Sci.* **2018**, 197, 19−29.

Polo, E., Ibarra-Arellano, N., Prent-Peñaloza, L., Morales-Bayuelo, A., Henao, J., Galdámez, A., Gutiérrez, M. Ultrasound-assisted synthesis of novel chalcone, heterochalcone and bis-chalcone derivatives and the evaluation of their antioxidant properties and as acetylcholinesterase inhibitors. *Bioorg. Chem.* **2019**, 90, Article ID 103034, https://doi.org/10.1016/j.bioorg.2019.103034.

Purser, S., Moore, P.R., Swallow, S., Gouverneur, V. Fluorine in medicinal chemistry. *Chem. Soc. Rev.* **2008**, 37, 327−432.

Rao, Y.K., Fang, S.H., Tzeng, Y.M. Differential effects of synthesised 2'-oxygenated chalcone derivatives: modulation of human cell cycle phase distribution. *Bioorg. Med. Chem.* **2004**, 12, 2679−2686.

Ridker, P.M., Danielson, E., Fonseca, F.A.H., Genest, J., Gotto, Jr., A.M., Kastelein, J.J.P., Koenig, W., Libby, P., Lorenzatti, A.J., MacFayden, J.G., Nordestgaard, B.G., Shepherd, J., Willerson, J.T., Glynn, R.J. Rouvastatin to prevent vascular events in men and women with elevated C-reactive protein. *N. Eng. J. Chem.* **2008**, 359, 2195−2207.

Rizk, O.H., Bekhit, M.G., Hazzaa, A.A.B., El-Khawass, E.M., Abdelwahab, I.A. Synthesis, antibacterial evaluation, and DNA gyrase inhibition profile of some new quinoline hybrids. *Arch. Pharm.* **2019**, 352, Article ID 1900086, https://doi.org/10.1002/ardp.201900086.

Rizvi, S.U.F., Siddiqui, H.L., Ahmad, M.N., Ahmad, M., Bukhari, M.H. Novel quinolyl-thienyl chalcones and their 2-pyrazoline derivatives with diverse substitution pattern as antileishmanial agents against *Leishmania major. Med. Chem. Res.* **2012**, 21, 1322−1333.

Rout, P.K., Kumar, P., Ramachandra Rao, Y., Kumar, A., Bawankule, D.U., Singh, R., Bahadur Singh, K., Chanotiya, C.S., Naik, S.N. A quinoline alkaloid rich *Quisqualis indica* floral extract enhances the bioactivity. *Nat. Prod. Res.* **2019**, https://doi.org/10.1080/14786419.2019.1634709.

Safari, J., Banitaba, S.H., Samiei, S.S. One-pot synthesis of quinaldine derivatives by using microwave irradiation without any solvent – a green chemistry approach. *J. Chem. Sci.* **2009**, 121, 481−484.

Sahu, N.P., Pal, C., Mandal, N.B., Banerjee, S., Raha, M., Kundu, A.P., Basu, A., Ghosh, M., Roy, K., Bandyopadhyay, S. Synthesis of a novel quinoline derivative, 2-(2-methylquinolin-4-ylamino)-*N*-phenylacetamide – a potential antileishmanial agent. *Bioorg. Med. Chem.* **2002**, 10, 1687−1693.

Sashidhara, K.V., Avula, S.R., Mishra, V., Palnati, G.R., Singh, L.R., Singh, N., Chhonker, Y.S., Swami, P., Bhatta, R.S., Palit, G. Identification of quinoline-chalcone hybrids as potential antiulcer agents. *Eur. J. Med. Chem.* **2015**, 89, 638−653.

Selepe, M.A., Van Heerden, F.R. Application of the Suzuki-Miyaura reaction in the synthesis of flavonoids. *Molecules* **2013**, 18, 4739−4765.

Shah, M.S., Najam-ul-Haq, M., Shah, H.S., Umar, S., Rizvi, F., Iqbal, J. Quinoline containing chalcone derivatives as cholinesterase inhibitors and their *in silico* modelling studies. *Comput. Biol. Chem.* **2018**, 76, 310−317.

Shen, S., Huang, X., Zhang, Y., Zhu, Y., Hou, C., Ge, Y., Cao, X. Ratiometric fluorescent probe for the detection of HOCl in lysosomes based on FRET strategy. *Sensor Actuat. B-Chem.* **2018**, 263, 252−257.

Shylesh, S., Samuel, P.P., Srilakshmi, C., Parischa, R., Singh, A.P. Sulfonic acid functionalised mesoporous silicas and catalytic applications. *J. Mol. Catal. A:Chem.* **2007**, 274, 153−158.

Shinozaki, T., Ono, M., Higashi, K., Moribe, K. A novel drug-drug cocrystal of levofloxacin and metacetamol: reduced hygroscopicity and improved photostability of levofloxacin. *J. Pharm. Sci.* **2019**, 108, 2383−2390.

Song, G.J., Ma, H.L., Luo, J., Cao, X., Zhao, B. A new ratiometric fluorescent probe for sensing HOCl based on TBET in real time. *Dyes Pigments* **2018**, 148, 206−211.

Sriramurthy, V. and Kwon, O. Synthesis of indolines, dihydropyrrolopyridines, benzimidazolines, tetrahydroquinolines, tetrahydroisoquinolines, dihydrobenzo-1,4-oxazines, and dihydrobenzo-3,1-oxazines. *Org. Lett.* **2010**, 12, 1084−1087.

Sulzipio, C., Breibeck, J., Rompel, A. Recent progress in synthesis and characterisation of metal chalcone complexes and their potential as bioactive agents. *Coord. Chem. Rev.* **2018**, 347, 497−524.

Tang, W., Gao, Y., Liu, B., Tong, H. Catalyst for synthesis of chalcone compound and its application. Chinese patent CN 110124744, June 12, 2019.

Takahashi, S., Murata, E., Sonogashira, K., Hagihara, N. Studies on polyene polymers containing transition metals in the main chain. IV. Polymer synthesis by oxidative coupling of transition metal-bis(acetylide) complexes. *J. Polymer Sci. Polymer Chem. Ed.* **1980**, 18, 661−669.

Tomar, V., Bhattacharjee, G., Kamaluddin, Kumar, A. Synthesis and antimicrobial evaluation of new chalcones containing piperazine or 2,5-dichlorothiophene moiety. *Bioorg. Med. Chem. Lett.* **2007**, 17, 5321−5324.

Tseng, C.H., Chen, Y.L., Hsu, C.Y., Chen, T.C, Cheng, C.M., Tso, H.C., Lu, Y.J., Tzeng, C.C. Synthesis and antiproliferative evaluation of 3-phenylquinolinylchalcone derivatives against non-small cell lung cancers and breast cancers. *Eur. J. Med. Chem.* **2013**, 59, 274−282.

Vander Mierde, H., Van Der Voort, P., De Vos, D., Verpoort, F. Ruthenium-catalysed approach to the Friëdlander Quinoline Synthesis. *Eur. J. Org. Chem.* **2008**, 9, 1625−1631.

Vilsmeier, A., Haack, A. About the action of halogenophosphorus on alkyl formanilides. A new method for the preparation of secondary and tertiary alkylaminobenzaldehydes. *Ber. Dtsch. Chem. Ges.* **1927**, *60*, 119−122.

Volpi, G., Lace, B., Garino, C., Priola, E., Artuso, E., Vioglio, P.C., Barolo, C., Fin, A., Genre, A., Prandi, C. New substituted imidazo[1,5-a]pyridine and imidazo[5,1-a]isoquinoline derivatives and their application in fluorescence cell imaging. *Dyes Pigments* **2018**, 157, 298−304.

Wang, F., Xu, J., Dubois, J.L., Ueda, W. Catalytic oxidative dehydration of glycerol over a catalyst with iron oxide domains embedded in an iron orthovanadate phase. *Chem. Sus. Chem.* **2010**, 3, 1383−1389.

Wu, W., Liu, Y., Ye, H., Li, Z. Millepachine showed novel antitumor effects in cisplatin-resistant human ovarian cancer through inhibiting drug efflux function of ATP-binding cassette transporters. *Phytother. Res.* **2018**, 32, 2428−2435.

Wu, W., Ye, H., Wan, L., Han, X., Wang, G., Hu, J., Tang, M., Duan, X., Fan, Y., He, S., Huang, L., Pei, H., Wang, X., Li, X., Xie, C., Zhang, R., Yuan, Z., Mao, Y., Wei, Y., Chen, L. Millepachine, a novel chalcone, induces G$_2$/M arrest by inhibiting CDK1 activity and causing apoptosis *via* ROS-mitochondrial apoptotic pathway in human hepatocarcinoma cells *in vitro* and *in vivo*. *Carcinogenesis* **2013**, 34, 1636–1643.

Wu., X. -F., Neumann, H., Spannenberg, A., Schulz, T., Jiao, H., Beller, M. Development of a general palladium-catalysed carbonylative Heck reaction of aryl halides. *J. Am. Chem. Soc.* **2010**, 132, 14596–14602.

Xu, J., Wenlong, L., Xu, S., Xu, F., Wen, S., Sun, H., Zhu, Z., Yao, H. Preparation of quinoline substituted chalcone compounds useful as tubulin polymerization inhibitors for the treatment of cancer. Chinese patent CN 109467549, December 7, 2018.

Xu, Q., Zhigao, Y., Dulin, Y., Zhang, F. Synthesis of chalcones catalysed by a novel solid sulfonic acid from bamboo. *Catal.* **2008**, 9, 1579–1582.

Yan, J., Chen, J., Zhang, S., Hu, J., Huang, L., Li, X. Synthesis, evaluation, and mechanism study of novel indole-chalcone derivatives exerting effective anti-tumor activity through microtubule destabilisation *in vitro* and *in vivo*. *J. Med. Chem.* **2016**, 59, 5264–5283.

Yu, P., Zhao, L., Zhao, Y., Miao, A., Hao, L., Fu, Y., Ding, Y., Xiang, C., Lu, K., Teng, Y. Selenium-containing chalcone derivative compound 1, and its synthesis method and application in preparation of drug for treating non-alcoholic steatohepatitis. Chinese patent CN 110143902, June 12, 2019.

Yu, X., Wang, J., Guo, W., Tian, Y., Wang, J. Efficient approach to construct unsymmetrical biaryls through oxidative coupling reactions of aromatic primary alcohols and arylboronic acids with a rhodium catalyst. *Organometallics* **2016**, 35, 1876–1884.

Zenger, K., Dutta, S., Wolff, H., Genton, M.G., Kraus, B. *In vitro* structure-toxicity relationship of chalcone in human hepatic stellate cells. *Toxicology* **2015**, 336, 26–33.

Zhou, Y., Wang, J., Gu, Z., Wang, S., Zhu, W., Aceña, J.L., Soloshonok, V.A., Izawa, K., Liu, H. Next generation of fluorine-containing pharmaceuticals, compounds currently in phase II-III clinical trials of major pharmaceutical companies: new structural trends and therapeutic areas. *Chem. Rev.* **2016**, 116, 422–518.

UNIVERSITY OF KWAZULU-NATAL

SYNTHESIS, CHARACTERISATION AND ANTIBACTERIAL

ACTIVITY OF QUINOLINE CHALCONE HYBRIDS

APPENDIX

2019

GILLEAN PAMELA FRASER
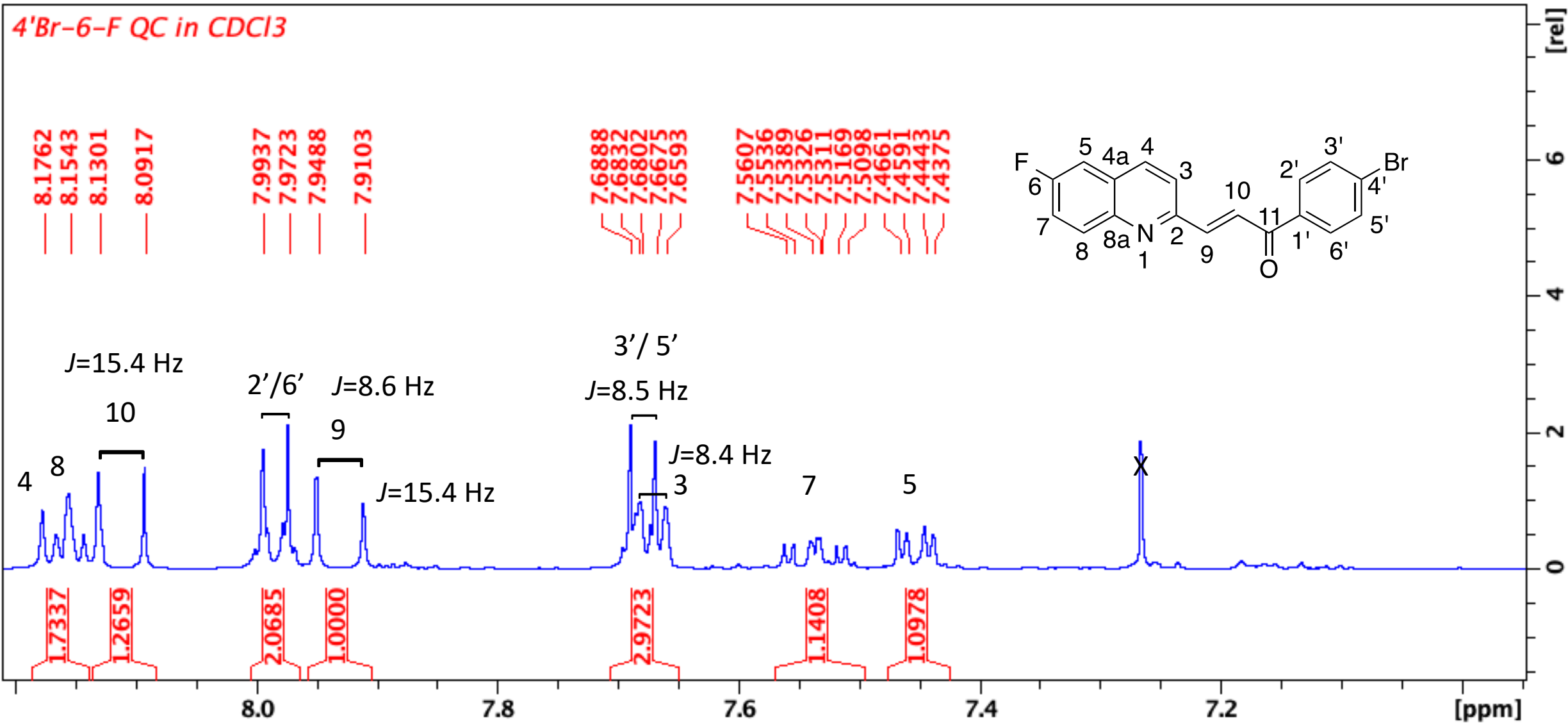
The ^{1}H NMR of compound **8a**

The ^{13}C NMR of compound **8a**

2
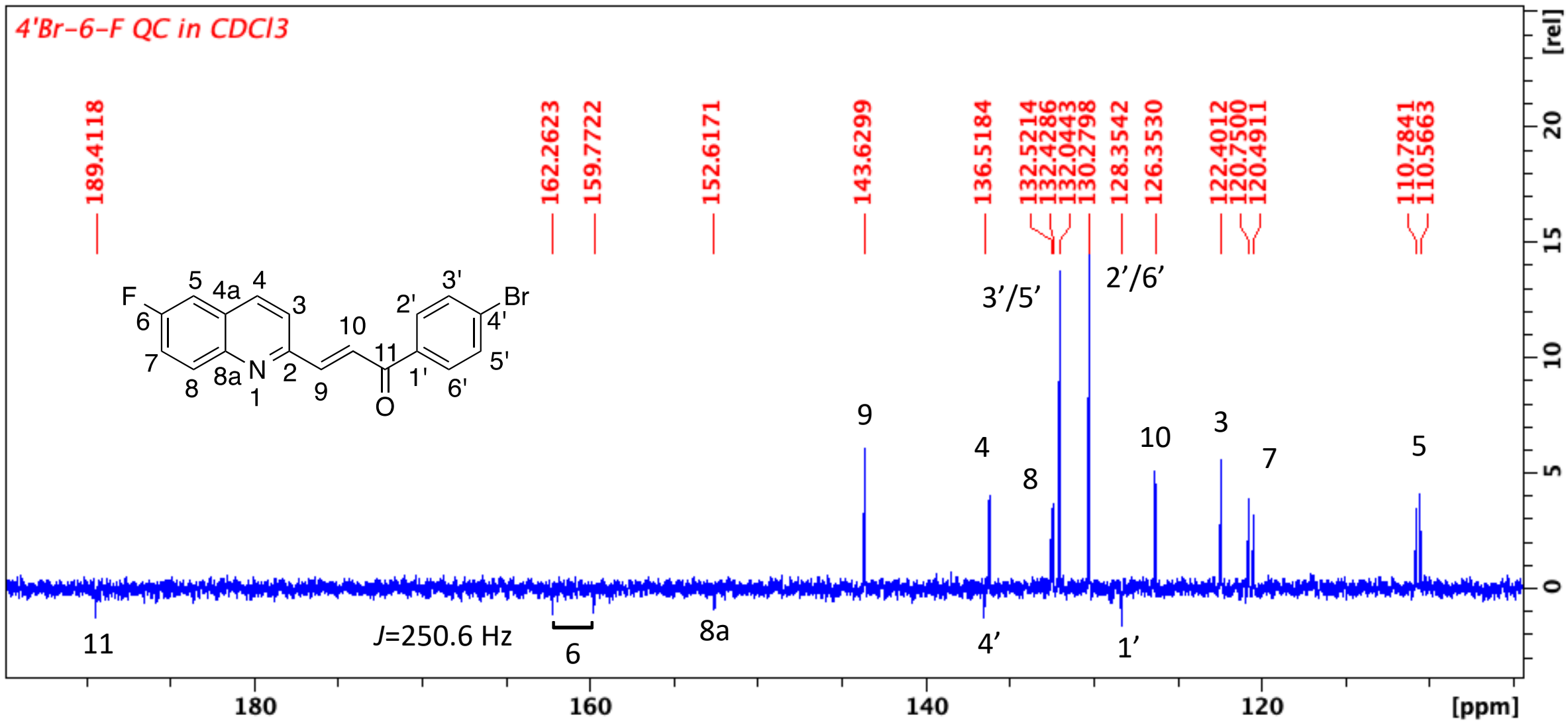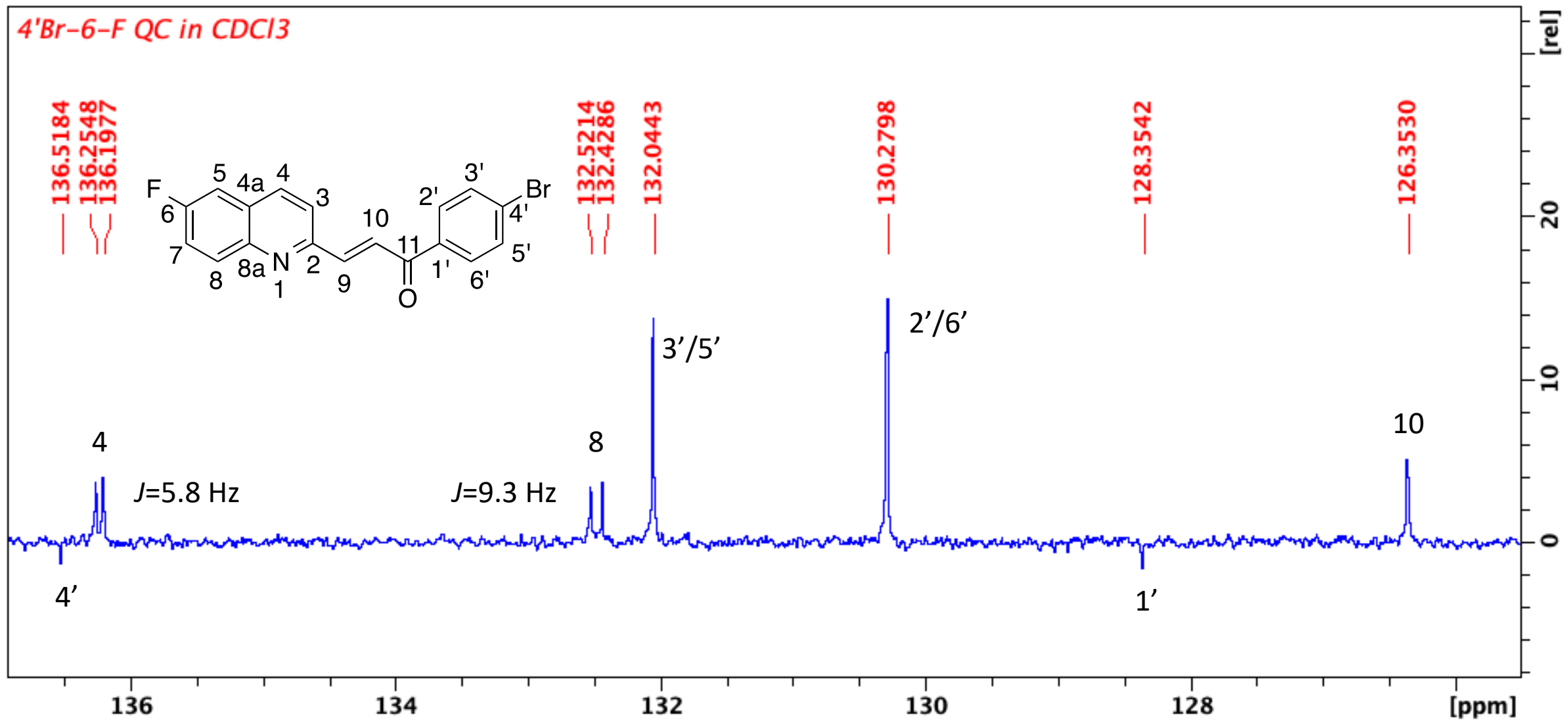
The expanded ^{13}C NMR of compound **8a**
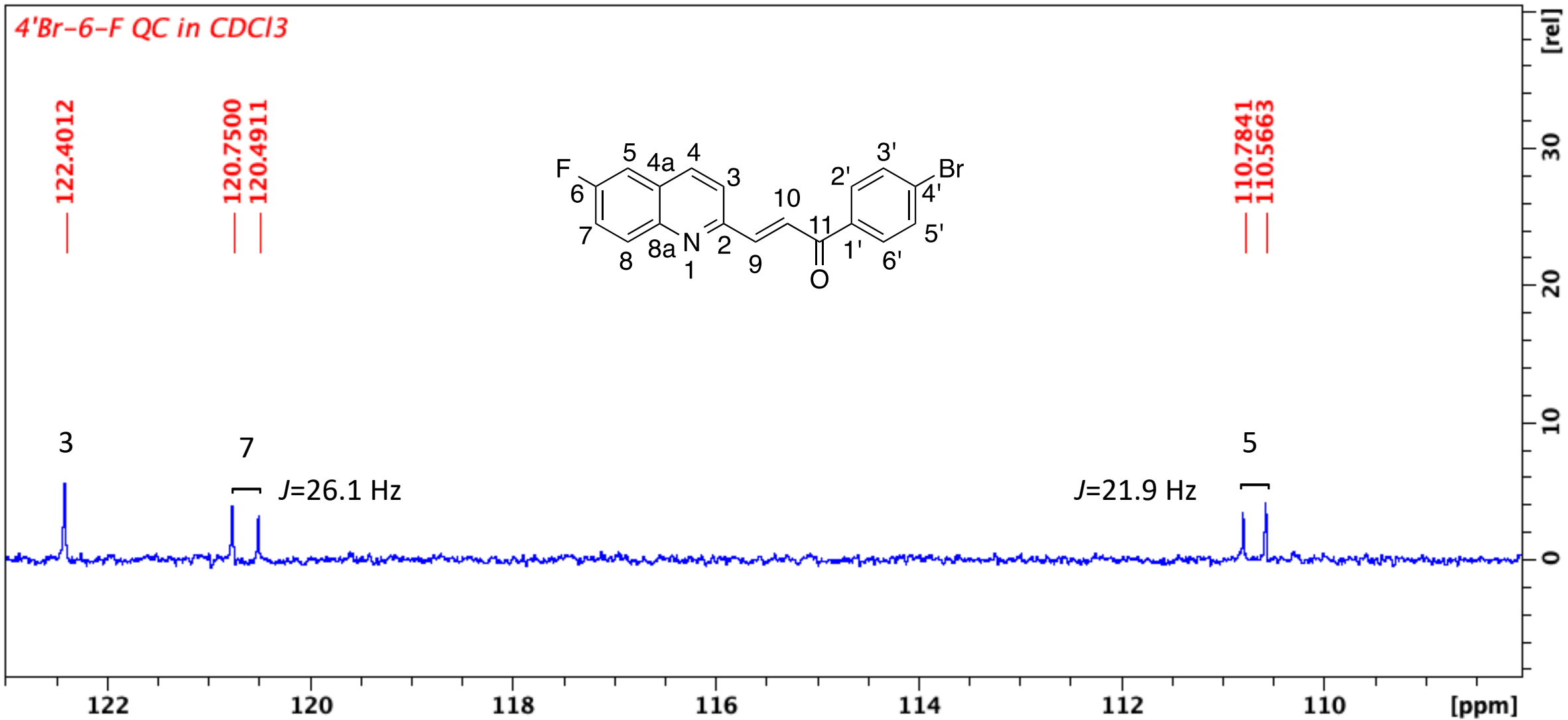
The expanded ^{13}C NMR of compound **8a**
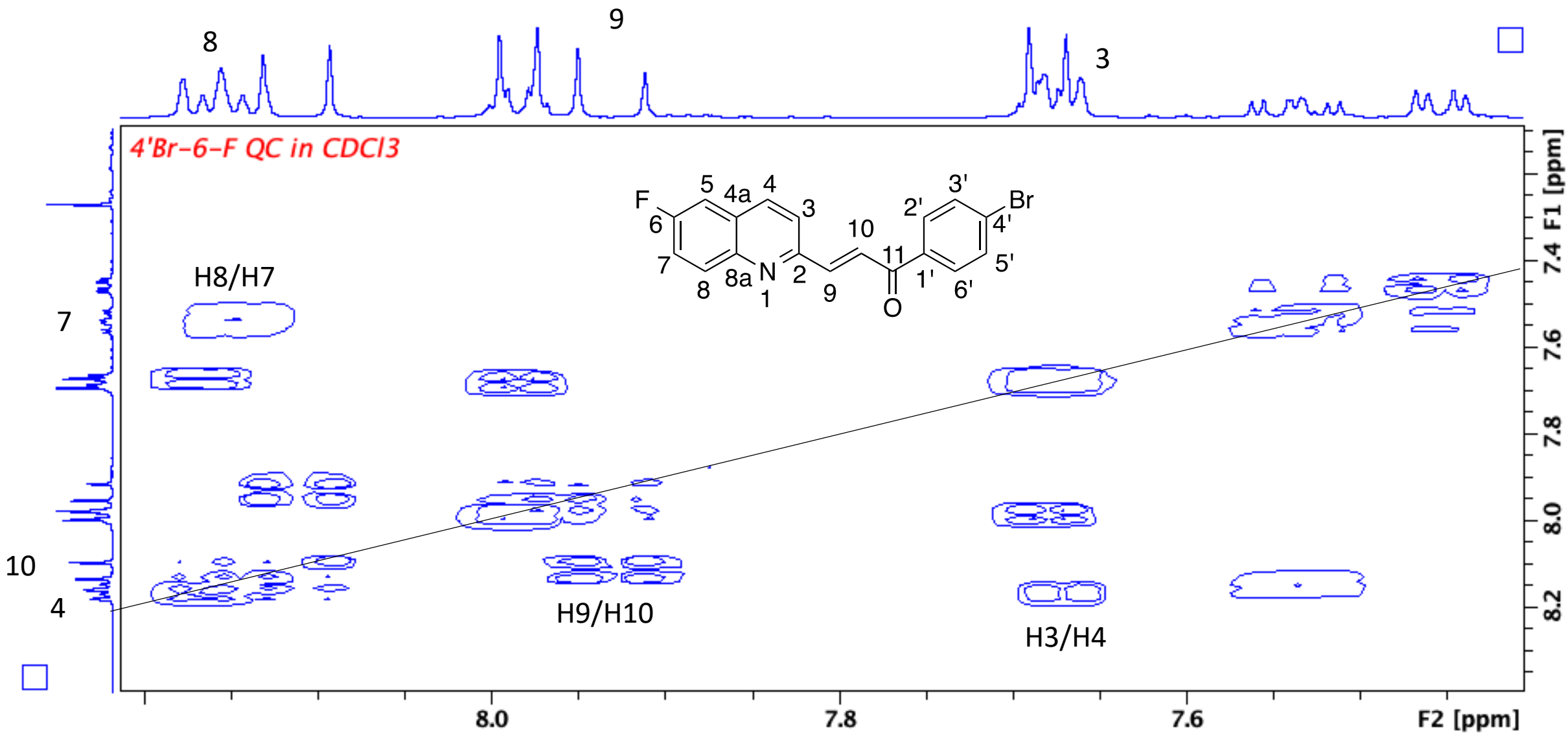
The COSY spectrum of compound **8a**
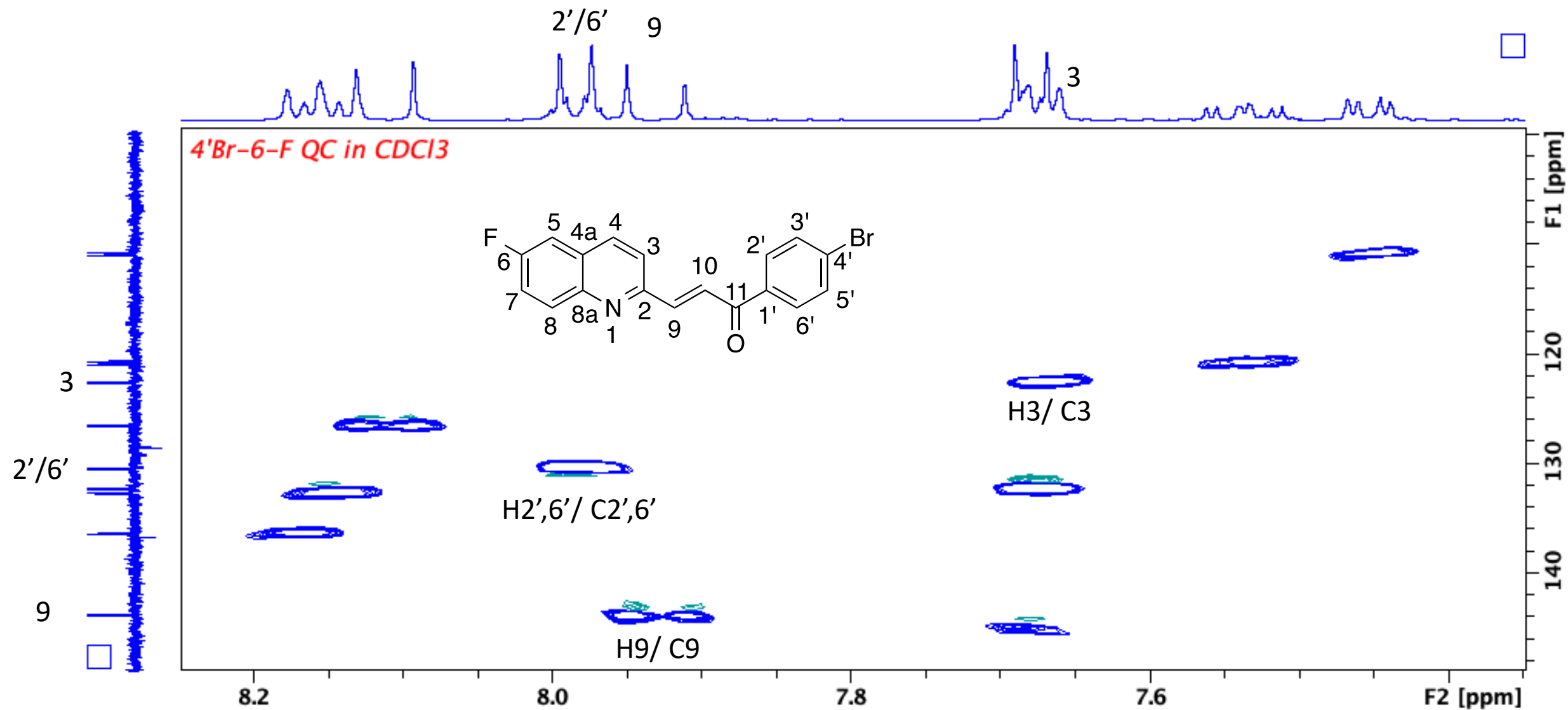
The HSQC of compound **8a**
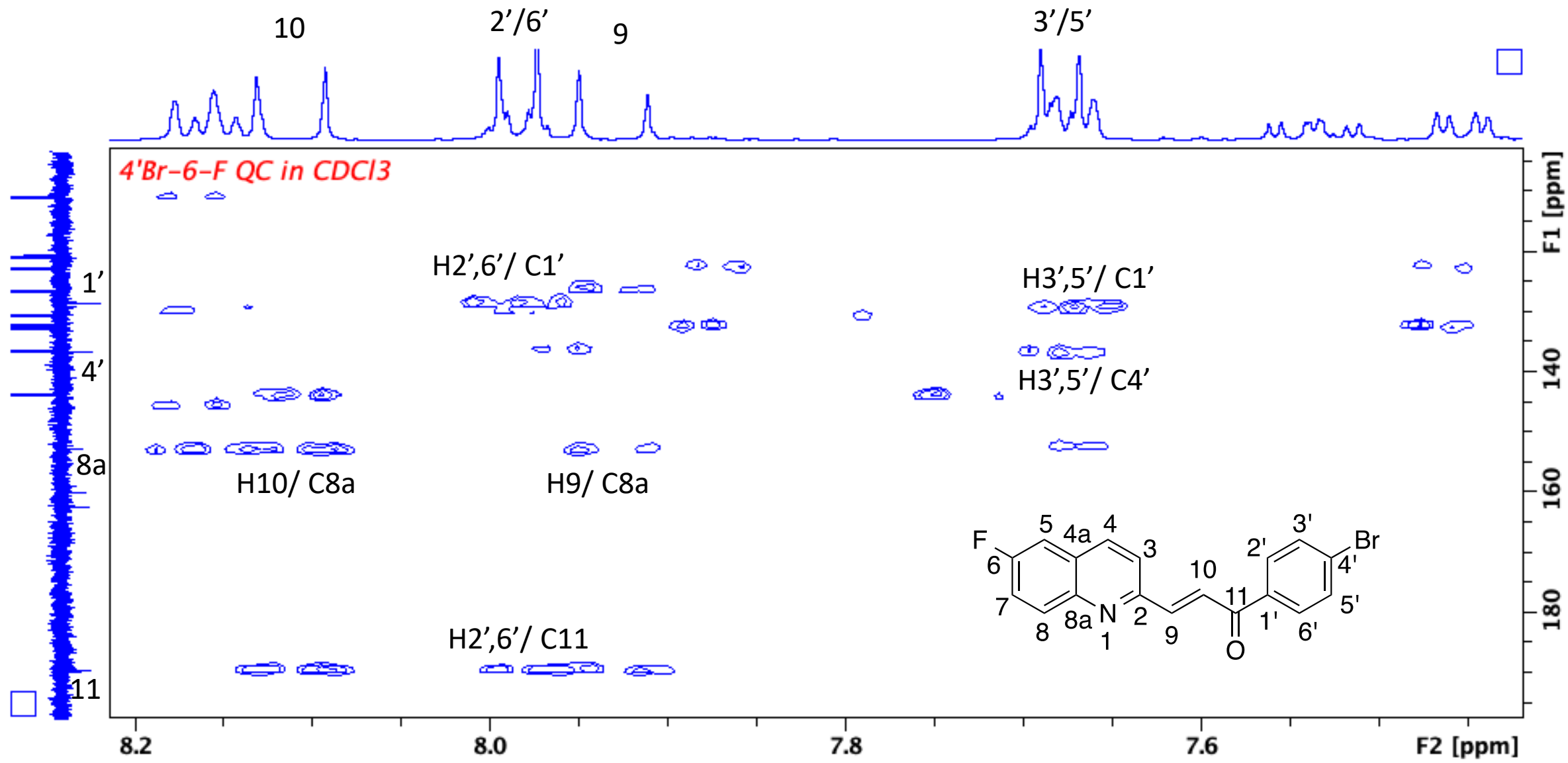
The HMBC of compound **8a**

Single Mass Analysis
Tolerance = 5.0 PPM   /   DBE: min = -1.5, max = 50.0
Element prediction: Off
Number of isotope peaks used for i-FIT = 3

Monoisotopic Mass, Even Electron Ions
37 formula(e) evaluated with 1 results within limits (all results (up to 1000) for each mass)
Elements Used:
C: 15-20   H: 10-15   N: 0-5   O: 0-5   F: 1-1   Br: 0-1

Cmpd 1 14 (0.438) Cm (1:61)
TOF MS AP+
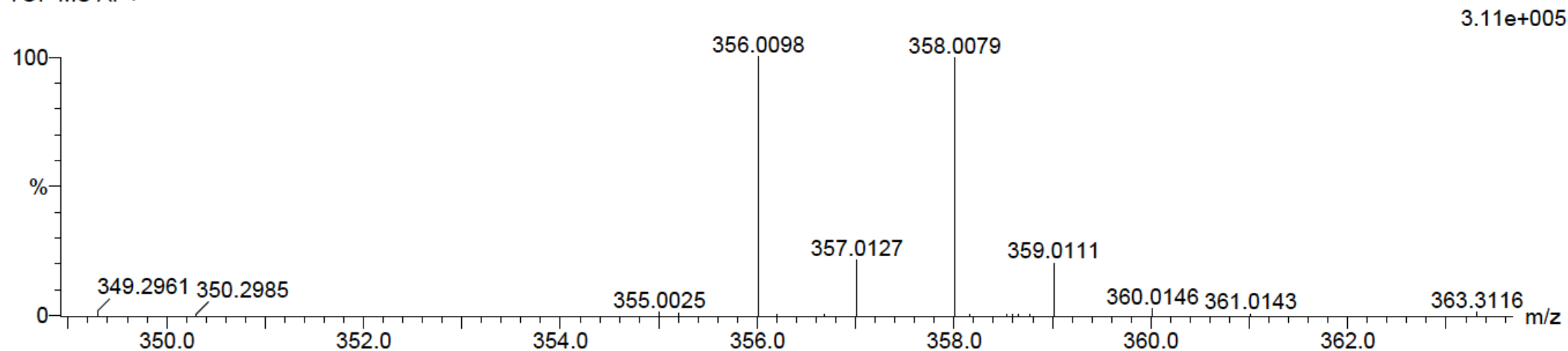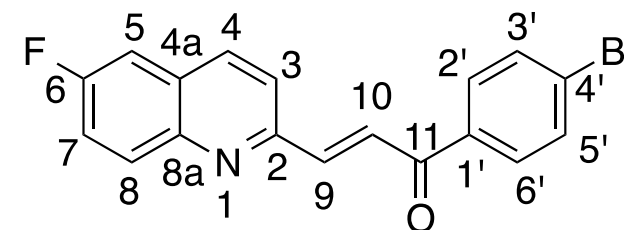
HRMS spectrum of compound **8a**

Infrared spectrum of compound **8a**

4'-Br-6-F quinoline chalcone

c:\pel_data\spectra\gillean msc\4'-br-6f qc.sp

9
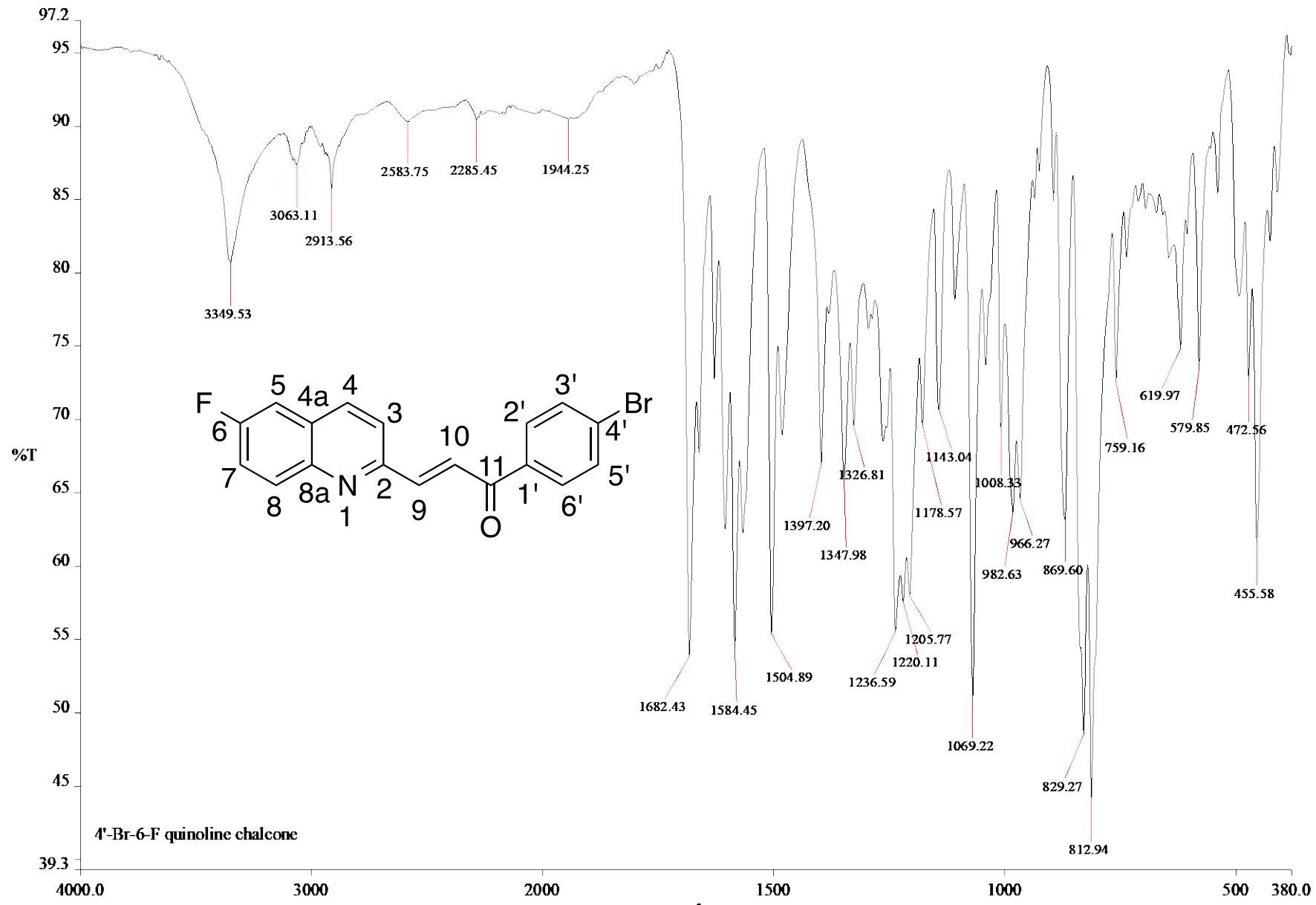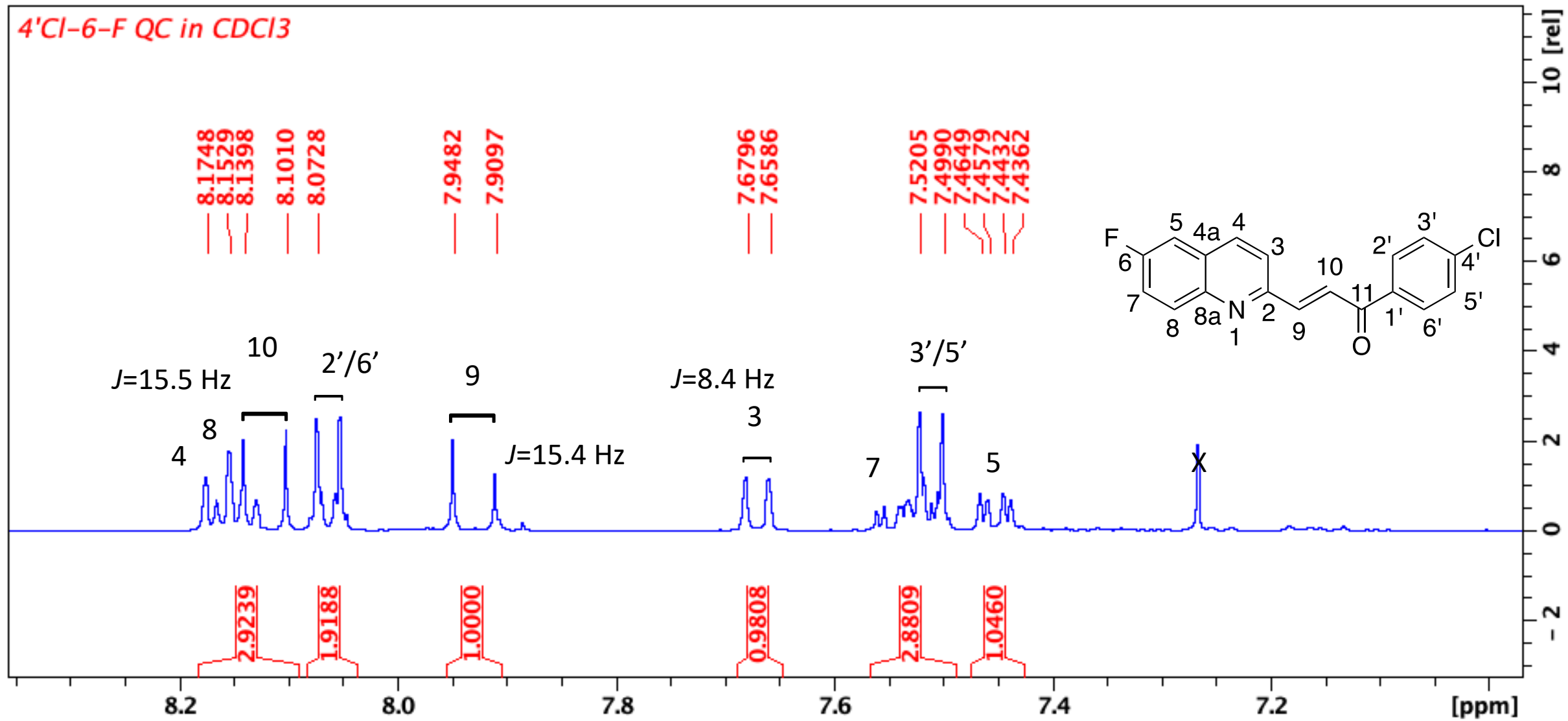
The ¹H NMR of compound **8b**
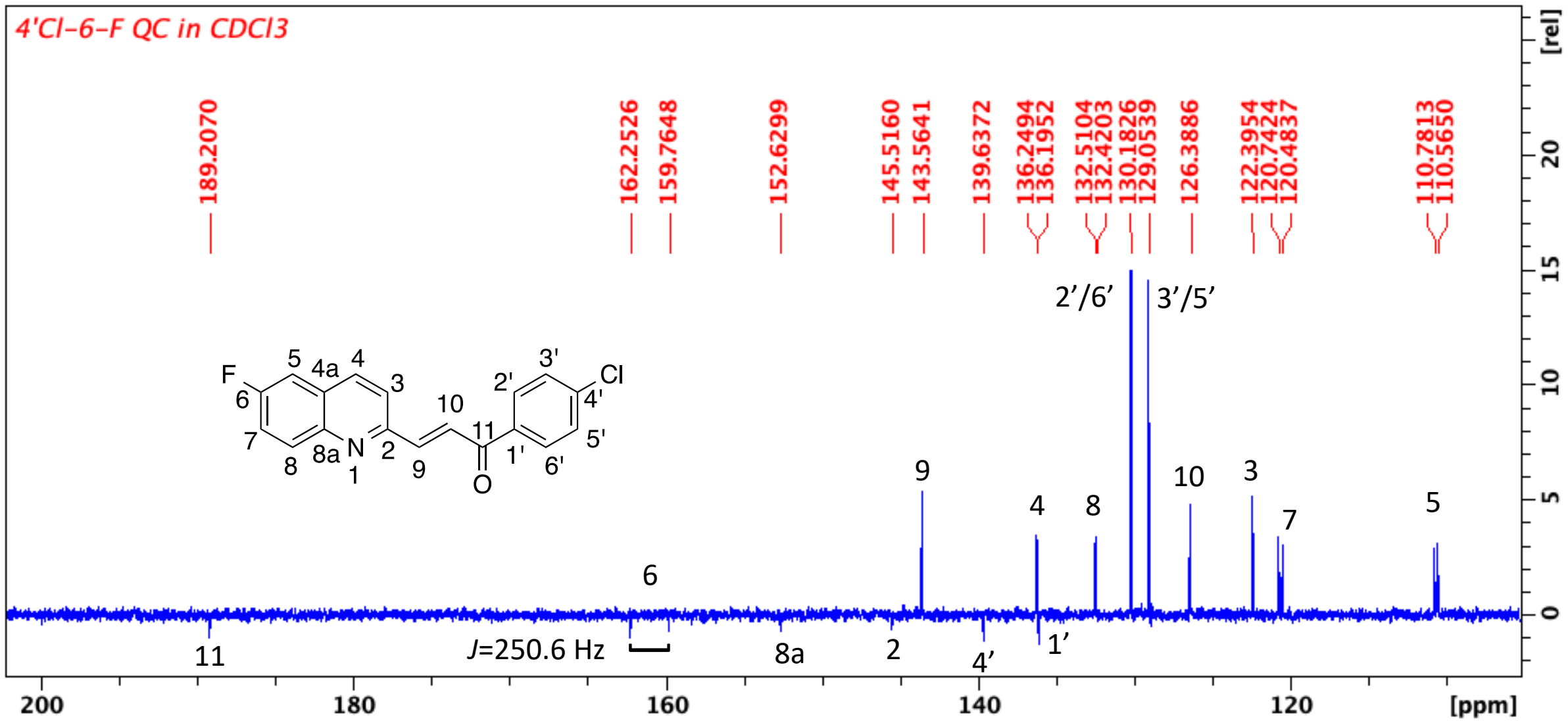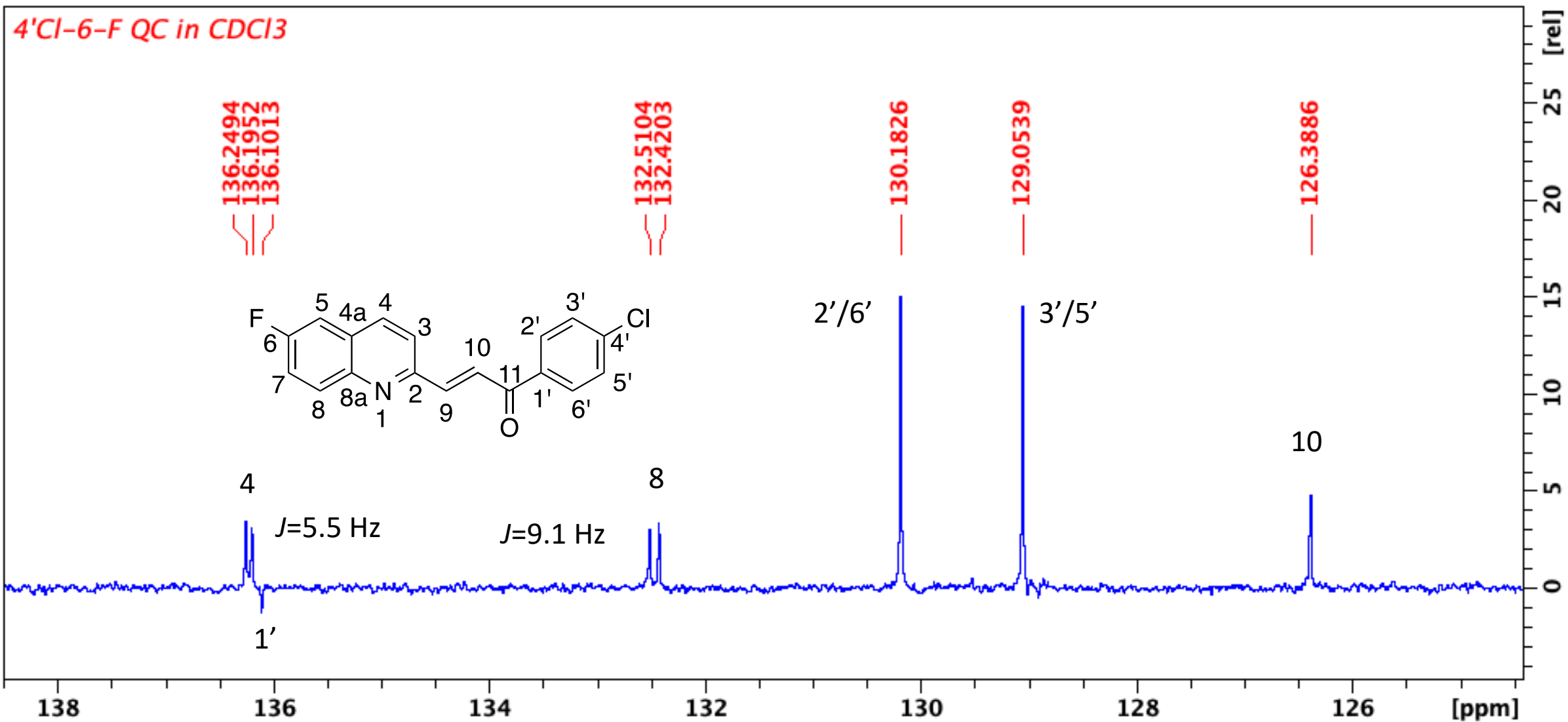
The ^{13}C NMR of compound **8b**

The expanded ^{13}C NMR of compound **8b**

12
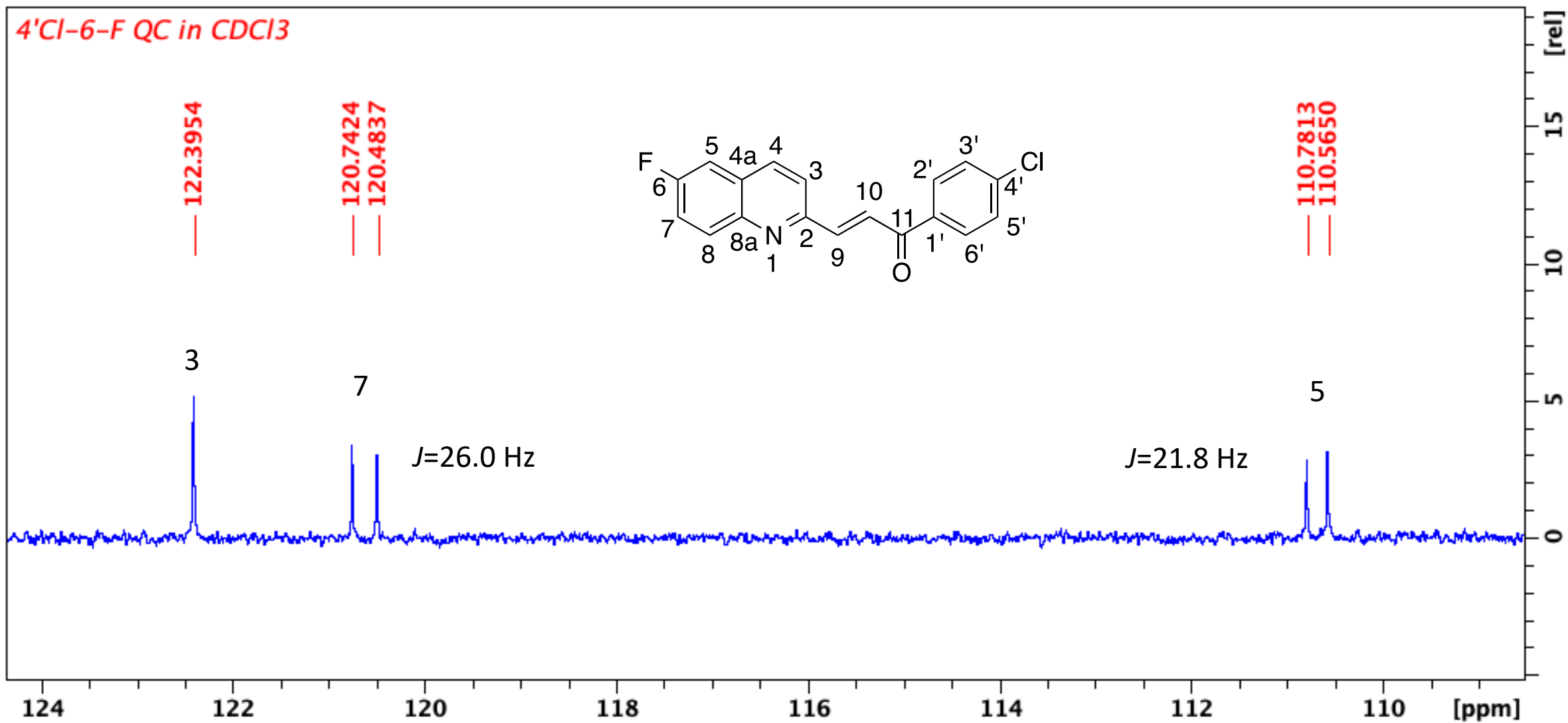
The expanded ^{13}C NMR of compound **8b**

The COSY spectrum of compound **8b**

14
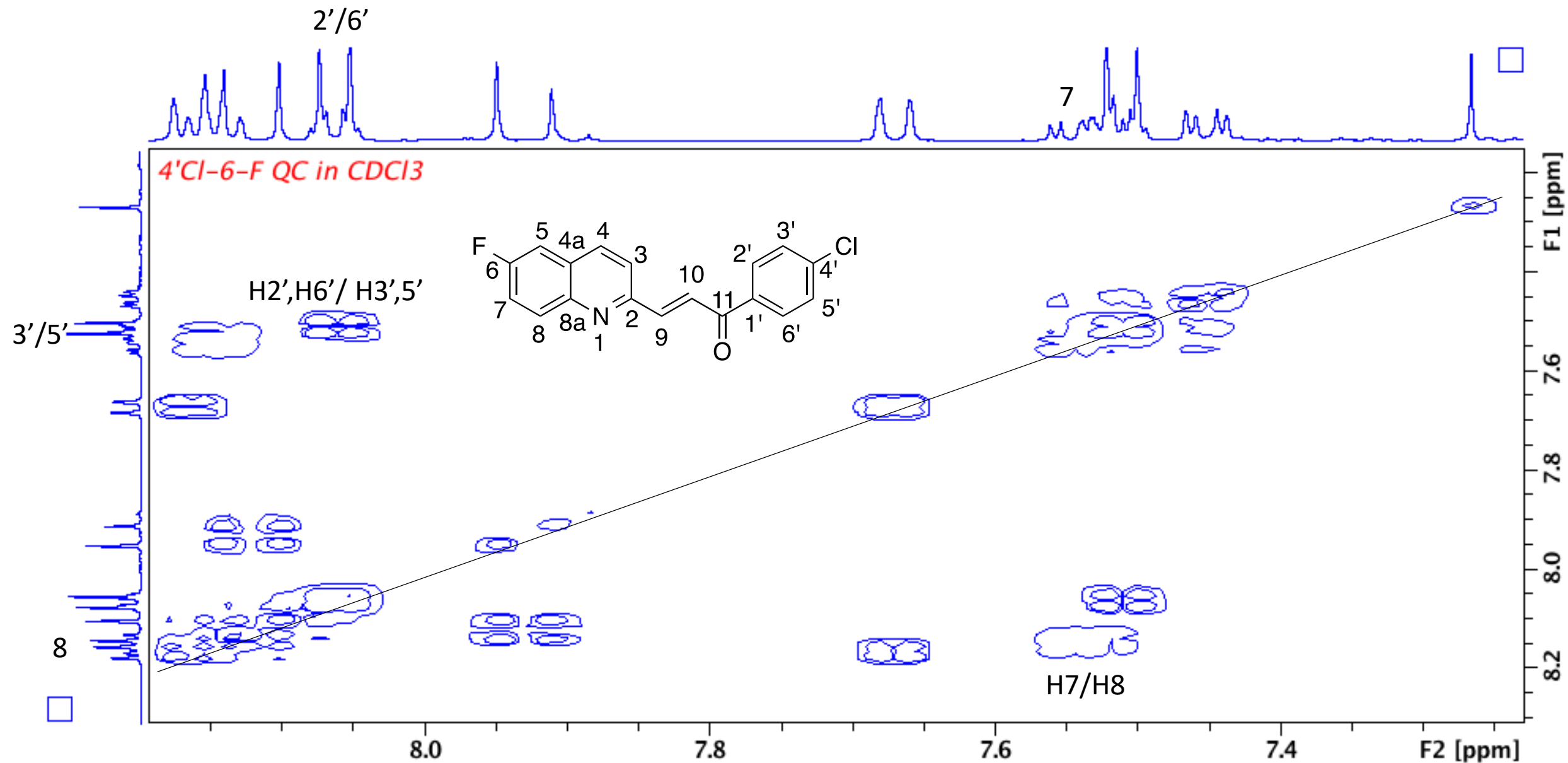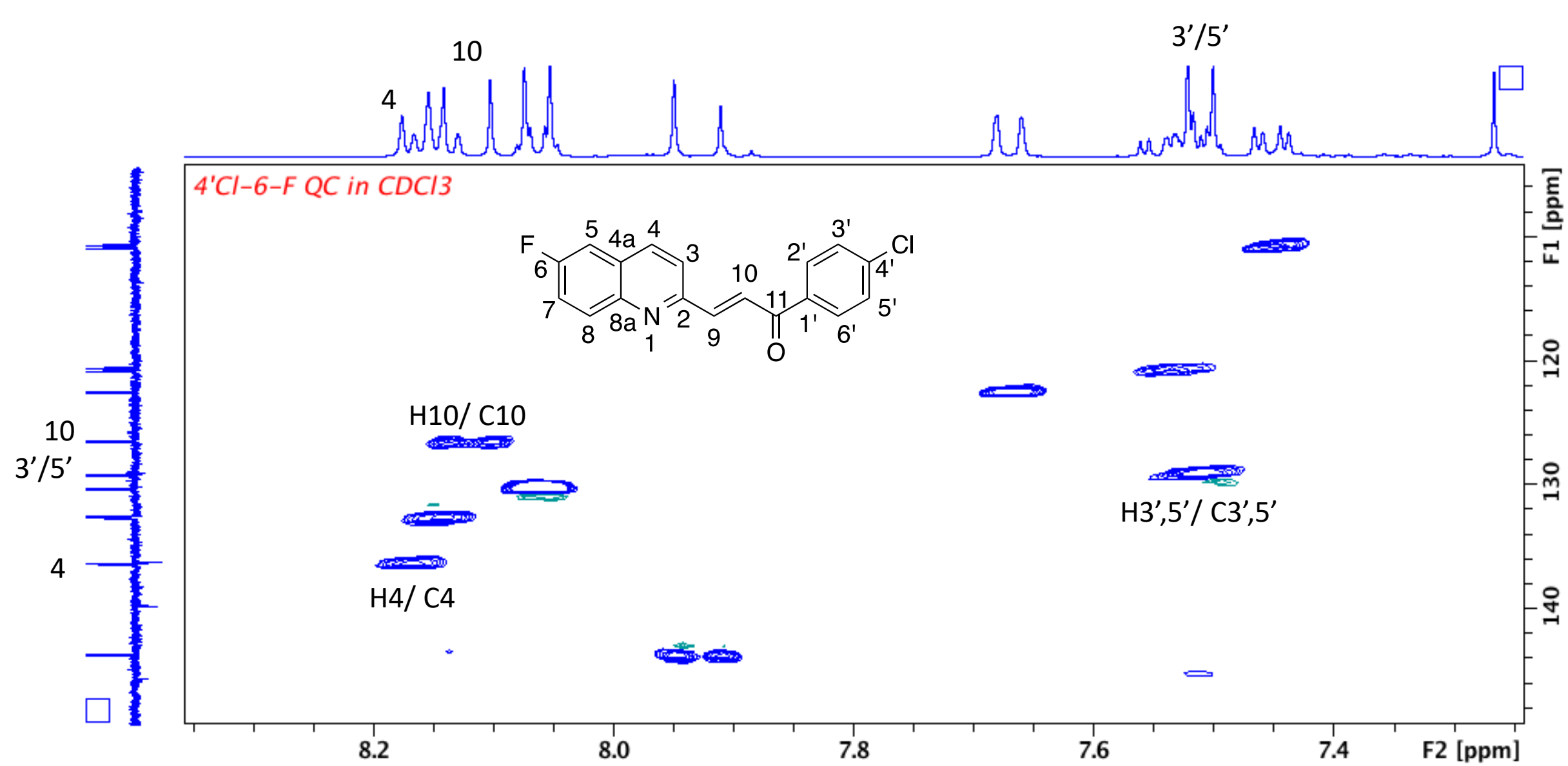
The HSQC of compound **8b**
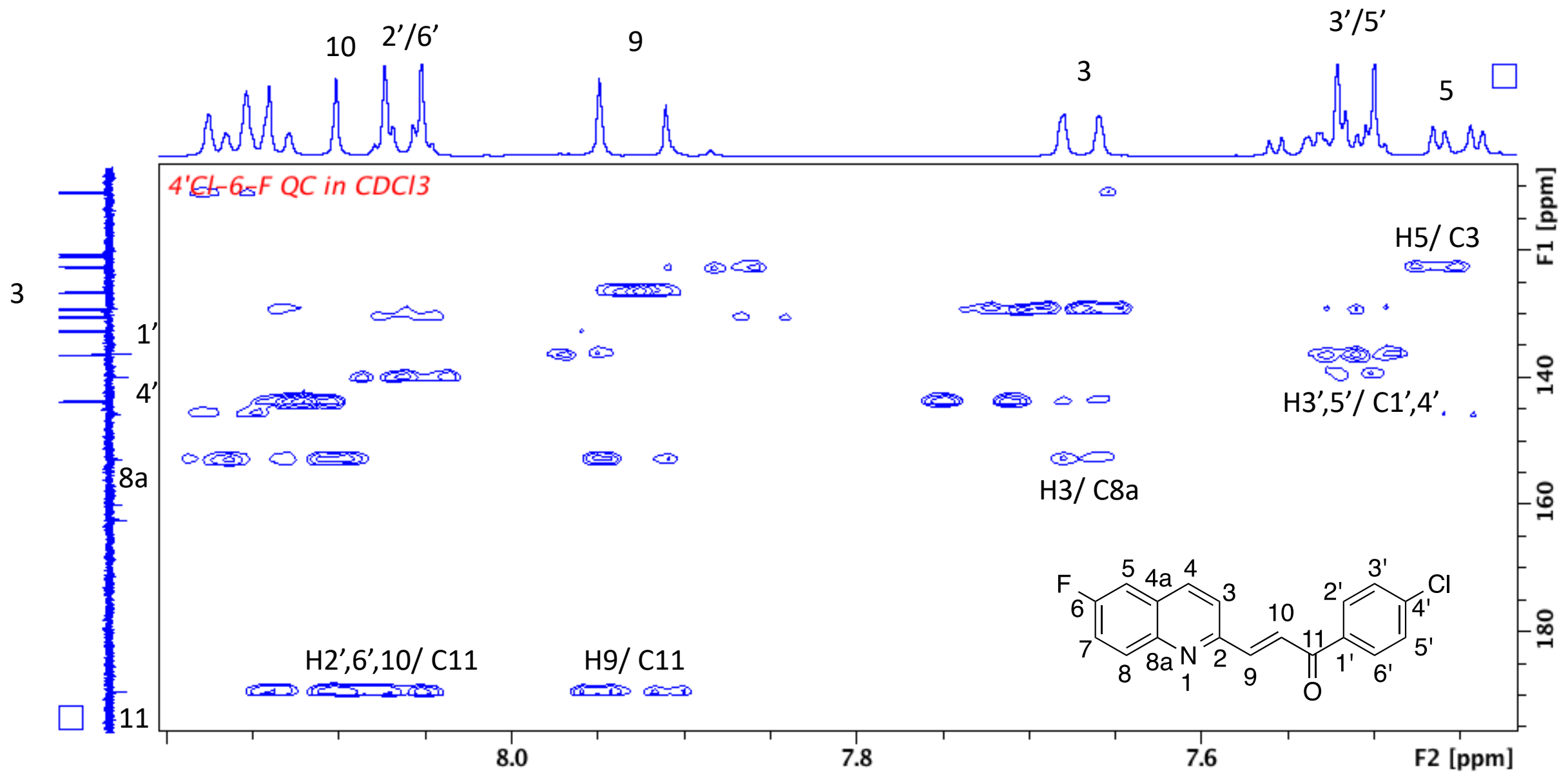
The HMBC of compound **8b**

Single Mass Analysis
Tolerance = 5.0 PPM   /   DBE: min = -1.5, max = 50.0
Element prediction: Off
Number of isotope peaks used for i-FIT = 3

Monoisotopic Mass, Even Electron Ions
38 formula(e) evaluated with 1 results within limits (all results (up to 1000) for each mass)
Elements Used:
C: 15-20   H: 10-15   N: 0-5   O: 0-5   F: 1-1   Cl: 0-1
Cmpd 2 51 (1.687) Cm (1:61)
TOF MS AP+
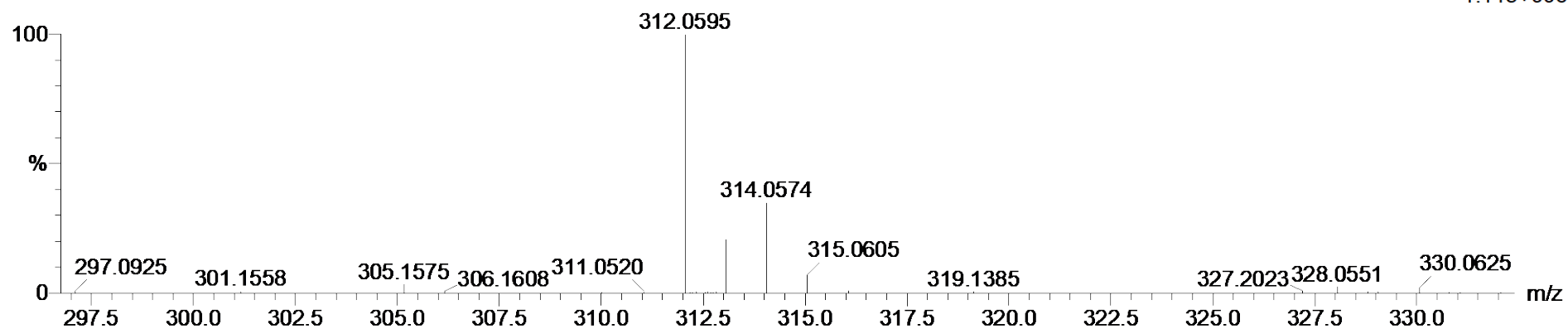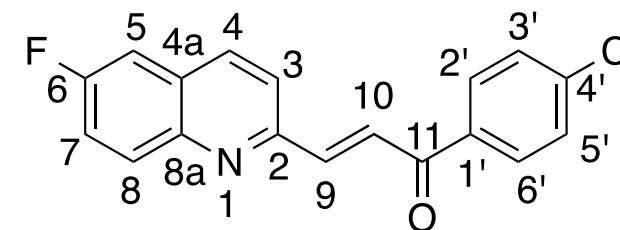
1.11e+005

Mass	Calc. Mass	mDa	PPM	DBE	i-FIT	i-FIT (Norm)	Formula
Minimum:				-1.5			
Maximum:		5.0	5.0	50.0			
312.0595	312.0591	0.4	1.3	12.5	106.7	0.0	C18 H12 N O F Cl

HRMS spectrum of compound **8b**
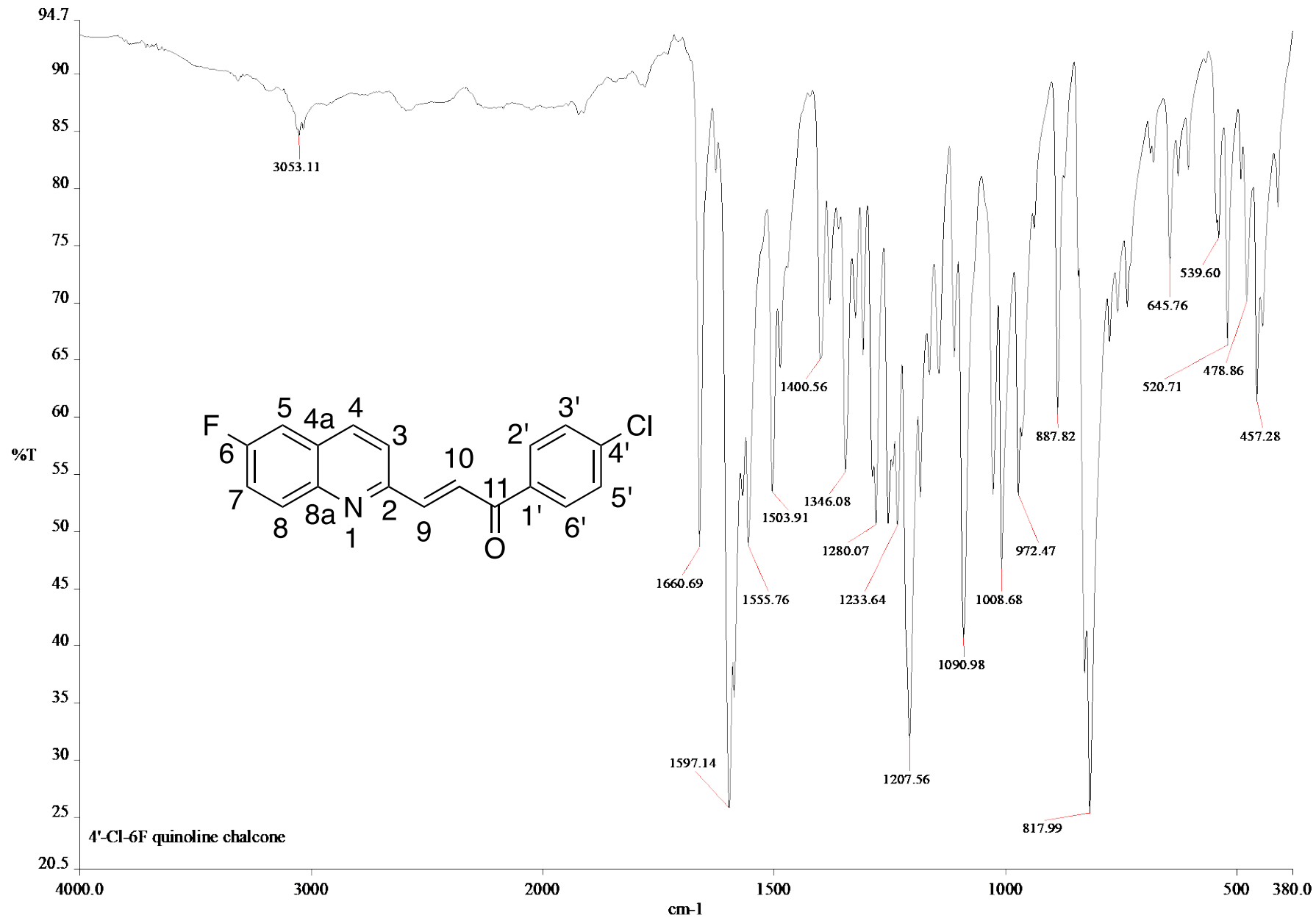
Infrared spectrum of compound **8b**

4'-Cl-6F quinoline chalcone

c:\pel_data\spectra\gillean msc\4'-cl-6f qc.sp

18
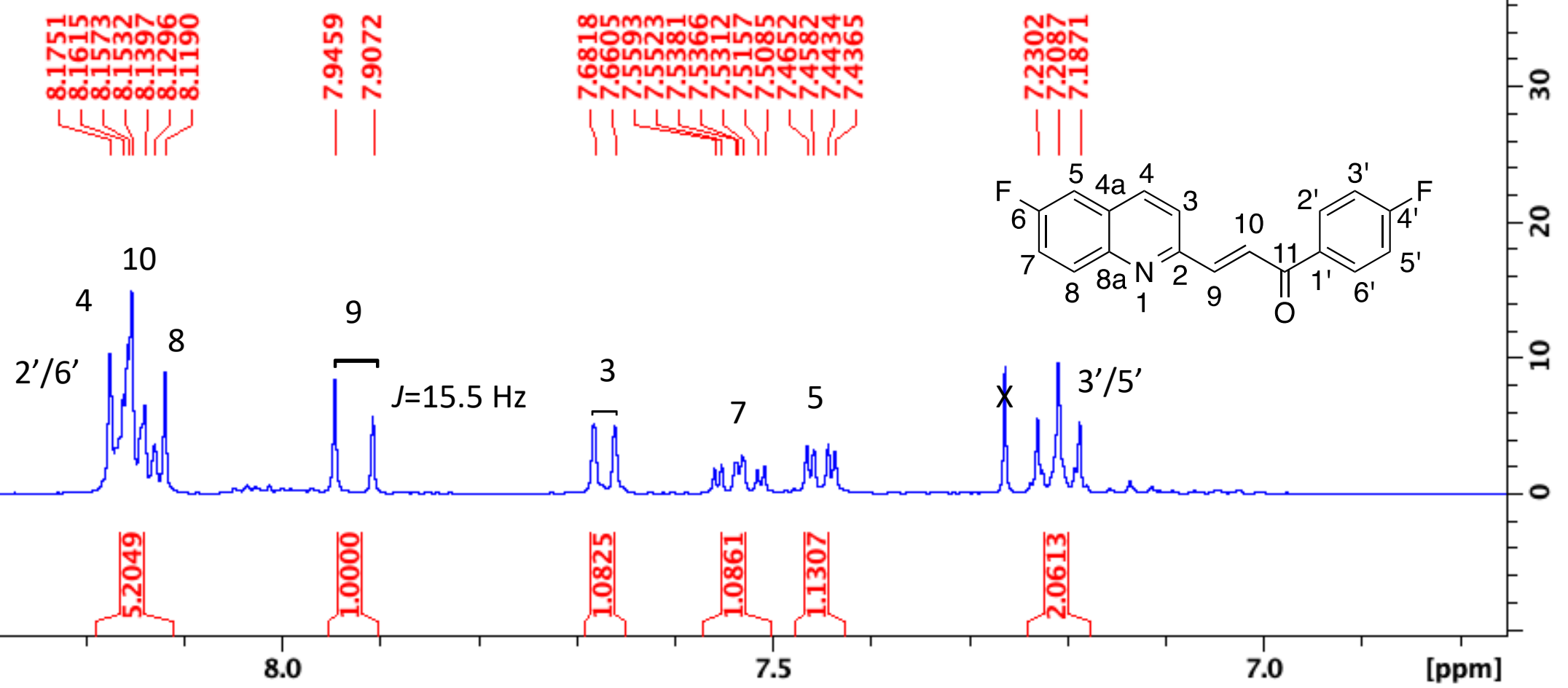
The ^{1}H NMR of compound **8c**
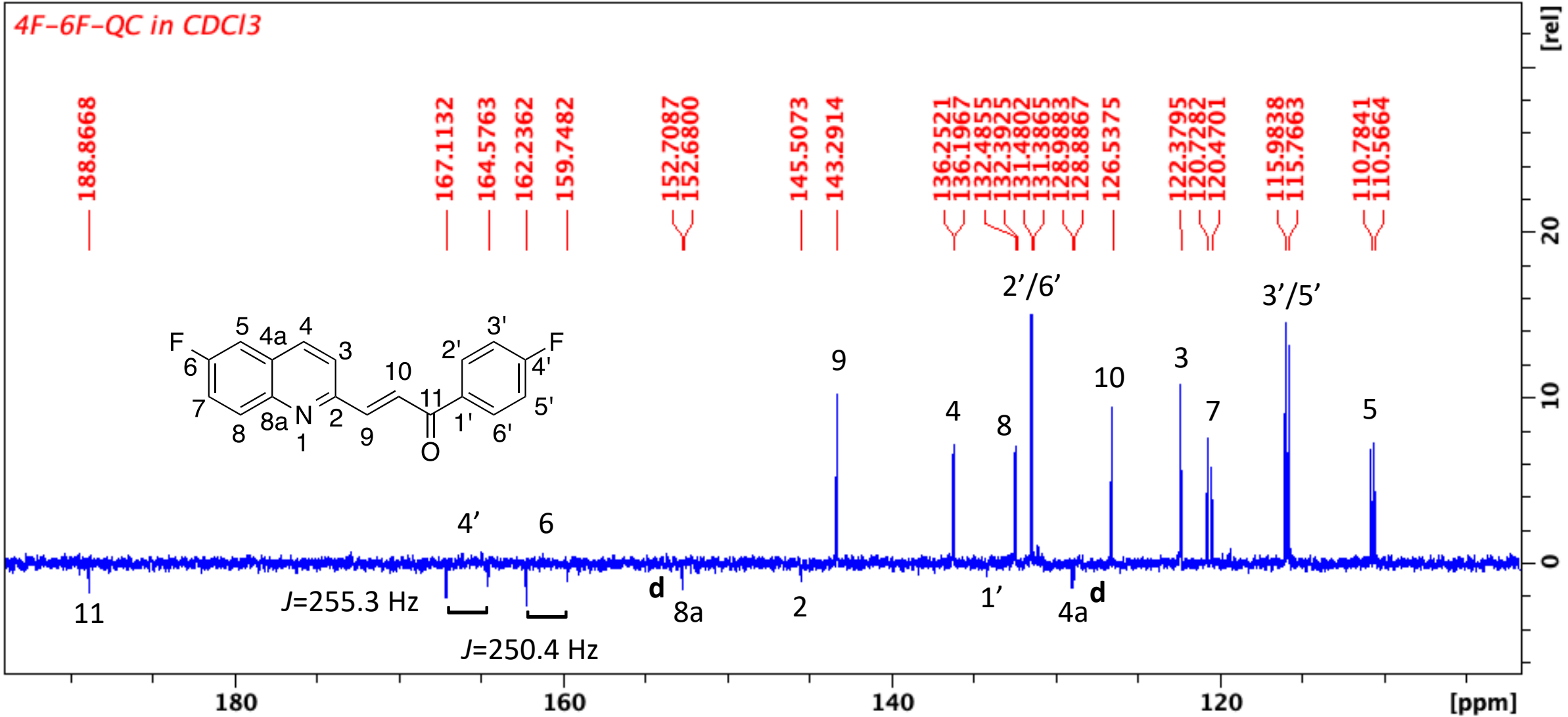
The ^{13}C NMR of compound **8c**

20

The expanded ^{13}C NMR of compound **8c**

21

The COSY spectrum of compound **8c**

22
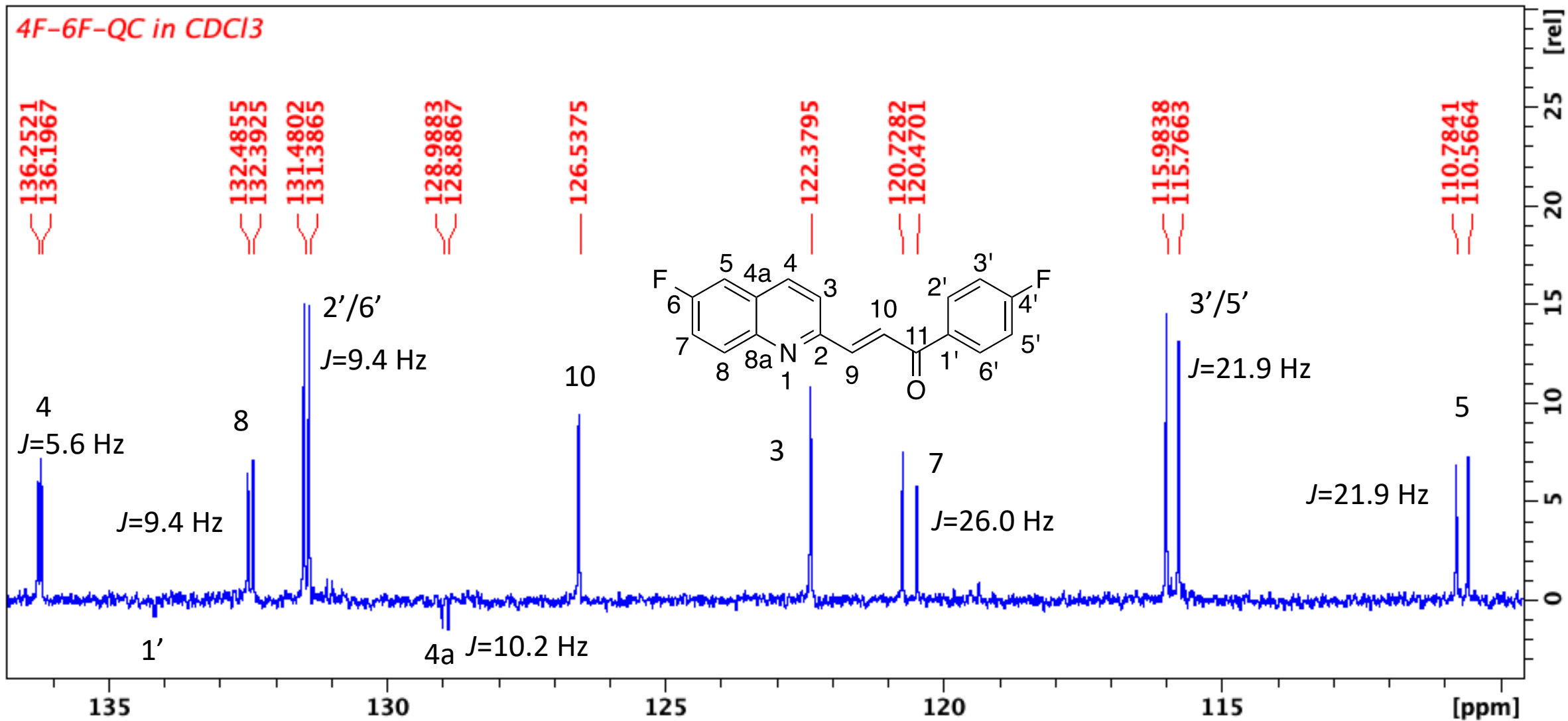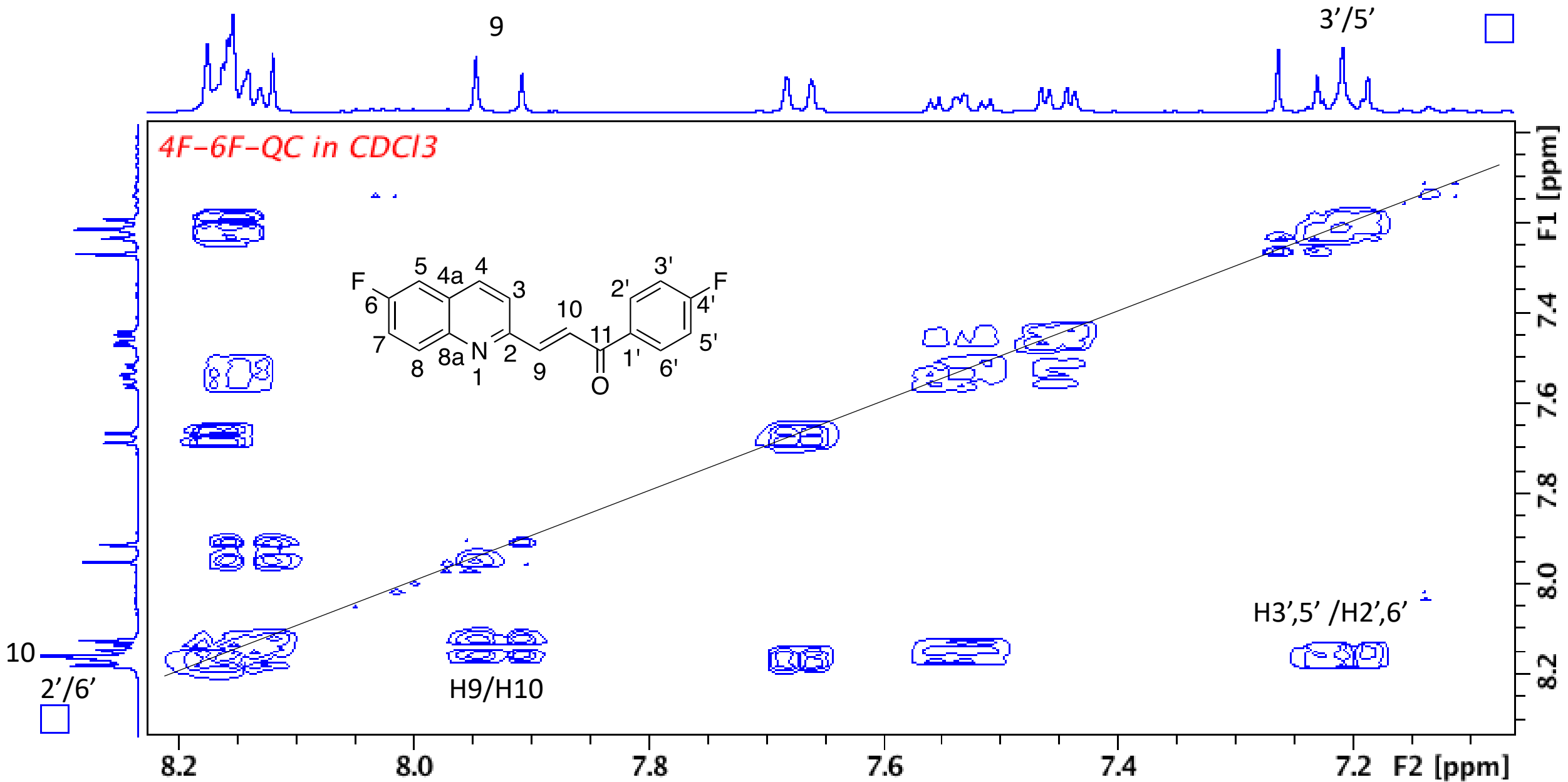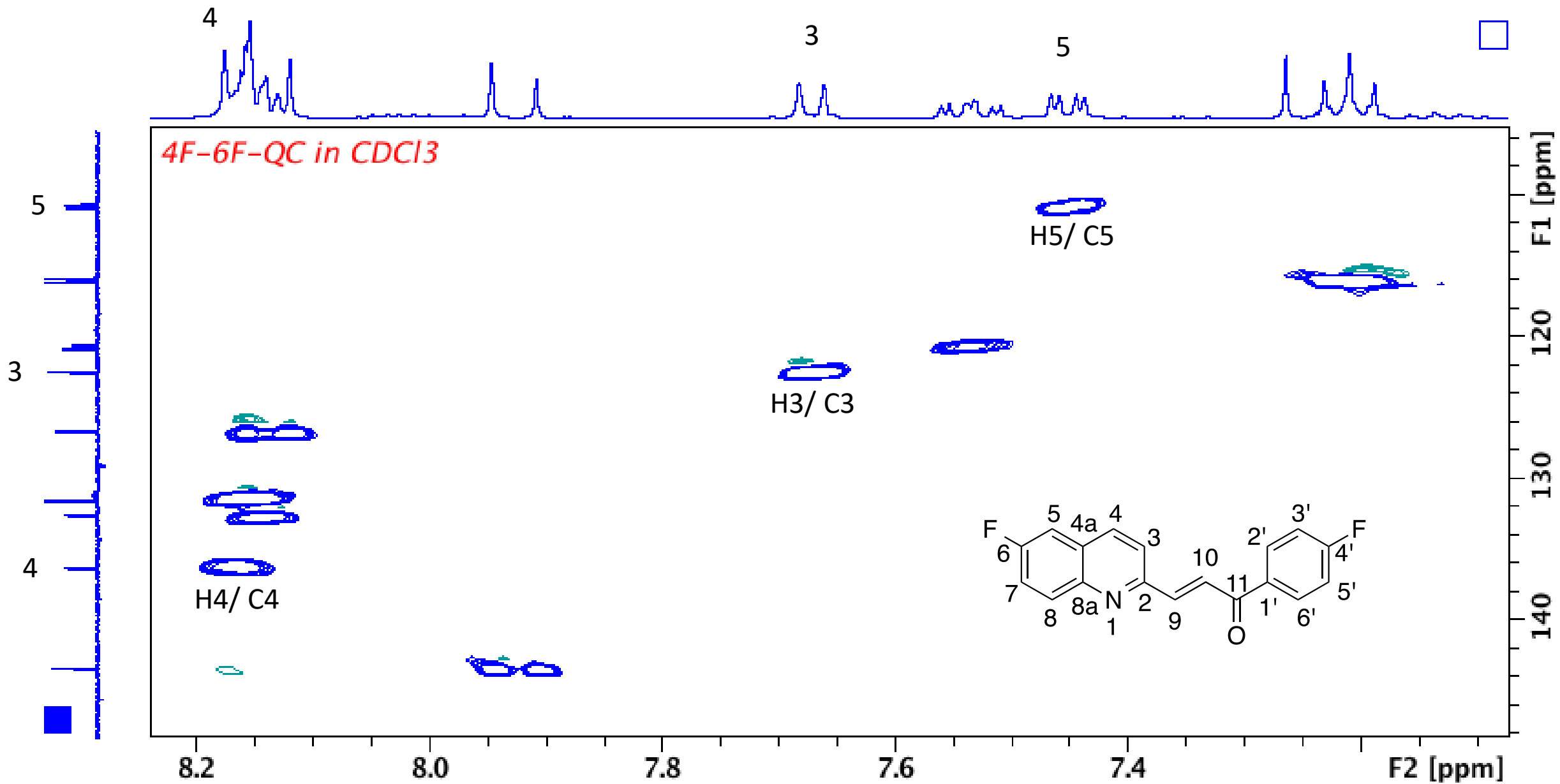
The HSQC of compound **8c**
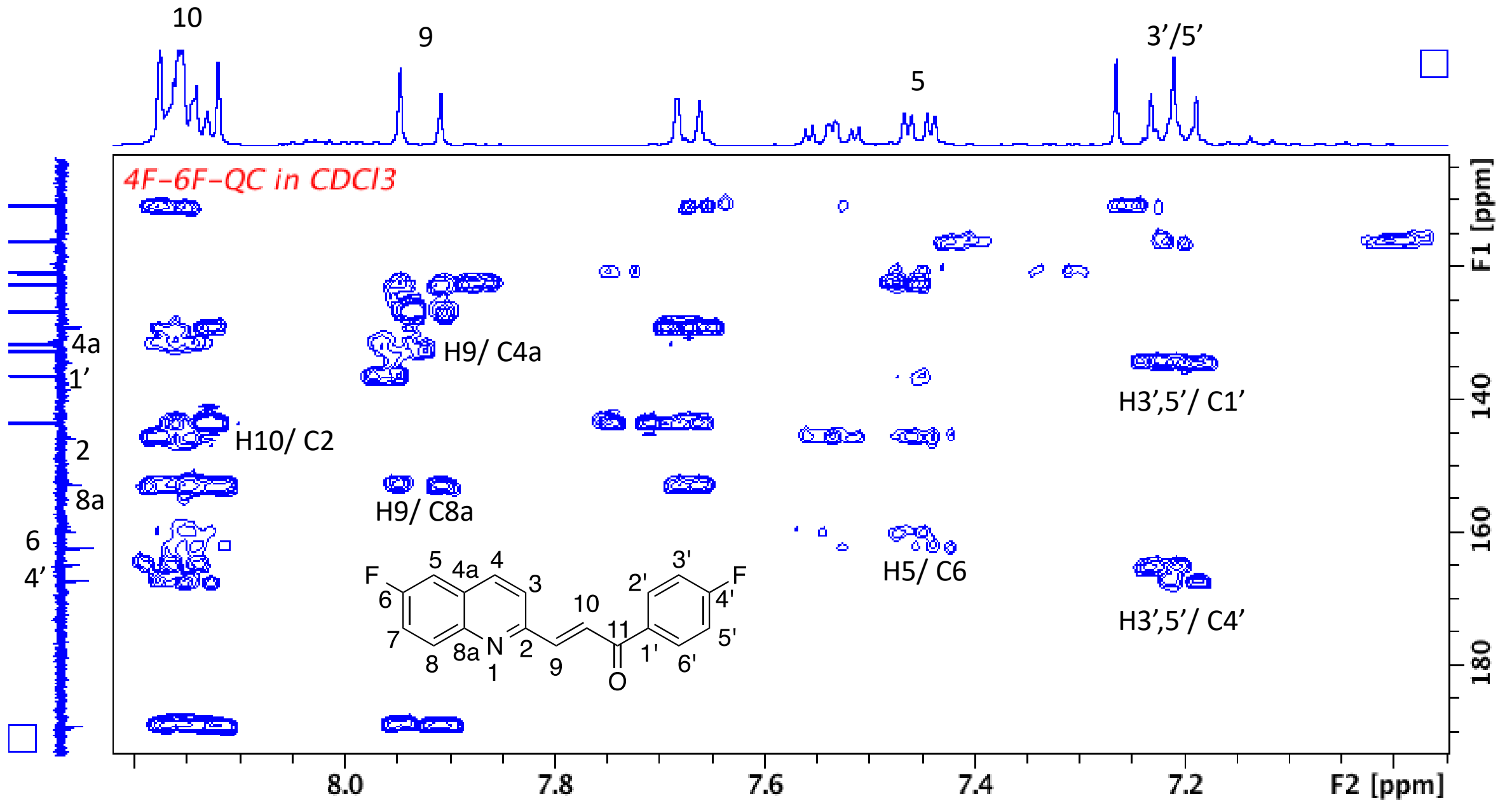
The HMBC of compound **8c**

24

Single Mass Analysis
Tolerance = 5.0 PPM   /   DBE: min = -1.5, max = 50.0
Element prediction: Off
Number of isotope peaks used for i-FIT = 3

Monoisotopic Mass, Even Electron Ions
58 formula(e) evaluated with 1 results within limits (all results (up to 1000) for each mass)
Elements Used:
C: 15-20   H: 10-15   N: 0-5   O: 0-5   F: 0-2
Cmpd 3 53 (1.754) Cm (1:61)
TOF MS AP+

2.07e+005
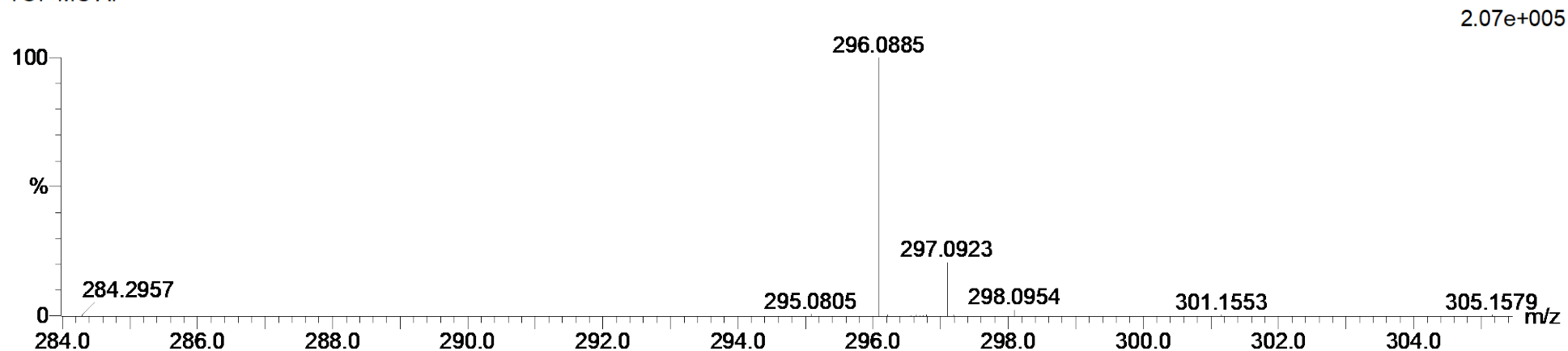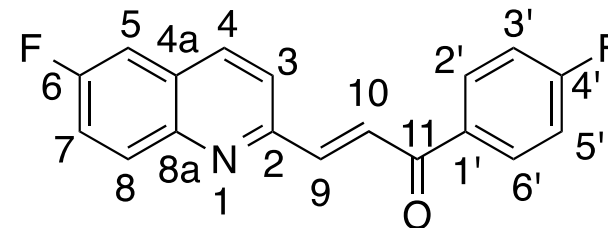
Minimum:				-1.5			
Maximum:		5.0	5.0	50.0			
Mass	Calc. Mass	mDa	PPM	DBE	i-FIT	i-FIT (Norm)	Formula
296.0885	296.0887	-0.2	-0.7	12.5	105.0	0.0	C18 H12 N O F2

HRMS spectrum of compound **8c**

25
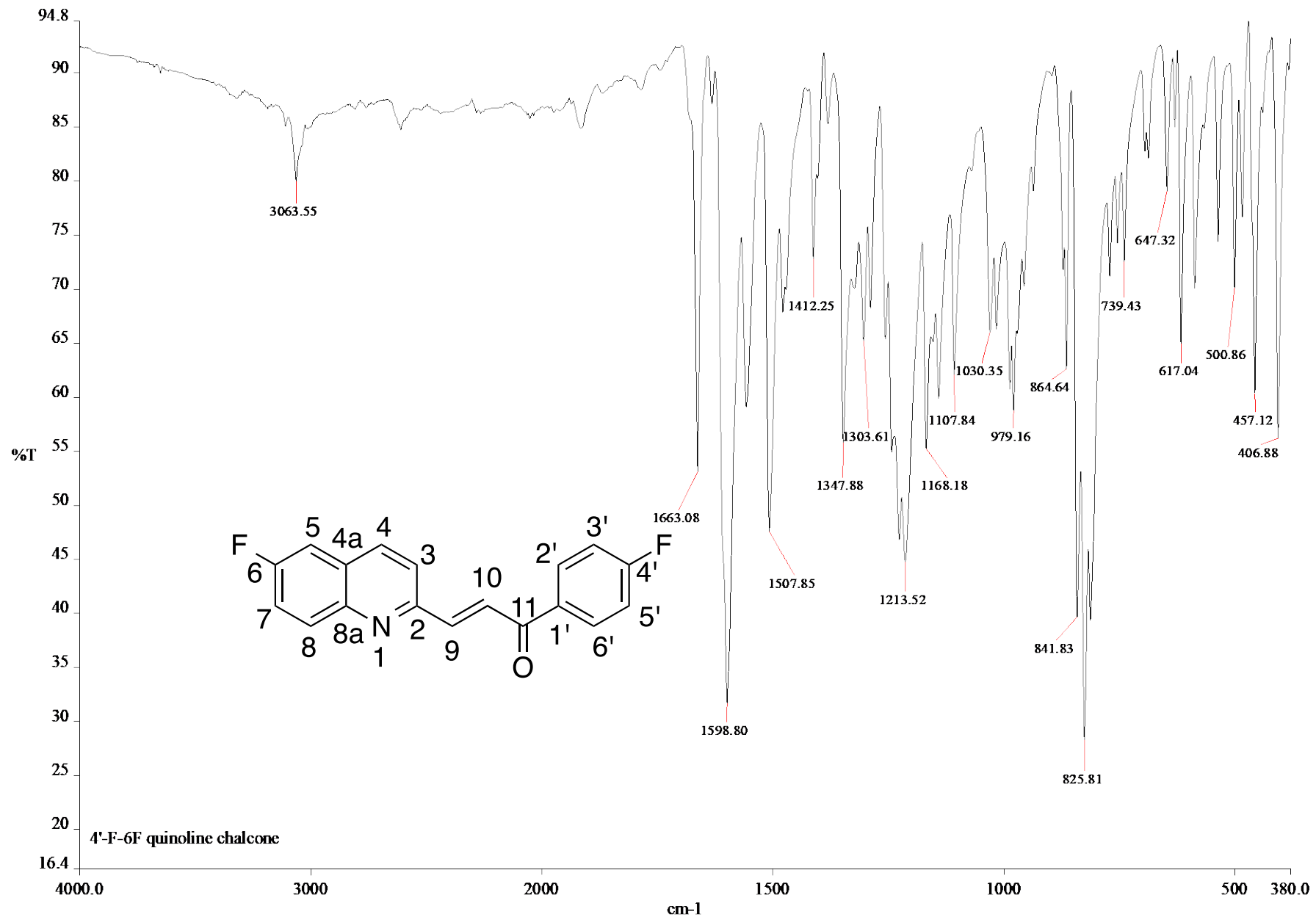
Infrared spectrum of compound **8c**

The ^{1}H NMR of compound **8d**

The ^{13}C NMR of compound **8d**

The expanded ^{13}C NMR of compound **8d**

The expanded ^{13}C NMR of compound **8d**

The COSY spectrum of compound **8d**
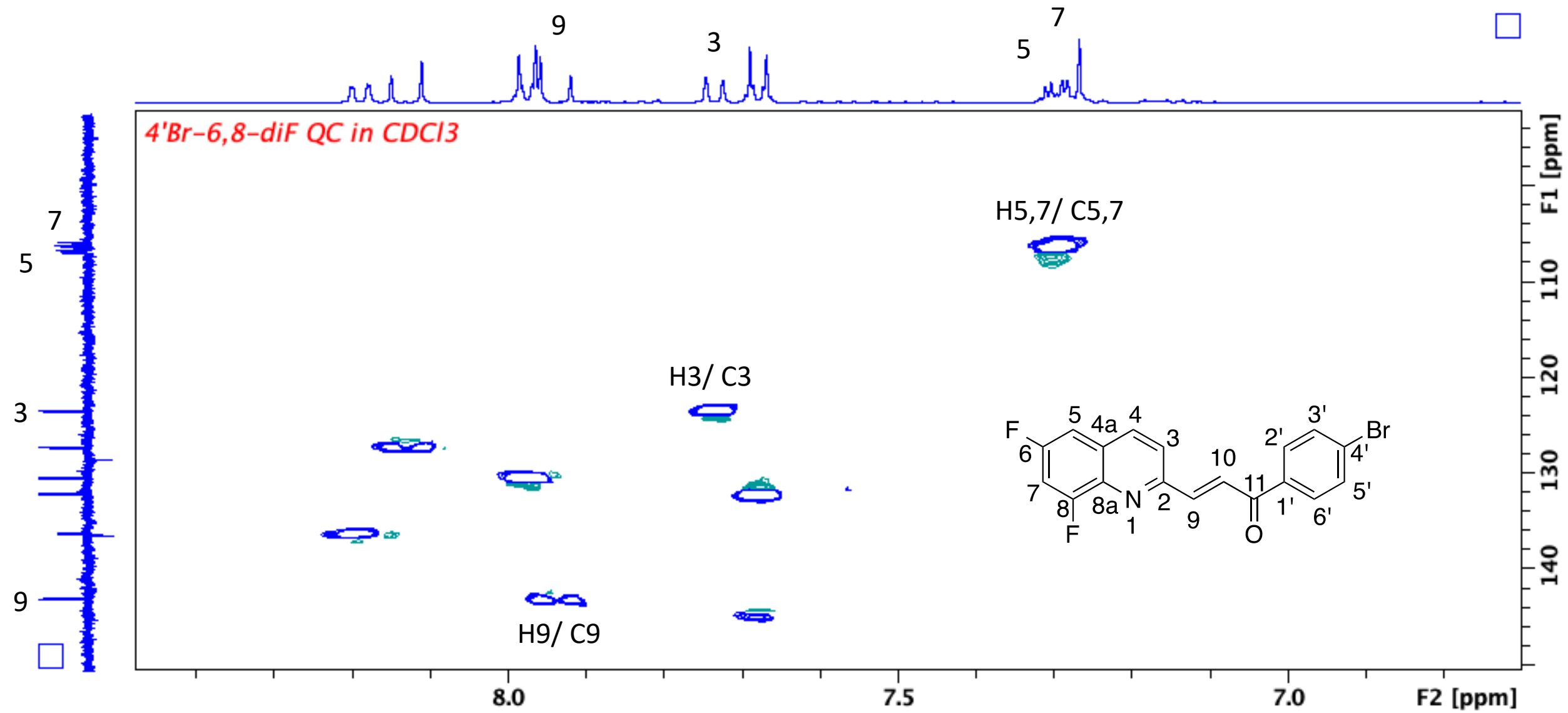
The HSQC of compound **8d**
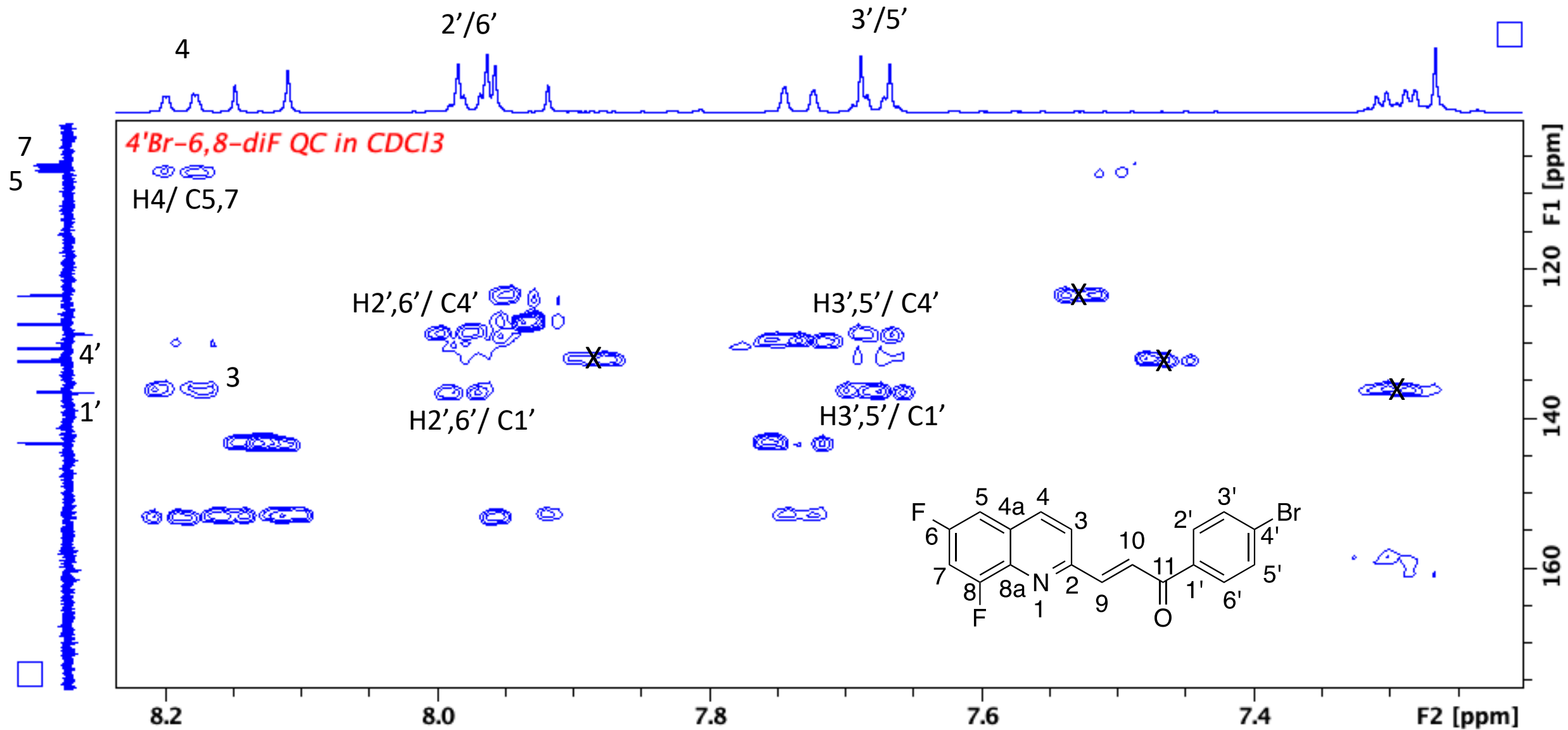
The HMBC of compound **8d**

Single Mass Analysis
Tolerance = 5.0 PPM   /   DBE: min = -1.5, max = 50.0
Element prediction: Off
Number of isotope peaks used for i-FIT = 3

Monoisotopic Mass, Even Electron Ions
108 formula(e) evaluated with 1 results within limits (all results (up to 1000) for each mass)
Elements Used:
C: 15-20   H: 10-15   N: 0-5   O: 0-5   F: 0-2   Br: 0-1

Cmpd 4 20 (0.641) Cm (1:61)
TOF MS AP+
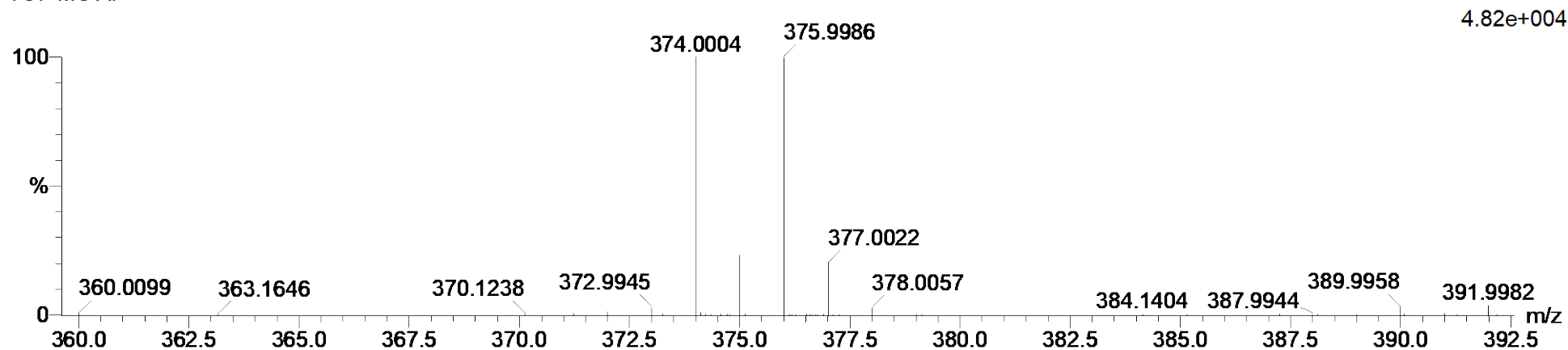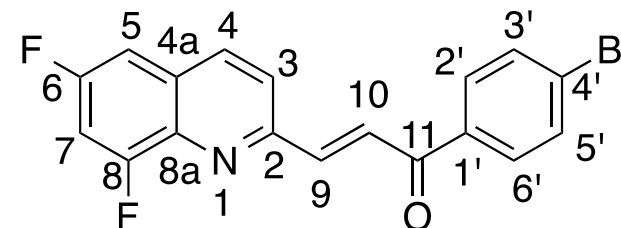
Minimum:			-1.5			
Maximum:	5.0	5.0	50.0			

Mass	Calc. Mass	mDa	PPM	DBE	i-FIT	i-FIT (Norm)	Formula
374.0004	373.9992	1.2	3.2	12.5	124.5	0.0	C18 H11 N O F2 Br

HRMS spectrum of compound **8d**

34

Infrared spectrum of compound **8d**

4'-Br-6,8-diF quinoline chalcone

c:\pel_data\spectra\gillean msc\4'-br-6,8-dif qc.sp

35
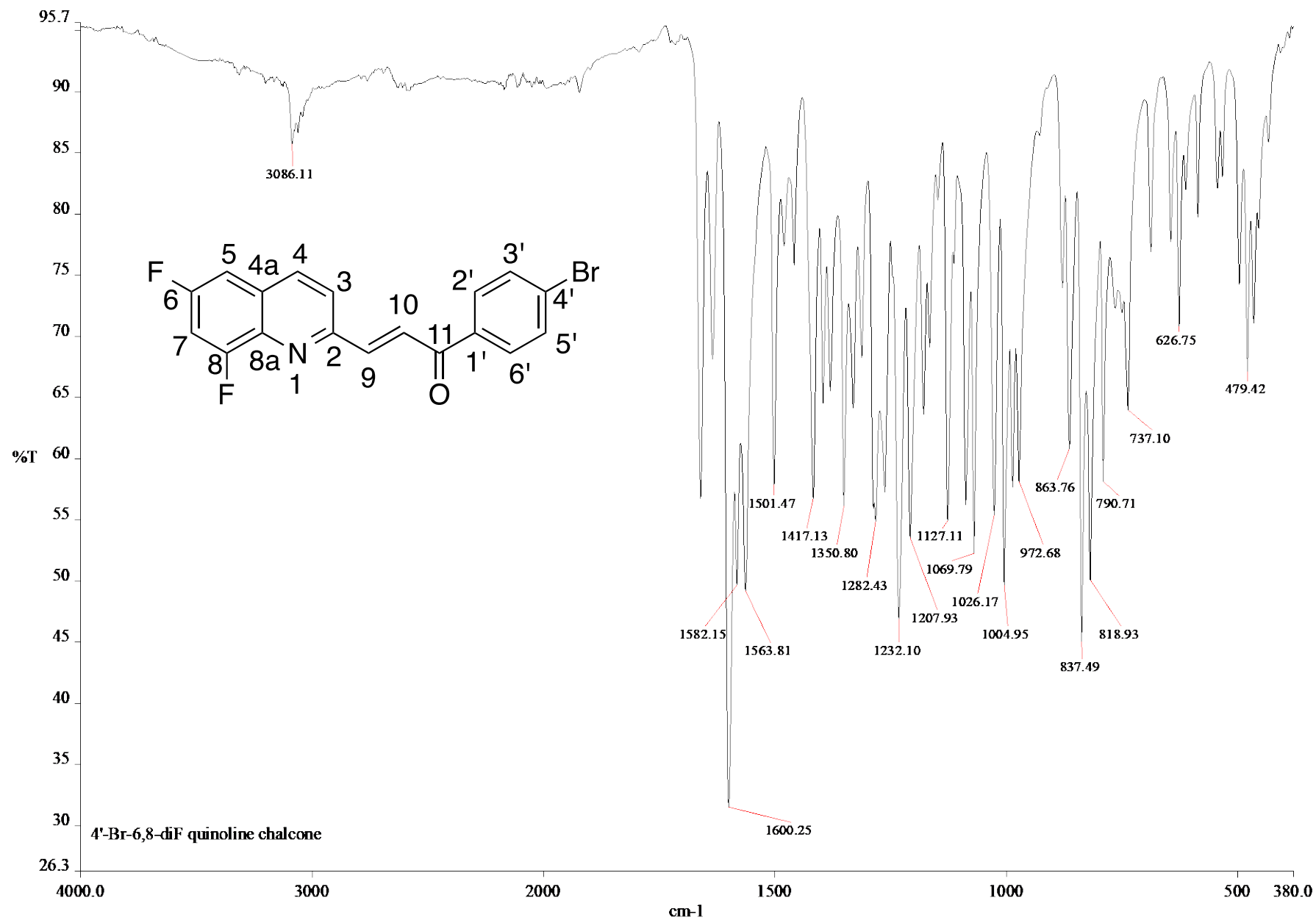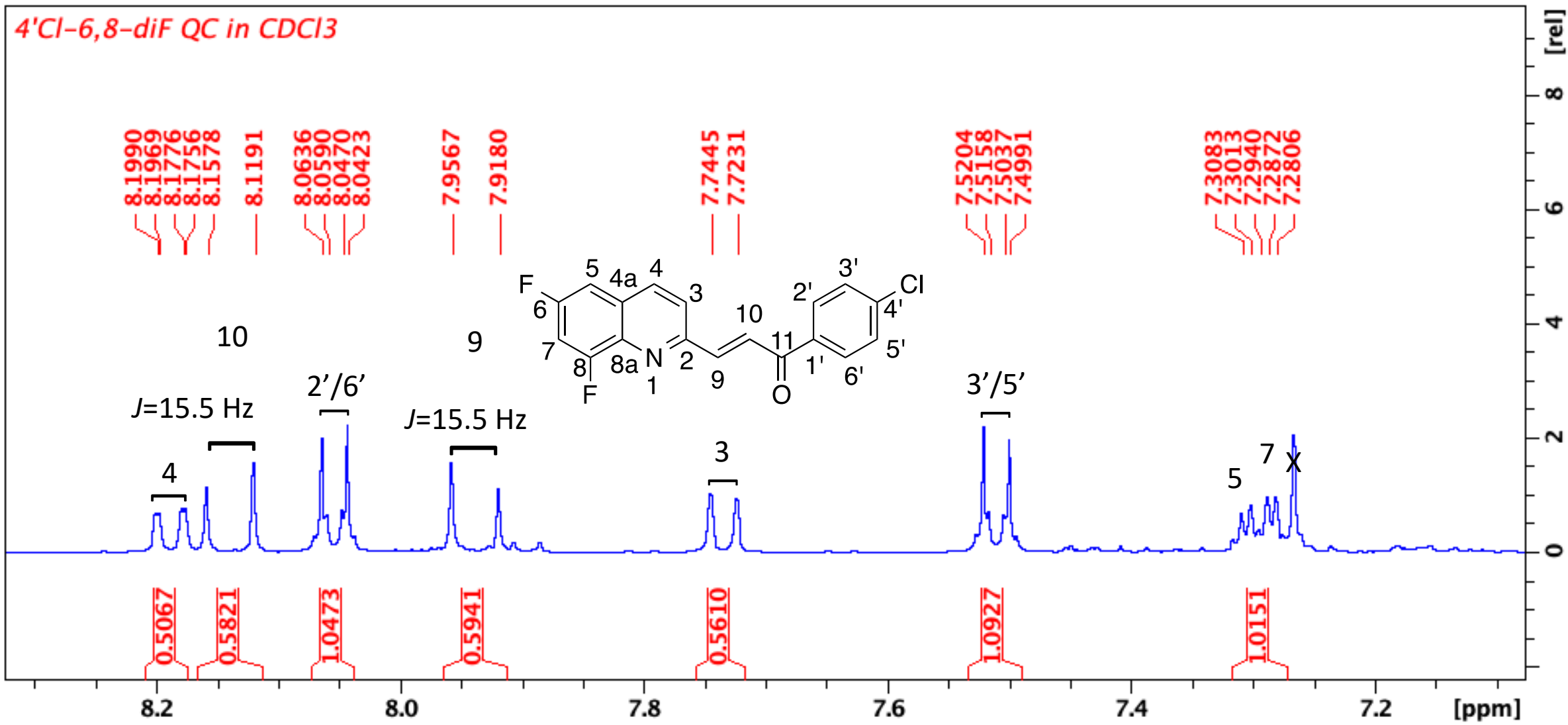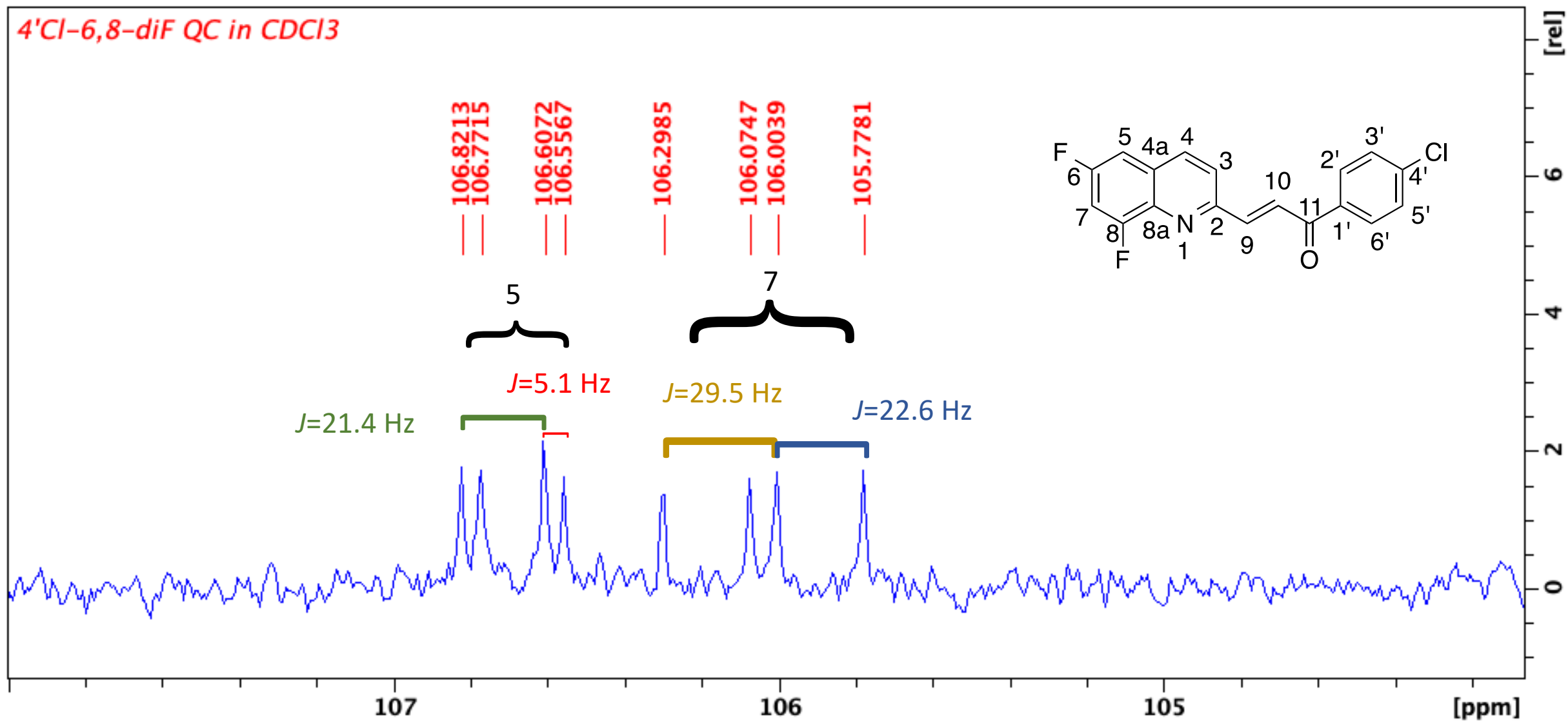
The ^{1}H NMR of compound **8e**

The ^{13}C NMR of compound **8e**

The expanded ^{13}C NMR of compound **8e**

38
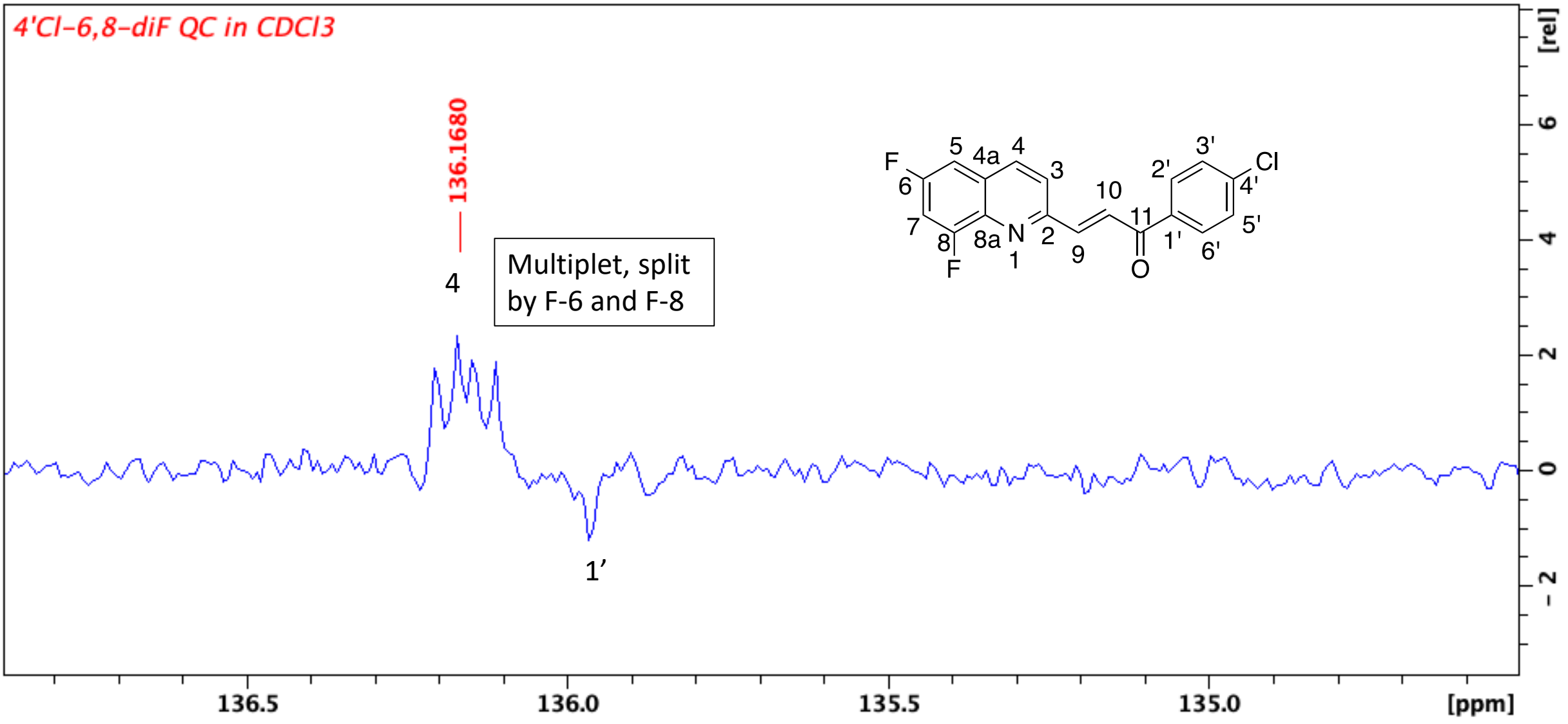
The expanded ^{13}C NMR of compound **8e**
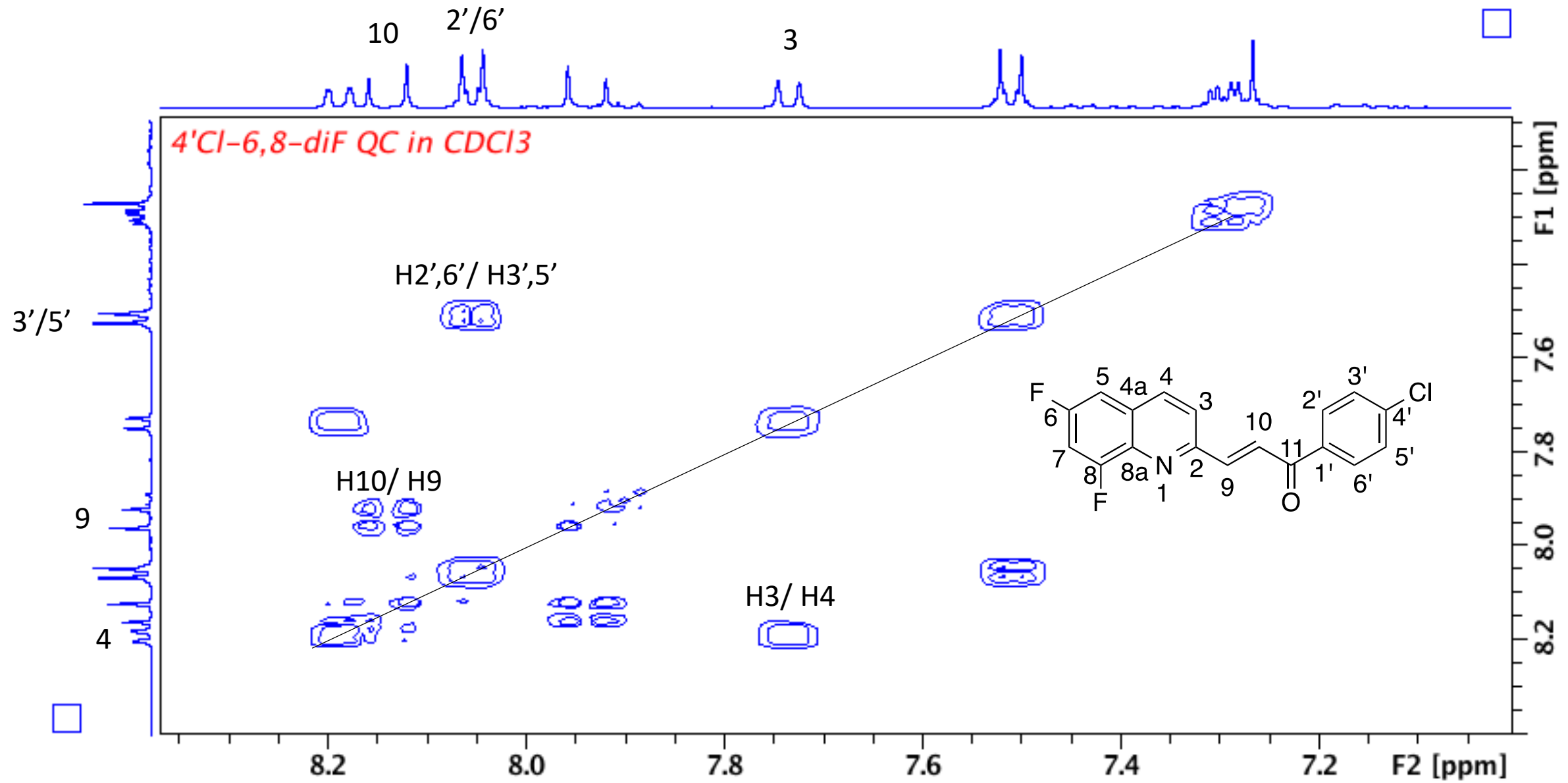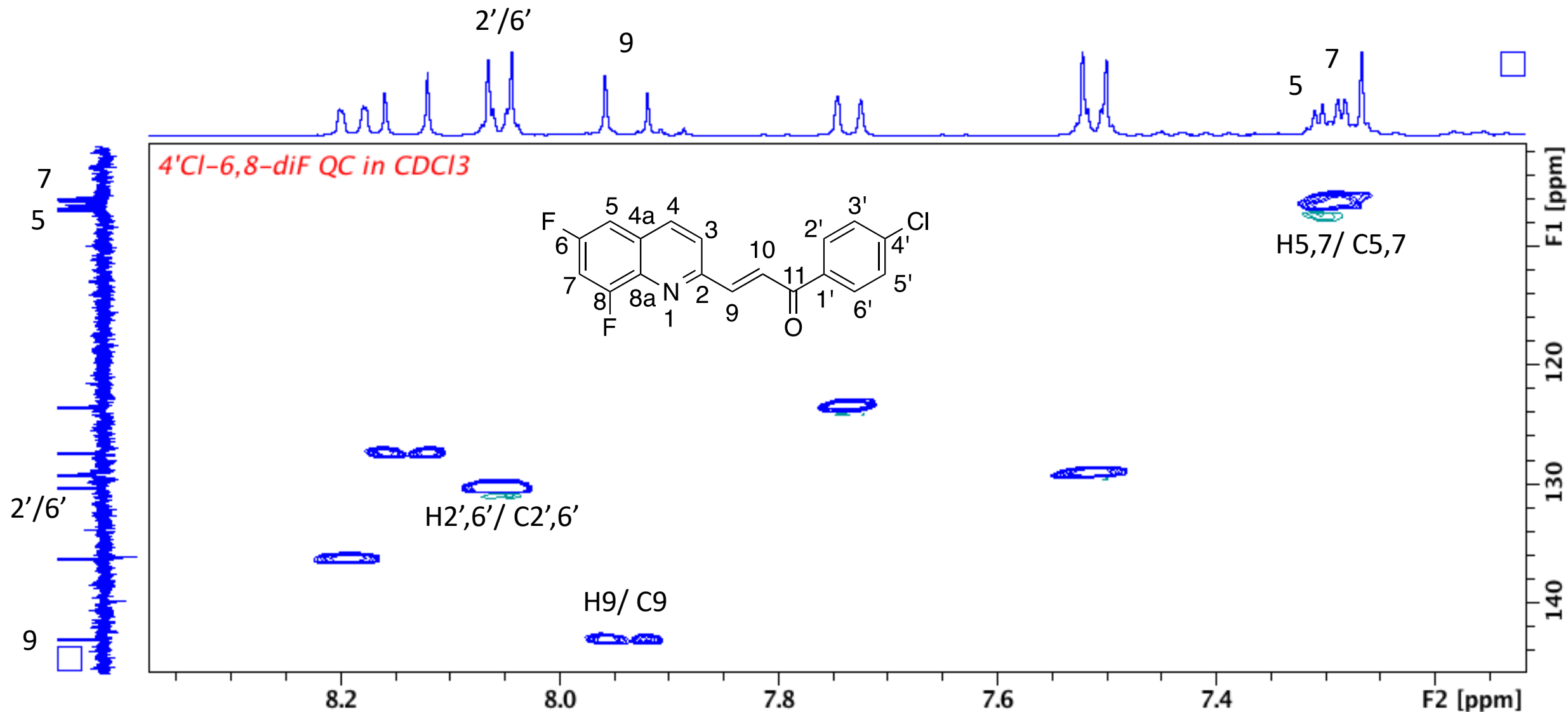
The COSY spectrum of compound **8e**

The HSQC of compound **8e**
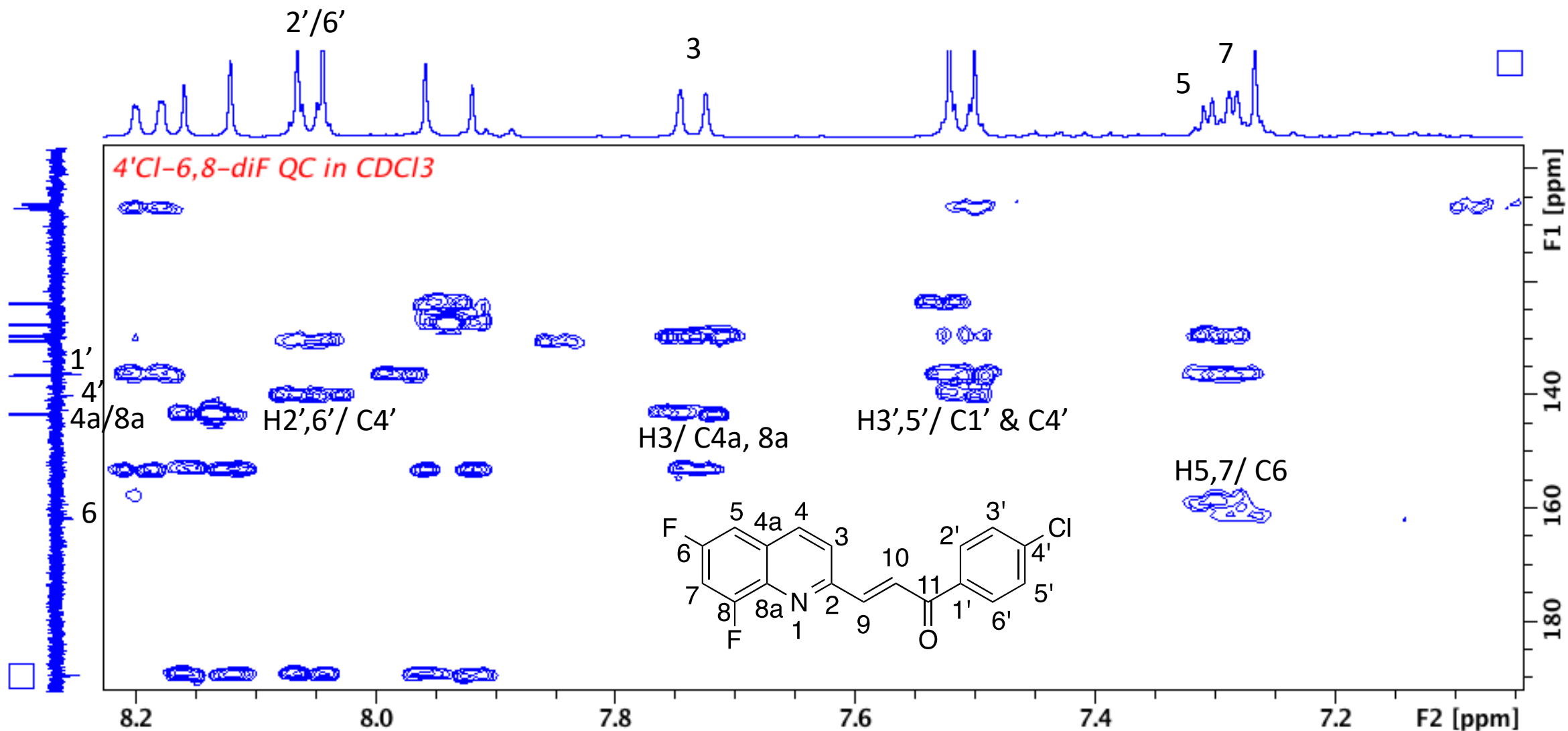
41

The HMBC of compound **8e**

Single Mass Analysis
Tolerance = 5.0 PPM   /   DBE: min = -1.5, max = 50.0
Element prediction: Off
Number of isotope peaks used for i-FIT = 3

Monoisotopic Mass, Even Electron Ions
101 formula(e) evaluated with 1 results within limits (all results (up to 1000) for each mass)
Elements Used:
C: 15-20   H: 10-15   N: 0-5   O: 0-5   F: 0-2   Cl: 0-1
Cmpd 5 14 (0.438) Cm (1:61)
TOF MS AP+
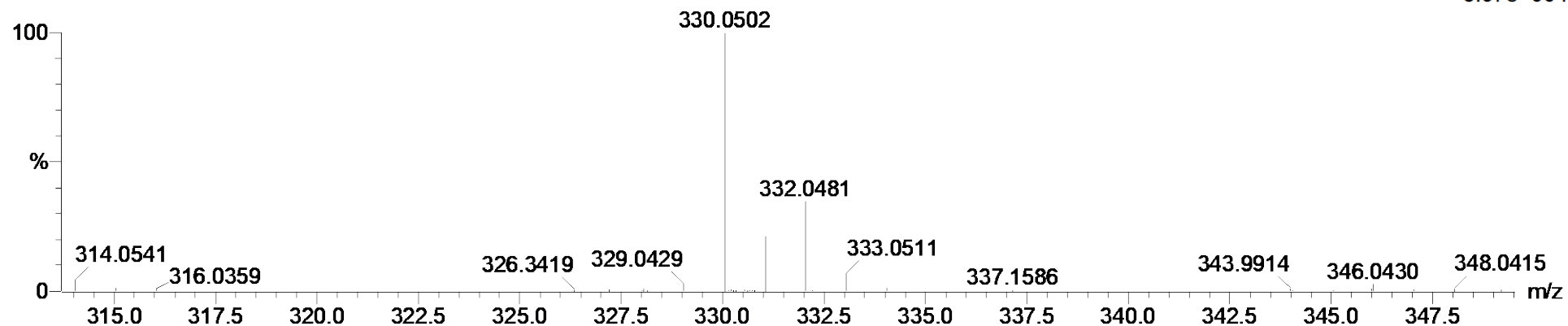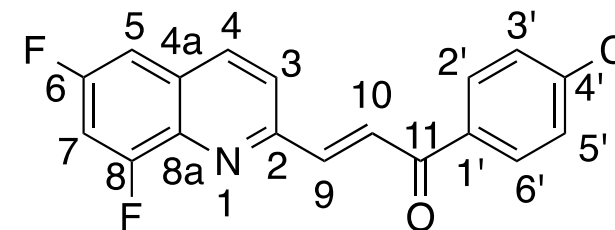
8.97e+004

Mass	Calc. Mass	mDa	PPM	DBE	i-FIT	i-FIT (Norm)	Formula
Minimum:				-1.5			
Maximum:		5.0	5.0	50.0			
330.0502	330.0497	0.5	1.5	12.5	124.3	0.0	C18 H11 N O F2 Cl

HRMS spectrum of compound **8e**
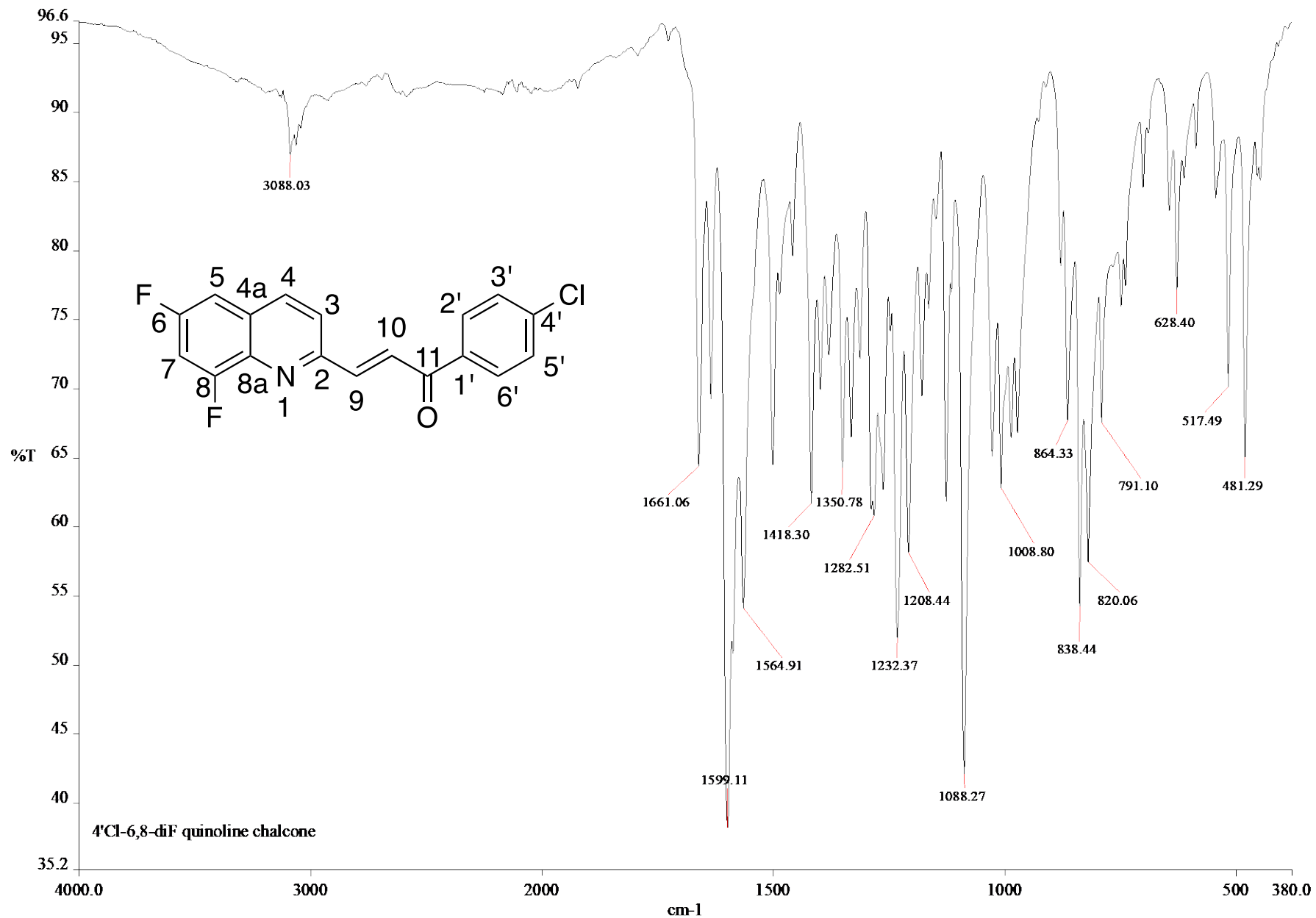
Infrared spectrum of compound **8e**
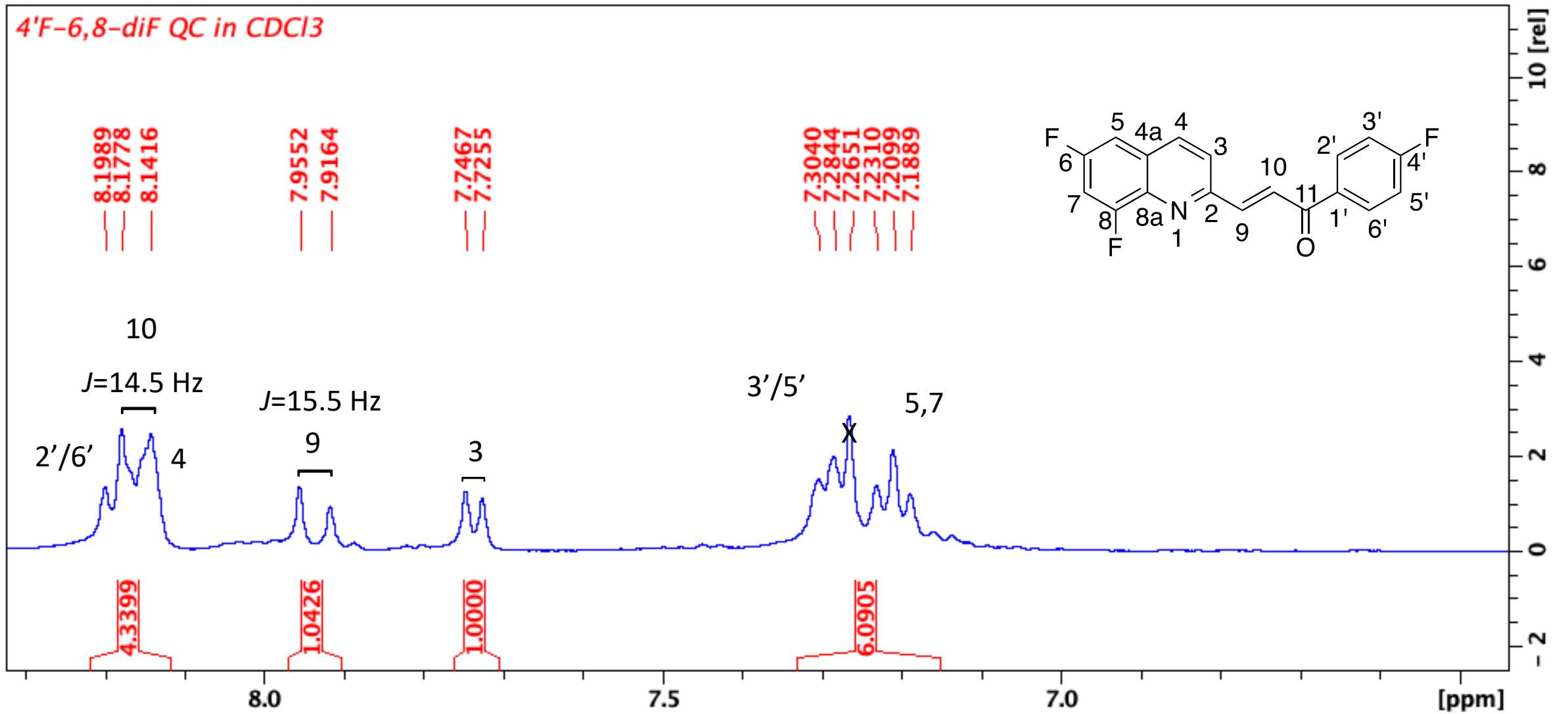
The ^{1}H NMR of compound **8f**
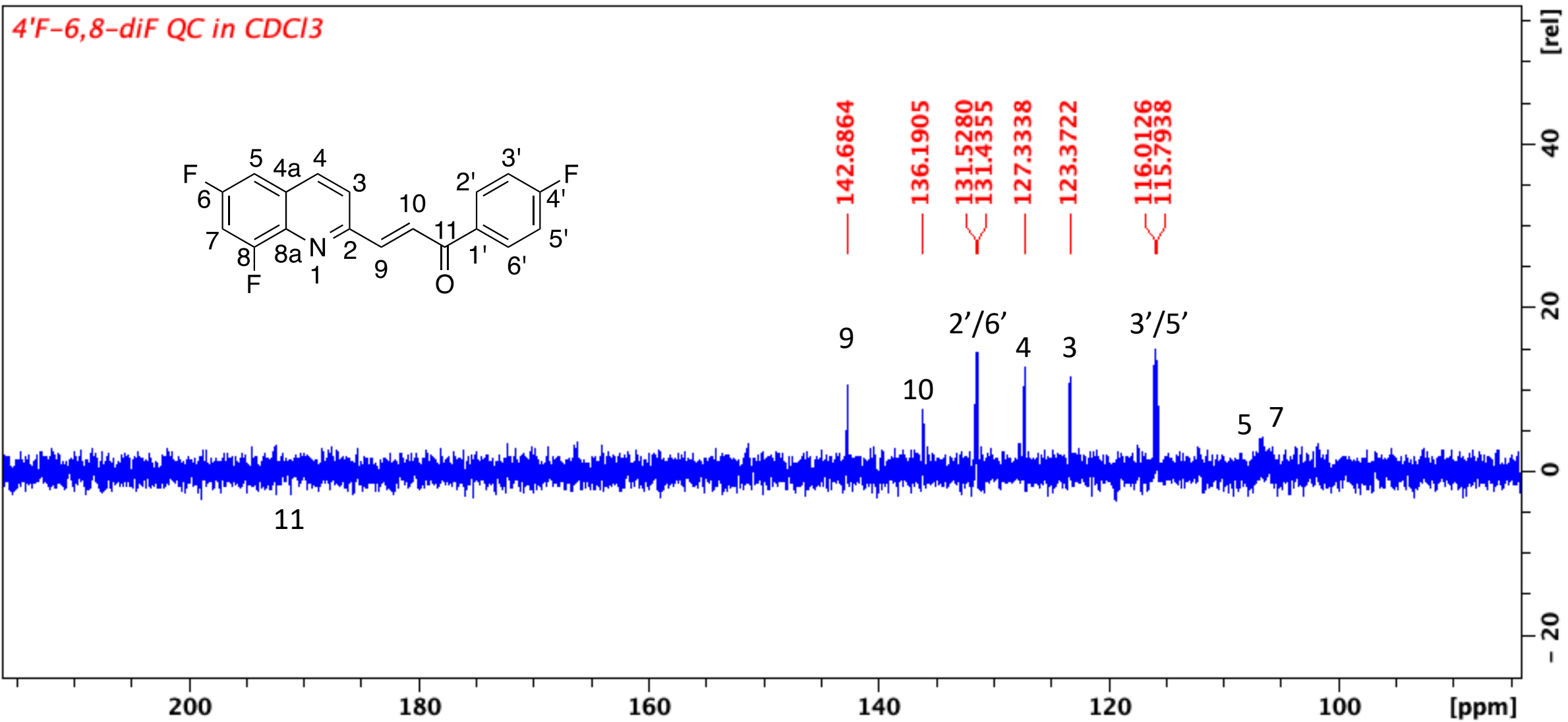
The ^{13}C NMR of compound **8f**
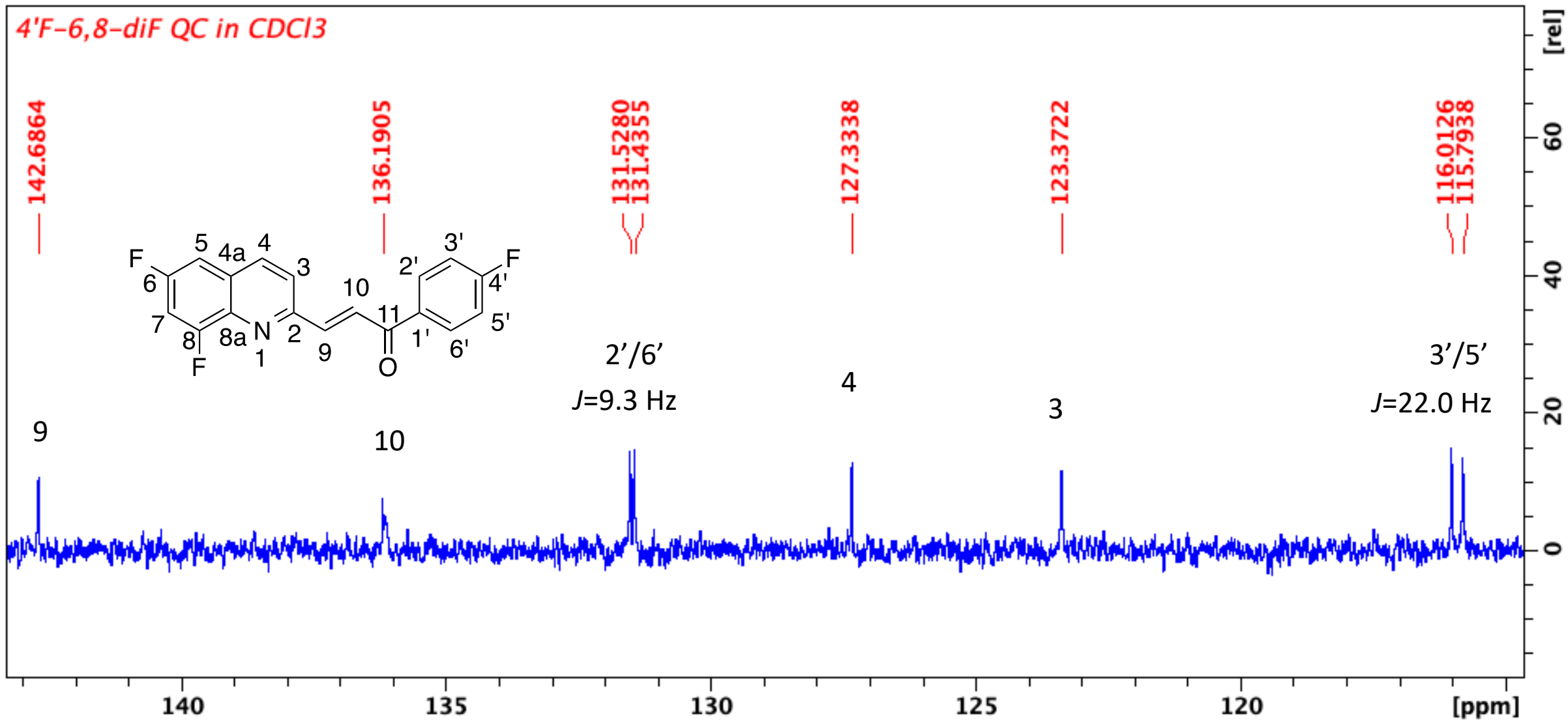
The expanded ^{13}C NMR of compound **8f**
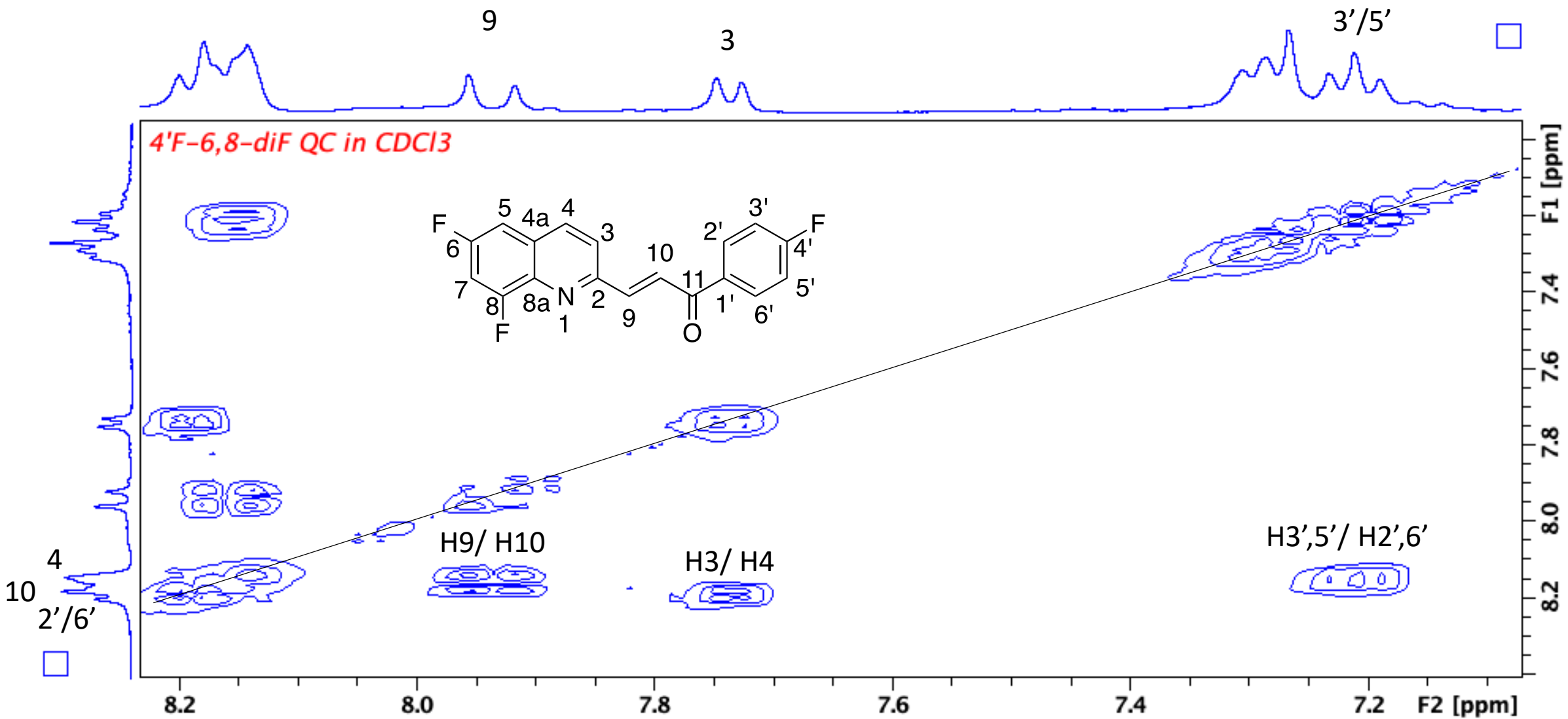
The COSY spectrum of compound **8f**
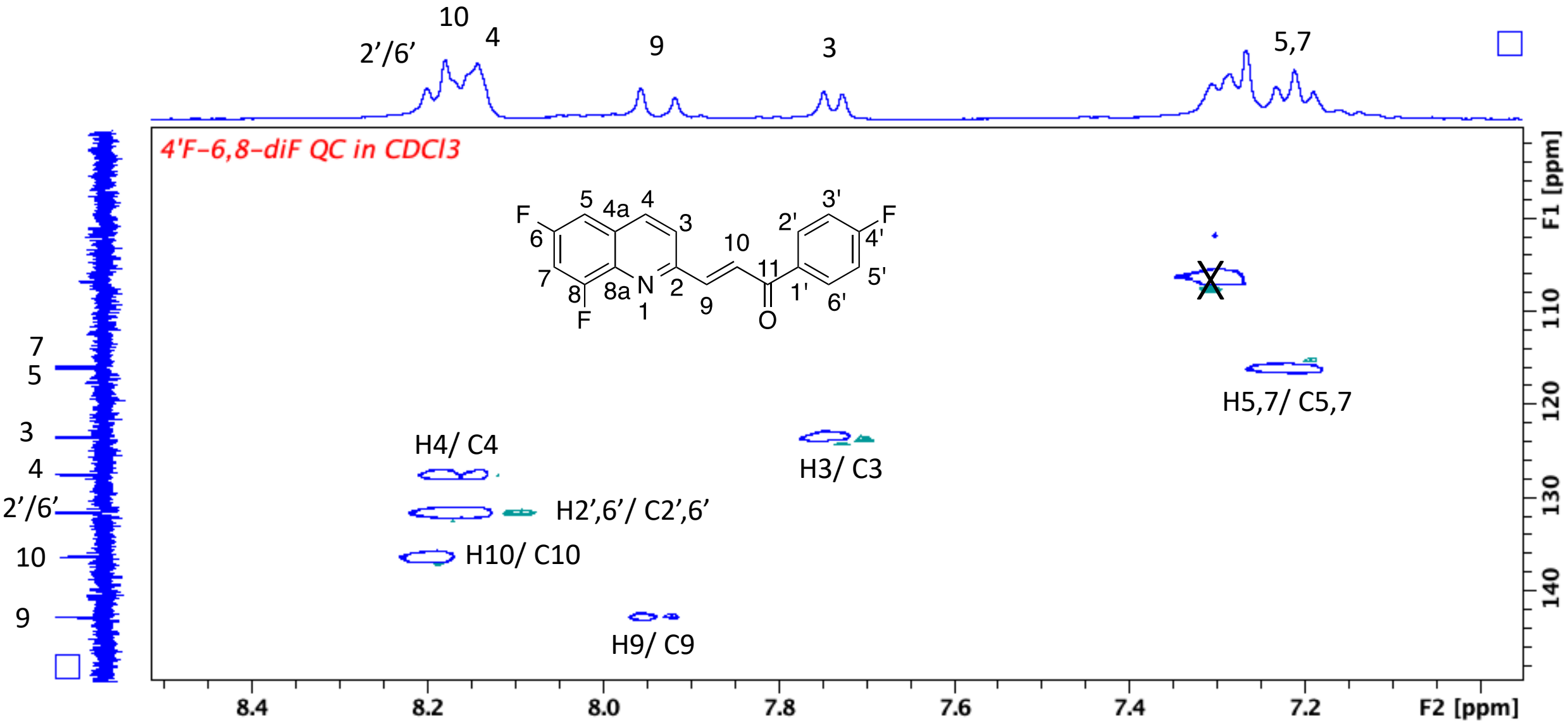
The HSQC of compound **8f**
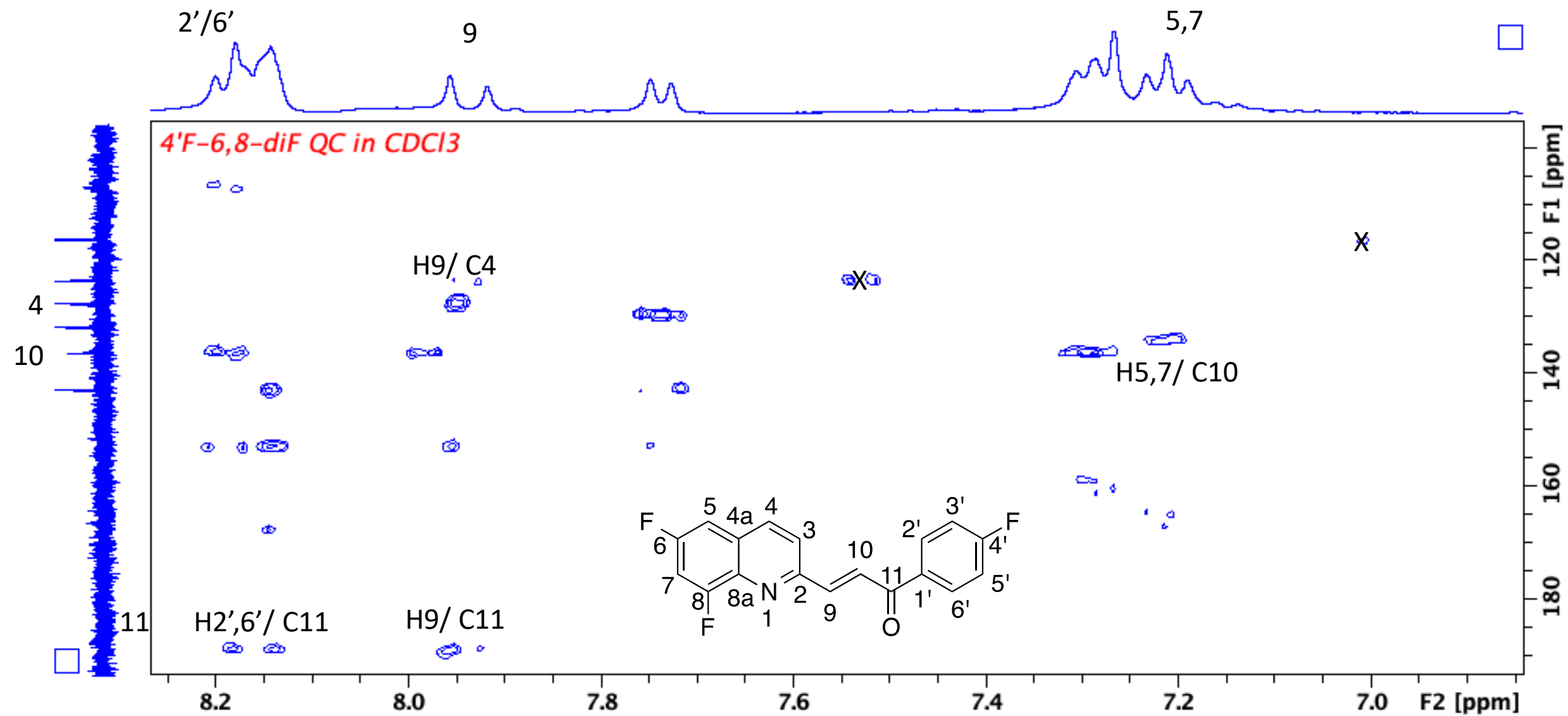
The HMBC of compound **8f**

Single Mass Analysis
Tolerance = 5.0 PPM   /   DBE: min = -1.5, max = 50.0
Element prediction: Off
Number of isotope peaks used for i-FIT = 3

Monoisotopic Mass, Even Electron Ions
71 formula(e) evaluated with 1 results within limits (all results (up to 1000) for each mass)
Elements Used:
C: 15-20   H: 10-15   N: 0-5   O: 0-5   F: 0-3
Cmpd 6 46 (1.518) Cm (1:61)
TOF MS AP+
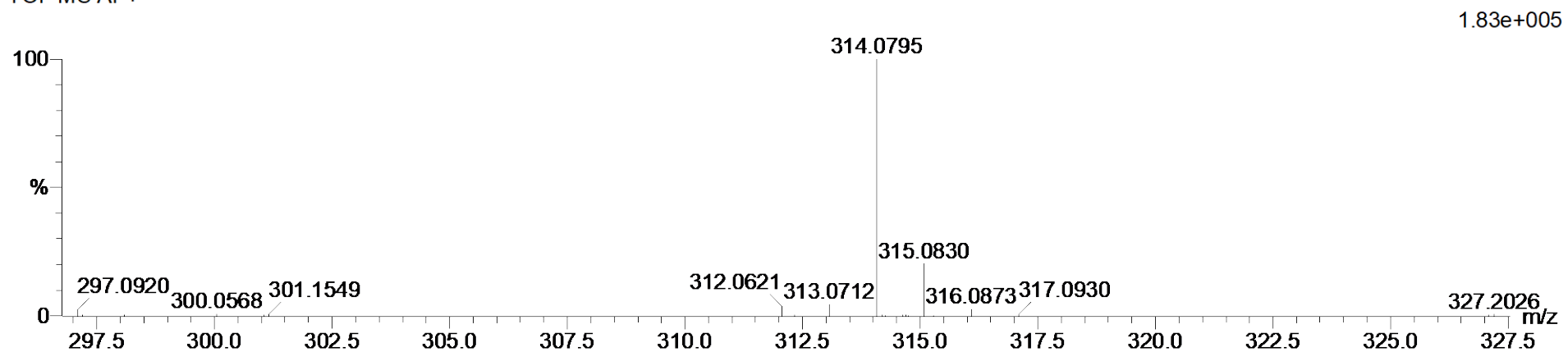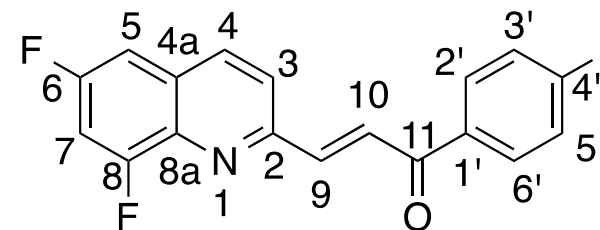
1.83e+005

Mass	Calc. Mass	mDa	PPM	DBE	i-FIT	i-FIT (Norm)	Formula
				Minimum:			-1.5
		Maximum:	5.0	5.0	50.0		
314.0795	314.0793	0.2	0.6	12.5	96.9	0.0	C18 H11 N O F3

HRMS spectrum of compound **8f**
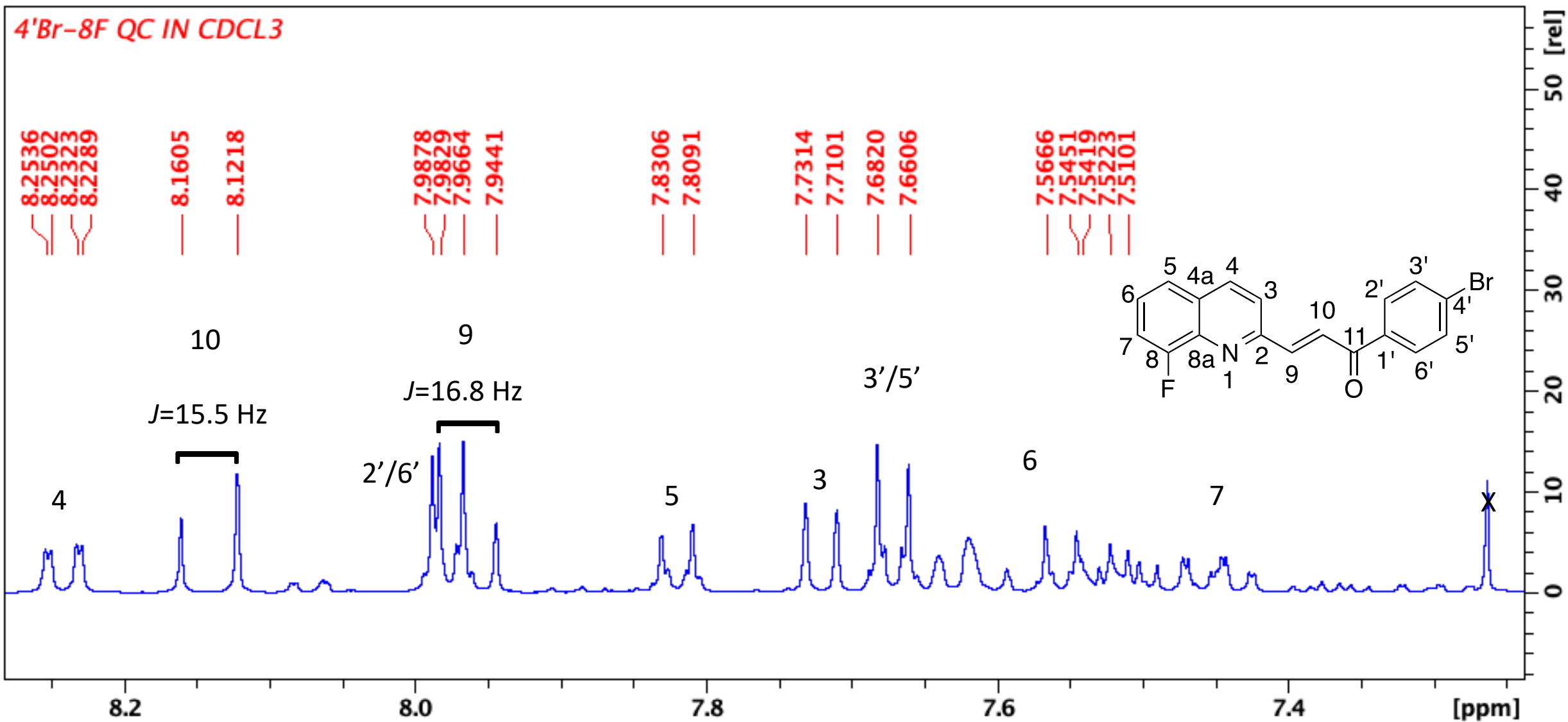
51

Infrared spectrum of compound **8f**

The ^{1}H NMR of compound **8g**
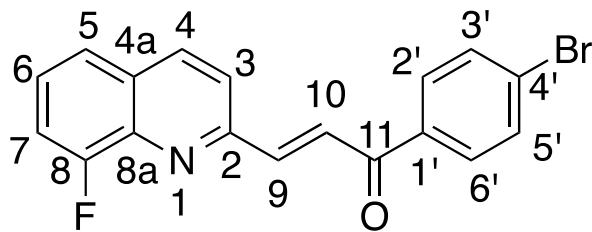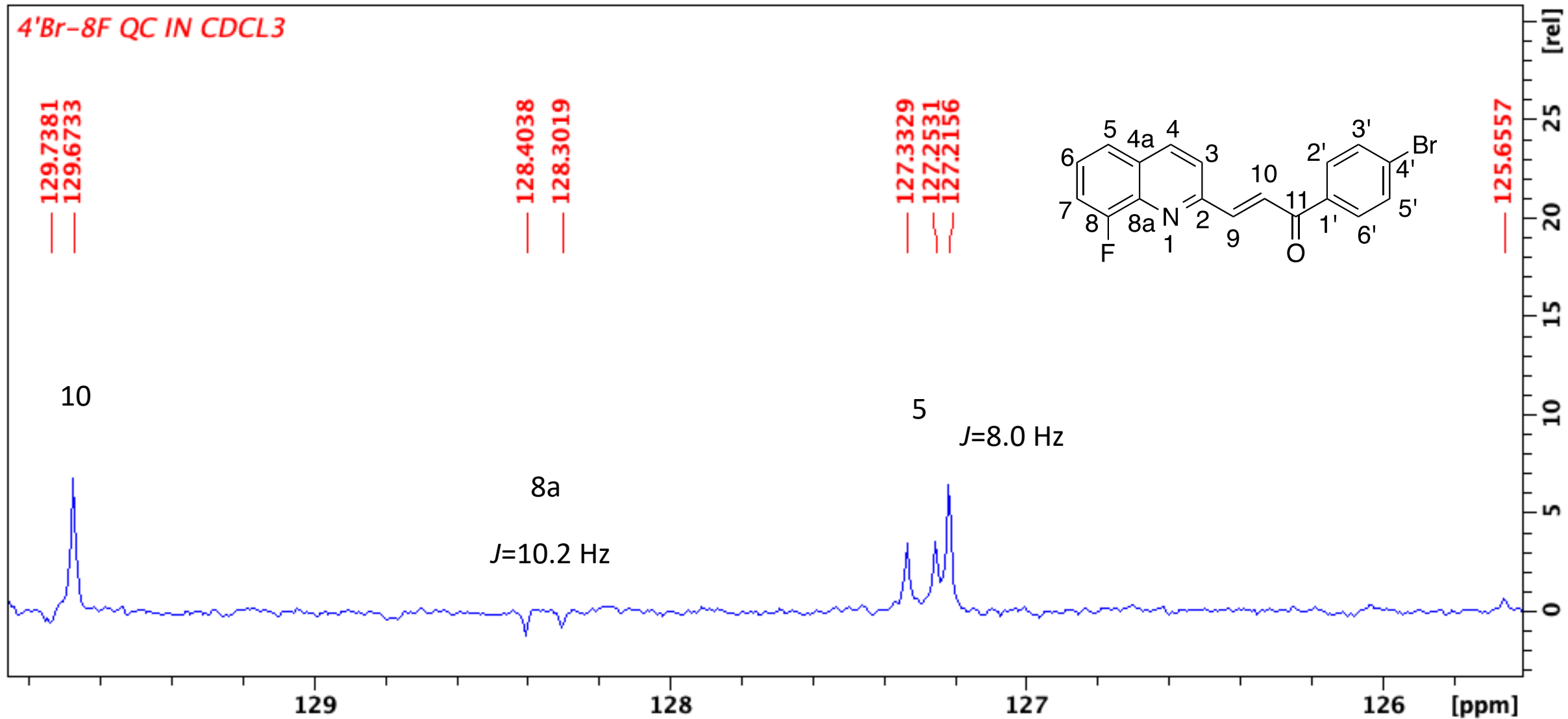
The ^{13}C NMR of compound **8g**

The expanded ^{13}C NMR of compound **8g**

55
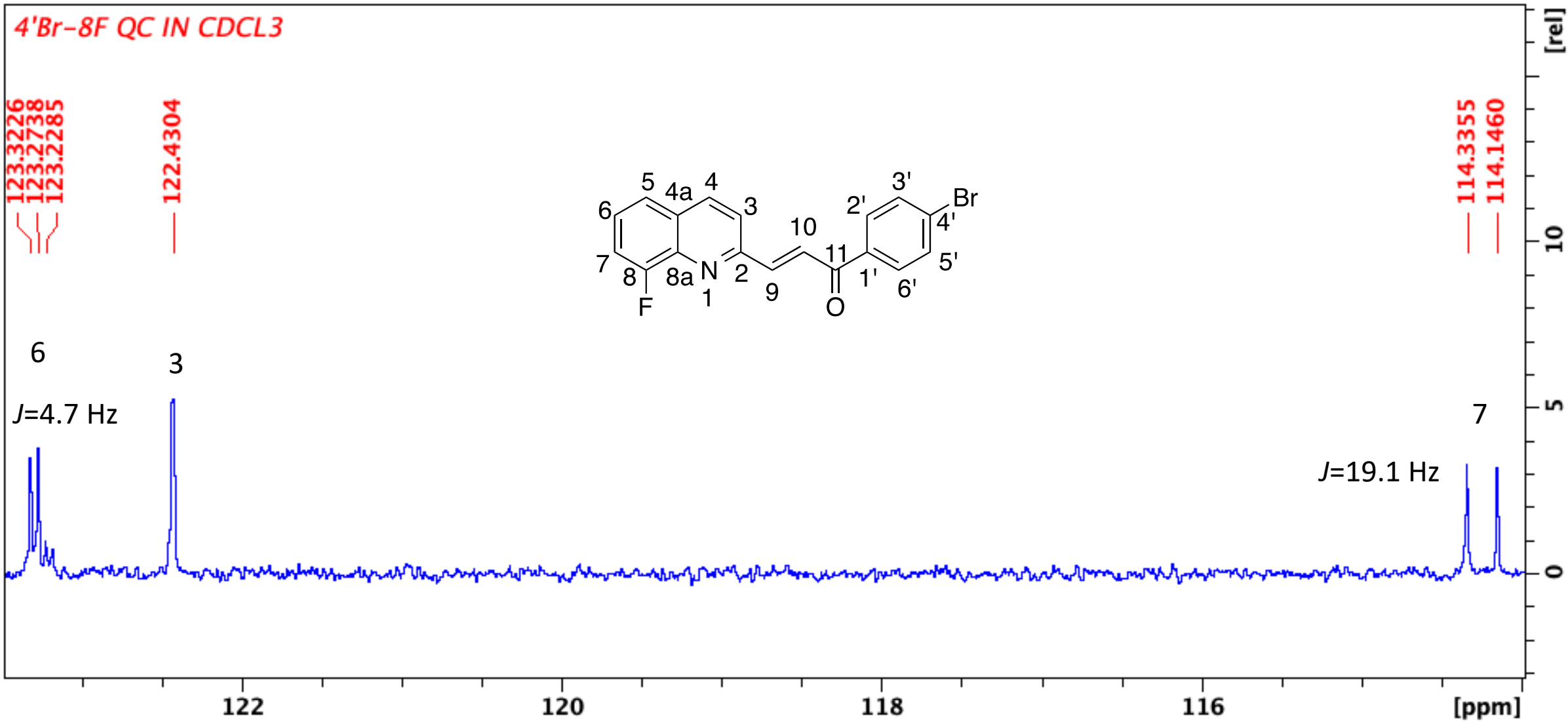
The expanded ¹³C NMR of compound **8g**
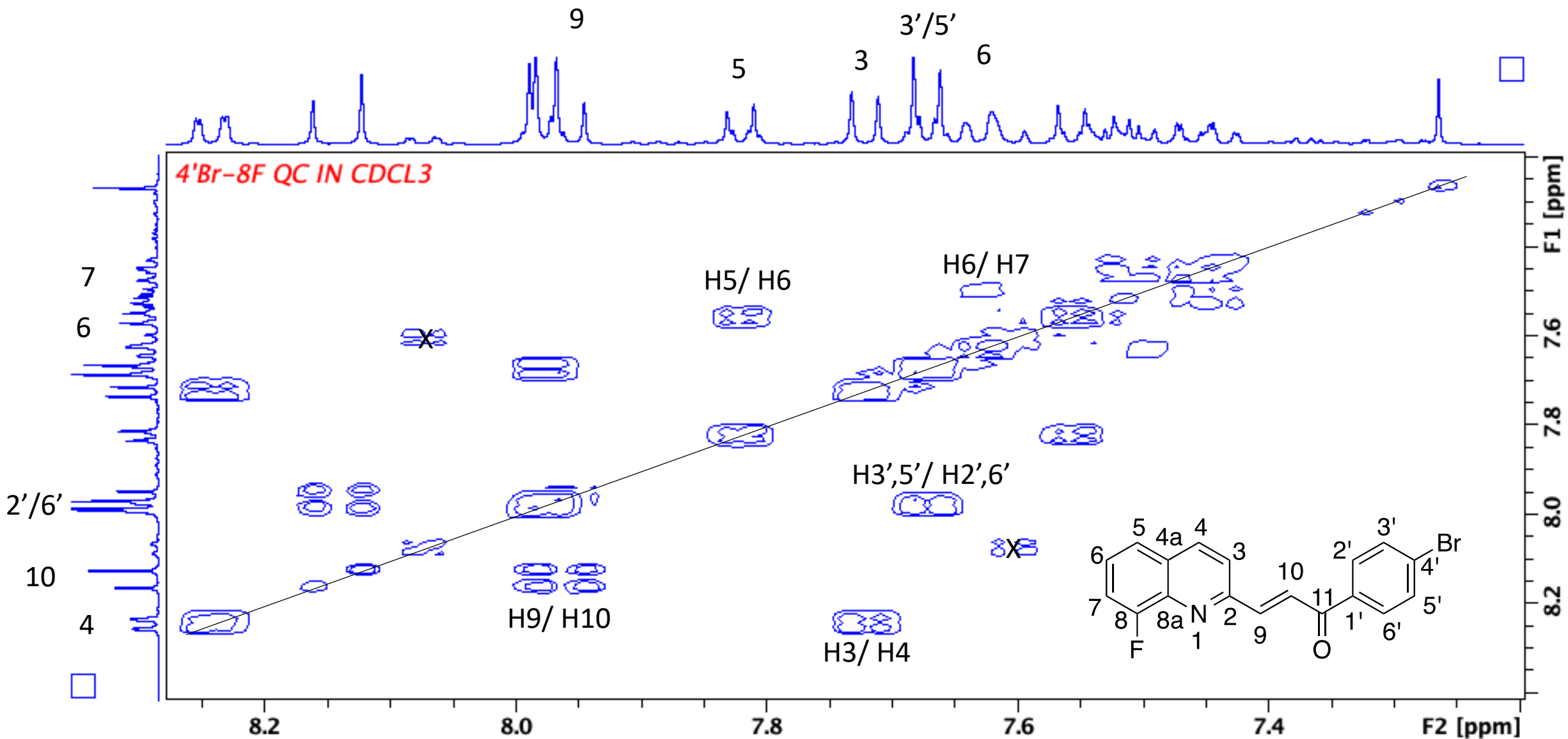
The COSY spectrum of compound **8g**
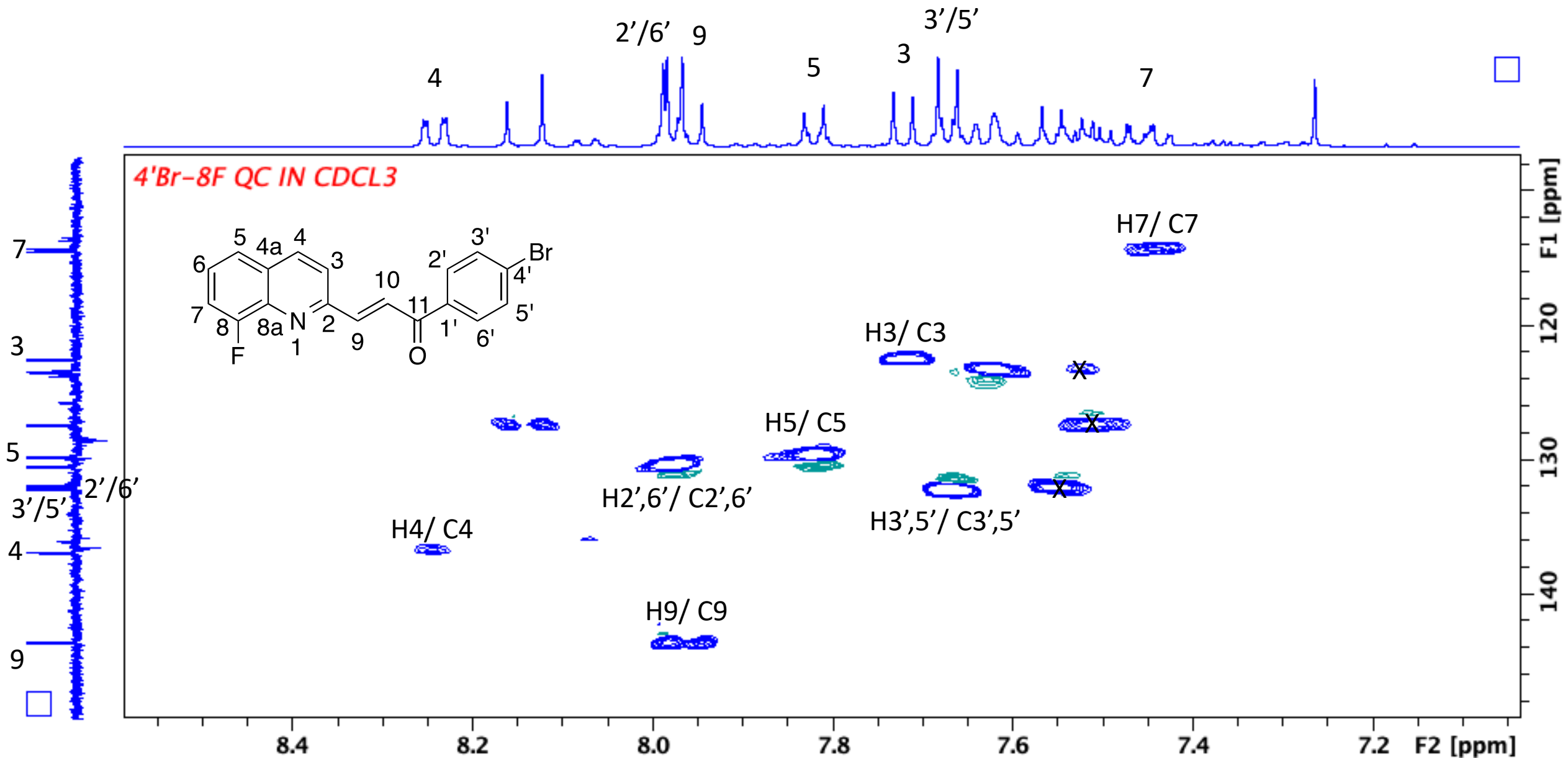
The HSQC of compound **8g**
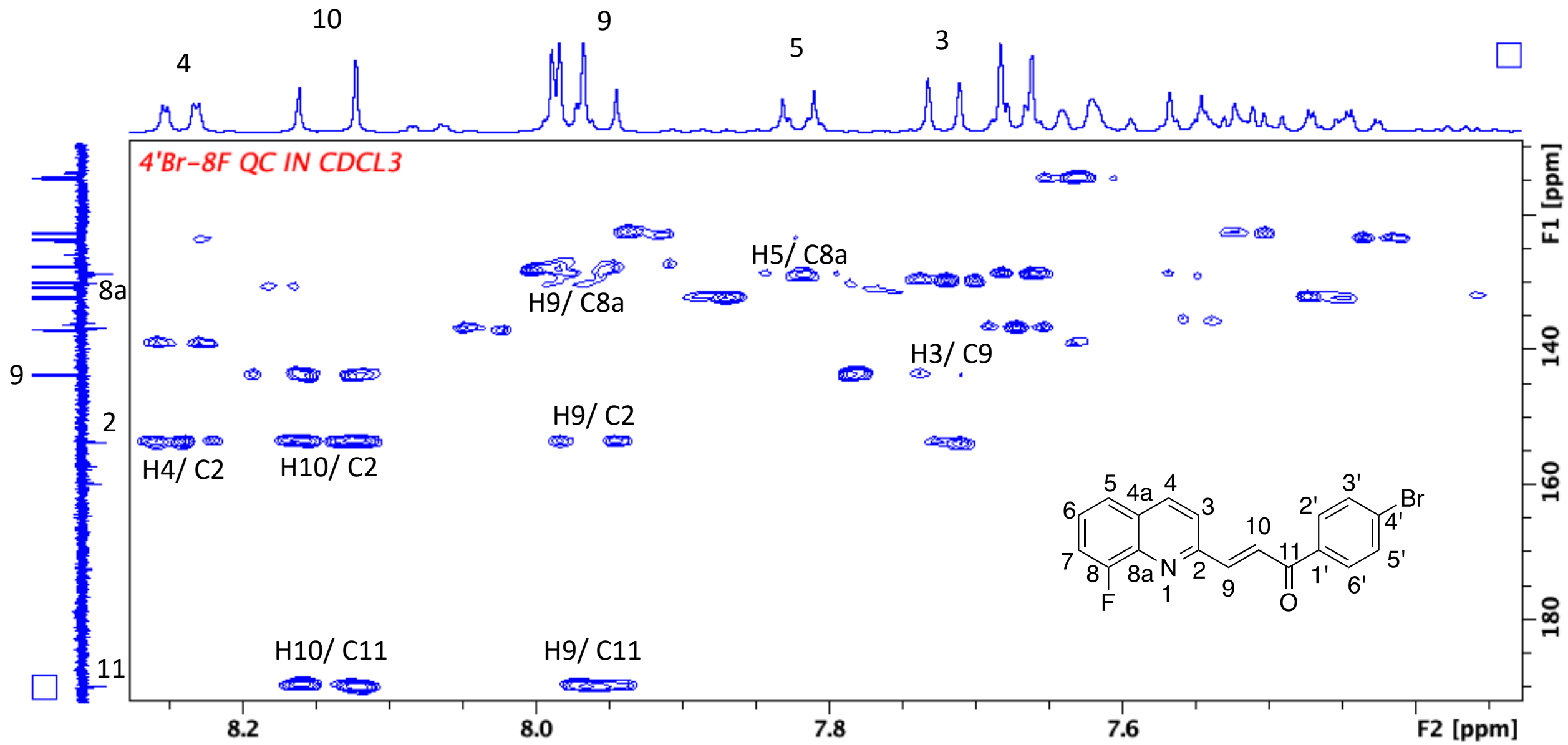
The HMBC of compound **8g**

Single Mass Analysis
Tolerance = 5.0 PPM   /   DBE: min = -1.5, max = 50.0
Element prediction: Off
Number of isotope peaks used for i-FIT = 3

Monoisotopic Mass, Even Electron Ions
72 formula(e) evaluated with 1 results within limits (all results (up to 1000) for each mass)
Elements Used:
C: 15-20   H: 10-15   N: 0-5   O: 0-5   F: 0-1   Br: 0-1

Cmpd 7 59 (1.956) Cm (1:61)
TOF MS AP+

1.01e+004
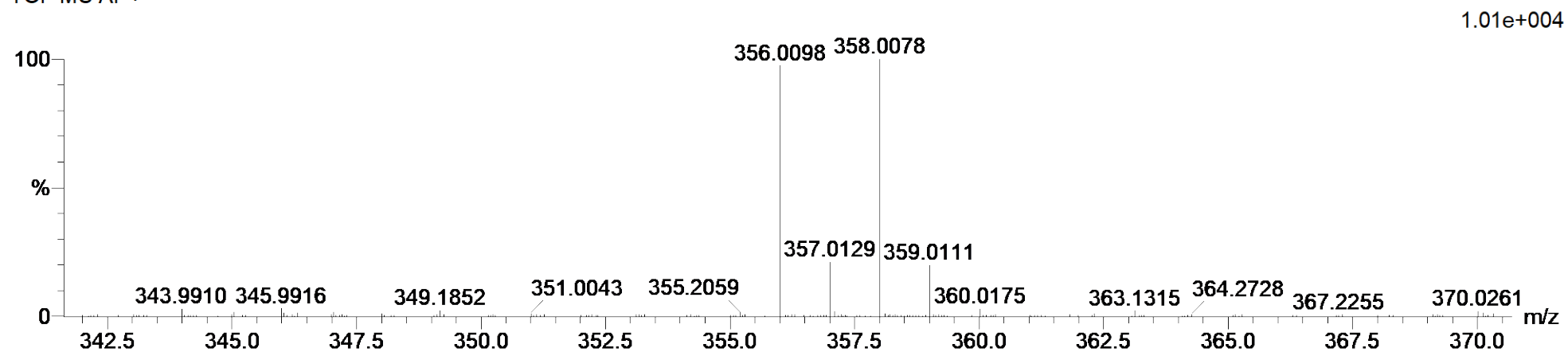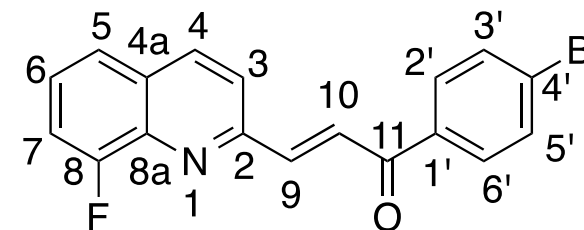
Minimum:				-1.5			
Maximum:		5.0	5.0	50.0			
Mass	Calc. Mass	mDa	PPM	DBE	i-FIT	i-FIT (Norm)	Formula
356.0098	356.0086	1.2	3.4	12.5	237.1	0.0	C18 H12 N O F Br

HRMS spectrum of compound **8g**
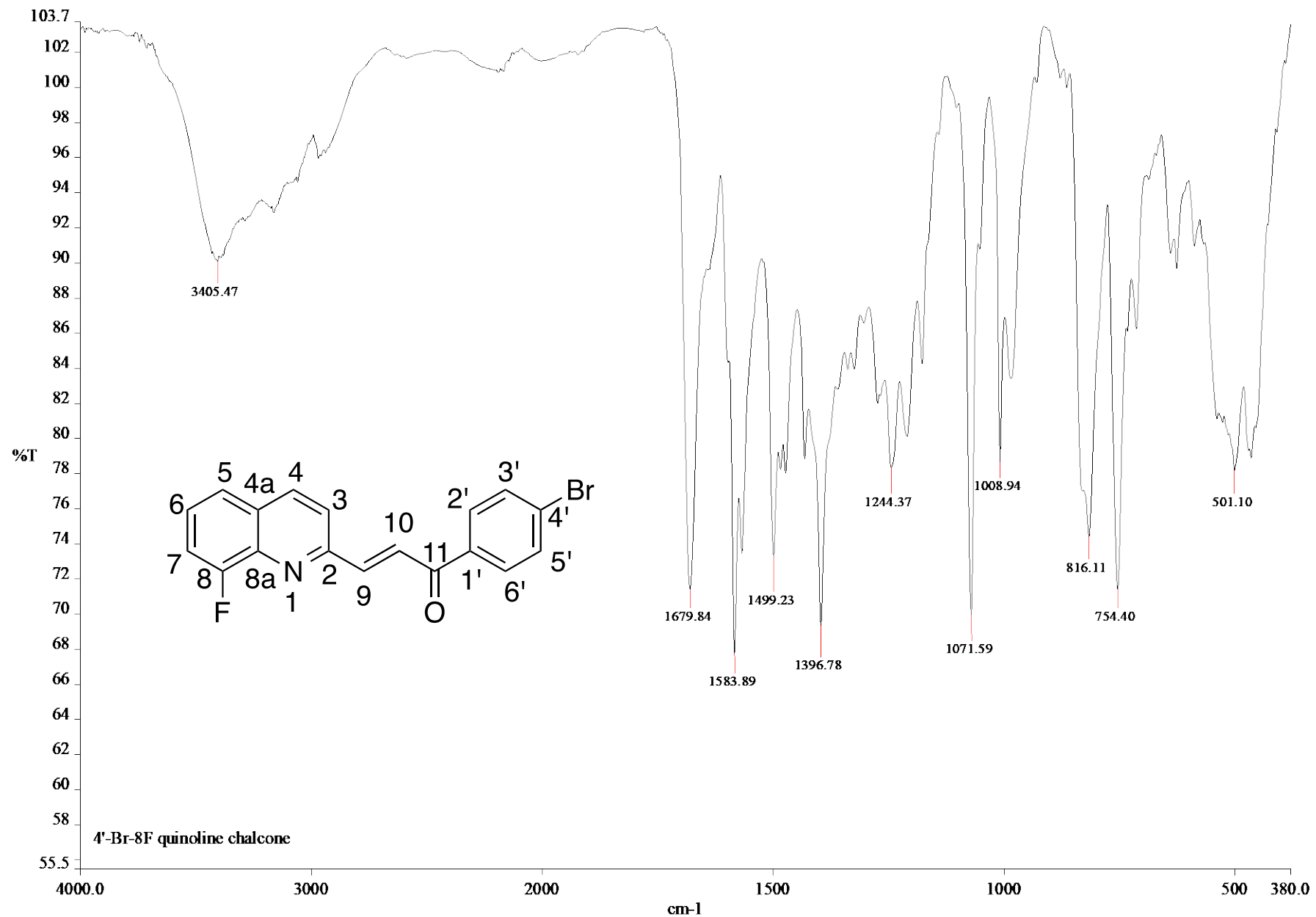
Infrared spectrum of compound **8g**
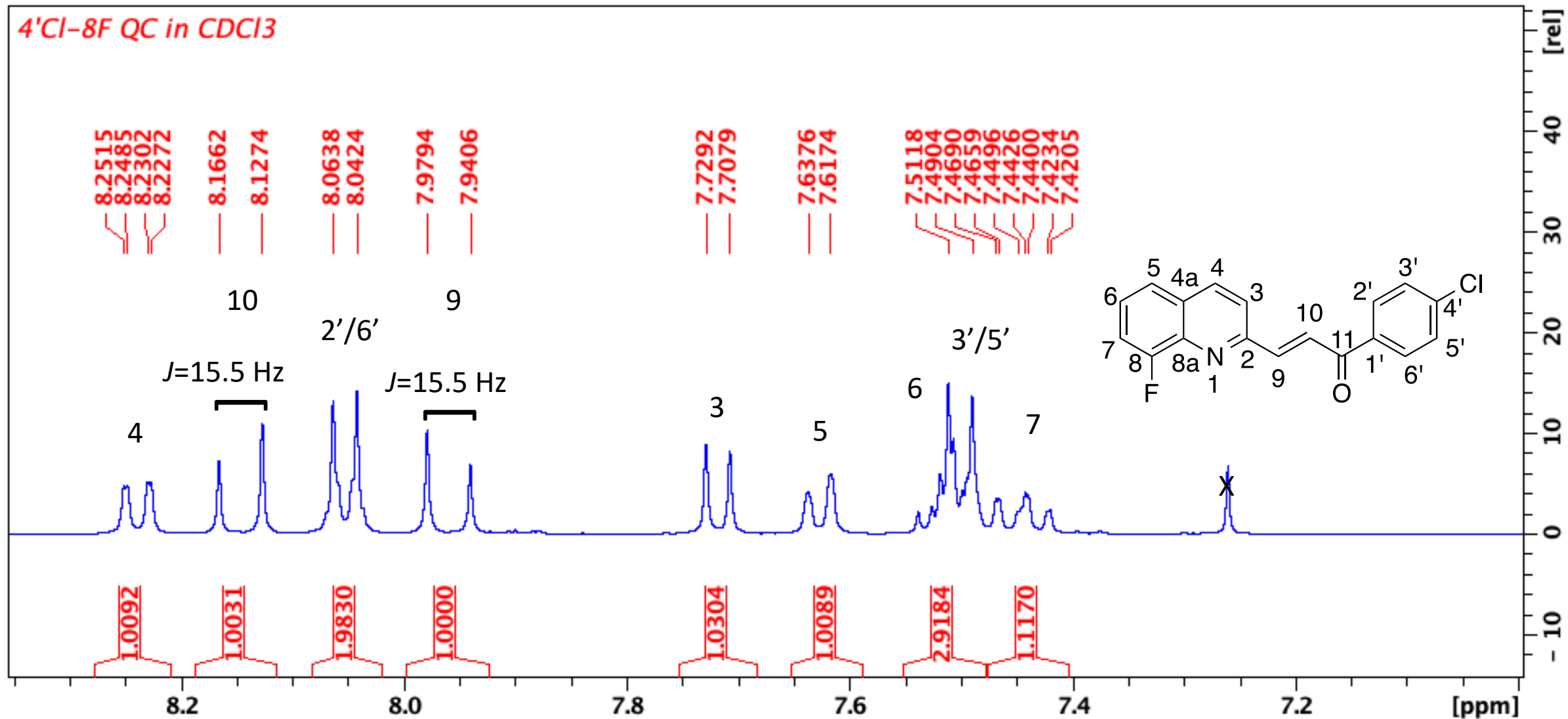
The ^{1}H NMR of compound **8h**
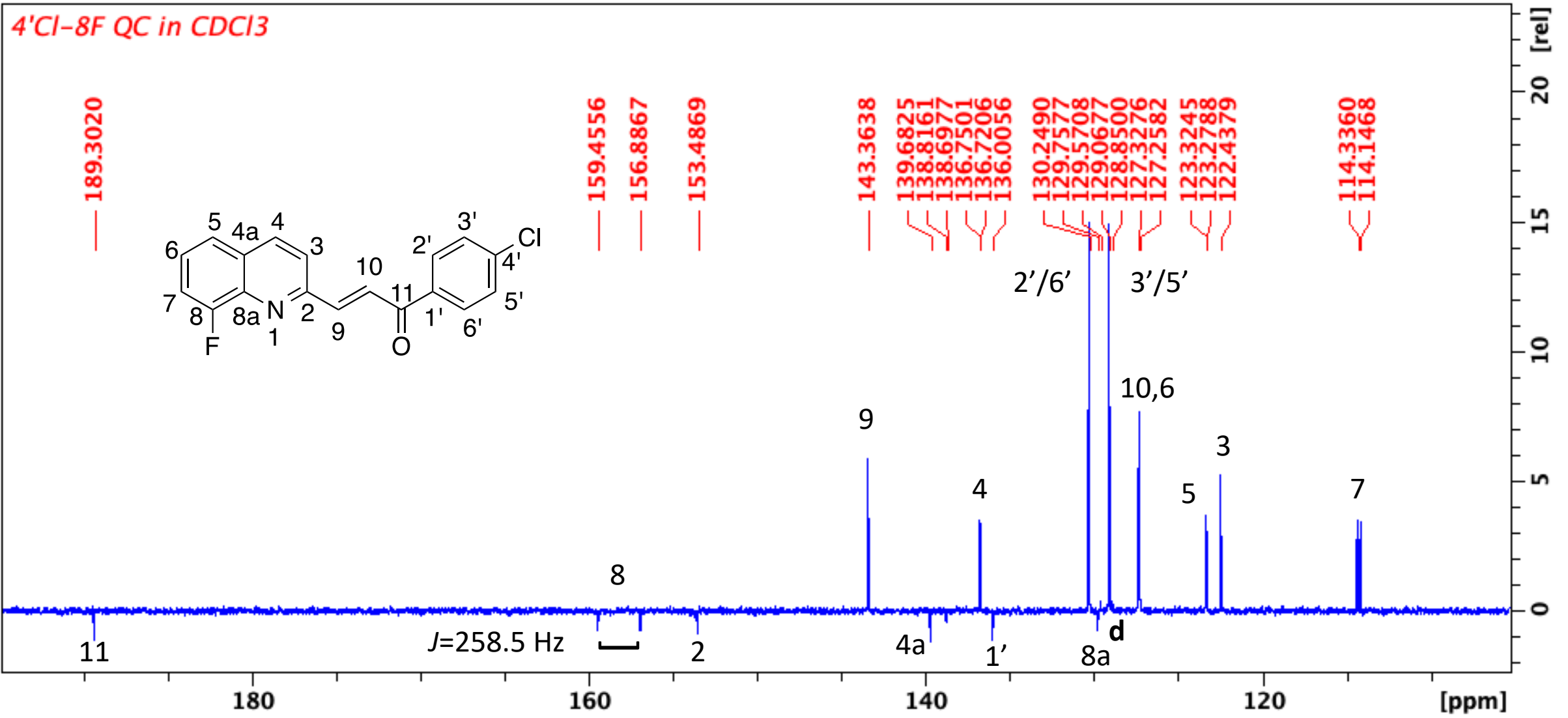
The ^{13}C NMR of compound **8h**
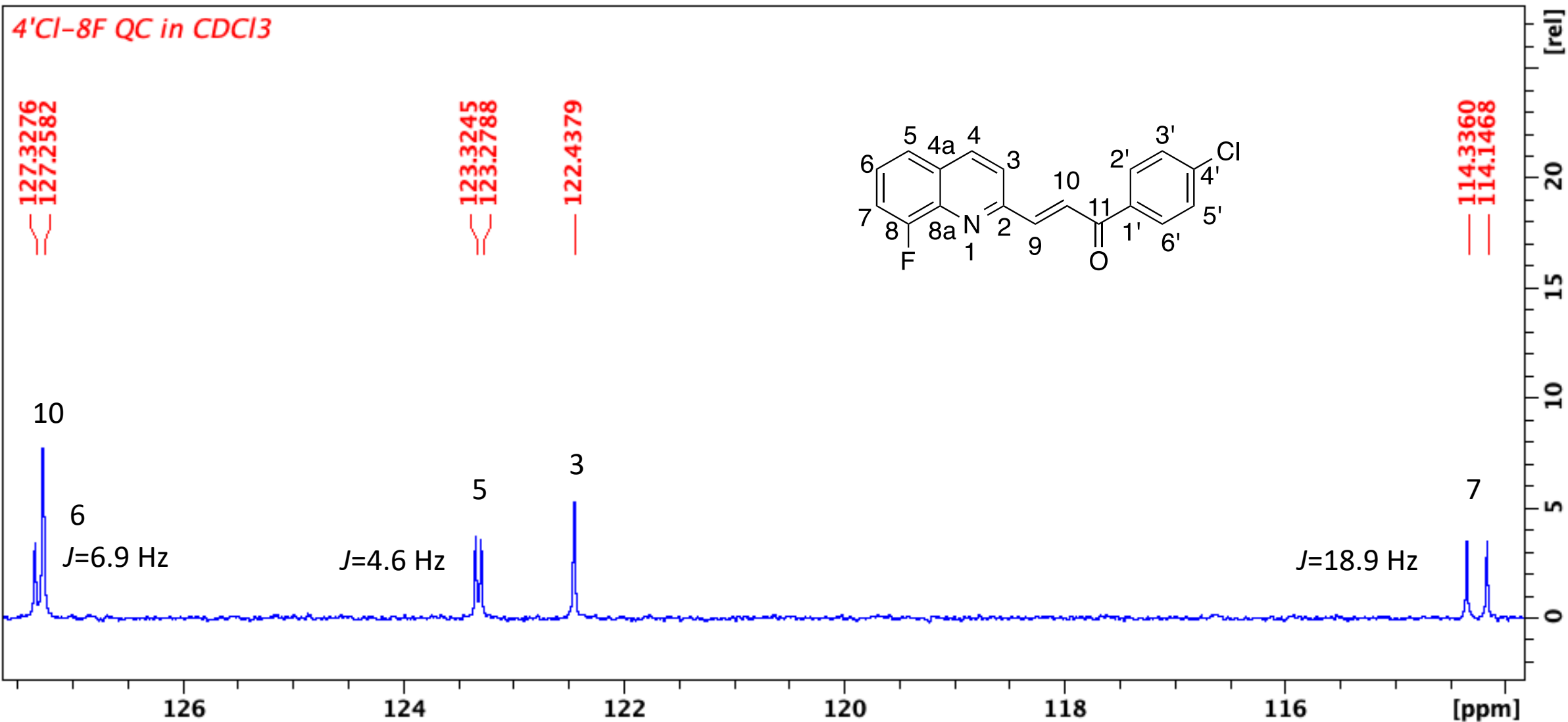
The expanded ^{13}C NMR of compound **8h**
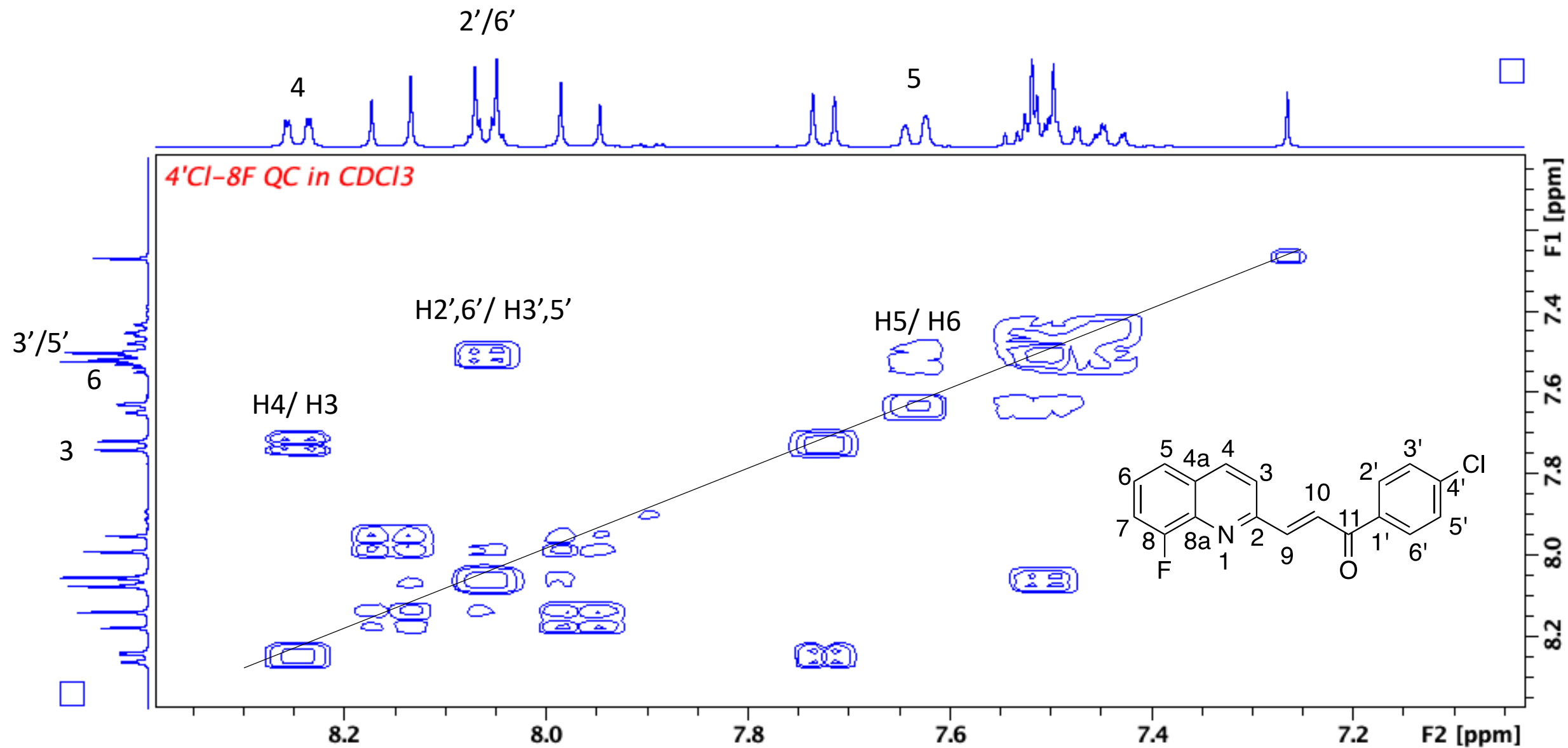
The COSY spectrum of compound **8h**
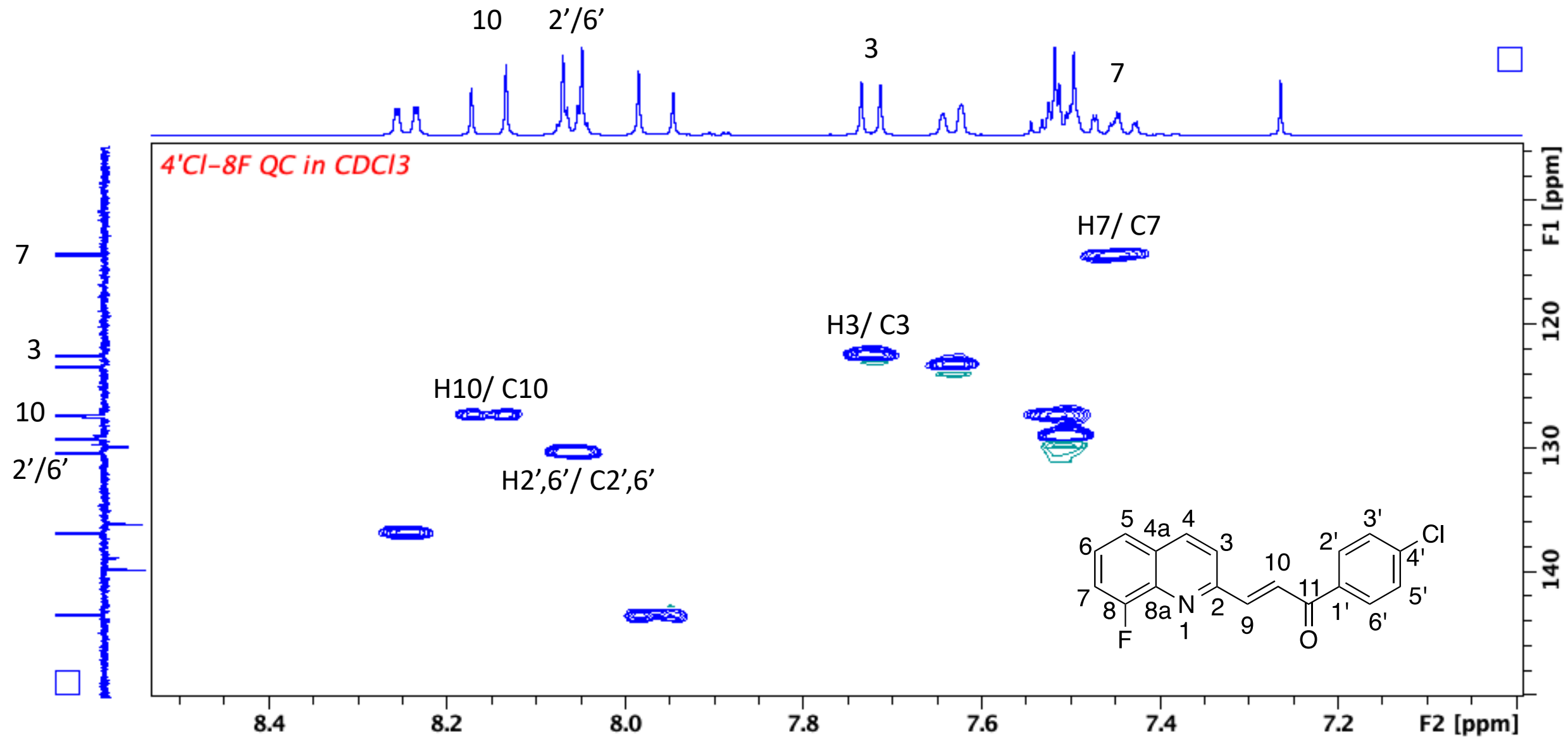
The HSQC spectrum of compound **8h**

66
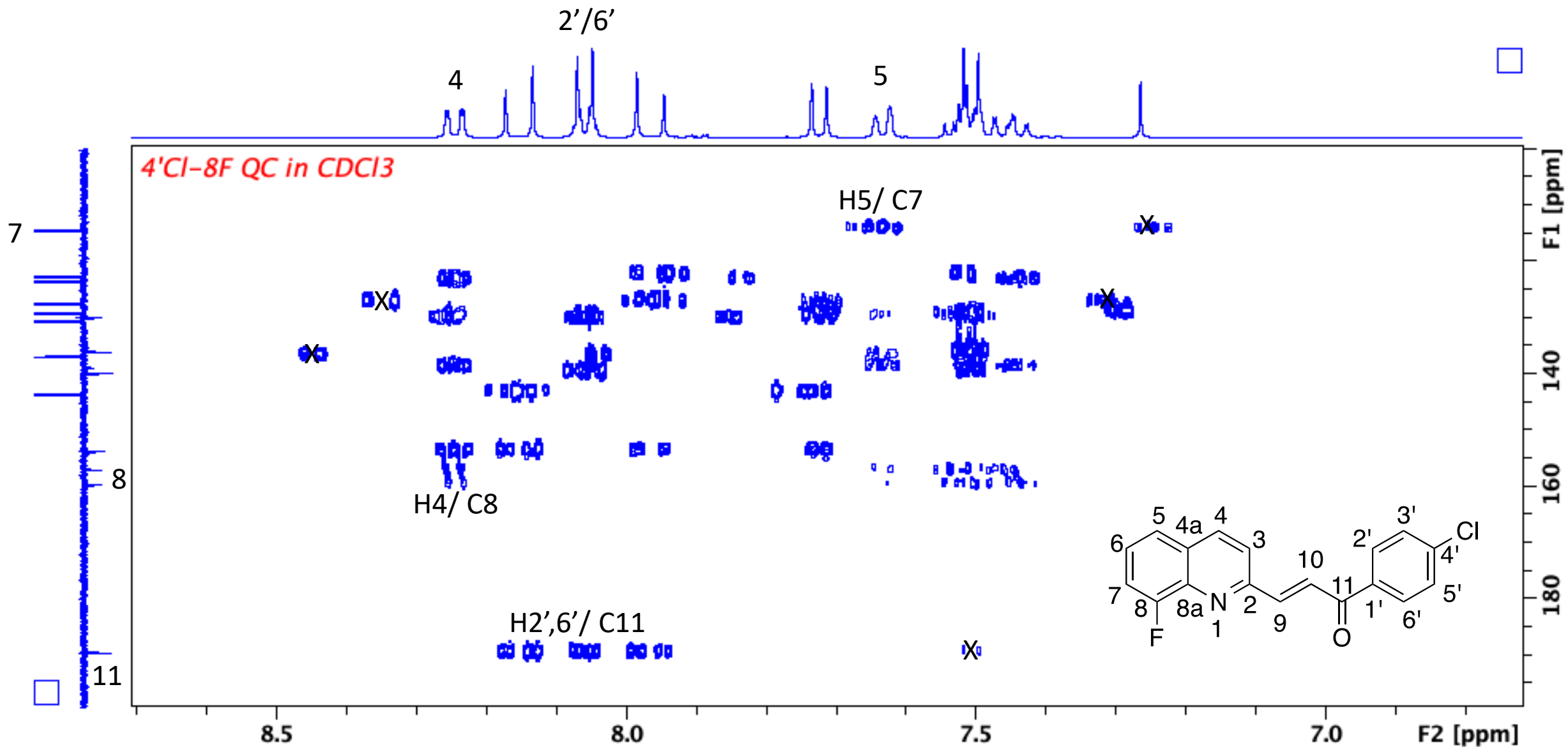
The HMBC spectrum of compound **8h**

Single Mass Analysis
Tolerance = 5.0 PPM   /   DBE: min = -1.5, max = 50.0
Element prediction: Off
Number of isotope peaks used for i-FIT = 3

Monoisotopic Mass, Even Electron Ions
72 formula(e) evaluated with 1 results within limits (all results (up to 1000) for each mass)
Elements Used:
C: 15-20   H: 10-15   N: 0-5   O: 0-5   F: 0-1   Cl: 0-1
Cmpd 8 8 (0.237) Cm (1:61)
TOF MS AP+

2.57e+005
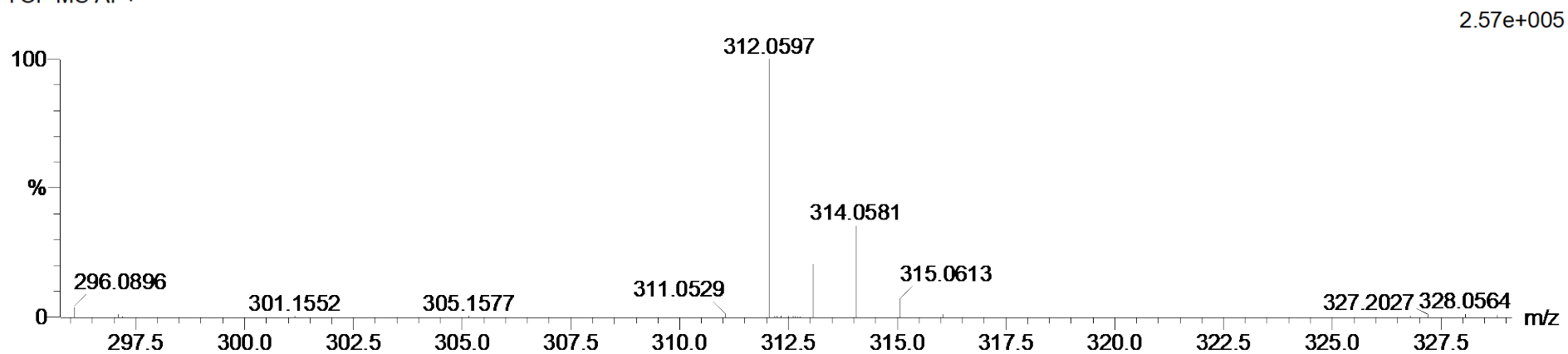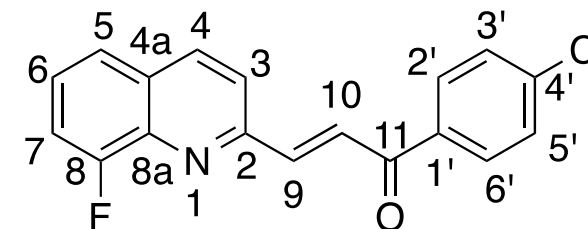
Minimum:				-1.5			
Maximum:		5.0	5.0	50.0			
Mass	Calc. Mass	mDa	PPM	DBE	i-FIT	i-FIT (Norm)	Formula
312.0597	312.0591	0.6	1.9	12.5	125.9	0.0	C18 H12 N O F Cl

HRMS spectrum of compound **8h**
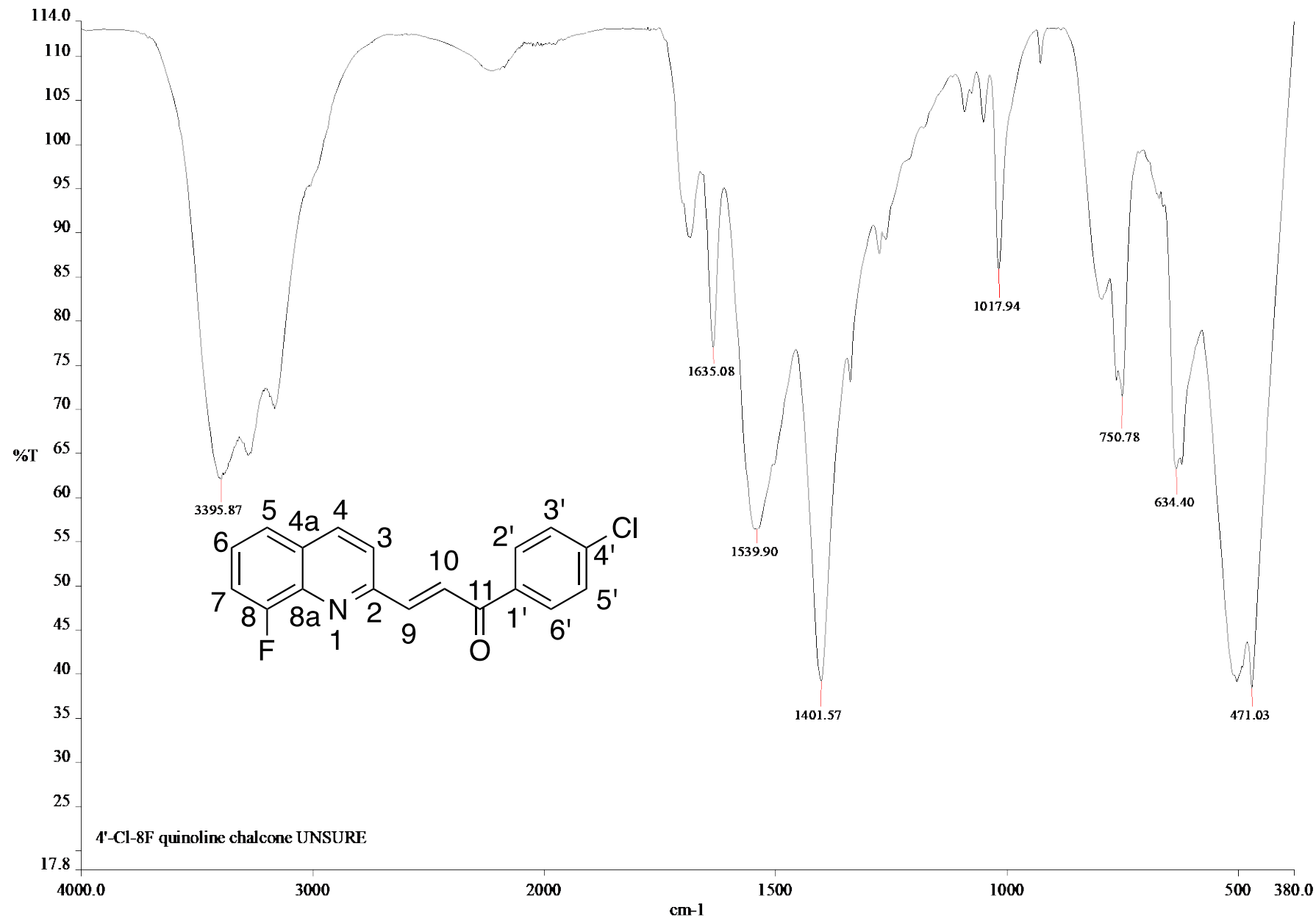
Infrared spectrum of compound **8h**
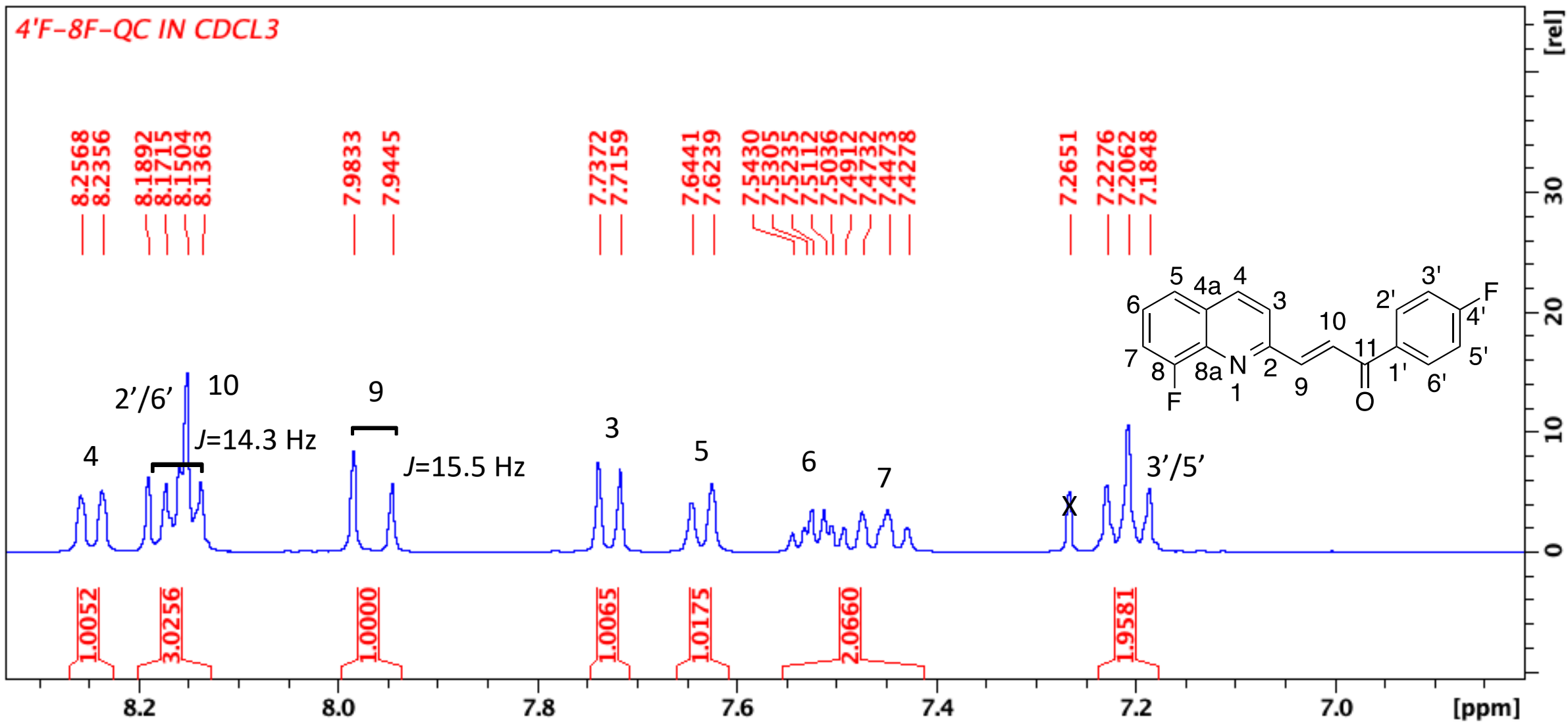
The ^{1}H NMR of compound **8i**

The ^{13}C NMR of compound **8i**

71
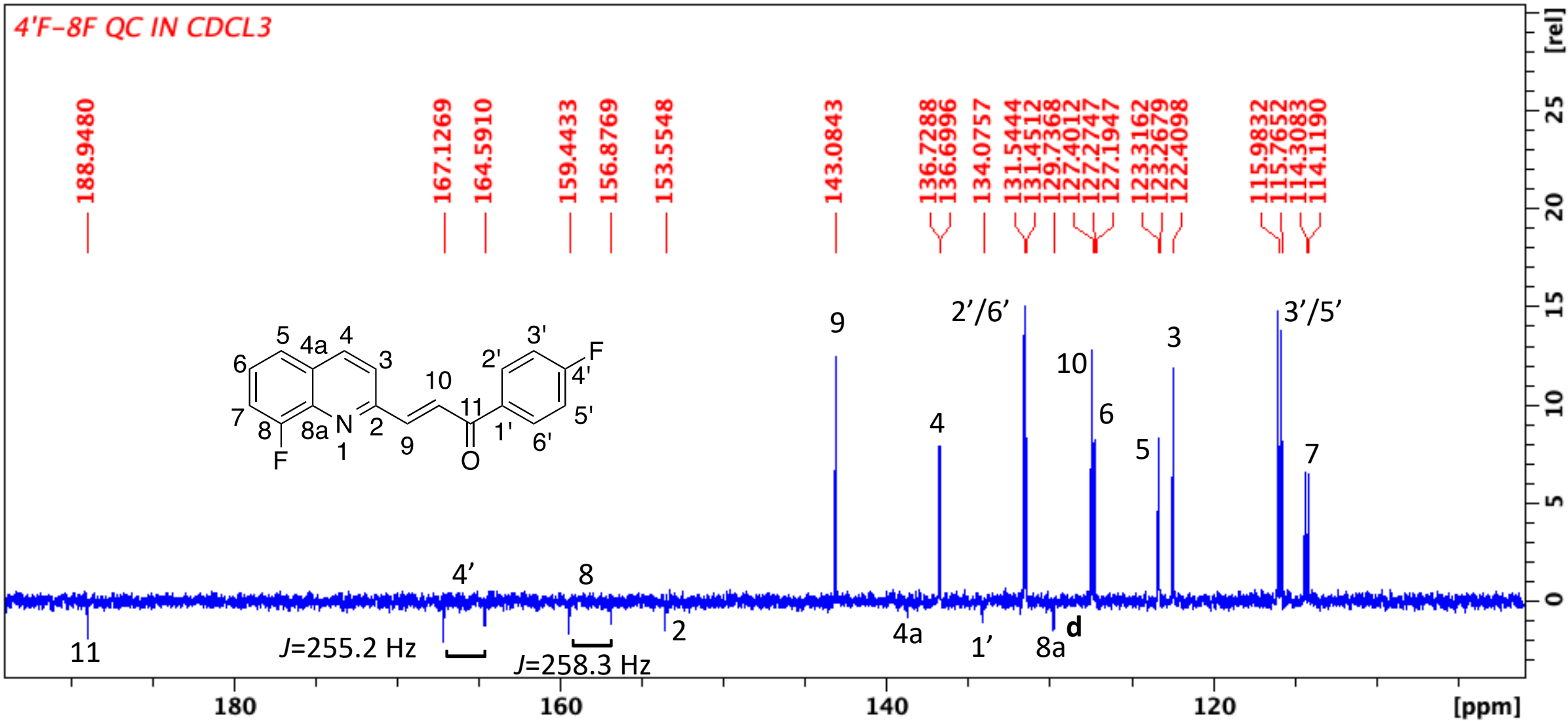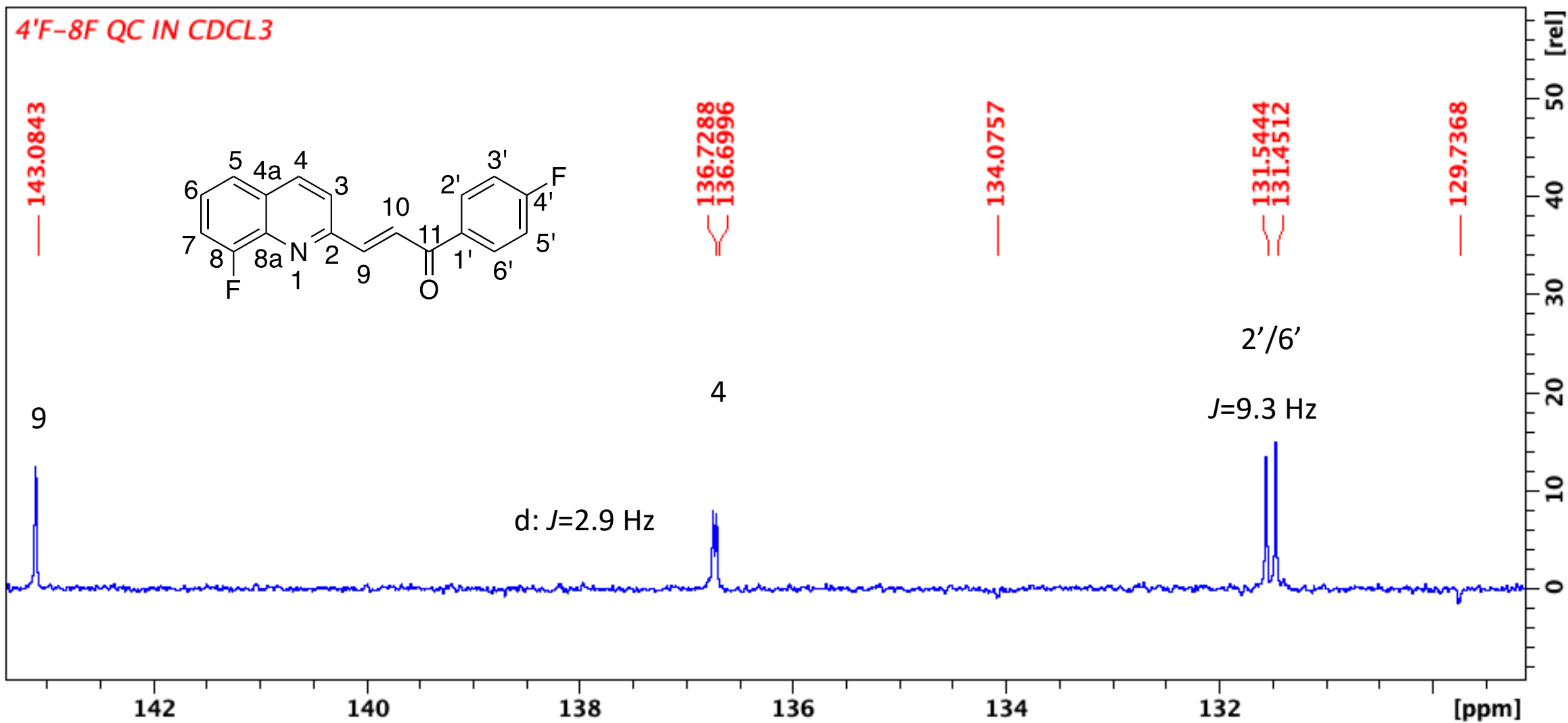
The expanded ^{13}C NMR of compound **8i**
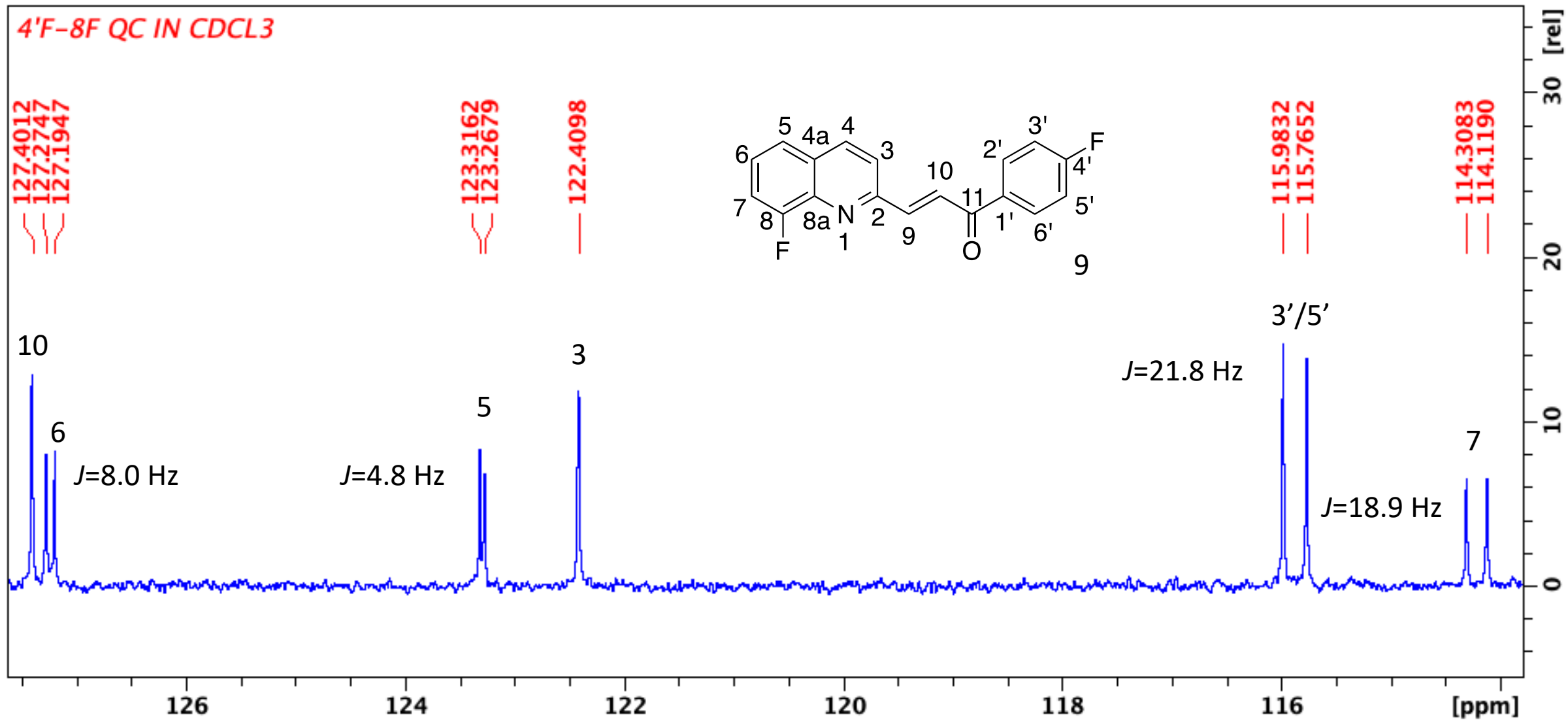
The expanded ^{13}C NMR of compound **8i**
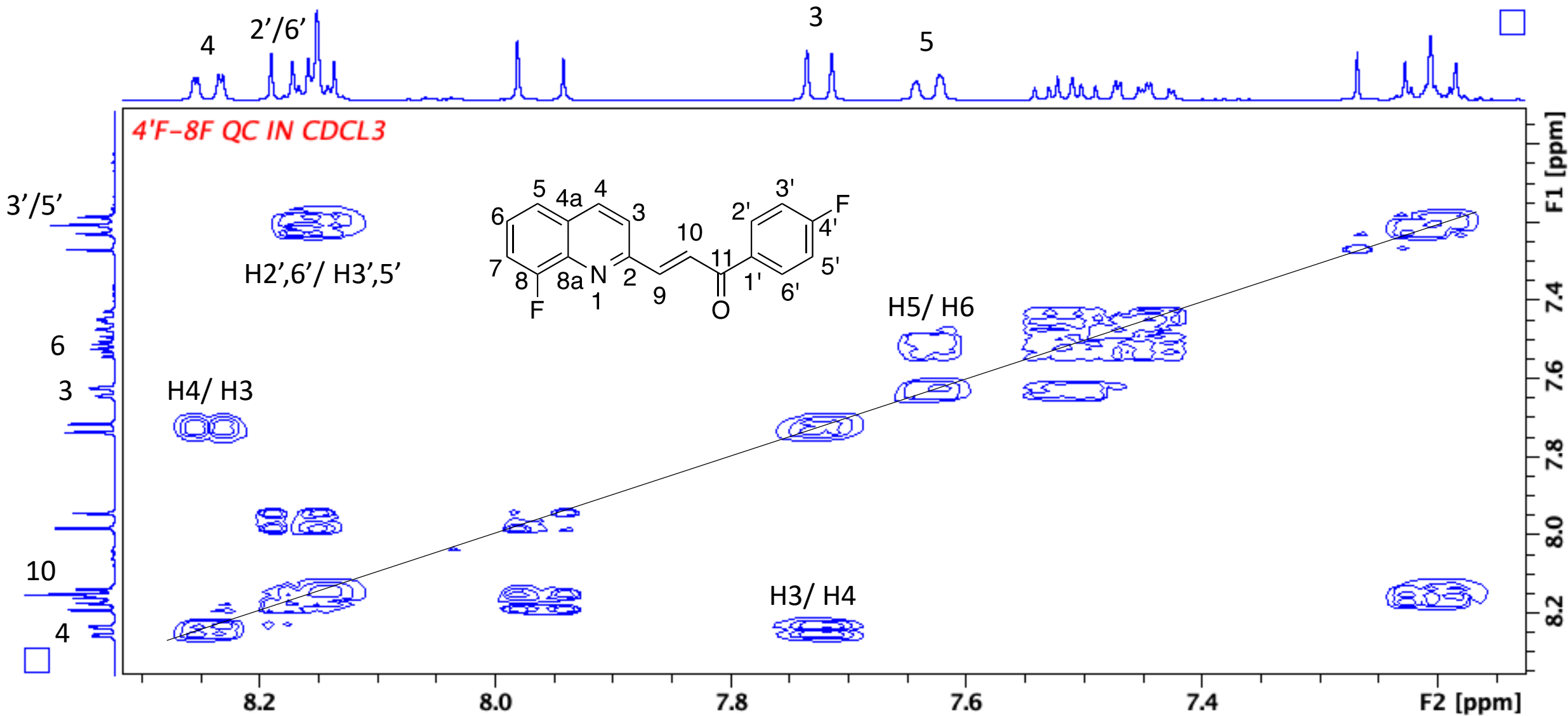
The COSY spectrum of compound **8i**
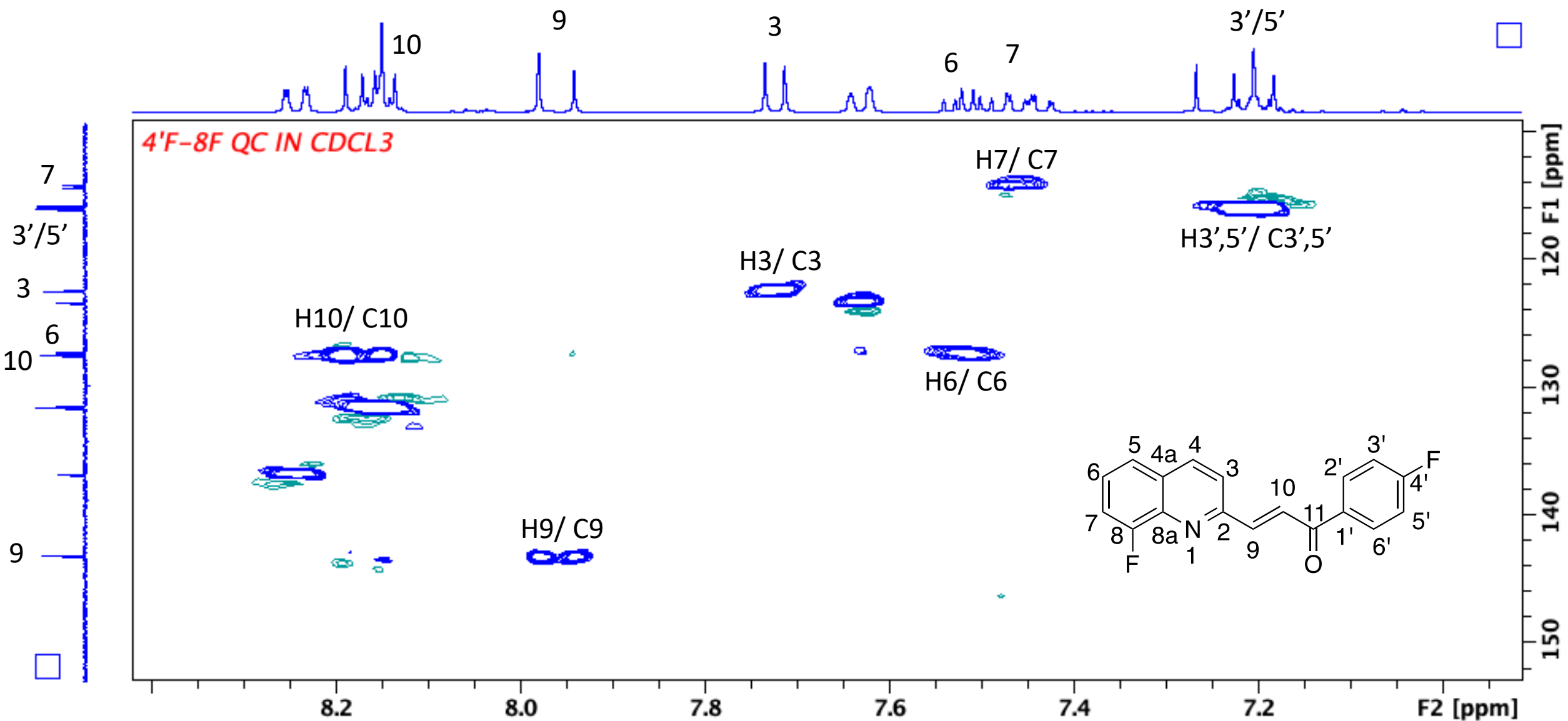
The HSQC of compound **8i**
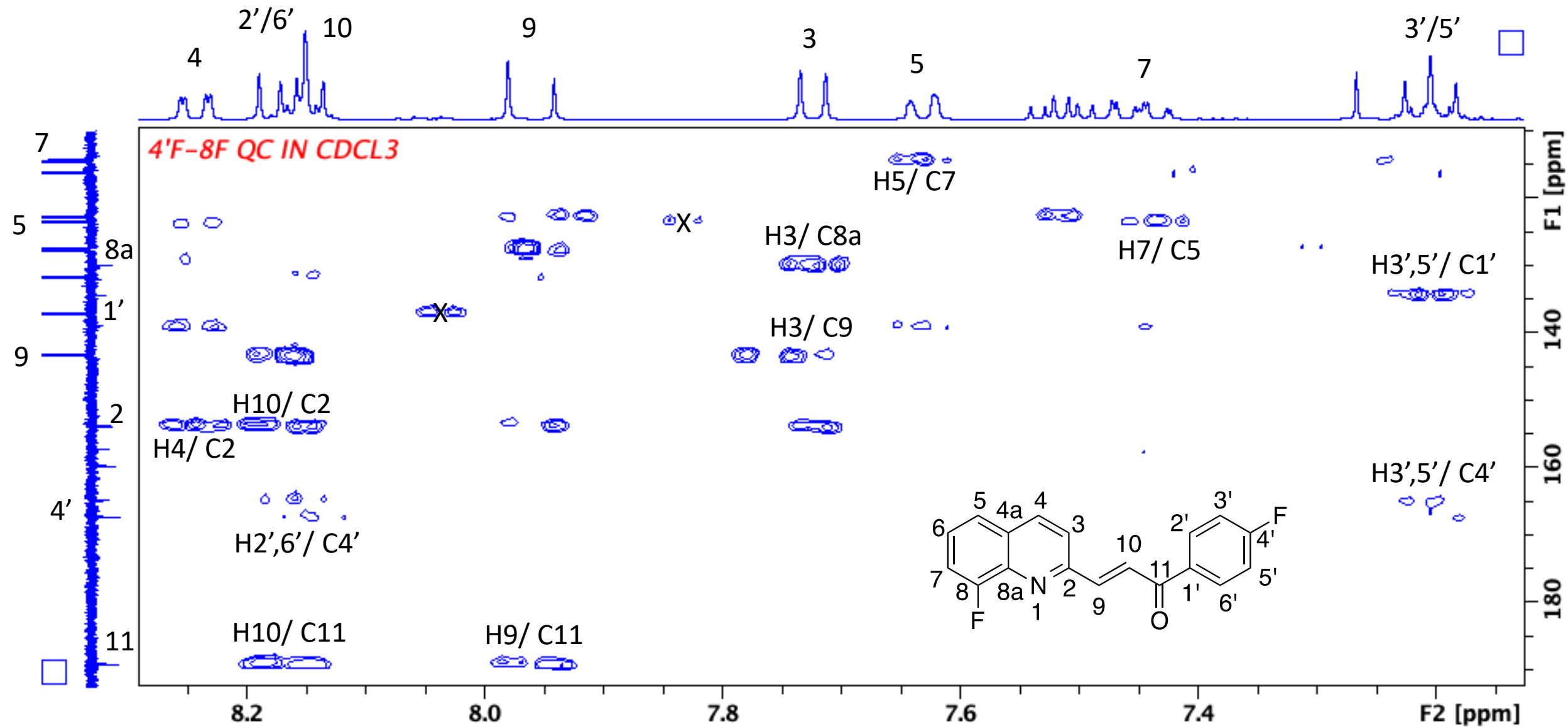
The HMBC of compound **8i**

Single Mass Analysis
Tolerance = 5.0 PPM   /   DBE: min = -1.5, max = 50.0
Element prediction: Off
Number of isotope peaks used for i-FIT = 3

Monoisotopic Mass, Even Electron Ions
58 formula(e) evaluated with 1 results within limits (all results (up to 1000) for each mass)
Elements Used:
C: 15-20   H: 10-15   N: 0-5   O: 0-5   F: 0-2
Cmpd 9 49 (1.619) Cm (1:61)
TOF MS AP+

2.63e+005
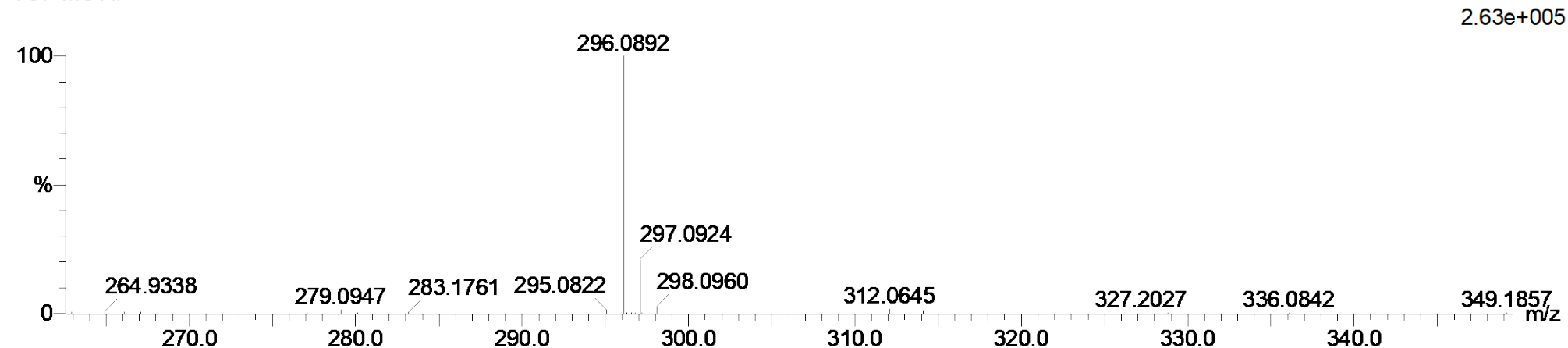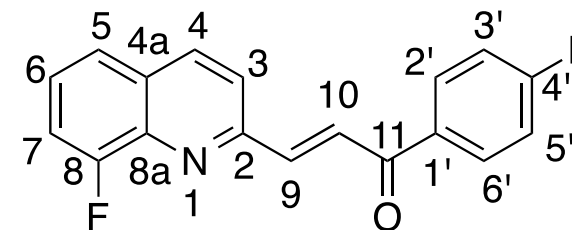
Minimum:				-1.5			
Maximum:		5.0	5.0	50.0			
Mass	Calc. Mass	mDa	PPM	DBE	i-FIT	i-FIT (Norm)	Formula
296.0892	296.0887	0.5	1.7	12.5	97.7	0.0	C18 H12 N O F2

HRMS spectrum of compound **8i**

77

Infrared spectrum of compound **8i**